NO. ST6
NOVEMBER 1956

JOURNAL of the

Structural Division

PROCEEDINGS OF THE

AMERICAN SOCIETY OF CIVIL ENGINEERS

VOLUME 82

BASIC REQUIREMENTS FOR MANUSCRIPTS

This Journal represents an effort by the Society to deliver information to the reader with the greatest possible speed. To this end the material herein has none of the usual editing required in more formal publications.

Original papers and discussions of current papers should be submitted to the Manager of Technical Publications, ASCE. The final date on which a discussion should reach the Society is given as a footnote with each paper. Those who are planning to submit material will expedite the review and publication procedures by complying with the following basic requirements:

1. Titles should have a length not exceeding 50 characters and spaces.

2. A 50-word summary should accompany the paper.

3. The manuscript (a ribbon copy and two copies) should be double-spaced on one side of 8½-in. by 11-in. paper. Papers that were originally prepared for oral presentation must be rewritten into the third person before being submitted.

4. The author's full name, Society membership grade, and footnote reference stating present employment should appear on the first page of the paper.

5. Mathematics are reproduced directly from the copy that is submitted. Because of this, it is necessary that capital letters be drawn, in black ink, 3/16-in. high (with all other symbols and characters in the proportions dictated by standard drafting practice) and that no line of mathematics be longer than 6½-in. Ribbon copies of typed equations may be used but they will be proportionately smaller in the printed version.

6. Tables should be typed (ribbon copies) on one side of 8½-in. by 11-in. paper within a 6½-in. by 10½-in. invisible frame. Small tables should be grouped within this frame. Specific reference and explanation should be made in the text for each table.

7. Illustrations should be drawn in black ink on one side of 8½-in. by 11-in. paper within an invisible frame that measures 6½-in. by 10½-in.; the caption should also be included within the frame. Because illustrations will be reduced to 69% of the original size, the capital letters should be 3/16-in. high. Photographs should be submitted as glossy prints in a size that is less than 6½-in. by 10½-in. Explanations and descriptions should be made within the text for each illustration.

8. Papers should average about 12,000 words in length and should be no longer than 18,000 words. As an approximation, each full page of typed text, table, or illustration is the equivalent of 300 words.

Further information concerning the preparation of technical papers is contained in the "Technical Publications Handbook" which can be obtained from the Society.

This Journal is published bi-monthly by the American Society of Civil Engineers. Publication office is at 2500 South State Street, Ann Arbor, Michigan. Editorial and General Offices are at 33 West 39 Street, New York 18, New York. $4.00 of a member's dues are applied as a subscription to this Journal. Second-class mail privileges are authorized at Ann Arbor, Michigan.

Journal of the

STRUCTURAL DIVISION

Proceedings of the American Society of Civil Engineers

CONTENTS

November, 1956

Papers

Paper 1096 ST 6

Journal of the
STRUCTURAL DIVISION
Proceedings of the American Society of Civil Engineers

INTERNAL TIES IN SLOPE DEFLECTION AND MOMENT DISTRIBUTION

Morris Ojalvo,[1] J.M. ASCE

Synopsis

The purpose of this paper is to outline a procedure which can be used in the slope deflection and moment distribution methods of analysis when the joints of a rigid frame are free to translate. This procedure makes use of imaginary internal ties. In moment distribution these ties may be considered as the restraints which prevent joint translation during the balancing of the moments. The procedure becomes increasingly useful for the more complicated structures and does not complicate the analysis of the simpler structures. The versatility of moment distribution and slope deflection is retained or enhanced.

INTRODUCTION

If the plane structures of figures 1.a and 1.b are made of inextensible members, the displacements of the joints can be expressed completely in terms of the changes in length of the diagonal distances such as AE and BD. Both structures are said to have two degrees of freedom as far as joint translation is concerned. If imaginary hinged diagonals AE and BE are introduced in each structure, the joints are fully restrained. Figure 1.a then becomes a simple pin connected truss. A Williot diagram can be used to graphically determine the relative movement δ of the ends of any member in a direction perpendicular to their original direction when one of the diagonals changes in length by an amount Δ. The same relative movement δ for any member of the rigid frame of figure 1.b may be similarly determined in terms of the Δ change in length of a diagonal. This allows the computation of the fixed end moments due to the change in length of a diagonal. If a more accurate determination of the fixed end moments is desirable, the Williot diagram provides a figure from which distances may be trigonometrically determined.

Note: Discussion open until April 1, 1957. Paper 1096 is part of the copyrighted Journal of the Structural Division of the American Society of Civil Engineers, Vol. 82, No. ST 6, November, 1956.

1. Asst. Prof., Dept. of Civ. Eng., Princeton Univ., Princeton, N. J.

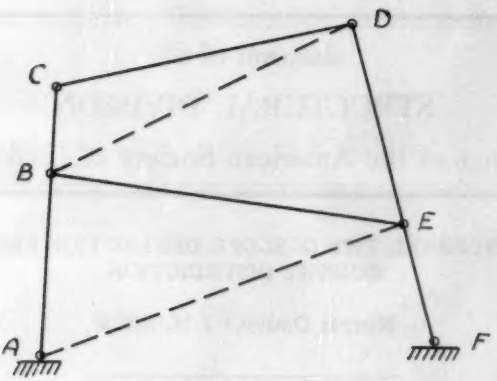

Fig. 1a

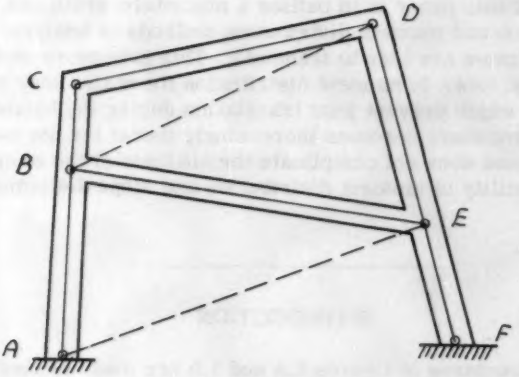

Fig. 1b

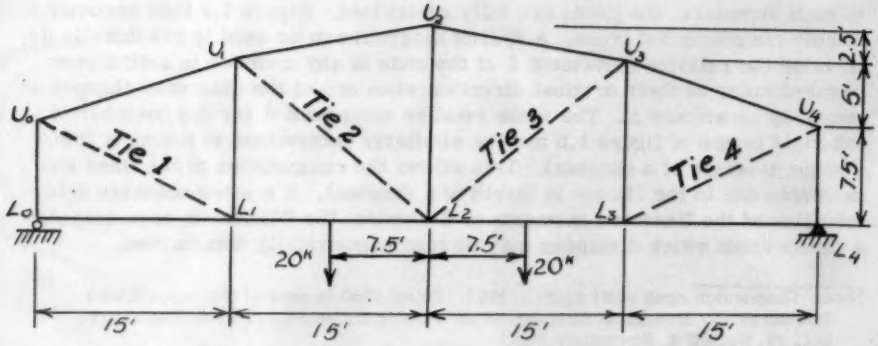

Fig. 2

Procedure in Slope Deflection

In slope deflection, equations of equilibrium are written in terms of the rotations of the angles and the displacements of the joints. These equations may be classified in two categories; e.g. those that equate moments at a joint to zero and those that concern the equilibrium of forces acting on a portion of the structure.

At the beginning of an analysis all joints of the structure are considered hinged and imaginary internal ties are located so that the structure becomes stable and statically determinate. The unknowns will be the rotations of the joints and the changes in length of the diagonals. Let the ties be numbered 1, 2, 3, . . . and the changes in length of the ties designated $\Delta_1, \Delta_2 \ldots$ For a member NF the δ distortion will be $\delta_1 + \delta_2 + \delta_3 \ldots$ where δ_n is the δ due to the change in length Δ_n of tie n. The final moment at N will be the fixed end moment due to the loads + $2EK \left(2\theta_N + \theta_F - 3\frac{\Sigma\, \delta_1 + \delta_2 + \delta_3 \cdots}{1_{NF}} \right)$

As stated previously, the equilibrium equations by which the Δs and θs are solved can be divided into two categories. The first (summation of moments at each joint) can be thought of as expressing the condition that the structure in its deflected equilibrium position requires no external moment restraints at the joints to prevent further joint rotation. The second category implies that in the equilibrium position, internal ties are not necessary to prevent further joint translation. Each of the equations of the second category must therefore solve for the force in a tie and then equate it to zero. In this manner these equations turn out to be independent of the joint equations and therefore useful in the solution of the unknown Δs and θs.

Procedure in Moment Distribution

The internal ties are located as described previously in the slope deflection method. Fixed end moments due to the load system are determined and then balanced in the usual way. The forces in the ties are calculated from statics. Analysis for these forces is identical to the analysis of a pin connected structure except that known shears and moments must be considered where a section cuts through a member to isolate a portion of the structure. In subsequent steps each tie is allowed to take a change in length and the fixed end moments throughout the structure are determined. These moments are balanced and the stresses in the ties are again determined. The results of each of these balances are combined with the first balance in such ratios that the forces in the ties disappear.

Analysis of a Vierendeel Truss

Figure 2 shows a Vierendeel truss loaded symetrically. The chords are 10WF49 steel beams and the verticals are 10WF21. The imaginary internal ties are indicated by dotted lines. From left to right the ties are designated 1, 2, 3, and 4. Various properties of the members are given in table 1.

Figure 3 shows the shape the truss would take when tie number 1 is shortened a small amount. Joints U_1, L_1, U_2, L_2, U_3, L_3, U_4 and L_4 are rotated clockwise by the angle α and joints U_0 and L_0 are rotated clockwise

TABLE 1

Properties of the Vierendeel Truss Members

Member	Length (in.)	I ($in.^4$)	K ($in.^3$)	Area ($in.^2$)
U_0U_1	190	273	1.435	14.4
U_1U_2	183	"	1.492	"
U_2U_3	183	"	1.492	"
U_3U_4	190	"	1.435	"
L_0L_1	180	"	1.515	"
L_1L_2	180	"	1.515	"
L_2L_3	180	"	1.515	"
L_3L_4	180	"	1.515	"
U_0L_0	90	106	1.178	6.2
U_1L_1	150	"	0.707	"
U_2L_2	180	"	0.589	"
U_3L_3	150	"	0.707	"
U_4L_4	90	"	1.178	"

by angle β. Members U_0U_1 and L_0L_1 are rotated counterclockwise by γ. In this manner only U_0U_1 and L_0L_1 have fixed end moments induced in them by this distortion. Angles α and γ may be easily determined as the vertical movement of L_1 is equal to the product of the shortening of tie number 1 and the influence line ordinate for tie number 1 at L_1. This influence line ordinate is obtained for the structure as though it were pin connected. If a unit couple is applied to L_0U_0 and the resultant stress in tie number 1 determined, then β may be similarly obtained. The fixed end moment of this distortion in U_0U_1 would $2EK(2\beta + \alpha + 3\gamma)$.

Figure 4 is used to determine fixed end moments in U_1U_2 and L_1L_2 when tie number 2 is shortened. The shortening of the tie in each case was made 0.5 inches. Fixed end moments and balanced moments for the distortion of ties 1 through 4 and for the applied loads are tabulated in table 2. The information for columns 8 and 9 can be obtained from columns 7 and 5 because of the symmetry of the structure. Table 3 gives the forces in the ties for each case.

In the equations below R_1, R_2, R_3, and R_4 are ratios of the translational effects which must be combined with the results of the initial balance to cause the forces in the ties to vanish. By symmetry:

$$R_1 = R_4$$

$$R_2 = R_3$$

$$25.83R_1 - 8.437R_2 + 28.54 = 0$$

$$-8.451R_1 + 23.76R_2 + 9.27 = 0$$

$$R_1 = R_4 = -1.394$$

$$R_2 = R_3 = -0.886$$

The final moments are given in figure 5.

Deflections

Joint deflections may be determined by virtual work or a Williot diagram. If virtual work is used the deflection at any points is equal to the summation of s x e for all members where s is the dummy load force in a member and e is the change in length of the member. This also includes the ties whose change in length would be 0.5 inches times the corresponding ratio R. The summation of s times e for the ties would give the deflection due to bending and the remainder would be the contribution of the changes in length of the real members. The vertical deflection of joint L_2 is computed in table 4.

Secondary Effects

The analysis by moment distribution ignored the effects of axial changes in length on the final moments. These can best be evaluated by successive approximations as in evaluating secondary moments in trusses.[2]

2. Statically Indeterminate Structures, L. C. Maugh.

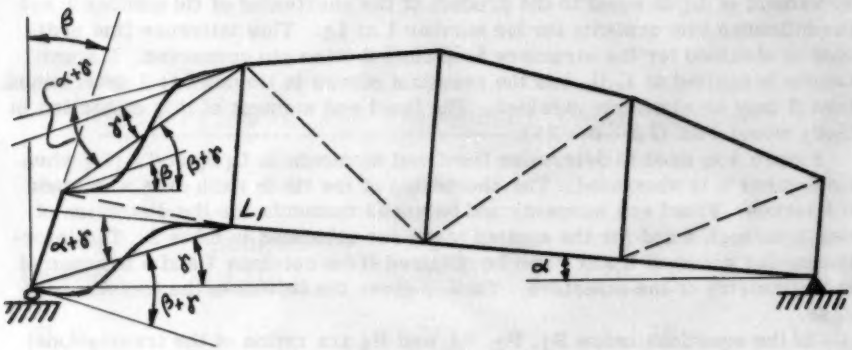

Fig.3
TIE 1 SHORTENED

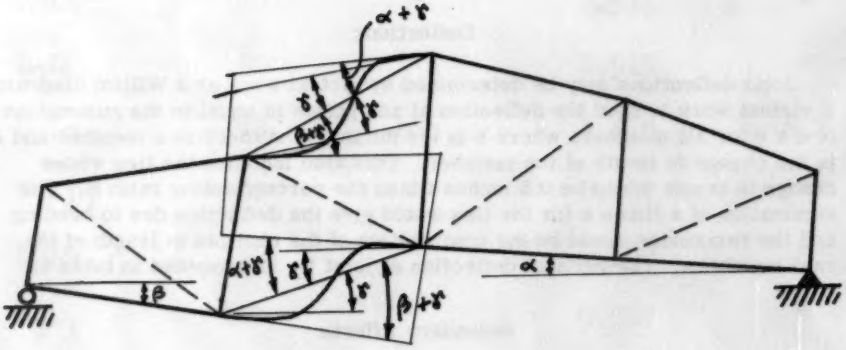

Fig.4
TIE 2 SHORTENED

TABLE 2 - Moments in inch kips

Moment	Applied Loads FEM	Applied Loads Balanced Moments	Δ_1=0.5 in. FEM	Δ_1=0.5 in. Balanced Moments	Δ_2=0.5 in. FEM	Δ_2=0.5 in. Balanced Moments	Δ_3=0.5 in. Balanced Moments	Δ_4=0.5 in. Balanced Moments
U_0U_1		7	1395	679		- 97	- 18	4
U_0L_0		- 7		-679		97	18	- 4
L_0U_0		- 38		-690		98	18	- 3
L_0L_1		38	1473	690		- 98	- 18	3
L_1L_0		165	1246	582		-322	- 60	12
L_1U_1		91		-254		-259	- 47	11
L_1L_2	-450	-256		-328	1121	581	107	- 23
L_2L_1	450	547		-110	1055	521	318	- 67
L_2U_2		0		43		-203	18	- 43
L_2L_3		-547		67		-318	-521	110
L_3L_2		256		23		-107	-581	328
L_3U_3		- 91		- 11		47	259	254
L_3L_4		-165		- 12		60	322	-582
L_4L_3		- 38		- 3		18	98	-690
L_4U_4		38		3		- 18	- 98	690
U_4L_4		7		4		- 18	- 97	679
U_4U_3		- 7		- 4		18	97	-679
U_3U_4		12		- 13		57	309	-568
U_3L_3		- 35		- 9		48	257	254
U_3U_2		23		22		-105	-566	314
U_2U_3		11		64		-308	-513	105
U_2L_2		0		41		-205	205	- 41
U_2U_1		- 11		-105	1034	513	308	**- 64**
U_1U_2		- 23		-314	1099	566	105	**- 22**
U_1L_1		35		-254		-257	- 48	**9**
U_1U_0		- 12	1180	568		-309	- 57	**13**

TABLE 3

Forces in the Ties in Kips

Tie	Applied Loads	$\Delta_1 = 0.5"$	$\Delta_2 = 0.5"$
1	28.54	25.56	- 7.119
2	9.27	- 7.115	17.40
3	9.27	- 1.336	6.357
4	28.54	0.273	- 1.318

TABLE 4

Vertical Deflection at L_2

Member	e(in.)	s_{L_2}	$s_{L_2} \cdot e$ (in.)
U_0U_1	-.0097	- .6325	.0061
U_1U_2	-.0121	-1.0138	.0123
L_0L_1	.0077	0	0
L_1L_2	.0115	1.2000	.0138
L_0U_0	-.0066	- .5000	.0033
L_1U_1	.0044	- .3000	-.0013
1/2 L_2U_2	.0080	.3333	.0027
Tie 1	.6971	.6708	.4676
Tie 2	.4430	.5207	.2307

Deflection of L_2 = 1.48" Σ = 0.7378

% due to bending = 95

Analysis of a Rigid Polygonal Truss

The second example is a rigid polygonal truss,[3] a structure midway between a truss and a rigid frame. The structure and its loading are shown in figure 6. All members are 10WF49 beams. Their properties are given in table 5. The ties 1 through 4 allow the greatest use of symmetry.

Williot diagrams are used in figures 7 and 8 to determine the δs when ties 1 and 2 are shortened 1 inch. Since the structure is a compound truss when considered with the ties, short additional computations giving the vertical movement of L_2 are necessary before the construction of the Williot diagrams can proceed. In the case of tie number 1 the portion U_3, U_5, M_6, L_6, L_4, M_4 is considered fixed and the support at L_0 is removed. A dummy load is placed at L_2. Assuming all joints hinged, the dummy load force in tie 1 gives the upward movement in inches of joint L_2 when tie 1 shortens one inch. The dummy force in tie 2 gives the upward movement of L_2 when tie 2 shortens one inch. These two deflections are 0.8544 and 0.2667 inches up.

The fixed end moments are $=6EK\frac{\delta}{I}$. Table 6 gives fixed end moments and balanced moments for the applied loads and the shortening of ties 1 through 4. Table 7 gives the forces in the ties and the following equations give the ratios in which the effects of the distortions must be combined with the moment balance of the applied loads to make the forces in the ties vanish.

$$205.65\ R_1 - 14.54\ R_2 - 29.66 = 0$$

$$-14.39\ R_1 + 97.51\ R_2 + 18.86 = 0$$

$$R_1 = R_4 = +0.1319$$

$$R_2 = R_3 = -0.1739$$

Figure 9 gives the final moments. The deflection at L_2 and L_4 is evaluated in table 8. The dummy load system for table 8 consists of unit loads placed at L_2 and L_4.

CONCLUSIONS

The use of internal ties can simplify the analysis of complex rigid frames by making possible the evaluation of deflections and distortions as in statically determinate pin connected trusses. The location of restraints for the optimum use of symmetry is more easily visualized.

NOTATION

δ - The displacement of one end of a member with respect to the other end, in a direction perpendicular to the original direction of the member; positive when the ends of the member rotate clockwise.

Δ - A change in length of an internal tie.

θ - Rotation of a joint; positive when it is clockwise.

3. Introduction to Semi-Rigid Determinate Polygonal Trusses, ASCE Proceedings Separate No. 828, A. H. Kenigsberg.

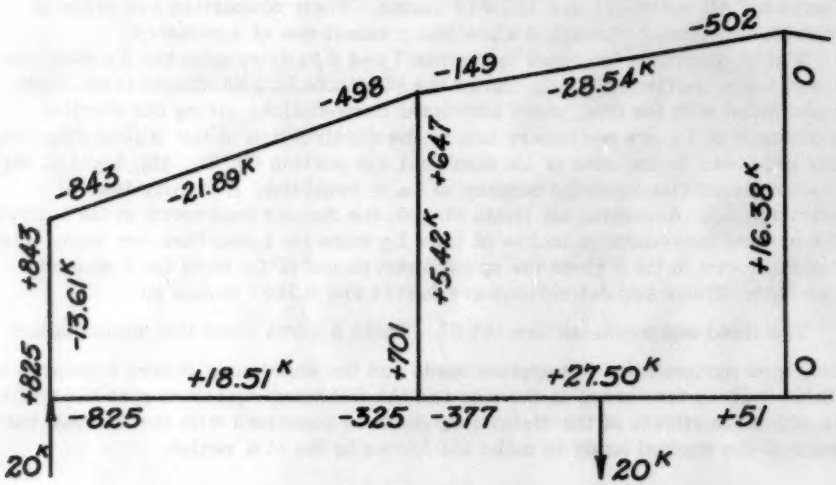

Fig.5
FINAL MOMENTS IN inch Kips
AND AXIAL FORCES IN kips

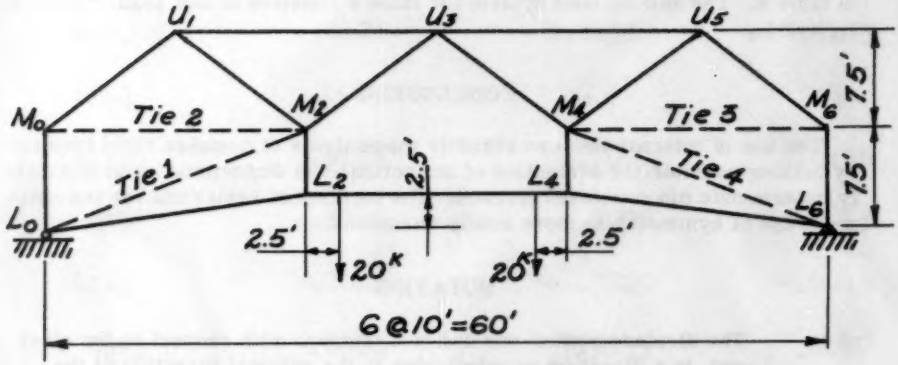

Fig.6

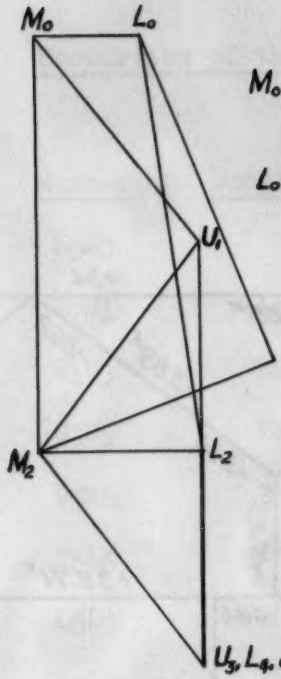

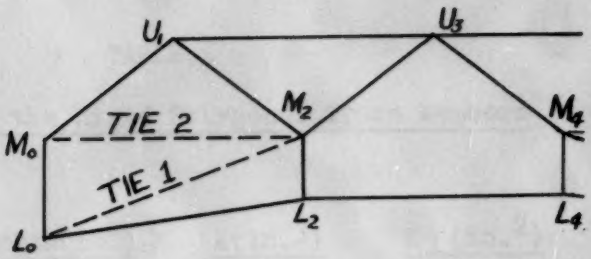

$\delta_{L_2L_4} = .854$ (computed)
$\delta_{L_2M_2} = -.648$
$\delta_{M_2U_1} = 1.078$
$\delta_{M_oU_1} = 1.074$
$\delta_{M_2U_3} = 1.073$
$\delta_{M_oL_o} = -.420$
$\delta_{L_oL_2} = 1.738$
$\delta_{U_1U_3} = 1.716$

Fig. 7
WILLIOT DIAGRAM
FOR TIE 1 SHORTENED

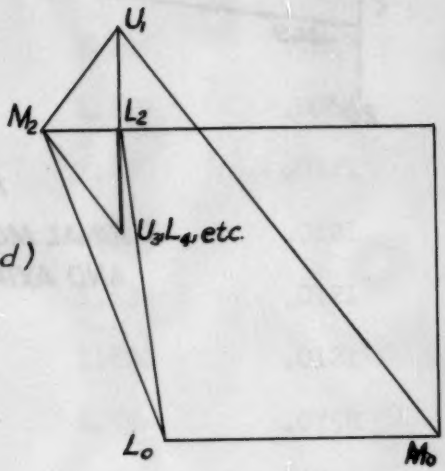

$\delta_{L_2L_4} = .267$ (computed)
$\delta_{L_2M_2} = -.200$
$\delta_{M_2U_3} = .333$
$\delta_{U_1U_3} = -.533$
$\delta_{U_1M_2} = .333$
$\delta_{U_1M_o} = -1.333$
$\delta_{L_oM_o} = .700$
$\delta_{L_oL_2} = -.806$

Fig. 8
WILLIOT DIAGRAM
FOR TIE 2 SHORTENED

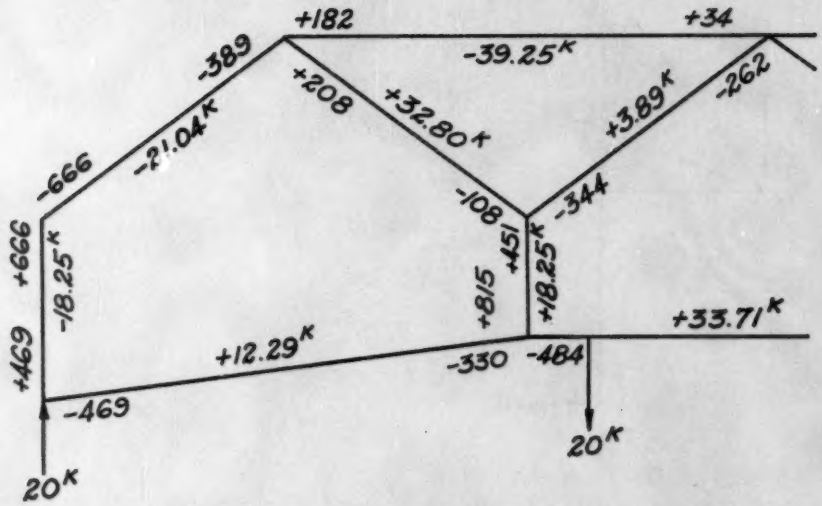

Fig.9

FINAL MOMENTS IN inch kips
AND AXIAL FORCES IN kips

TABLE 5

Properties of the Rigid Polygonal Truss Members

Member	Length(in.)	K(in.^{3})	K/A (in.^{2})
L_0M_0	70	3.033	.0337
M_0U_1	150	1.820	.0121
U_1U_3	240	1.138	.0047
U_3U_5	240	1.138	.0047
U_5M_6	150	1.820	.0121
M_6L_6	90	3.033	.0337
L_0L_2	242	1.129	.0047
L_2L_4	240	1.138	.0047
L_4L_6	242	1.129	.0047
U_1M_2	150	1.820	.0121
M_2U_3	150	1.820	.0121
U_3M_4	150	1.820	.0121
M_4U_5	150	1.820	.0121
L_2M_2	60	4.55	.0758
L_4M_4	60	4.55	.0758

$I = 273$ in.^{4}

$A = 14.4$ in.^{2}

TABLE 6

Moments in Inch Kips

Moment	Applied Loads FEM	Applied Loads Balanced Moments	Δ_1 = 1 in. FEM	Δ_1 = 1 in. Balanced Moments	Δ_2 = 1 in. FEM	Δ_2 = 1 in. Balanced Moments	Δ_3=1 in. Balanced Moments	Δ_4=1 in. Balanced Moments
L_0M_0		- 37	2548	1980	4246	1387	37	81
L_0L_2		37	-1461	-1980	677	1387	- 37	- 81
L_2L_0		99	-1461	-2420	677	562	- 103	- 227
L_2M_2		372	8845	3962	2730	243	- 329	- 721
L_2L_4	-525	-471	- 729	-1542	- 228	- 805	432	948
L_4L_2		471	- 729	- 948	- 228	- 432	805	1542
L_4M_4		-372		721		329	- 243	-3962
L_4L_6		- 99		227		103	- 562	2420
L_6L_4		- 37		81		37	-1387	1980
L_6M_6		37		- 81		- 37	1387	-1980
M_6L_6		11		15		3	2665	-1628
M_6U_5		- 11		- 15		- 3	-2665	1628
U_5M_6		- 10		- 96		- 30	-2232	139
U_5M_4		16		- 227		- 85	1452	333
U_5U_3		- 6		323		115	780	- 472
U_3U_5		- 3		661		269	407	- 4
U_3M_4		23		1011		402	264	1676
U_3M_2		- 23	-2347	-1676	- 728	- 264	- 402	-1011
U_3U_1		3	-1464	4	- 455	- 407	- 269	- 661
U_1U_3		6	-1464	472	- 455	- 780	- 115	- 323
U_1M_2		- 16	-2347	- 333	- 728	-1452	85	227

(Continued on following page)

TABLE 6 (Continued)

Moment	Applied Loads FEM	Applied Loads Balanced Moments	Δ_1 = 1 in. FEM	Δ_1 = 1 in. Balanced Moments	Δ_2 = 1 in. FEM	Δ_2 = 1 in. Balanced Moments	Δ_3=1 in. Balanced Moments	Δ_4=1 in. Balanced Moments
U_1M_0		10	-2347	- 139	2912	2232	30	96
M_0U_1		11	-2347	-1628	2912	2665	3	15
M_0L_0		- 11	2548	1628	-4246	-2665	- 3	- 15
M_2U_1		- 45	-2347	-2016	- 728	-1069	112	281
M_2L_2		94	8845	4706	2730	1543	17	57
M_2U_3		- 49	-2347	-2690	- 728	- 474	- 129	- 338
M_4U_3		49		338		129	474	2690
M_4L_4		- 94		- 57		- 17	-1543	-4706
M_4U_5		45		- 281		- 112	1069	2016

TABLE 7

Forces in the Ties in Kips

Tie	Applied Loads	$\Delta_1 = 1"$	$\Delta_2 = 1"$
1	-29.66	206.90	-12.84
2	18.86	- 12.91	98.77
3	18.86	- 1.48	- 1.26
4	-29.66	- 1.25	- 1.70

TABLE 8

Deflection at L_2 and L_4

Member	e(in.)	s	s.e(in.)
L_0L_2	.0069	1.613	.0111
1/2 L_2L_4	.0094	1.600	.0150
L_0M_0	-.0038	- .600	.0023
M_0U_1	-.0073	01.000	.0073
U_1U_3	-.0273	01.600	.0436
U_1M_2	.0114	1.000	.0114
M_2U_3	.0014	0	0
L_2M_2	.0025	1.200	.0030
tie 1	-.1319	01.709	.2255
tie 2	.1739	1.613	.2806
			$\Sigma = .5998$

Deflection = 0.60 in.

% due to bending = 85

M - Moment at the end of a member; positive when the joint tends to rotate the member clockwise.

FEM - Fixed end moment.

E - Modulus of elasticity.

1 - Length of a member.

α, β, γ - Rotations of portions of a structure.

I - Moment of inertia of a member.

K - $\frac{I}{1}$

R - A ratio giving the magnitude of a tie distortion.

e - Change in length of a member; positive when it is an elongation.

s - Force due to a dummy load.

Paper 1097 ST 6

Journal of the
STRUCTURAL DIVISION
Proceedings of the American Society of Civil Engineers

"INFLUENCE LINES FOR CIRCULAR RING REDUNDANTS"

Henry M. Lummis III,[1] J.M. ASCE
(Proc. Paper 1097)

SYNOPSIS

Circular ring design is required on many engineering design problems such as pipe lines, tanks, aircraft, submarines and wind tunnels. The circular ring is an indeterminate structure which requires the use of indeterminate structural analysis for its design. By using the influence lines for the redundants presented with this paper, the circular ring can be analyzed as a statically determinate structure.

INTRODUCTION

The circular ring lends itself readily to the determination of influence lines for its redundants, especially when the redundants are placed at the center of the ring (neutral point). When these neutral point reactions are known the ring can be analyzed by simple statics. Formulas have been derived for circular ring analysis for many different cases of loading.[2] By combining various cases practically any problem can be solved. However, as is the case with any solution by formulas, signs must be carefully watched especially when various cases are combined. By knowing the redundants and analyzing the ring by statics, it is possible to see exactly how the forces act on the particular section of the ring under consideration.

Basic Assumptions

The development of the influence lines and curves presented in this paper are based on the same assumptions as given by Raymond J. Roark;[3] i.e.

Note: Discussion open until April 1, 1957. Paper 1097 is part of the copyrighted Journal of the Structural Division of the American Society of Civil Engineers, Vol. 82, No. ST 6, November, 1956.

1. Design Engr., Union Carbide Nuclear Co., Paducah, Ky.
2. "Formulas for Stress and Strain," by Raymond J. Roark, McGraw Hill Book Co., Inc., New York, N. Y., 1943, pp. 151-160.
3. Ibid, Pg. 160

(1) the ring is of uniform cross-section; (2) it is of such large radius in comparison with its radial thickness that the deflection theory for straight beams is applicable; (3) it is nowhere stressed beyond the elastic limit; (4) it is not so severely deformed as to lose its essentially circular shape; (5) in the case of pipes acting as beams between widely spaced supports, the distribution of shear stress across the section of the pipe is in accordance with the usual shear theory $s = \frac{VQ}{Ib}$, and the direction of the resultant shear at any point on the ring is tangential.

Procedure and Development of Influence Line Ordinates

Influence lines for the neutral point redundants will be obtained for vertical loads, horizontal loads, and moments applied to the ring. This will be accomplished by utilizing the principle attributed to Muller Breslau and explained by Linton E. Grinter;[4] that is, when a unit deflection is imposed on a structure at the redundant and in the direction of the redundant the deflection at any point on the structure is the influence ordinate for the redundant. It follows that the curve of the deflected structure is actually the influence line for the redundant. Since the redundants are placed at the neutral point, movement in the direction of any one redundant will not cause movement in the direction of the other two.

Cut the ring at the top, anchor one side and place the redundants (M_o, V_o, H_o) at the neutral point. (See Figure 1.)

Nomenclature

$I_{V_o M}$ = Influence ordinate for V_o due to applied moment. (Other ordinates noted similarly.)
E = Modulus of elasticity of ring material.
I = Moment of inertia of ring section.
R = Radius of ring.
θ = angle to the point on the ring where Δx, Δy and Δb are desired.
a = angle to any arbitrary point on the ring.
M_a = bending moment at a due to M_o, V_o or H_o.
db = angle change along length ds = R da.
Δx = total horizontal movement at θ.
Δy = total vertical movement at θ.
Δb = total angular movement at θ.

Sign Convention

Positive moment causes tension on the inside and compression on the outside.
Clockwise rotation is positive.
Movement upward is positive.
Movement to the right is positive.

---

4. "Theory of Modern Steel Structures," by Linton E. Grinter, The Macmillan Company, New York, N. Y., 1949, pp. 87, 88 and 253.

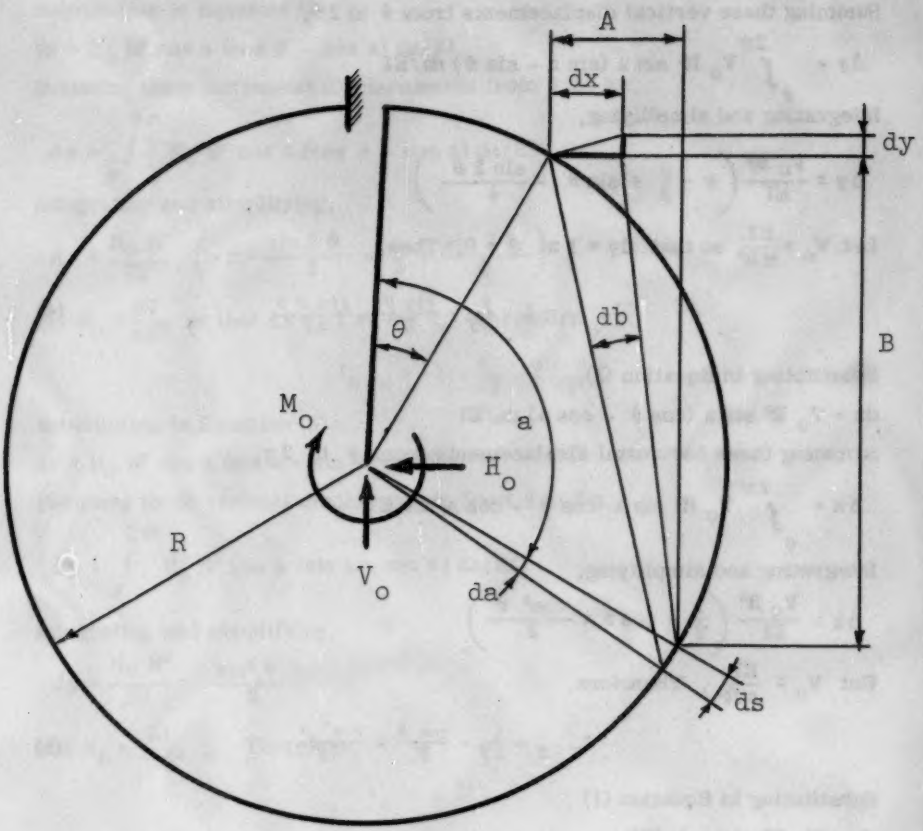

FIGURE 1

By simple trigonometry: (See Figure 1.)
$A = R(\sin a - \sin \theta)$
$B = R(\cos \theta - \cos a)$
By beam flexure theory:

$$db = M_a\, ds/EI = M_a\, R\, da/EI \qquad (1)$$

but

$$dx = B\, db = M_a\, R^2(\cos \theta - \cos a)\, da/EI \qquad (2)$$

$$dy = A\, db = M_a\, R^2(\sin a - \sin \theta)\, da/EI \qquad (3)$$

Derivation for $I_{V_0\, M}$, $I_{V_0\, H}$ and $I_{V_0\, V}$

Place only V_0 on the ring, then
$M_a = V_0\, R \sin a$
Substituting in Equation (3),
$dy = V_0\, R^3 \sin a\, (\sin a - \sin \theta)\, da/EI$

Summing these vertical displacements from θ to 2π,

$$\Delta y = \int_{\theta}^{2\pi} V_o R^3 \sin a (\sin a - \sin \theta)\, da/EI$$

Integrating and simplifying,

$$\Delta y = \frac{V_o R^3}{EI}\left(\pi - \frac{\theta}{2} + \sin\theta - \frac{\sin 2\theta}{4}\right)$$

Let $V_o = \frac{EI}{\pi R^3}$ so that $\Delta y = 1$ at $\theta = 0$, Then,

$$I_{V_o V} = 1 - \frac{\theta}{2\pi} + \frac{\sin\theta}{\pi} - \frac{\sin 2\theta}{4\pi} \qquad (4)$$

Substituting in Equation (2),

$dx = V_o R^3 \sin a (\cos\theta - \cos a)\, da/EI$

Summing these horizontal displacements from θ to 2π,

$$\Delta x = \int_{\theta}^{2\pi} V_o R^3 \sin a (\cos\theta - \cos a)\, da/EI$$

Integrating and simplifying,

$$\Delta x = \frac{V_o R^3}{EI}\left(\frac{1}{2} - \cos\theta + \frac{\cos^2\theta}{2}\right)$$

But $V_o = \frac{EI}{\pi R^3}$, Therefore,

$$I_{V_o H} = \frac{1}{2\pi} - \frac{\cos\theta}{\pi} + \frac{\cos^2\theta}{2\pi} \qquad (5)$$

Substituting in Equation (1)

$db = V_o R^2 \sin a\, da/EI$

Summing these rotational displacements from θ to 2π,

$$\Delta b = \int_{\theta}^{2\pi} V_o R^2 \sin a\, da/EI$$

Integrating and simplifying,

$$\Delta b = \frac{V_o R^2}{EI}(\cos\theta - 1)$$

But $V_o = \frac{EI}{\pi R^3}$, Therefore,

$$RI_{V_o M} = \frac{\cos\theta}{\pi} - \frac{1}{\pi} \qquad (6)$$

Derivation for $I_{H_o M}$, $I_{H_o H}$ and $I_{H_o V}$

Place only H_o on the ring, Then,

$M_a = H_o R \cos a$

Substituting in Equation (2)

$dx = H_o R^3 \cos a (\cos \theta - \cos a)\, da/EI$

Summing these horizontal displacements from θ to 2π,

$$\Delta x = \int_{\theta}^{2\pi} H_o R^3 \cos a (\cos \theta - \cos a)\, da/EI$$

Integrating and simplifying,

$$\Delta x = \frac{H_o R^3}{EI} \left(-\pi - \frac{\sin 2\theta}{2} + \frac{\theta}{2} + \frac{\sin 2\theta}{4} \right)$$

Set $H_o = \frac{EI}{\pi R^3}$ so that $\Delta x = -1$ at $\theta = 0$, Therefore,

$$I_{H_o H} = -1 + \frac{\theta}{2\pi} - \frac{\sin 2\theta}{4\pi} \qquad (7)$$

Substituting in Equation (3)

$dy = H_o R^3 \cos a (\sin a - \sin \theta)\, da/EI$

Summing these vertical displacements from θ to 2π,

$$\Delta y = \int_{\theta}^{2\pi} H_o R^3 \cos a (\sin a - \sin \theta)\, da/EI$$

Integrating and simplifying,

$$\Delta y = \frac{H_o R^3}{EI} \quad \frac{\sin^2 \theta}{2}$$

But $H_o = \frac{EI}{\pi R^3}$, Therefore,

$$I_{H_o V} = \frac{\sin^2 \theta}{2\pi} \qquad (8)$$

Substituting in Equation (1)

$db = H_o R^2 \cos a\, da/EI$

Summing these rotational displacements from θ to 2π,

$$\Delta b = \int_{\theta}^{2\pi} H_o R^2 \cos a\, da/EI$$

Integrating and simplifying,

$\Delta b = -H_o R^2 \sin \theta/EI$

But $H_o = \frac{EI}{\pi R^3}$, Therefore,

$$RI_{H_o M} = -\frac{\sin \theta}{\pi} \qquad (9)$$

Derivation for $I_{M_o M}$, $I_{M_o V}$, and $I_{M_o H}$

Place only M_o on the ring, Then

$M_a = M_o$

Substituting in Equation (1)

$db = M_o R\, da$

Summing these rotational displacements from θ to 2π,

$$\Delta b = \int_{\theta}^{2\pi} M_o R\, da/EI$$

Integrating and simplifying,

$$\Delta b = M_o R (2\pi - \theta)/EI$$

Set $M_o = \frac{EI}{2\pi R}$ so that $\Delta b = 1$ at $\theta = 0$, Then

$$I_{M_o M} = 1 - \frac{\theta}{2\pi} \tag{10}$$

Substituting in Equation (2)

$dx = M_o R^2 (\cos\theta - \cos a)\, da/EI$

Summing these horizontal displacements from θ to 2π,

$$\Delta x = \int_{\theta}^{2\pi} M_o R^2 (\cos\theta - \cos a)\, da/EI$$

Integrating and simplifying,

$$\Delta x = M_o R^2 (2\pi \cos\theta - \theta\cos\theta + \sin\theta)/EI$$

But $M_o = \frac{EI}{2\pi R}$, Therefore,

$$I_{M_o H}/R = \cos\theta - \frac{\theta\cos\theta}{2\pi} + \frac{\sin\theta}{2\pi} \tag{11}$$

Substituting in Equation (3)

$dy = M_o R^2 (\sin a - \sin\theta)\, da/EI$

Summing these vertical displacements from θ to 2π,

$$\Delta y = \int_{\theta}^{2\pi} M_o R^2 (\sin a - \sin\theta)\, da$$

Integrating and simplifying,

$$\Delta y = M_o R^2 (-1 - 2\pi\sin\theta + \cos\theta + \theta\sin\theta)/EI$$

But since $M_o = \frac{EI}{2\pi R}$, Then,

$$I_{M_o V}/R = -\frac{1}{2\pi} - \sin\theta + \frac{\cos\theta}{2\pi} + \frac{\theta\sin\theta}{2\pi} \tag{12}$$

Summary of Formulas for Influence Lines
For V_o

$$I_{V_o V} = 1 - \frac{\theta}{2\pi} + \frac{\sin\theta}{\pi} - \frac{\sin 2\theta}{4\pi} \quad (4)$$

$$I_{V_o H} = \frac{1}{2\pi} - \frac{\cos\theta}{\pi} + \frac{\cos^2\theta}{2\pi} \quad (5)$$

$$RI_{V_o M} = \frac{\cos\theta}{\pi} - \frac{1}{\pi} \quad (6)$$

For H_o

$$I_{H_o H} = -1 + \frac{\theta}{2\pi} - \frac{\sin 2\theta}{4\pi} \quad (7)$$

$$I_{H_o V} = \frac{\sin^2\theta}{2\pi} \quad (8)$$

$$RI_{H_o M} = -\frac{\sin\theta}{\pi} - \quad (9)$$

For M_o

$$I_{M_o M} = 1 - \frac{\theta}{2\pi} \quad (10)$$

$$I_{M_o H}/R = \cos\theta - \frac{\theta\cos\theta}{2\pi} + \frac{\sin\theta}{2\pi} \quad (11)$$

$$I_{M_o V}/R = -\frac{1}{2\pi} - \sin\theta + \frac{\cos\theta}{2\pi} + \frac{\theta\cos\theta}{2\pi} \quad (12)$$

Utilizing equations (4) through (12), influence line ordinates are computed for every 15° from 0 to 360° and are tabulated in Table 1. These values are then used to plot the influence lines for redundants as shown in Figures 2, 3 and 4.

Extension for Rings with Tangential Shear

In order to extend the usefulness of the influence lines to rings which are acted upon by tangential shear, equations will be derived for moment, shear and thrust at any point on the ring caused by various types of tangential shear. This type of loading on rings is quite common as is the case when a long circular cylinder acting as a beam is supported by rings.

Development of Formulas

The nomenclature for the subsequent derivations will vary somewhat from that used in the first portion of the paper. It will be explained as the development of equations proceeds.

TABLE 1

θ	$I_{V_o H}$	$I_{V_o V}$	$RI_{V_o M}$	$I_{H_o H}$	$I_{H_o V}$	$RI_{H_o M}$	$I_{M_o H}/R$	$I_{M_o V}/R$	$I_{M_o M}$
0°	0	1.0000	0	-1.0000	0	0	1.0000	0	1.0000
15°	.0002	1.0009	- .0109	- .9981	.0107	- .0824	.9667	- .2535	.9583
30°	.0029	1.0069	- .0426	- .9856	.0398	- .1592	.8734	- .4797	.9167
45°	.0137	1.0205	- .0932	- .9546	.0796	- .2251	.7313	- .6653	.8750
60°	.0398	1.0401	- .1592	- .9023	.1194	- .2757	.5545	- .8013	.8333
75°	.0874	1.0593	- .2359	- .8315	.1485	- .3075	.3586	- .8827	.7917
90°	.1592	1.0683	- .3183	- .7500	.1592	- .3183	.1592	- .9092	.7500
105°	.2522	1.0556	- .4007	- .6686	.1485	- .3075	- .0296	- .8845	.7083
120°	.3581	1.0113	- .4775	- .5978	.1194	- .2757	- .1955	- .8161	.6667
135°	.4638	.9297	- .5434	- .5454	.0796	- .2251	- .3294	- .7136	.6250
150°	.5542	.8114	- .5940	- .5144	.0398	- .1592	- .4256	- .5887	.5833
165°	.6151	.6638	- .6258	- .5019	.0107	- .0824	- .4820	- .4531	.5417
180°	.6366	.5000	- .6366	- .5000	0	0	- .5000	- .3183	.5000
195°	.6151	.3362	- .6258	- .4981	.0107	.0824	- .4839	- .1943	.4583
210°	.5542	.1886	- .5940	- .4856	.0398	.1592	- .4404	- .0887	.4167
225°	.4638	.0703	- .5434	- .4546	.0796	.2251	- .3777	- .0065	.3750
240°	.3581	- .0113	- .4775	- .4022	.1194	.2757	- .3045	.0499	.3333
255°	.2522	- .0556	- .4007	- .3315	.1485	.3075	- .2292	.0814	.2917
270°	.1592	- .0683	- .3183	- .2500	.1592	.3183	- .1592	.0908	.2500
285°	.0874	- .0593	- .2359	- .1685	.1485	.3075	- .0998	.0833	.2083
300°	.0398	- .0401	- .1592	- .0978	.1194	.2757	- .0545	.0648	.1667
315°	.0137	- .0205	- .0932	- .0454	.0796	.2251	- .0242	.0418	.1250
330°	.0029	- .0069	- .0426	- .0144	.0398	.1592	- .0074	.0204	.0833
345°	.0002	- .0009	- .0109	- .0019	.0107	.0824	- .0010	.0054	.0417
360°	0	0	0	0	0	0	0	0	0

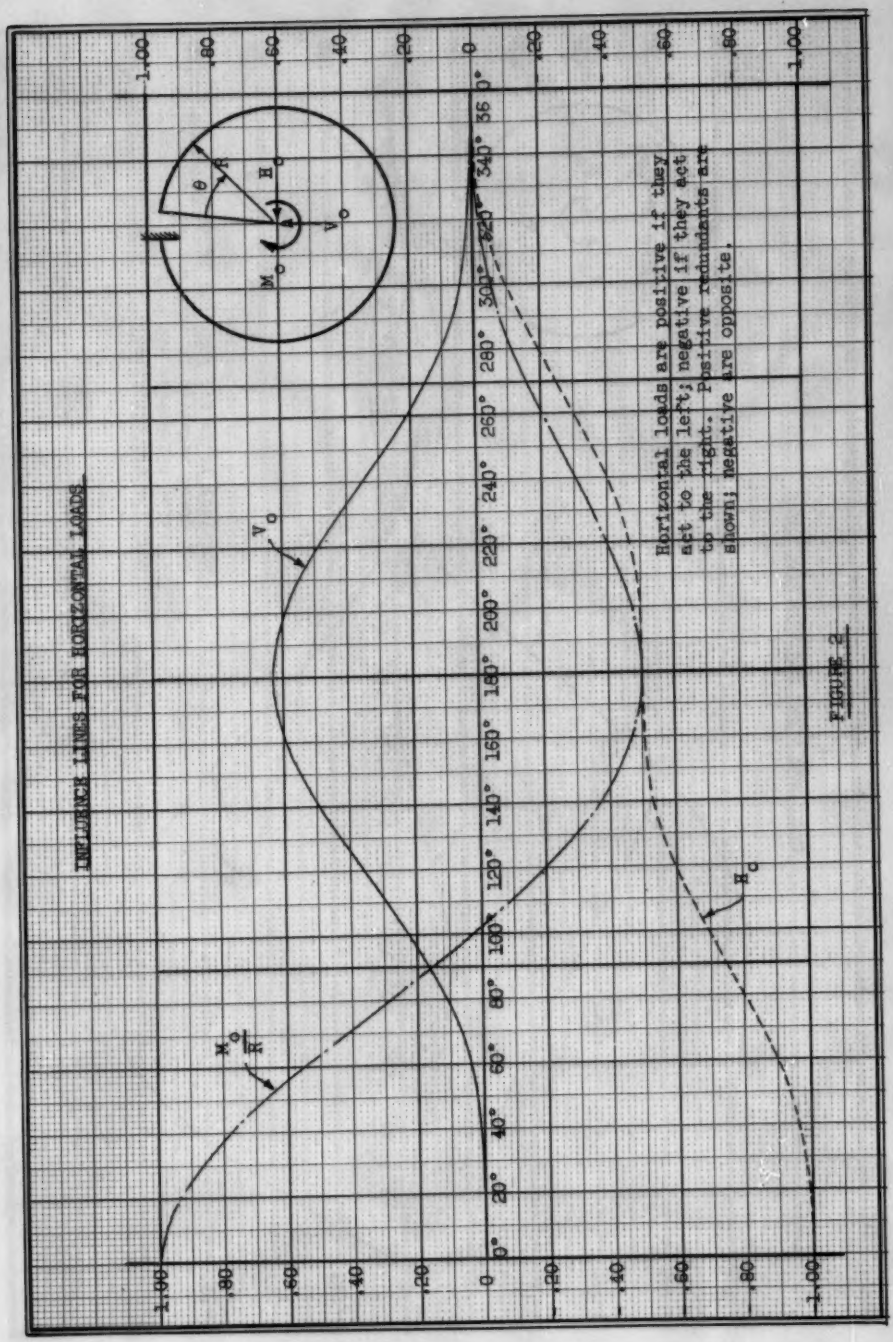
INFLUENCE LINES FOR HORIZONTAL LOADS
Horizontal loads are positive if they act to the left; negative if they act to the right. Positive redundants are shown; negative are opposite.
V_o
H_o
M_o
$\frac{M_o}{R}$
θ
R
0° 20° 40° 60° 80° 100° 120° 140° 160° 180° 200° 220° 240° 260° 280° 300° 320° 340° 360°
1.00 .80 .60 .40 .20 0 .20 .40 .60 .80 1.00

FIGURE 2

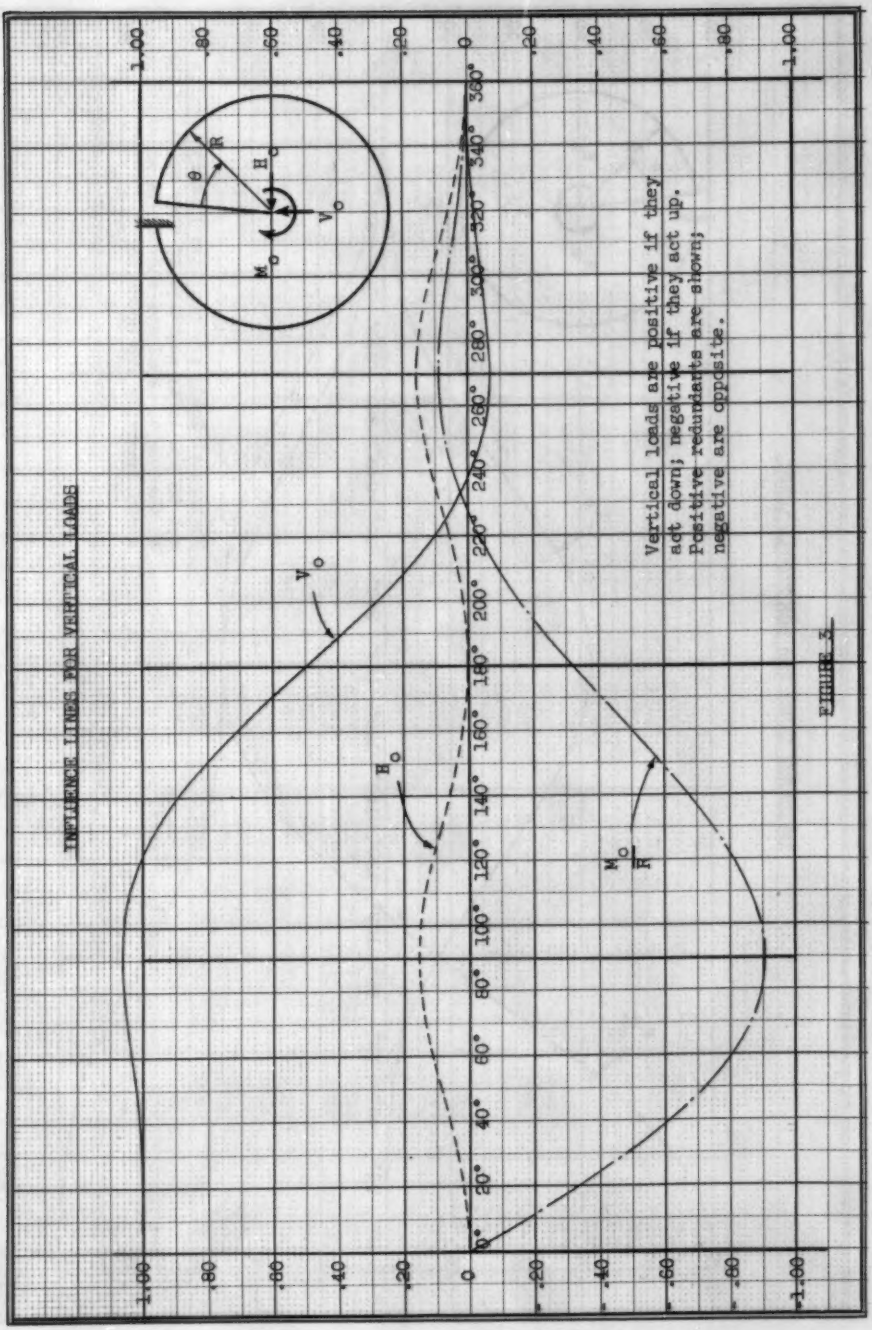
INFLUENCE LINES FOR VERTICAL LOADS
Vertical loads are positive if they act down; negative if they act up. Positive redundants are shown; negative are opposite.
V_o
H_o
$\frac{M_o}{R}$
θ
R
H_o
V_o
M_o
0° 20° 40° 60° 80° 100° 120° 140° 160° 180° 200° 220° 240° 260° 280° 300° 320° 340° 360°
1.00 .80 .60 .40 .20 0 .20 .40 .60 .80 1.00

FIGURE 3

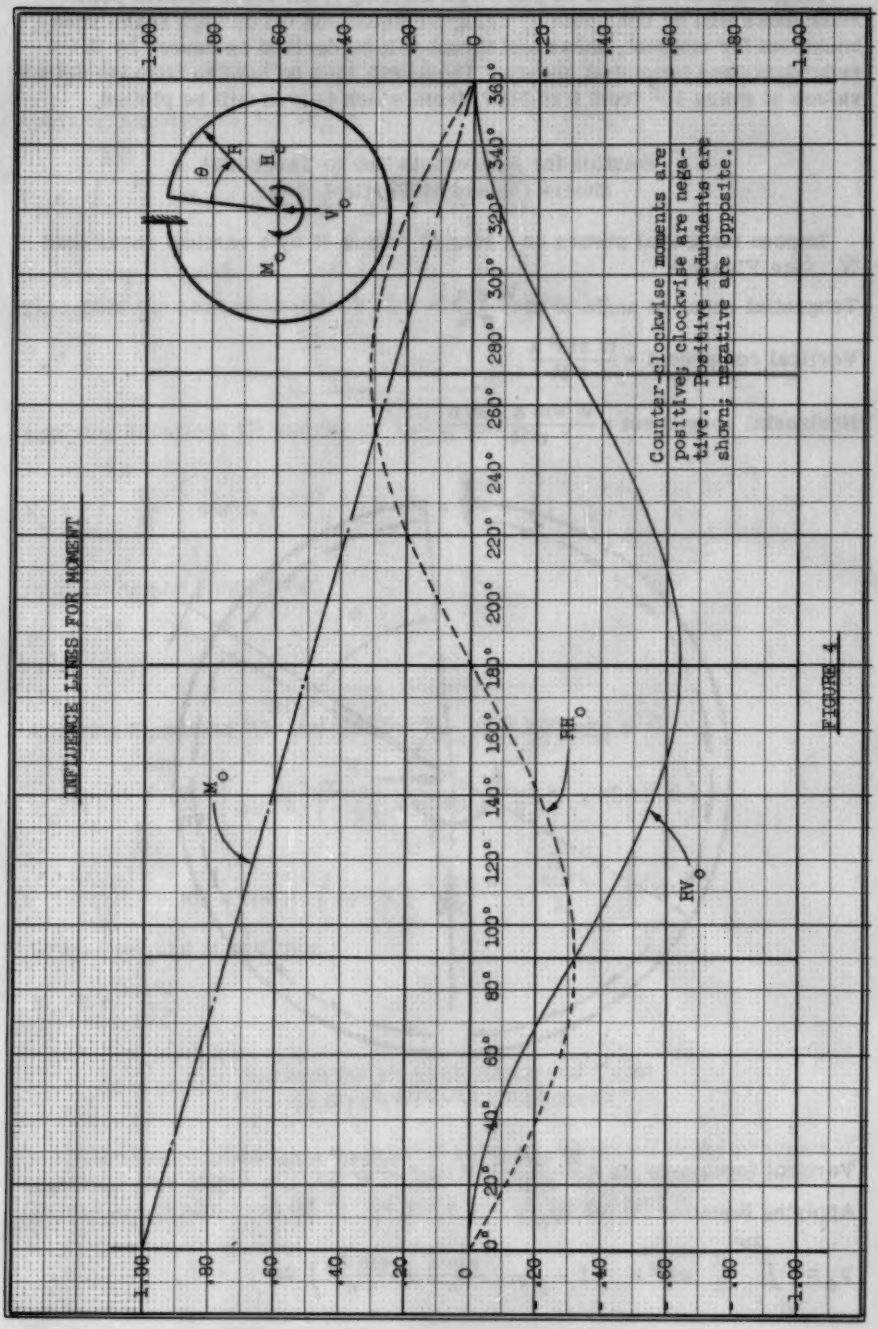
INFLUENCE LINES FOR MOMENT
Counter-clockwise moments are positive; clockwise are negative. Positive redundants are shown; negative are opposite.
M_o
HH_o
HV_o
θ
H
V
M
1.00
.80
.60
.40
.20
0
0°
20°
40°
60°
80°
100°
120°
140°
160°
180°
200°
220°
240°
260°
280°
300°
320°
340°
360°

FIGURE 4

Tangential shears will be placed on the ring from which neutral point redundants will be computed by using the equations (4) through (12). Then equations for moment, shear and thrust will be derived as caused by the redundants and tangential shears. These will then be used to compute actual values at every 15^{o} from 0 to 360^{o}, from which curves will be plotted.

Solution for Redundants Due to Tangential Shears Caused by Vertical Shear

Impose tangential shears on a ring of radius R by a vertical shear load W. (See Figure 5.)

Tangential shear at angle a is $\frac{W \sin a}{\pi R}$

Vertical component = $\frac{W \sin^2 a}{\pi R}$

Horizontal component = $\frac{W \sin a \cos a}{\pi R}$

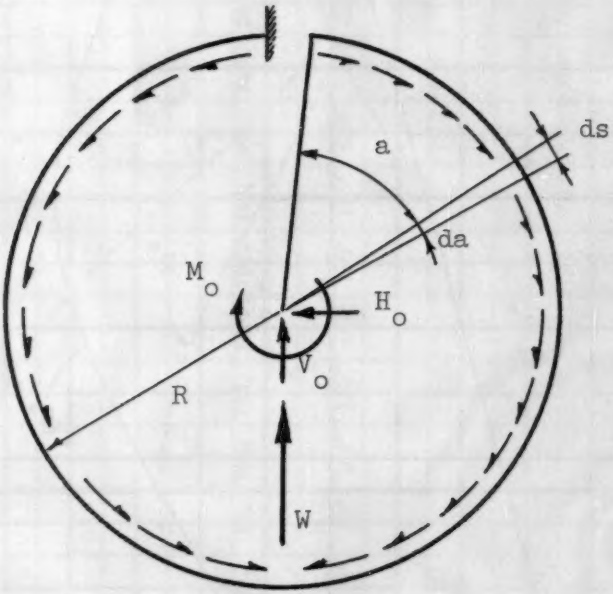

FIGURE 5

Vertical force over ds = $\frac{W \sin^2 a}{\pi R}$ R da = $\frac{W \sin^2 a \, da}{\pi}$

Applying Equation (4) for $I_{V_o V}$

$$V_o = \int_0^{2\pi} \frac{W}{\pi} \sin^2 a \left(1 - \frac{a}{2\pi} + \frac{\sin a}{\pi} - \frac{\sin 2a}{4\pi}\right) da$$

Integrating and simplifying,

V_o (due to vertical components) = $\frac{W}{2}$

Horizontal force over ds = $\frac{W \sin a \cos a}{\pi}$ da

Applying Equation (5) for $I_{V_o} H$

$$V_o = \int_0^{2\pi} \frac{W}{\pi} \sin a \cos a \left(\frac{1}{2\pi} - \frac{\cos a}{\pi} + \frac{\cos^2 a}{2\pi} \right) da$$

Integrating: $V_o = 0$

Therefore the total redundant V_o for shears shown is:

$V_o = \frac{W}{2}$

Applying Equations (7) and (8) for $I_{H_o} H$ and $I_{H_o} V$

$$H_o = \int_0^{2\pi} \frac{W}{\pi} \left[\sin^2 a \left(\frac{\sin^2 a}{2\pi} \right) + \sin a \cos a \left(1 - \frac{a}{2\pi} + \frac{\sin 2a}{4\pi} \right) \right] da$$

Integrating and simplifying,

$H_o = \frac{3W}{4\pi}$

Applying Equations (11) and (12) for $I_{M_o} H/R$ and $I_{M_o} V/R$

$$M_o/R = \int_0^{2\pi} \frac{W}{\pi} \left[\sin^2 a \left(-\frac{1}{2\pi} - \sin a + \frac{\cos a}{2\pi} + \frac{a \sin a}{2\pi} \right) - \sin a \cos a \left(\cos a - \frac{a \cos a}{2\pi} + \frac{\sin a}{2} \right) \right] da$$

Integrating and simplifying,

$M_o/R = -\frac{3W}{2\pi}$

Solution for Moment, Shear and Trust on Ring Due to Vertical Shear

Place the redundants at the neutral point as calculated in the previous section. (See Figure 6.) Let θ by the angle to the point where the ring forces are desired and let "a" be any angle between 0 and θ .

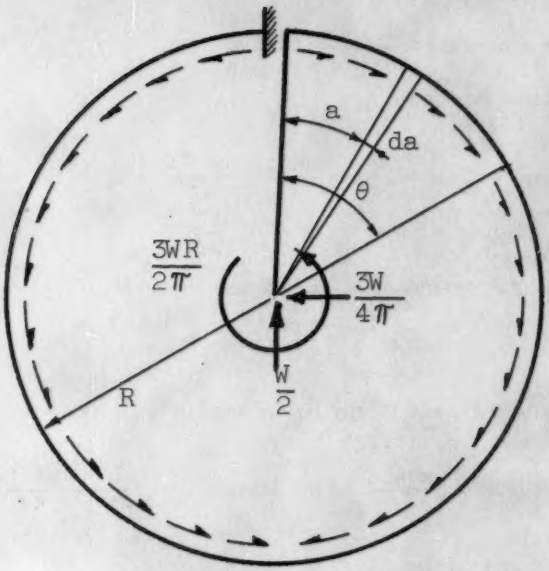

FIGURE 6

Moment at θ is:

$$M_\theta = \int_0^\theta W\left[-\frac{\sin^2 a}{\pi} R\,(\sin\theta - \sin a) + \frac{\sin a \cos a}{\pi} R\,(\cos a - \cos\theta)\right] da$$
$$+ W\left(\frac{R \sin\theta}{2} + \frac{3R\cos\theta}{4\pi} - \frac{3R}{2\pi}\right)$$

Integrating and simplifying,

$$\frac{M_\theta}{WR} = \frac{1}{\pi}\left(-\frac{1}{2} - \frac{\cos\theta}{4} - \frac{\theta \sin\theta}{2} + \frac{\pi \sin\theta}{2}\right) \qquad (13)$$

Shear at θ is:

$$V_\theta = W \int_0^\theta \frac{\sin a}{\pi} \sin(\theta - a)\, da + \frac{\cos\theta}{2} - \frac{3\sin\theta}{4\pi}$$

Integrating and simplifying,

$$\frac{V_\theta}{W} = \frac{1}{\pi}\left(-\frac{\sin\theta}{4} - \frac{\theta\cos\theta}{2} + \frac{\pi\cos\theta}{2}\right) \qquad (14)$$

Thrust at θ is:

$$T_\theta = W \int_0^\theta -\frac{\sin a}{\pi} \cos(\theta - a)\, da + \frac{\sin\theta}{2} + \frac{3\cos\theta}{4\pi}$$

Integrating and simplifying,

$$\frac{T_\theta}{W} = \frac{1}{\pi}\left(-\frac{\theta \sin\theta}{2} + \frac{\pi \sin\theta}{2} + \frac{3\cos\theta}{4}\right) \quad (15)$$

Solution for Redundants Due to Tangential Shears Caused by Torsion

Impose tangential shears on a ring of radius R by torsion M. (See Figure 7.)

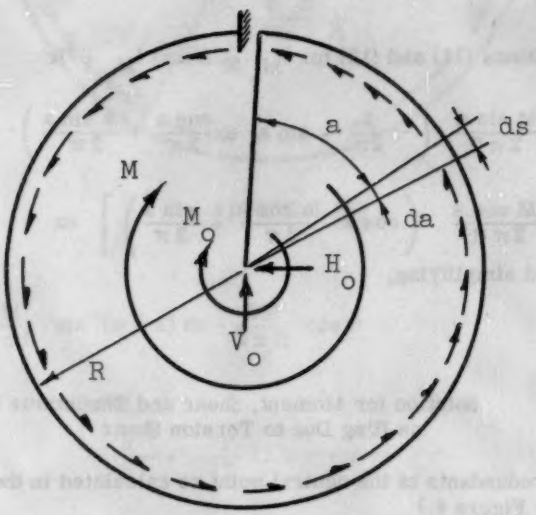

FIGURE 7

Unit shear is: $\frac{M}{2\pi R^2}$

Force on ds = $\frac{M\, ds}{2\pi R^2} = \frac{M\, da}{2\pi R}$

Vertical component is: $\frac{M \sin a\, da}{2\pi R}$

Horizontal component is: $\frac{M \cos a\, da}{2\pi R}$

Applying Equations (4) and (5) for $I_{V_o V}$ and $I_{V_o H}$

$$V_o = \int_0^{2\pi} \left[-\frac{M \sin a}{2\pi R} \left(1 - \frac{a}{2\pi} + \frac{\sin a}{\pi} - \frac{\sin 2a}{4\pi} \right) + \frac{M \cos a}{2\pi R} \left(\frac{1}{2\pi} - \frac{\cos a}{\pi} + \frac{\cos^2 a}{2\pi} \right) \right] da$$

Integrating and simplifying,

$$V_o = \frac{3M}{2\pi R}$$

Applying Equations (7) and (8) for $I_{H_o H}$ and $I_{H_o V}$

$$H_o = \int_0^{2\pi} \left[-\frac{M \sin a}{2\pi R} \left(\frac{\sin^2 a}{2\pi} \right) + \frac{M \cos a}{2\pi R} \left(-1 + \frac{a}{2\pi} - \frac{\sin 2a}{4\pi} \right) \right] da$$

Integrating and simplifying,

$$H_o = 0$$

Applying Equations (11) and (12) for $I_{M_o H}/R$ and $I_{M_o V}/R$

$$\frac{M_o}{R} = \int_0^{2\pi} \left[-\frac{M \sin a}{2\pi R} \left(-\frac{1}{2\pi} - \sin a + \frac{\cos a}{2\pi} + \frac{a \sin a}{2\pi} \right) + \frac{M \cos a}{2\pi R} \left(\cos a - \frac{a \cos a}{2\pi} + \frac{\sin a}{2\pi} \right) \right] da$$

Integrating and simplifying,

$$M_o = \frac{M}{2}$$

Solution for Moment, Shear and Thrust on Ring Due to Torsion Shear

Place the redundants at the neutral point as calculated in the previous section. (See Figure 8.)

Moment at θ is:

$$M_\theta = \int_0^{\theta} \left[\frac{M \sin a}{2\pi R} R(\sin\theta - \sin a) - \frac{M \cos a}{2\pi R} R(\cos a - \cos\theta) \right] da - \frac{3M}{2\pi R} R \sin\theta + \frac{M}{2}$$

Integrating and simplifying,

$$\frac{M_\theta}{M} = -\frac{\sin\theta}{\pi} - \frac{\theta}{2\pi} + \frac{1}{2} \qquad (16)$$

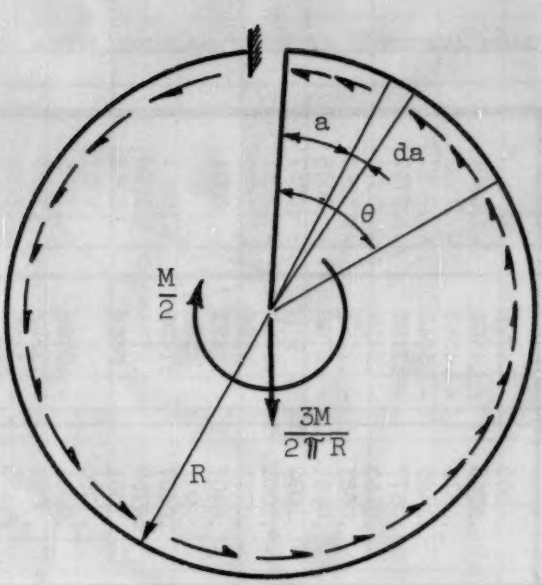

FIGURE 8

Shear at θ :

$$V_\theta = \int_0^\theta -\frac{M}{2\pi R} \sin(\theta - a)\, da - \frac{3M}{2\pi R} \cos\theta$$

Integrating and simplifying,

$$\frac{V_\theta R}{M} = -\frac{1}{2\pi}(1 + 2\cos\theta) \qquad (17)$$

Thrust at θ :

$$T_\theta = \int_0^\theta \frac{M}{2\pi R} \cos(\theta - a)\, da - \frac{3M}{2\pi R} \sin\theta$$

Integrating and simplifying,

$$\frac{T_\theta R}{M} = -\frac{\sin\theta}{\pi} \qquad (18)$$

Using equations (13) through (18), values for moment, shear and thrust at every 15° around the ring are computed and are tabulated in Table 2. From these values curves are plotted as shown in Figures (9) and (10).

TABLE 2

θ	VERTICAL SHEAR			TORSIONAL SHEAR		
	$\frac{M_\theta}{WR}$	$\frac{V_\theta}{W}$	$\frac{T_\theta}{W}$	$\frac{M_\theta}{M}$	$\frac{V_\theta R}{M}$	$\frac{T_\theta R}{M}$
0°	- .2387	.5000	.2387	.5000	- .4775	0
15°	- .1174	.4221	.3492	.3760	- .4666	- .0824
30°	- .0197	.3211	.4151	.2575	- .4348	- .1592
45°	.0498	.2089	.4340	.1499	- .3842	- .2251
60°	.0897	.0978	.4080	.0577	- .3183	- .2757
75°	.1020	- .0014	.3435	- .0158	- .2415	- .3075
90°	.0909	- .0796	.2500	- .0683	- .1592	- .3183
105°	.0627	- .1308	.1395	- .0991	- .0768	- .3075
120°	.0250	- .1523	.0250	- .1090	0	- .2757
135°	- .0145	- .1447	- .0804	- .1001	.0659	- .2251
150°	- .0486	- .1120	- .1651	- .0758	.1165	- .1592
165°	- .0715	- .0609	- .2198	- .0407	.1483	- .0824
180°	- .0796	0	- .2387	0	.1592	0
195°	- .0715	.0608	- .2198	.0407	.1483	.0824
210°	- .0486	.1120	- .1651	.0758	.1165	.1592
225°	- .0145	.1447	- .0804	.1001	.0659	.2251
240°	.0250	.1523	.0250	.1090	0	.2757
255°	.0627	.1308	.1394	.0991	- .0768	.3075
270°	.0909	.0796	.2500	.0683	- .1592	.3183
285°	.1020	.0014	.3435	.0158	- .2415	.3075
300°	.0897	- .0978	.4080	- .0577	- .3183	.2757
315°	.0497	- .2089	.4340	- .1499	- .3842	.2251
330°	- .0197	- .3211	.4151	- .2575	- .4348	.1592
345°	- .1174	- .4221	.3492	- .3760	- .4666	.0824
360°	- .2387	- .5000	.2387	- .5000	- .4775	0

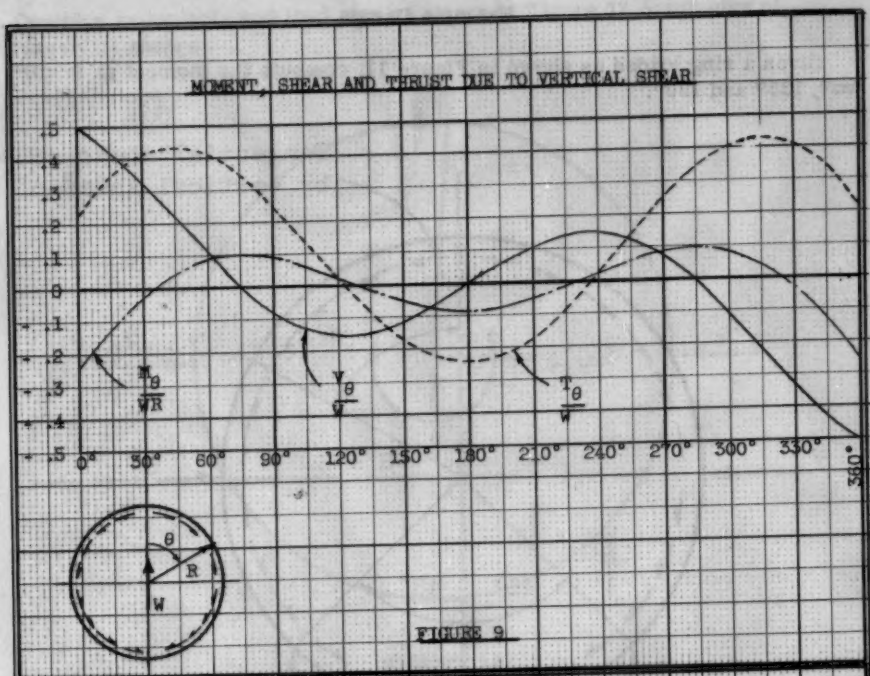

FIGURE 9

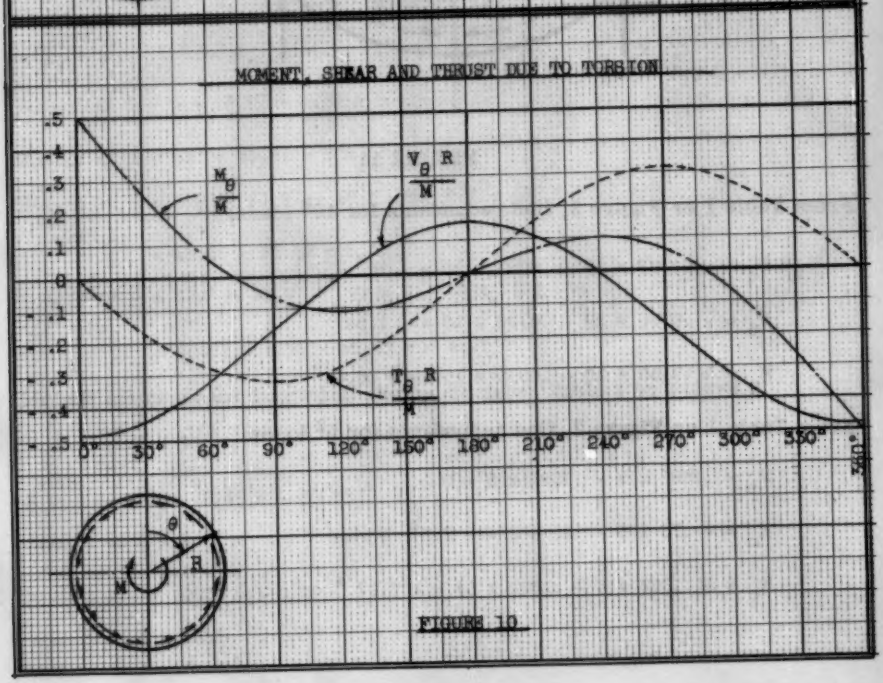

FIGURE 10

Example Design

Given a ring loaded as shown in Figure 11, compute the moment at $\theta = 0^o$, 90^o, 135^o and 180^o.

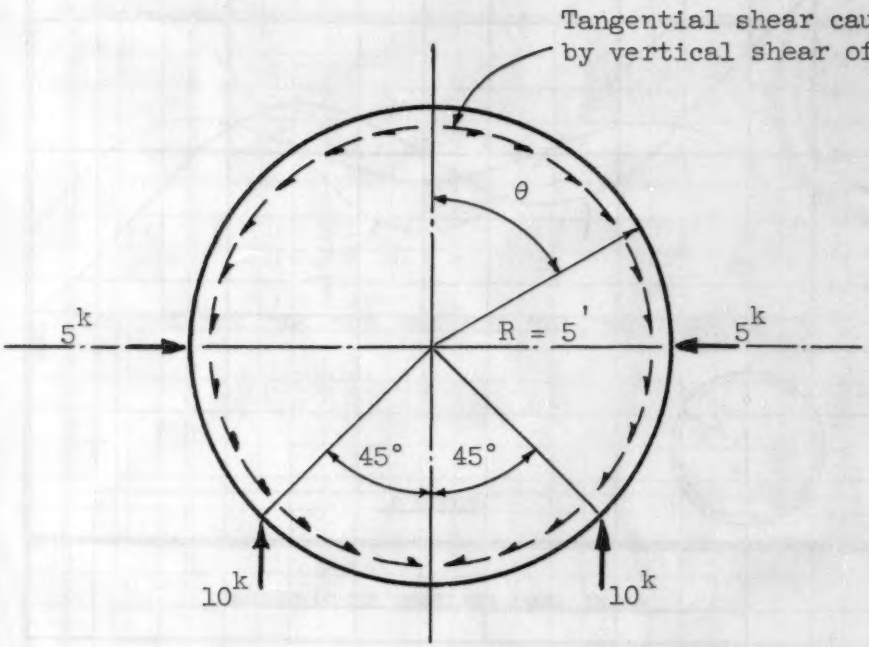

FIGURE 11

From Table 1 or Figure 3, find redundants for 10^k loads:

$$V_o = - .9297 \times 10 - .0703 \times 10 = - 10^k$$

$$H_o = - .0796 \times 10 - .0796 \times 10 = - 1.59^k$$

$$M_o = 5(.7136 \times 10 + .0065 \times 10) = + 36.0'^k$$

From Table 1 or Figure 2, find redundants for 5^k loads:

$$V_o = .1592 \times 5 - .1592 \times 5 = 0$$

$$H_o = - .75 \times 5 + .25 \times 5 = - 2.5^k$$

$$M_o = 5(.1592 \times 5 + .1592 \times 5) = + 7.97'^k$$

Combine redundants and load ring as shown in Figure 12 (exclusive of tangential shears).

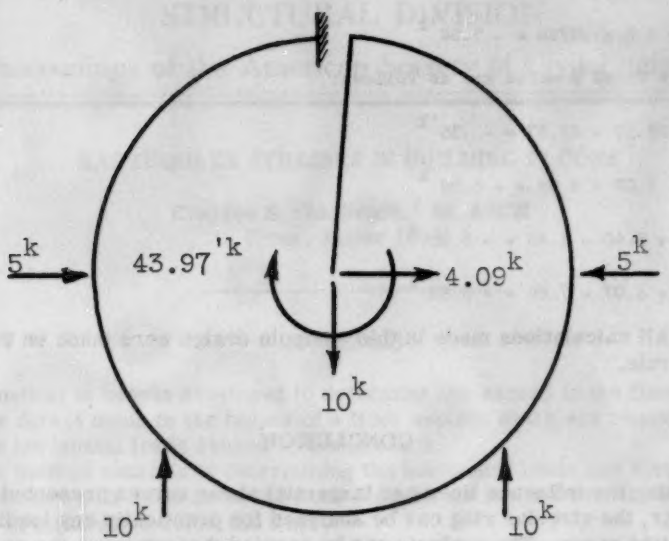

FIGURE 12

Moment at $\theta = 0 = 43.97 - 4.09 \times 5 = +23.52$ 'k

Moment at $\theta = 90° = 43.97 - 5 \times 10 = -6.03$ 'k

Moment at $\theta = 135° = 43.97 - 10 \times .707 \times 5 - .91 \times .707 \times 5$

$= 43.97 - 38.57 = 5.40$ 'k

Moment at $\theta = 180° = 43.97 - .91 \times 5 - 10 \times .707 \times 5$

$= 43.97 - 4.55 - 35.35 = +4.07$ 'k

Include moments for tangential shears by using Table 2 or Figure 9.

Moment at $\theta = 0$

$M = -20 \times 5 \times .2387 = -23.87$ 'k

Moment at $\theta = 90°$

$M = 20 \times 5 \times .0909 = +9.09$ 'k

Moment at $\theta = 135°$

$M = 20 \times 5 \times - .0145 = - 1.45$ 'k

Moment at $\theta = 180°$

$M = - 20 \times 5 \times .0796 = - 7.96$ 'k

Therefore final moments are as follows:

$M_{0°} = + 23.52 - 23.87 = - .35$ 'k

$M_{90°} = - 6.03 + 9.09 = + 3.06$ 'k

$M_{135°} = + 5.40 - 1.45 = + 3.95$ 'k

$M_{180°} = + 4.07 - 7.96 = - 3.89$ 'k

NOTE: All calculations made in this example design were made on the slide rule.

CONCLUSION

By using the influence lines and tangential shear curves presented with this paper, the circular ring can be analyzed for practically any loading which might occur. The analysis can be carried through much the same as any simple structure is analyzed. Should it be necessary to compute moment, shear or thrust for small angle increments around the ring, a simple tabular form can be set up giving the sine and cosine functions for each angle. It is hoped that the data and curves compiled in this paper will help the engineer in circular ring design.

ACKNOWLEDGMENT

The writer appreciates the incentive given him while employed in the Wind Tunnel Section of Sverdrup and Parcel, Inc. Consulting Engineers, St. Louis, Missouri. The excellent design atmosphere which exists in that office was primarily responsible for the conception of this paper.

Journal of the
STRUCTURAL DIVISION
Proceedings of the American Society of Civil Engineers

EARTHQUAKE STRESSES IN BUILDING FLOORS

Charles S. Glazbrook,[1] M. ASCE
(Proc. Paper 1098)

SYNOPSIS

A method is herein developed to determine the shears in the floor panels and the direct loads in the beams of a floor system which are required to distribute horizontal loads caused by earth shock.

The method consists of determining the horizontal loads and their points of application which come on to the floor from above and the reactions and their points of application below the floor.

The analysis is then made statically determinate by assuming that the floor beams in a bay of the building resist "overturning" moment in proportion to their distances from the center of gravity of the group of beams in the bay.

INTRODUCTION

The assumption, sometimes made, that floor systems of buildings are infinitely rigid and are capable of distributing horizontal earth shock loads without further investigation, is not always valid.

This is true in particular of multistory buildings having offset exterior walls and of buildings which are irregular in plan configuration.

Example

The following example illustrates the method.

For simplicity the panels of the floor in the example are assumed to be square and of the same size. The method may be adapted to floors having rectangular panels of various sizes.

The floor chosen for the example is assumed to have little shear

Note: Discussion open until April 1, 1957. Paper 1098 is part of the copyrighted Journal of the Structural Division of the American Society of Civil Engineers, Vol. 82, No. ST 6, November, 1956.

1. Structural Engr., Holmes & Narver, Inc., Los Angeles, Calif.

resistance making necessary the installation of a horizontal bracing system. This system is assumed to be capable of taking both tension and compression. No particular difficulty would be encountered if the system was to be designed for rods taking tension only.

In the example, computations are carried only far enough to illustrate the method and cover an earth shock moving from South to North. One moving from North to South will reverse the signs of the loads and computed forces. To completely analyze the floor, similar computations are required for a shock in the East-West direction.

The method checks itself since it will be impossible to balance out the moments, shears, and direct loads unless all computations are reasonably accurate and proper signs are given to the forces.

It will be noted that no great complications are involved when some of the floor panels are left open to accommodate elevator or duct shafts.

Figure 1 shows the plan of the floor and the elevation of one exterior wall and its bracing system above and below the floor. The figures on the plan are the assumed relative stiffnesses of the vertical bents above and below the floor. These are inversely proportional to their deflections under unit load and should be evaluated for any particular case.

Figure 2 shows the horizontal loads coming on to the floor from above plus the horizontal load increments due to the dead load of the floor. It also shows the reactions under the floor and the points of application of these loads and reactions.

In arriving at the loads a total shear of 966 kips was assumed just above the floor.

The total stiffness of the vertical bents in the North-South direction above the floor is 69. This gives a value of 14 kips for a vertical bent with a relative stiffness of unity.

At each point of application of the above horizontal loads on the floor two (2) kips were added as the assumed floor weight increment load. This gives a total shear of 1050 kips just under the floor.

The total stiffness of the vertical bents under the floor is 70, which gives a value of 15 kips to a bent having a relative stiffness of unity.

It will be noted as shown in Figure 2 that the center of gravity of the loads does not coincide with the center of gravity of the reactions. For simplicity in the example, equilibrium is established by assuming that the resulting moment is entirely resisted by the vertical bents in the North and South exterior walls. Actually the moment is taken by all vertical bents in proportion to their rigidities and distances from their center of gravity, and should be so distributed in an actual analysis. It is felt that bents with a relative stiffness of unity may be omitted in this distribution.

In practice every effort should be made to minimize eccentricity by making adjustments in the vertical braced bents above and below the floor. Since the purpose of this example is to illustrate the method only, no adjustments will be made.

Figure 3 shows the floor system, separated by bays for convenience, and the reactions as computed for each bay. From these the shears in each panel are readily obtained and may be recorded in the center of each panel as shown.

Figure 4 shows the computations for the direct loads in the beams along line (3) and is typical for such calculations for the beams in the North-South direction.

Figure 5 shows the computations for the direct loads in the beams along line (C) and is typical for such calculations for the beams in the East-West direction.

CONCLUSION

The method illustrated is considered to be a rough tool which may be useful in producing a design which may be further examined in the light of diaphragm deflections.

The method will give most accurate results for buildings in which the floor bracing system is relatively stiff as compared to the vertical bracing elements.

Where a great many such calculations are required for a given building, forms or charts for the orderly recording of the computations may be devised which will expedite the work.

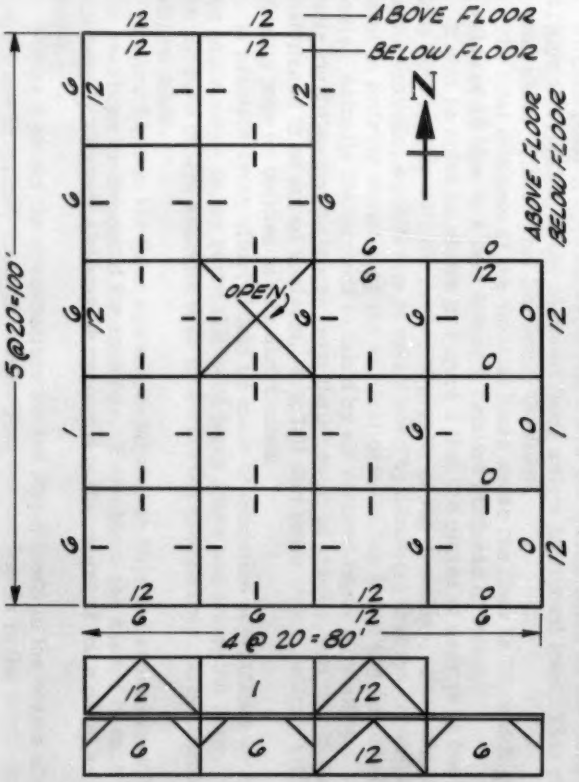

FIG. 1.- RELATIVE STIFFNESSES OF VERTICAL BENTS

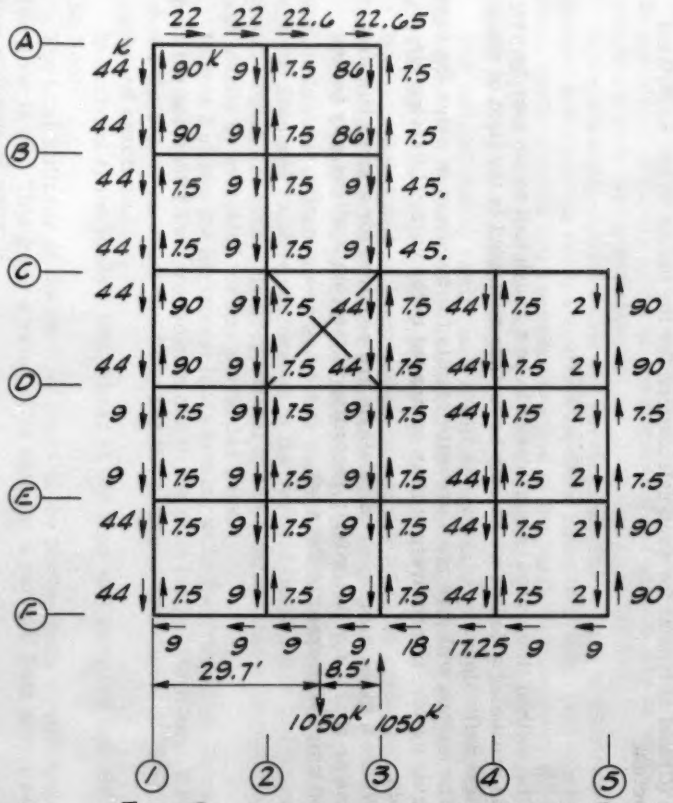

FIG. 2. LOADS AND REACTION ON FLOOR

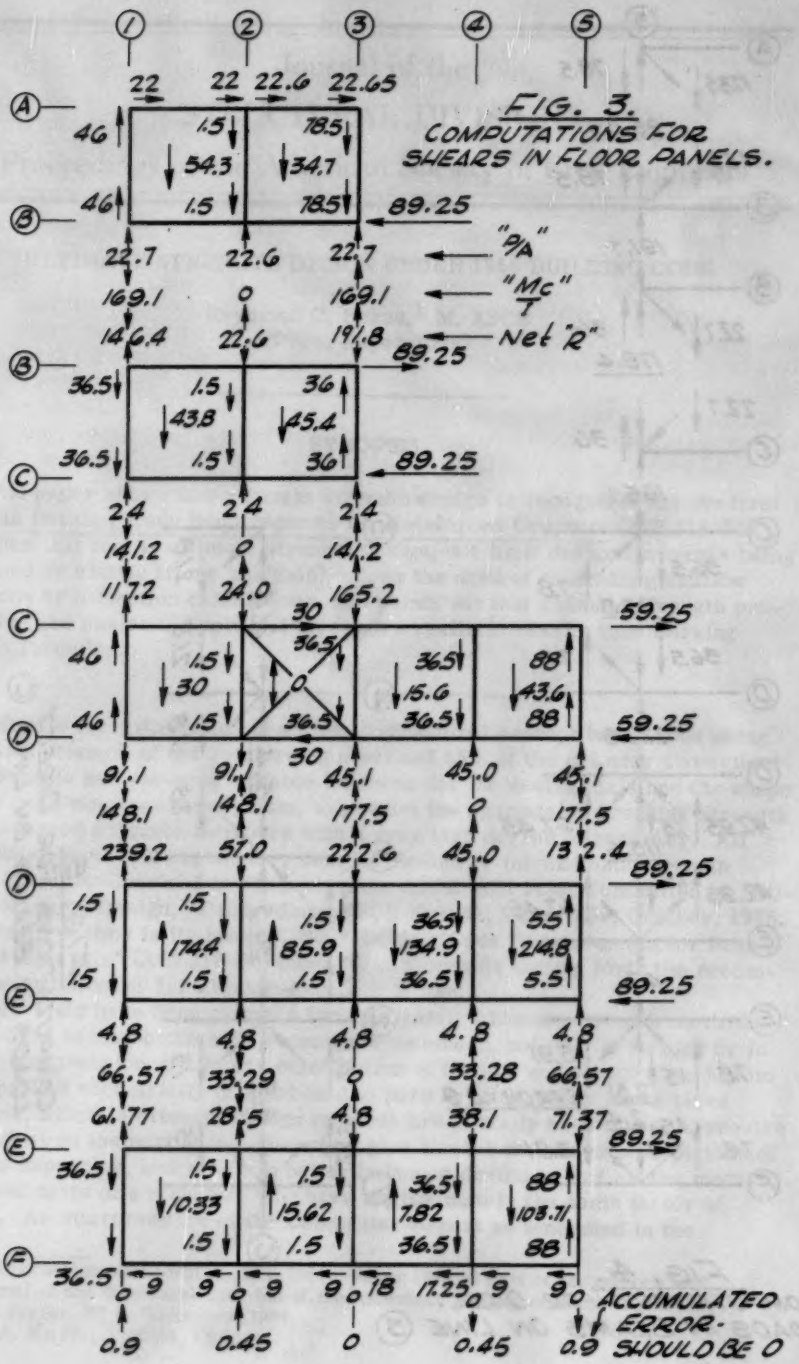

FIG. 3.
COMPUTATIONS FOR SHEARS IN FLOOR PANELS.

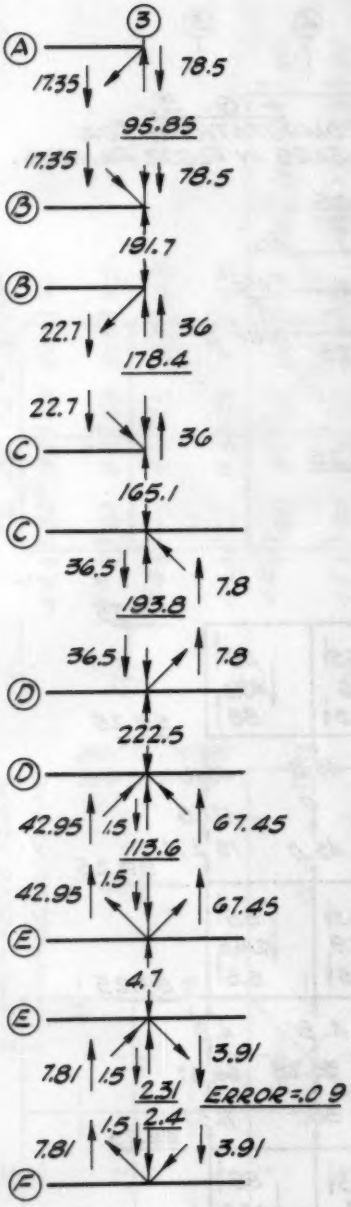

FIG. 4.
COMPUTATIONS FOR DIRECT LOADS IN BEAMS ON LINE (3)

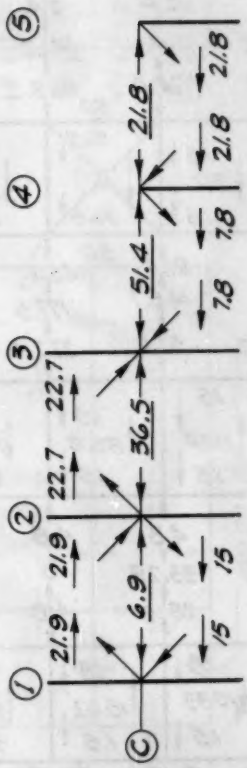

FIG. 5.
COMPUTATIONS FOR DIRECT LOADS IN BEAMS ON LINE (C)

Journal of the
STRUCTURAL DIVISION
Proceedings of the American Society of Civil Engineers

ULTIMATE STRENGTH DESIGN UNDER 1956 BUILDING CODE

Raymond C. Reese,[1] M. ASCE
(Proc. Paper 1099)

SYNOPSIS

This paper shows how ultimate strength design is recognized for the first time in Building Code Requirements for Reinforced Concrete (ACI 318-56), explains that this is ultimate strength design, not limit design (moments being obtained by elastic frame analysis), shows the need of controlling shallow sections by deflection calculations, and points out that ultimate strength procedures are easier to apply and give more realistic results than working stress formulas.

Ultimate strength design is a simple structural concept based upon using the yield strength of the reinforcing steel and 85% of the cylinder strength of the concrete and choosing suitable locations for the neutral axis and the shape of the compression stress prism, to predict the ultimate or breaking strength of reinforced concrete members with a very high degree of accuracy. All necessary basic and explanatory data for design by the ultimate strength method are summarized in "Report of the ASCE-ACI Joint Committee on Ultimate Strength Design," Proceedings ASCE Vol. 81, Paper 809, October, 1955. For the first time in its history, the "Building Code Requirements for Reinforced Concrete" (ACI 318-56) contains an Appendix setting forth the recommended procedures for ultimate strength design.

Many tests have demonstrated how accurately ultimate strength methods predict the breaking strength of concrete members, not only in flexure or in direct compression, but in any combination of flexure and direct stress from the smallest eccentricity of axial load to pure bending. With just a bit of practice, ultimate strength design methods are actually easier to use, require less effort on the part of the computer, give a much more realistic picture of what is happening, and result in better balanced design in that all the members and parts of a structure will have approximately the same factor of safety. An interpretation of the Committee Report as embodied in the

Note: Discussion open until April 1, 1957. Paper 1099 is part of the copyrighted Journal of the Structural Division of the American Society of Civil Engineers, Vol. 82, No. ST 6, November, 1956.
1. Cons. Engr., Toledo, Ohio.

Appendix of the Building Code and an explanation for some of the provisions are in order.

The best place to start may be with the legal status of ultimate strength design under the 1956 ACI Code. As stated in the body of the Code, ultimate strength design may be used for the design of reinforced concrete members, and a footnote calls attention to recommended criteria given in the Appendix, which is based directly on the Joint Committee Report. Thus there is authority in the 1956 Code for the use of the method whenever the designer sees fit to do so. This is an optional method and not mandatory. Printing the recommendations in the Appendix does nothing to detract from the legal status. The separation of the recommendations for ultimate strength design from the body of the Code avoids the possibility of confusing requirements with the working stress method. Moreover it allows time for engineers to become familiar with the alternate method before its incorporation into the body of the Code.

Ultimate strength design as considered by the Joint Committee and embodied in the Appendix is not limit design but is only a step in that direction since the recommended ultimate strength procedure governs only the design of sections. It is assumed that external bending moments will be computed by elastic analysis as for any rigid framework. This is clearly stated in the Committee Report and in the Code. The Joint Committee anticipates that limit design may well be the next advancement in the design of reinforced concrete structures. Limit design goes further by taking advantage of the fact that when any section of a statically indeterminate reinforced concrete framework is gradually overstressed to the extent that the tension steel undergoes a stress equal to its elastic limit, then with further increase of load that section will not take additional moment, though it will hold what it already has, and so will become a plastic hinge, transferring moments to less heavily stressed sections.

In using ultimate strength methods, the engineer does not have to change his methods of computing loads, moments or shears, with the one exception that live loads and dead loads will be separated as will appear shortly. The engineer is free to choose his own methods of rigid frame analysis. The use of arbitrary coefficients for moments or the more exact methods of analysis are to be applied under the same conditions as for designs made under the working stress method.

One provision in the ultimate strength method that differs from present practice is the inclusion of a minimum eccentricity in proportioning all columns. In spirally reinforced columns, an eccentricity of at least 0.05 times the depth of member and in tied columns of at least 0.10 times the depth is required. The Committee recognized that almost unavoidable small eccentricities exist and made provision for them even where loads are usually regarded as concentric. It appears reasonable and properly conservative to do so because if we are to predict more closely the actual strength of members, we must, on the other hand, be realistic and include all load conditions involved. Recent tests of eccentrically loaded columns[2,3] have taken the

2. "A Study of Combined Bending and Axial Load in Reinforced Concrete Members" by E. Hognestad, Bulletin 399, University of Illinois Experiment Station, November, 1951.
3. "Sustained Load Strength of Eccentrically Loaded Short Reinforced Concrete Columns" by Viest, Elstner, and Hognestad, Journal ACI, Vol. 27, March, 1956.

problem of the design of members subject to axial load and bending out of the realm of purely theoretical analysis and put it on a readily-understood basis.

Ultimate strength design could result in shallower and more flexible members. If advantage is taken of this fact, and it is often desirable to do so, some limitation must be provided to guard against too great deflections and excessive cracking. The Committee Report as embodied in the Code reminds the designer of the need for considering deflections whenever the net ratio of tension reinforcement in any section of a flexural member exceeds $0.18\, f'_c/f_y$. In the case of 20,000 psi steel, 3000 psi concrete, and n = 10, balanced reinforcement according to the elastic theory is 0.0136. With ultimate strength design, the steel and concrete attain their allowed stresses simultaneously with a steel ratio between 0.03 and 0.04. Using 3000 psi concrete and 40,000 psi yield strength steel, the prescribed limiting value for the ratio of reinforcement works out to be 0.0135, which is almost identical with the 0.0136. This is tantamount to saying that since satisfactory structures have resulted so far as deflection and cracking are concerned, under the working stress design procedure, only shallower members need be investigated for deflection.

The relative costs of steel and concrete, however, make it likely that greater economy may lie in lower percentages of steel, and shallow beams may not actually occur as frequently as might at first seem possible. There are several ways to keep deflections under control. One is the rule-of-thumb limitation of maintaining a maximum ratio of span to depth. Solid slabs were frequently limited to a ratio of 32 for floors or 40 for roofs. Joists and beams have sometimes been limited to a ratio of 20 or 24. These are rough and ready rules and somewhat conservative, but they serve to guide the designer against getting too shallow members. A second possibility is to require the computing of deflections, at least in borderline cases. Researchers differ somewhat on the simplest method for computing the probable deflection of a single span reinforced concrete beam, and the problem becomes more difficult if continuity is taken into account. Still it is possible to make a fairly good approximation. Even with that accomplished, there is still no definite criterion to measure against. The classic L/360 established well over a century ago as a limitation to prevent excessive cracking of plastered ceilings survived a change from lime to cement and then to vermiculite plaster and finally was applied to exposed concrete slabs free of any plaster at all. In spite of this lack of rational derivation, no better rule has been advanced, though this is obviously a fairly strict requirement for a monolithic concrete structure. Permissible sagging is largely a matter of esthetics and psychology as to what the general public will accept as a satisfactory structure, because deflections, within the ranges likely to be encountered, will not materially affect the safety of the structure.

The question is often raised, "Does one need better concrete to use ultimate strength design?" Probably not, because one wants as good concrete as he can reasonably get for any method of design. However, the Committee Report and the Code do put a more strict limitation on random low cylinder tests than is required in common practice. Controlled concrete is a requisite to the use of ultimate strength design, with all that the term "controlled" means technically. It is required that only one test in ten may fall below the minimum strength specified, and the average of any three consecutive tests shall not be less than the designed strength, each test consisting of at least three standard cylinders. By contrast, the 1956 ACI Code applying to designs made by the working stress method permits one test in ten to fall below 90

per cent of the required strength and requires the average of five consecutive tests to equal or exceed the design strength. This difference is somewhat greater than it may sound when casually stated. The difficulty of meeting specified concrete strengths is greatly increased when the number of cylinders averaged is reduced. Under ultimate strength design requirements, the possibility of the concrete strength being under the design strength is practically nonexistent.

A good deal of discussion has been carried on regarding the shape of the compression prism, and experiments have been undertaken to feel out its contours. There is no practical difference in the final results whether a parabola, trapezoid, rectangle, or parabola-plus-secant is chosen, and for that reason the Committee leaves the choice up to the designer, with the stipulation that whatever shape is chosen the ultimate capacity so computed can not exceed a fixed value. The rectangle is by far the simplest to use because its area and centroid can be located immediately. The parabola-plus-secant probably approaches most closely to the known facts, but is somewhat awkward for regular design use. It has been advanced that tables and diagrams will be developed to simplify the work. The writer prefers a simple theory that can be carried in the head and the results run off on a slide rule without the need for burdening one's self with books, charts, and diagrams. It might be that the researcher will prefer the more complicated form in analyzing his problems and the designer, the more simple rectangle for his work. Only time can tell which stress prism will be preferred, but, in the meantime, choose the one most easily understood and for which the properties are clearly in mind. Let me repeat that there is little difference in the final result obtained by the various compression prisms within the range permitted in ultimate strength design.

In passing, attention is directed to the fact that ultimate strength design takes advantage of steels with yield points as high as 60,000 psi. If a higher yield point is available, advantage can not be taken of that fact under the present recommendation. Studies are under way on the use and advantages of high strength steels. The outcome is still unknown. There are at present sufficient supporting data to justify the use of yield point steels up to 60,000 psi.

One of the thorniest problems confronting the Committee was the selection of appropriate load factors. Before discussing the recommended load factors, consider for a moment the procedure under the working stress design method, where, to take care of all reasonable contingencies, the yield point strengths are reduced to 40 or 45 per cent of their true values and that reduced strength is called the safe working stress. In ultimate strength design, the necessary factor of safety is obtained by multiplying the effect of the normal service loads by a load factor and designing for ultimate capacity at such overload. In the immediately following discussion, it is the effect of such overloads that is being considered.

An increase in the live load on a heavy reinforced concrete structure generally is not serious because it results in only a relatively small increase in the total load. On the other hand, any increase in live load makes a substantial difference in the total load on a structure built of relatively light-weight materials. This inherent characteristic of reinforced concrete structures should be kept in mind. Though nearly obvious, it is worth repeating that the more combinations of possible loads one considers, the closer he can approach the ultimate capacity of a structure with safety because he is then

including numerically certain items that were previously absorbed in a theoretical factor of safety. If only dead and live loads are considered, a large load factor is needed to compensate for loads not taken into account. If wind or any other item is included, the load factor could be reduced. If wind and another item, such as earthquake loading, is included, the factor might be still further reduced. If temperature effects, braking or centrifugal forces, vibrations, impact, and the like are all combined, the load factor can be decreased even further. The design of structures subjected to various combinations of all these forces should be approached through the theory of probabilities to determine the combination most likely to occur; which is just the same problem under ultimate strength design as when using working stresses, except that in the former case we have our ultimate capacity much more accurately known.

The Committee recommends factors for live and dead loads only and for these loads combined with wind or earthquake. This is most easily stated as 1.2 basic loads plus 2.4 live loads, with this sum increased by 0.6 wind or earthquake loads. (The report uses the term "basic load" and explains that this consists of dead load plus volume change due to plastic and elastic actions, shrinkage, and temperature. All of these effects are to be included in the basic load.) There is also provision for 1.2 basic loads plus 0.6 live loads and 2.4 wind or earthquake loads when the latter are a determining factor. The reasons for load factors of about these values and for variations in the load factors applied to the different types of loading can readily be understood. The dead load is capable of quite accurate determination. Perhaps in the early stages of a design considerable approximating may be necessary, but as work progresses, it is possible to compute the magnitude of dead loads to a high degree of precision (as witness the computations of counterweights for a bascule bridge). Furthermore, there should be nothing more than small changes in the dead load during the life of the structure. Hence, little need be added for possible increases or underestimates. However, it is not proper to assume that all other factors affecting the strength of the member will be as determinable. Therefore, some increase is required to cover errors in assumptions and methods of computing, irregularities in construction, failure of materials to be exactly in accordance with their prescribed strengths, and similar items. It seems proper, therefore, to increase basic loads by about 20 per cent for these contingencies.

Live loads are a different matter. They are established by general code as a fair appraisal of what should be provided for given types of occupancy. Only rough approximations can be made as to the weights of crowds of people, office equipment, parked automobiles, or highway or railroad loadings. Even warehouses, which would seem easier to study, may in time have the aisles and stock piles rearranged or method of conveying materials changed, upsetting the most carefully planned computations. Some consideration must also be given to changes of occupancy because types of occupancy do change during the life of a structure; outdated stores turn up as garages, obsolete churches as warehouses. Some minimum live load must be established that appears likely to serve throughout the useful life of the structure. A load factor must be applied to the minimum live load established by code to take into account all the foregoing possible variations in load, and to account for the various minor variations in design techniques, material strengths, and construction processes previously mentioned. An increase of 140 per cent was assigned to this load factor. Extensive studies were made by the

Committee and others upon the effects of varying these factors. Perhaps it is sufficient to state here that designs made with these factors, i.e., 1.2 basic loads plus 2.4 live loads, agree closely with designs made by the working stress method. Not that this is necessarily a criterion; it is merely a statement. Many designers have long felt that monolithic reinforced concrete frames have much greater reserve strength than designs in any other materials. Those who have test-loaded actual structures are aware that many types of construction used in light-occupancy buildings will fail at loads just above double the designed live-plus-dead load. This may be quite enough capacity for this type of structure. Monolithic concrete structures, on the other hand, have carried much greater overloads with little or no damage to the building. The whole subject of load factors is by no means settled. In the Report, these load factors have been formulated for present use and will produce structures that often compare closely with those designed by the working stress method. The separation of live and dead loads is a forward step in design and will make it possible to appraise live load requirements and load factors more realistically. Being able to predict failure quite accurately, we can gradually improve the recommendations in the interest of economy coupled with safety.

Because the ratio of the effect of live to dead load may be small, a second set of load factors must be satisfied. These are not alternative to the ones just discussed but supplementary to them. The designer is required to combine dead and live loads and increase the sum 100 per cent on columns or columns combined with bending and 80 per cent for members in flexure only. Similarly, if wind or earthquake load is included, it is required that half of the wind or earthquake load be added to the dead and live loads and that the sum be increased by 100 per cent or 80 per cent, depending upon the type of member.

The Committee recommendation for maximum permissible steel percentage is based upon the thought of always having under-reinforced sections. There is seldom economy in balanced or over-reinforced sections. Then again, tension failures are gradual, accompanied with considerable deflection and cracking, and thus plenty of warning. Compression failures may, on the other hand, occur without warning. From all considerations, the under-reinforced section is to be desired. Hence the maximum net percentage of tensile reinforcement in beams is limited to $0.40\, f'_c/f_y$. This value is reduced when concrete in excess of 5000 psi is being used. For 3000 psi concrete and 40,000 psi steel, this formula limits the maximum reinforcement to 0.03, which is a bit below ultimate strength balanced reinforcement, but more than double balanced reinforcement computed by the working stress method.

Since 1941, and in the 1956 Revision of the ACI Code, concentrically loaded columns have been designed more or less in conformity with ultimate strength methods, so little change would be expected in the design of axially loaded members. In one manner, however, ultimate strength design introduces a somewhat different approach to the differentiation between the capacity of spirally reinforced and tied columns. Recent Codes have recognized the somewhat tougher nature of spirally reinforced columns by reducing the allowable stresses on a tied column to 80 per cent of the spirally reinforced one. There is not much difference in the ultimate capacity of the two types of column, but the spiral reinforcement produces a column that substitutes considerable bending or buckling for the crushing type of failure experienced with

tied columns. Codes have chosen to recognize this desirable characteristic by varying working stresses. Ultimate strength design, being based solely upon the ultimate capacity, can not differentiate between the two types in this manner. The Report sets up only one formula for the carrying capacity of a reinforced concrete compression member whether spirally reinforced or tied. Because spirally reinforced columns have shown themselves in tests to be somewhat tougher for concentric loads, the Report varies the required minimum eccentricity of load from 0.05t on a spiralled column to 0.10t on a tied column.

Under present design methods, slender or long columns are not too common in reinforced concrete structures. The Code allows some increase in the capacity of such slender columns by raising the limit for unreduced carrying capacity from 10 to 15 diameters and the load reduction for lengths above that from (1.3 - 0.03h/d) to (1.6 - 0.04 h/d), thus giving some credit to the increased knowledge of the behaviour of long columns and combined bending and direct stress, particularly under sustained loads. The previous codes seemed rather conservative in this regard. Foreign practice is much more liberal, the recommended formula being identical with British Regulations and more conservative than Czechoslovakian requirements.

The report is silent on the problem of web stresses, i.e., diagonal tension and bond. Experiments recently completed and those now under way are shedding a good deal of light upon the whole subject of web stresses. The tests indicate that with concentrated loads the shear-span is an important factor. This simply means that if two equal concentrated loads are placed symmetrically upon a beam and the unit intensity of shear is computed as exactly the same regardless of the position of the loads, it will be found that the beam is much better able to resist such concentrations when they are close to the supports, and that as the loads are moved progressively towards the center, the ability to resist the diagonal tension forces is reduced. Uniformly distributed loads would seem to be a summation of pairs of concentrated loads, but to be sure what happens, tests are under way simulating uniform loads. Experiments also show that diagonal tension in a zone of zero moment is much more serious than exactly the same amount of diagonal tension combined with high bending, where the internal couple acts to divert the diagonal tension into a position more nearly parallel to the neutral axis. Many other factors are coming to light in these studies. Soon all the results will be collected and studied as a whole. A joint committee of ASCE-ACI under the chairmanship of Charles S. Whitney has been engaged for some time in suggesting the direction the tests should take and in collecting and studying the data. In the meantime, web stresses should be determined by working stress procedures.

It would be possible to extend these remarks indefinitely, explaining the reasons for each recommendation in the Committee Report and the study and discussion behind each one of them. For those who have not been actively in touch with the enormous amount of testing and analysis of such tests, suffice it to say that probably no other structural concept has such an impressive amount of testing and analysis to support it. Tests have extended over a long period, at many institutions, and under numerous researchers. Similarly, analysis has progressed under the thoughtful direction of analysts all over the world. There should be no hesitation on the part of the designer to use this method whenever he wishes. The work of the computer is not made more difficult, as the actual computations are about the same, but the mental images

behind such computations are a bit simpler and easier to apply. There is a consistent procedure through simple compression, direct stress and flexure, to pure bending. The results give a much more realistic picture of the actual strength of a structure, and this allows the designer to take full advantage of the materials. Similar methods are in use in practically all the countries of Europe and South America. True, we need further data and recommendations in such fields as allowable deflections and the handling of web stresses, but the latter subject in particular has almost passed through the experimental and testing stage and is practically ready for correlation and analysis. Shortly these areas should be ready for codification.

Journal of the
STRUCTURAL DIVISION
Proceedings of the American Society of Civil Engineers

THE PAINTING OF STRUCTURAL STEEL

E. J. Ruble,[1] M. ASCE
(Proc. Paper 1100)

SYNOPSIS

A review of research being conducted on the painting of steel structures is presented. The contents and use of the Painting Manual prepared by the Steel Structures Painting Council is discussed. A description of the many tests being conducted by the Council on actual structures to determine the best methods of protecting the steel against severe corrosive conditions, such as brine drippings from refrigerator cars, is included.

INTRODUCTION

The protection of structural steel against the ravages of rust has exercised the minds of engineers for many years, and has been the subject of practical investigations and research in several countries. As an indication of the importance of this subject, the American Railroads' annual loss due to corrosion has been estimated at $260,000,000 per year of which $190,000,000 covers corrosion damage to rolling stock and $70,000,000 to track, bridges and other physical assets. The large losses on the railroads can be attributed to a large extent to the brine from refrigerator cars accentuated within recent years by the transportation of frozen foods. Heavy corrosion also takes place on steel near large industrial centers.

In 1950, through the efforts of the American Institute of Steel Construction, representatives of nineteen technical associations, interested in the protection of steel against corrosion, met in Pittsburgh, Pennsylvania, at the Mellon Institute and formally organized the Steel Structures Painting Council. The sponsoring technical associations were from both the consumer and the producer; typical associations being the American Institute of Steel Construction, Association of American Railroads, Steel Plate Fabricators Association,

Note: Discussion open until April 1, 1957. Paper 1100 is part of the copyrighted Journal of the Structural Division of the American Society of Civil Engineers, Vol. 82, No. ST 6, November, 1956.

1. Research Engr., Structures, Assn. of Am. R. R., Chicago, Ill.

Federation of Paint and Varnish Production Clubs, Lead Industries Association and the American Zinc Institute.

The Council adopted as its "Purposes" the following:

1) To review the art of cleaning and painting steel structures through literature surveys, conferences and other means and to determine and outline the best methods developed up to the present time.

2) To issue, if found feasible, a code or specification covering practical and economical methods of surface preparation and painting steel structures based on the present knowledge of the membership of the Council.

3) To perform in its own organization or by engaging outside individuals or organizations, further research to reduce or prevent the corrosion of steel structures by surface preparation and by the application of coatings, paint and other materials and to determine the initial and annual costs thereof.

4) To issue from time to time recommendations intended to further improve and to make more effective and more economical the protection of steel structures; such recommendation to be made available to specification and code writing committees.

One of the first acts of the Council was to employ Dr. Joseph Bigos, a chemical engineer, as its Director of Research with headquarters at the Mellon Institute in Pittsburgh. Dr. Bigos received his doctors degree in 1948 from the University of Pittsburgh after an extended period of military service, where he had considerable experience in ship repair and marine work, including drydocking, cleaning and painting of ships and floating equipment. Dr. Bigos has devoted full time to the work of the Council since his employment and must be given full credit for his contribution to the outstanding accomplishments of the Council to date.

Paint Manual

In order to obtain information as to current good cleaning and painting practices, a very comprehensive questionnaire was distributed to a large list of companies, organizations and trade associations representing the principal users of paint for steel structures. The replies to the questionnaire indicated that there was a wide divergence in current practices, even in organizations in the same industries, but even so, the replies indicated that there were many paint systems from which satisfactory results could be expected. The answered questionnaires constituted the foundation for the preparation of Volume 1. Good Painting Practice, of the Steel Structures Painting Manual, See Fig. 1, by the assignment of chapters on painting in the various fields to men who had found means for securing satisfactory paint performance. Volume 1 of the Paint Manual consists of eighteen chapters, describing in complete detail the methods of surface preparation and the paint systems which have been found by the individual authors to give satisfactory results.

The first chapter in the Manual is entitled "Simplified Theory of Corrosion" and covers the complete field of chemical and electrochemical reaction of steel with its environment. Typical examples of the practical application of the theory are included.

The chapter on Mechanical Surface Preparation covers the entire field

Fig. 1. View of Painting Manual

from hand cleaning to blast cleaning. Various pictures and detail drawings showing the equipment and use of equipment are included. The detailed information on equipment, tools, abrasions and procedures merit particular attention.

The chapter on Chemical Surface Preparation describes various types of chemical surface treatment designed to increase the life of paint on structures.

Chapters on the application of Paint, Inspection, Quality Control of Paint and Comparative Costs are quite extensive and contain a vast amount of data and latest information on the particular subjects.

The chapters on the Shop Painting of Steel in Fabricating Plants, Painting of Railroad Bridges and Structures and Painting of Highway Bridges and Structures cover present day practice in the shop and field painting of bridges. These three chapters contain many tables of time and cost data, diagrams and pictures of cleaning and painting tools and painting operations.

The chapters on the Painting of Steel Vessels for Salt Water Service, the Painting of Steel Vessels for Fresh Water Service, the Painting of Steel Tanks, the Painting of Hydraulic Structures and the Protection of Underground Structures give complete information on these subjects.

The chapter on the Painting of Industrial Plants covers Water and Sewage Works Structures, Maintenance Painting of Steel and Coke Oven Plants, Petroleum Refineries and Chemical Plants. A section is also included on the use of color to improve working conditions in industrial plants.

A chapter on Metallizing is included as this is the only method of applying metallic coatings which lends itself to field application. Metallizing offers a solution to some corrosion problems where organic coatings systems are partially or completely inadequate. This chapter evaluates metallizing in connection with specific corrosion problems.

The final chapter covers the Causes and Prevention of Paint Failures. The importance of the various factors influencing failure and the common types of paint failure are discussed.

The second volume of the Manual entitled "Systems and Specifications," see Fig. 1, was prepared by the Council to fulfill the need for specific recommendations for the painting of various types of steel structures in a manner similar to the specific recommendations of the American Society for Testing Materials whereby the structural steel for any bridge can be ordered by just referring to the current ASTM Specification A7. Very few consulting engineers or architects are sufficiently versed in paint technology to qualify them as specialists. Volume 2 of the Manual was accordingly planned so that it could be used with confidence as a reference by those who must make recommendations for the painting of structural steel.

The Council realized that seldom is there a single solution to any painting problem, but usually a number of solutions exist. For this reason Volume 2 of the Manual contains several specific recommendations for the particular painting problem and possibly others could have been added. However, the recommendations that are made are considered the best solutions, based on experience over the years.

Volume 2 of the Manual contains nine separate and complete Paint System Specifications, each system developed for a separate exposure classification. Each Paint System Specification stipulates the surface preparation, pretreatment, paint application, primers, intermediate and finish paints by reference to individual specifications for each item. Detailed requirements such as dry

paint film thickness, drying time, color contrast between coats, and other necessary information are included. If the engineer specifies the Paint System by number only, the contractor will be required to use the "standard" specifications. If particular primers, finish coats or surface preparations are desired, the engineer may specify any of the numerous "alternates" listed for the particular system.

In addition to the various specifications and paint systems, the Manual contains a very complete table of indexed recommendations for the painting of steel. The table contains a list of about 600 different types of steel structures, such as Acetic Acid Tanks, Belt Conveyors, Bridges, Offshore Drilling Platforms, Roof Gutters, Smokestacks, Transformers and Yachts. A recommended Painting System or Systems are shown for each of these 600 steel structures for various types of exposure, such as Rural, Industrial, Marine or Chemical Atmosphere, Fresh Water, Salt Water or Alternate Immersion and High Humidity or Dry Interiors.

As an example in using Volume 2 of the Manual, suppose a consulting engineer is preparing the plans and specifications for a railroad bridge which will be constructed in a rural atmosphere, but will carry a large number of refrigerator cars. If the bridge is to be designed and constructed in accordance with the AREA Specification, the consulting engineer will be required to paint the bridge in accordance with the recommendations of the Council. By referring to the table of indexed recommendations, he will note that Paint Systems 1 or 2 are satisfactory for the parts of the bridge not subjected to brine; such as the upper part of a through bridge, but Paint System 3, 4, 5 or 9 should be used for the lower chord, floor system and lower chord bracing as this steel will be subjected to severe corrosive conditions.

If the engineer selects Paint System 1, which is an Oil Base Paint System designed for structural steel surfaces exposed to the weather or moderately corrosive atmospheres, for the upper part of the bridge, it is only necessary for him to state "The bridge members above the top of rail shall be painted in accordance with the provisions of the Steel Structures Painting Council's Paint System Specification SSPC-PS1-55T." This notation will require the contractor to do the following:

1) Prepare the steel surface in accordance with either Surface Preparation Specification 2-52T for Hand Cleaning or Specification 3-52T for Power Tool Cleaning, as elected by the contractor. These Surface Preparation Specifications establish definite Cleaning Standards for each method.

2) Prime the steel with paint of highest quality conforming to either SSPC Specification 1-55T, a Red Lead and Raw Linseed Oil Primer, AASHO Specification M72-51, Type 1, a Red Lead Ready Mixed Paint, Federal Specification TT-P-86A, Type 1, a Red-Lead-Base, Ready-Mixed, Type 1, SSPC Specification 2-55T, a Red Lead, Iron Oxide, Raw Linseed Oil and Alkyd Paint or SSPC Specification 3-55T, a Red Lead, Iron Oxide and Fractionated Linseed Oil Paint. Complete Specifications for the Council Paints are included in the Manual.

3) Apply an intermediate coat the same as the primer coat except the paint shall be tinted with carbonblack or lampblack paste-in-oil to a color contrasting with the primer coat.

4) Apply an aluminum finish coat conforming to either:

a) Federal Specification TT.A-468A, Type 2, Class B.
b) American Society for Testing Materials Specification D962-49, Type 2, Class B.
c) U. S. Coast Guard Specification GGS-5-P-2a.

5) Apply the paint in accordance with SSPC Specification PA1-53T, Shop, Field and Maintenance Painting to a controlled thickness.

If the engineer selects Paint System 4, which is a Vinyl Paint System designed for structural steel surfaces exposed to fresh and salt water immersion, alternate immersion, high humidity and condensation or chemical fumes, for the lower part of the bridge where brine from the refrigerator cars are deposited on the steel, it is only necessary for him to state "The bridge members below the top of rail shall be painted in accordance with the provisions of the Steel Structures Painting Council's Paint System Specification SSPC-PS3-55T. This notation will then require the contractor to do the following:

1) Prepare the steel surface in accordance with either Surface Preparation Specification SSPC-SP6-52T for Commercial Blast Cleaning or SSPC-SP9-52 for Pickling, as elected by the contractor.

2) Pretreat the steel with a wash primer according to Council Specification SSPC-PT3-53T.

3) Prime the steel with paint conforming to U. S. Military Specification MIL-P-15929A, a Vinyl Red Lead Type Primer (Formula 119) of the Bureau of Ships.

4) Apply an intermediate coat the same as the primer coat except the paint shall be tinted with lampblack to a color contrasting with the first coat.

5) Apply an Aluminum Vinyl Finish Coat conforming to SSPC-Paint 8-55T.

6) Apply the paint in accordance with Steel Structures Painting Council Specification PA153T for Shop, Field and Maintenance Painting to a specified dry film thickness.

Field Tests

As previously mentioned, the purposes of the Council are to prepare and issue paint specifications based on the most reliable data to date and then conduct research in the laboratory and on actual structures in the field to improve our specifications and recommendations. With the completion of the Manual, the Council is now concentrating its activities on research.

One high aim of Railroad and Highway Officials is to develop a chemical treatment which can be sprayed on steel structures to remove all dirt, rust and debris from the flat surfaces, interiors of members, re-entrant angles and around bearings. In order to obtain some data on this subject, the AAR Research Staff cooperated with the Steel Structures Painting Council in determining the suitability for painting of chemically cleaned and pretreated surfaces in comparison with surfaces cleaned by hand-chipping and wire-brushing methods. A secondary purpose was to evaluate the comparative performance of a number of paints and coatings.

For this investigation, portions of two through-plate girders of a railroad bridge in Chicago were first chemically cleaned by use of a "flush-off" paint stripper and steam, and then pretreated with a proprietary cold phosphate rust remover, see Fig. 2. Other portions were cleaned by hand chipping and wire brushing in the usual manner by painters from a railroad. Six primers were applied to both types of cleaned surfaces, and one-half of each primed surface was top coated with a black finish paint.

The six paint primers tested on the two types of cleaned surfaces were:

1) A paint equivalent to Steel Structures Paint Council Paint No. 2, containing 75 percent red lead and 25 percent iron oxide in the pigment, and two parts of linseed oil to one part alkyd solids in the vehicle.

2) A red lead paint, in common use by the railroads, containing pure red lead as the pigment and a mixture of raw and bodied linseed oil as the vehicle. This paint complied with Federal Specification TT-P-86a, Type 1.

3) A state highway department red lead paint supposedly complying to the above Federal Specification, but the paint that was received and applied did not have the proper viscosity and, as a result, was applied at about one-half the recommended thickness.

4) A paint containing some rust-inhibitive pigment and iron oxide in the pigment and a vehicle based upon processed fish oil.

5) Another proprietary paint for rusty surfaces, the composition of which is unknown.

6) An extended red lead, semi-quick-drying paint.

An inspection of the paints was held three years after their application by a large group of railroad engineers and representatives from the AAR Research Staff and the Steel Structures Painting Council. The paint panels were rated for rusting only in accordance with the ASTM standard method of evaluating degree of resistance to rusting. See Fig. 3. Remarkably consistent ratings were obtained from the various engineers for each test panel and it should be pointed out that the ratings were made without knowledge of which materials were being rated. Based on the average ratings for the various test sections, the following conclusions appeared to be valid for these tests.

1) The surfaces prepared by chemical cleaning and cold phosphate pretreating were inferior to those prepared by hand chipping and hand wire brushing. However, the surfaces chemically cleaned, but without the cold phosphate pretreatment were satisfactory.

2) The two paints meeting the Council's Specification and the Federal Specification were superior to the other paints.

3) None of the paints tested was effective in painting over very heavy rust scale; all rust scale which was painted failed by loosening of the rust scale and exposure of fresh metal in a few months, as shown at the bottom of Fig. 4.

The most common method of painting steel bridges in the past has been two coats of red lead and oil with a finish coat applied over hand cleaned surfaces. Satisfactory results have been obtained with this system for most

Fig. 2. Paint tests on chemical cleaned steel surfaces.

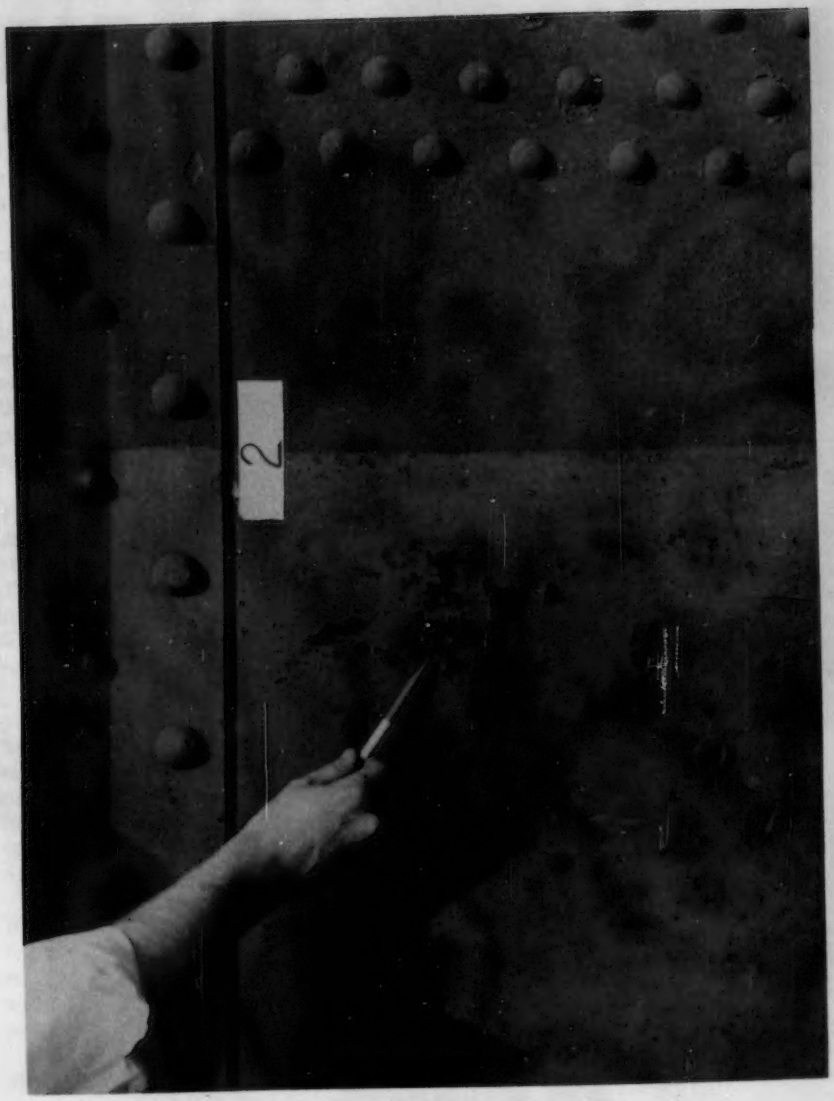

Fig. 3. The rating of rusty surfaces.

Fig. 4. The failure of paint when applied to heavy rust scale.

exposures, but on certain bridges carrying a large number of refrigerator cars, the paint on the lower surfaces has only lasted a very short time. In many cases, where the bridges are located on a curved track or near the end of a curve, it has been necessary to clean the steel and paint every year to keep the steel from rusting.

In order to determine if some of the newer synthetic resin paints would prove satisfactory on steel surfaces subjected to brine drippings, arrangements were made with the Missouri Pacific Railroad to test paints on two of their bridges where considerable trouble had been encountered with paint failures. The bridges selected are near the ends of curves and the red lead and oil paints only lasted a year. Both bridges are of the through type with an open timber floor, as shown in Fig. 5.

In these tests, which consisted essentially of about 300 sq. ft. on the floorbeams, stringers, lower chord and lateral bracing between panel points for each test panel, two methods of surface preparation were used. On one bridge seventeen test areas or panels were available so these surfaces were sandblasted to what was supposed to be a commercial grade, but in order to remove all of the grease and rust, it was necessary to blast to a grade almost equal to white metal. On the other bridge, the seven test panels were thoroughly cleaned by hand chipping, scraping and a combination of hand and power wire brushing. The surfaces were then steam cleaned to remove the salt residue.

The type of sand drier used in the sandblasting operations is shown in Fig. 6. The drier is powered by a small gasoline engine and has a very high drying capacity. It will easily keep two 1/4 in. nozzles supplied. In operation, sand is shoveled from the pile into the inlet end of the rotating kiln. The exit end is heated by means of the flame from an oil-fired unit. A screen is attached to the exit end and all material which passed through the screen was caught in a large box. The oversize material, which amounted to about one-fourth of the sand, was discarded.

After the sand is thoroughly dried, it is emptied into the sandblasting tank, as shown in Fig. 7. A screen is used on the inlet to the tank to prevent oversize material, such as splinters, pieces of sack, etc., from entering the blast tank and clogging the exit valve on the blast nozzle. An important accessory on the tank is a water separator at the air liner before entrance to the sandblast tanks. Compressed air will generally carry sufficient condensed water to cause caking of the sand in the sandblast tanks unless water separators are used.

The type of air mask used in the sandblasting operation is shown in Fig. 8. It is absolutely mandatory that the blast cleaning operator be provided with a fresh air supply to prevent silicosis. Gloves and apron are also recommended, as well as tight fitting clothing. The mask used in these tests is equipped with a filter type of cartridge which filters out traces of oil decomposition products generated in the oil compressor, oil, dust and water.

The air supply for the operator's mask may be obtained from the air supplied to the blast cleaning tanks, but the air should be taken off past the oil and water separator, and before it enters the blast tank.

Thick rust deposits on the steel are shown in Fig. 9 being removed by the hand chipping, scraping and wirebrushing operation. Even where sandblasting is used, it is generally considered more economical to remove the heavy deposits of rust by chipping.

The power wire brushing operation, shown in Fig. 10, is not very effective

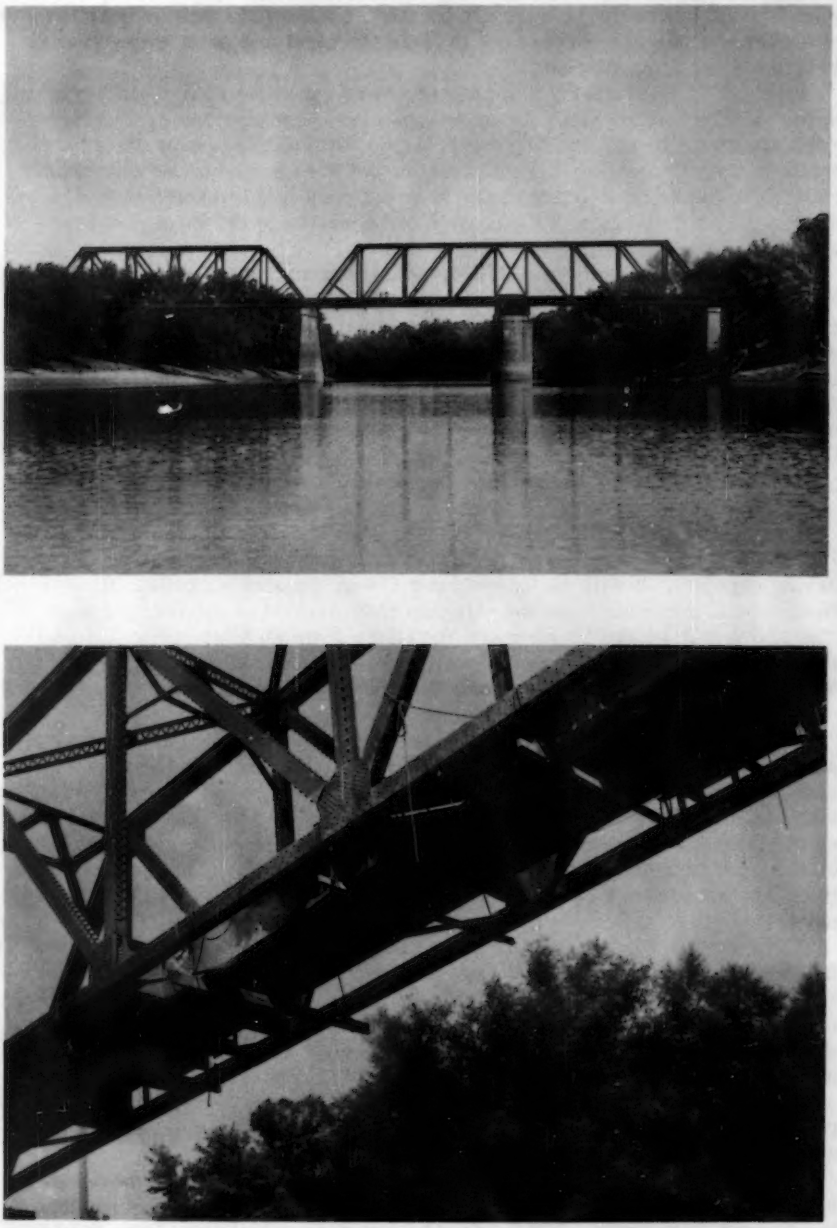

Fig. 5. Paint tests on the Missouri Pacific Railroad.

Fig. 6. General view of sand drier used in sandblasting.

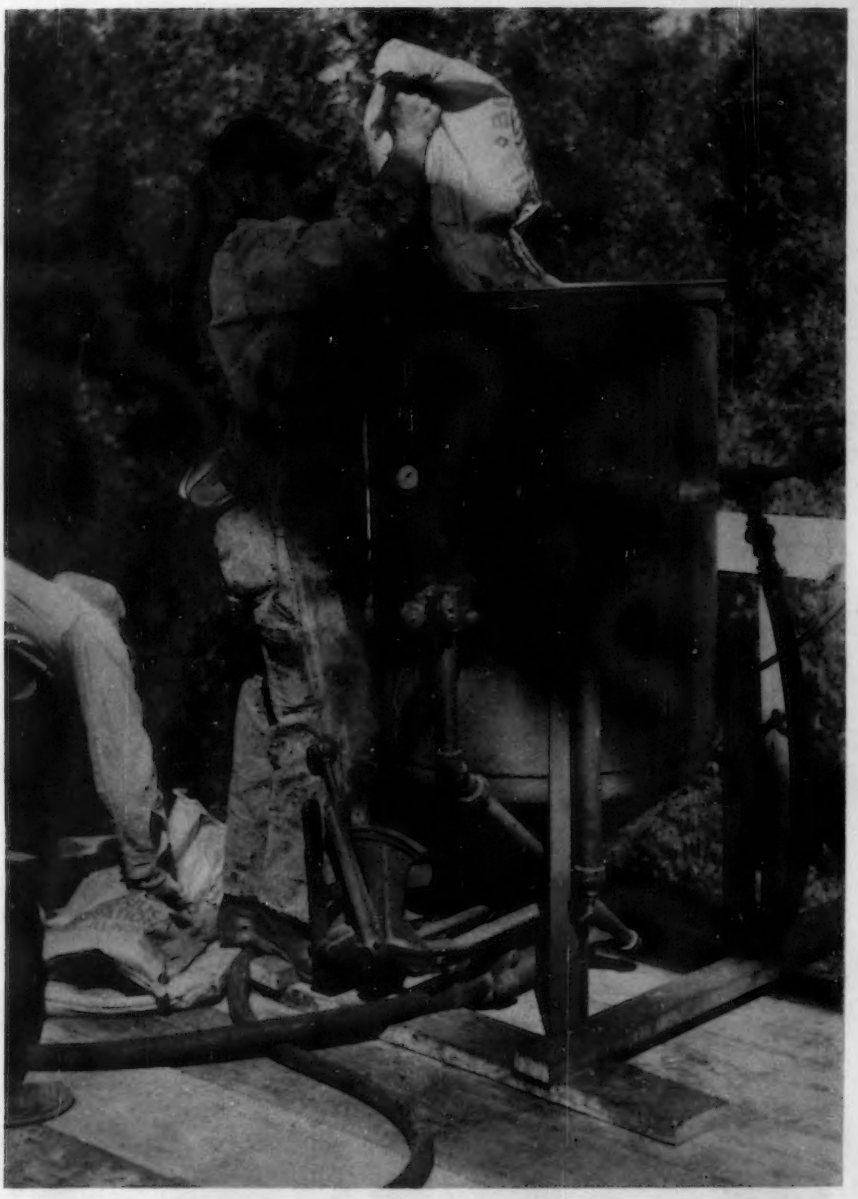

Fig. 7. View of sandblasting tank.

Fig. 8. Sandblasting steel surfaces.

Fig. 9. Removing thick rust scale by hand chipping.

for removing thick rust deposits but will remove tightly adherent rust. Power wire brushing is considered more economical than hand brushing. The brush shown has a 6-in. diameter cup wire brush of knotted wire construction. There is no serious hazard associated with power brushing, but the eyes of the workmen must be protected by safety goggles due to flying debris from the surface and to wire bristles which break off.

The hot suds for cleaning the steel after the hand and wire brushing was supplied by the steam cleaner shown in Fig. 11. Steam cleaning is an excellent method of surface preparation for the parts of structures subjected to brine drippings as the water and detergents that are supplied by the cleaner at about 350°F and 150 psi pressure will remove the soluble salts. However, a final rinse with steam or hot water without the detergents must be used as no alkali must be permitted to remain on the steel.

After considerable preliminary laboratory studies, a number of paints and coatings were selected as having sufficient chemical resistance to be considered for these tests. Of the various materials studied, the vinyl paints appeared to have the greatest potentiality for resisting the brine dripping corrosion. Vinyl resins are synthetic materials which are formulated into quick drying lacquer type paints. Two vinyl paint systems were selected, the first being a system based upon a basic zinc chromate vinyl butyral wash coat pretreatment, two coats of red lead vinyl paint and a top coat of black vinyl paint. The second system is based upon the same wash primer pretreatment and three coats of an aluminum vinyl paint.

The second most potential source of currently available paint systems are those based upon phenolic resins. The phenolic resins are incorporated into paints by cooking with oil to form varnish vehicles. The following four basic phenolic paint systems are included in the tests:

1) Two coats of red lead phenolic primer and a top coat of black phenolic paint.

2) Red lead, zinc chromate, zinc oxide. Alkyd and phenolic varnish primer, and intermediate coats with a black phenolic finish coat.

3) A primer and intermediate coat of a paint consisting of a zinc chromate, red lead, iron oxide, mixed pigment phenolic varnish with a black phenolic finish coat.

4) A red lead, iron oxide, phenolic varnish primer and intermediate coat with a black phenolic finish coat.

In addition to the Vinyl and Phenolic Paints, a paint using a dehydrated castor oil alkyd was applied. This material appears to have improved chemical resistance over linseed oil. Other paints included the Chlorinated Rubbers, Neoprene Coatings, and a paint based upon the Epoxy Resins.

Several coatings were based upon the coal tar and asphalt mastics. Some low cost materials were included in the tests to evaluate the economics of their use as compared with the more expensive paints. Four proprietary materials of a rust-proofing nature in common use by the railroads and an asphalt automobile underbody coating were used.

As a control to test the effectiveness of the change in paints, a standard paint system was included on each bridge. This system consisted of a proprietary paint containing red lead, lead chromate, iron oxide and extender in a linseed oil vehicle in the primer, with a conventional black topcoat.

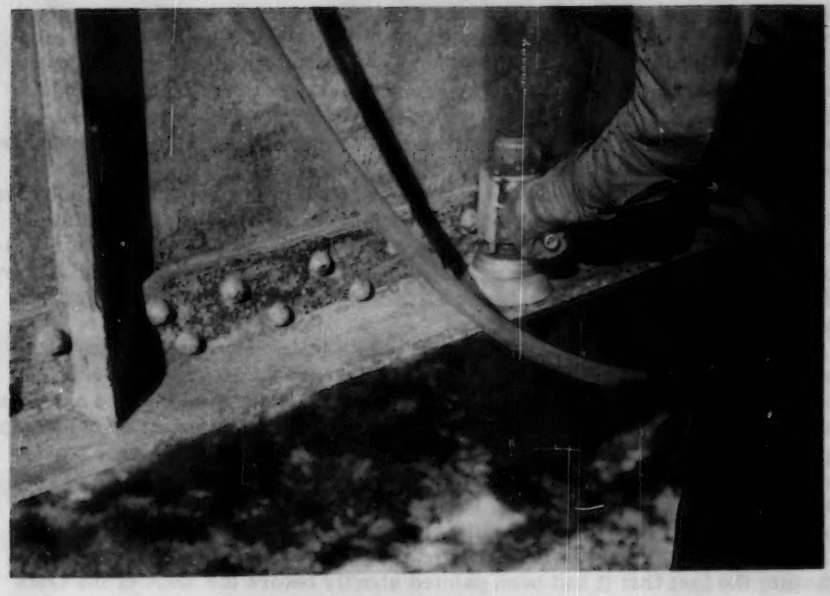

Fig. 10. Power wire brushing of steel surfaces.

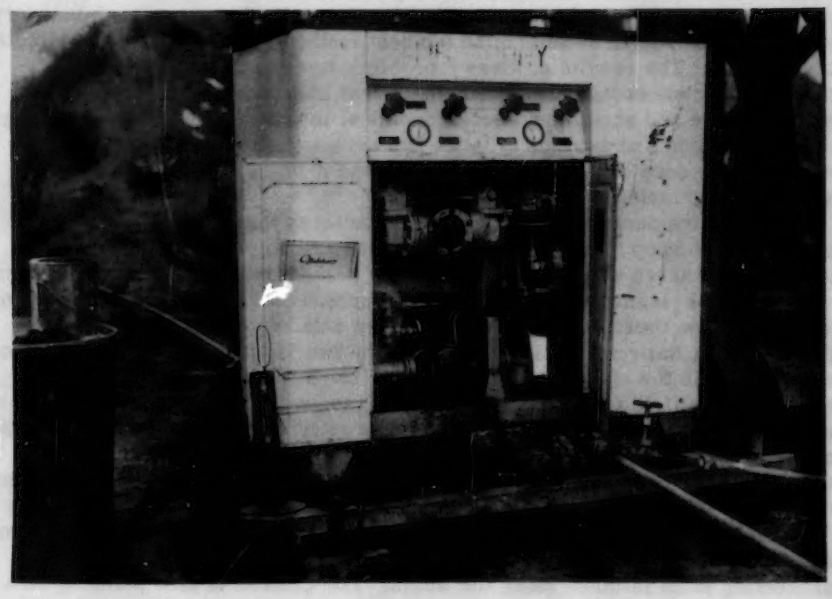

Fig. 11. View of steam cleaner.

The bridges were inspected after one year of test service and it appeared that all the paints and coatings on the sand blasted surfaces were in perfect condition except for the control paint of red lead, lead chromate and iron oxide where slight rusting on the floorbeam web was obvious. All of the paints and coatings on the hand cleaned surfaces are performing extremely well, with the exception of the control paint and the two proprietary rust-proofing greases. The two rust preventive compounds were complete failures with bad scaling and rusting.

The paint and coatings on the bridges were again inspected after about two years' service and it was found that the synthetic resin paints—such as the vinyls, phenolics, alkyds and chlorinated rubbers are still in excellent condition on the sand blasted surfaces, but there is some evidence of initial failure in these paints on the hand cleaned surfaces. However, the conventional paints are in poor condition.

The advantage of the synthetic resin paints for steel surfaces exposed to brine is apparent from the results of the Missouri Pacific tests on sand-blasted surfaces on surfaces that have been thoroughly hand cleaned and then steam cleaned to remove the salt. The question was then asked by bridge engineers if the synthetic resins could be used on hand and power tool cleaned surfaces without the steam cleaning. In order to answer this question, two bridges on the Seaboard Airline Railroad near Charleston, South Carolina, were selected. These bridges, like the Missouri Pacific bridges, carry a large number of refrigerator cars and the steel was in very bad condition, despite the fact that it had been painted shortly before the start of the tests with a proprietary paint for use over rust.

The use of such paints over hand or power tool cleaned, brine-contaminated surfaces was considered questionable unless something was done to neutralize the effects of the brine. Accordingly, extensive laboratory tests were conducted to determine the best method of neutralizing the effects of the brine. The results of these laboratory tests indicated that the phosphoric acid cleaners and emulsifiable solvent cleaners remove most of the brine residue and should be more economical to use than the steam cleaning.

The cleaning and painting of these two bridges using various synthetic resins, were done during the fall of 1955, and it is, of course, too early to state any conclusions.

The relative performance of painted structures that are cleaned and primed in the shop as compared to those that are shipped and erected unpainted, weathered about a year to remove mill scale by rusting and then hand or power tool cleaned and painted has been discussed for years. In order to secure data on these two methods, arrangements have been made with the Pennsylvania Railroad to clean and paint the two 75 ft. 6 in. girders of a two-span bridge in the shop. Four different primers will be used on the two girders. The field painting, consisting of a second primer coat and two finish coats will be completed as soon as possible after erection. The two girders of the second span will be erected without any paint and then in about nine months they will be cleaned and painted, using the same paints as those used on the first span.

In addition to the many field tests now underway, the Council is conducting extensive laboratory tests of welded joints to determine the best method of preventing paint failures along the welds. The Council is also planning on a laboratory investigation to evaluate all of its recommended paint systems and comparative evaluations with the outstanding proprietary products.

CONCLUSION

In conclusion, we feel that the Steel Structures Painting Council, has done much to reduce the annual loss due to corrosion and should be able to reduce this loss still more by further research.

Paper 1101 ST 6

Journal of the
STRUCTURAL DIVISION
Proceedings of the American Society of Civil Engineers

ANALYSIS OF RIBBED DOMES WITH POLYGONAL RINGS

Tsze-Sheng Shih[a]
(Proc. Paper 1101)

SYNOPSIS

This paper presents methods of analysis of ribbed domes for both fully symmetrical loading and for a general load condition. The members of the structure are considered to be rigidly connected as exists in most practical construction. Under a fully symmetrical loading the dome is analyzed by direct application of Castigliano's theorem. For a general load condition on the dome, the internal forces and displacements are determined by superimposing the effects of separate loads on individual ribs. The latter solution is made by combining the cases of two corresponding opposite ribs under antisymmetrical and symmetrical load. In the analysis of domes for these particular loading conditions, (symmetrical and antisymmetrical) auxiliary force systems are used to control translations of the joints and, for the symmetrical loads, the numerical solution is much simplified by the use of finite trigonometric series.

The methods of analysis presented in this paper can be applied to domes constructed of rib and ring elements either curved or polygonal in shape. Numerical examples are presented to illustrate the application of the methods of solution.

INTRODUCTION

A dome is a structural unit that is round or polygonal in plan and, on a vertical section through the axis of the dome, it may be curved or polygonal, usually the former as shown in Figs. 1 and 2. Most domes have a circular or polygonal base and are of a circular shape on a section through the vertical axis.

According to the type of construction domes may be divided into two classes; shell domes and ribbed domes. The former is made of a thin membrane as shown in Fig. 1, while the latter is made with a framework consisting

Note: Discussion open until April 1, 1957. Paper 1101 is part of the copyrighted Journal of the Structural Division of the American Society of Civil Engineers, Vol. 82, No. ST 6, November, 1956.

[a]Prof. of Civ. Eng., Tsing Hwa Univ., Peking, China.

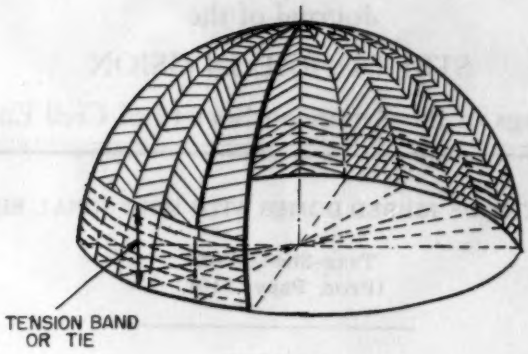

FIG. 1

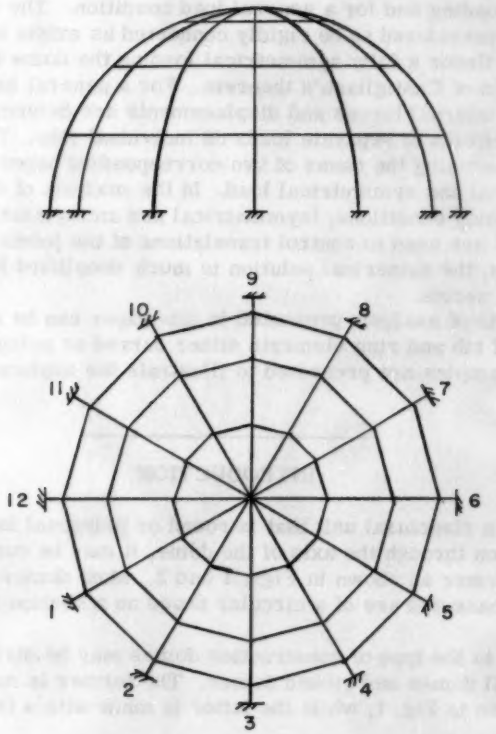

FIG. 2

of ribs in the meridian planes as illustrated in Fig. 2 connected by a series of horizontal rings.

Domes are now constructed either of reinforced concrete or of steel. Of the domes now existing in the world most shell domes are of reinforced concrete, while ribbed domes are made of either reinforced concrete or steel. A majority of the large domes are of the ribbed type, which may be due to the fact, that the form-work for large reinforced concrete shell domes is comparatively expensive and difficult to construct. However, in the United States, as a consequence of the fact that methods for the practical analysis of shell domes have been greatly improved in the past twenty years over the design of ribbed domes, many of the domes built have been of the shell type. Hence, improvement of analytical methods for the accurate design of ribbed domes is necessary if they are to be used more extensively.

Nomenclature

The nomenclature which will be used is as follows:

A = Cross-sectional area of ribs

A_i = Cross-sectional area of ring i

C = EI/R^3

E = Tensile modulus of material in ribs and rings

G = Shear modulus of material in ribs and rings

I = Moment of inertia of section of ribs

I_i = Moment of inertia of section of ring i

i = a, b, c . . . m, refer to number of rings

j = 1, 2, 3 . . . n, refer to number of ribs

K = AE/R; $K_i = A_iE/R_i$

k = 1, 2, 3 . . . , refer to harmonic components

ℓ_i = Length of sides of ring i

M = Bending moment in rib or ring

N = Axial force in rib or ring

Q = Shear force in rib or ring

R = Radius of ribs

R_i = Radius of ring i

r = Radius of gyration of rib cross-section

r_i = Radius of Gyration of cross section of ring i

V = Tangential displacement of joint in horizontal plane

W = Radial displacement of joint in horizontal plane

α = One-half the angle between meridian planes of two adjacent ribs

ρ = $(R/r)^2$ is a measure of slenderness of ribs

$\rho_i = (R_i/r_i)^2$ is a measure of slenderness of ring i

Further symbols will be defined as they are used.

Dischinger's Method of Analysis

During the past thirty years, the most popular method for the analysis of ribbed domes has been the one presented by Professor F. Dischinger in 1928.[1] For rigidly connected dome under fully symmetrical load, Dischinger assumed that the dome is statically determinate. By reason of axial symmetry, he considered only the action of one rib and assumed that each rib is hinged at the joints where the horizontal rings are connected. By removing the rings a curved member is obtained which is subjected to the forces shown in Fig. 3a. To illustrate the application of this method of analysis, a dome of four rings, including the base ring, is used. The bending moments in any individual arch rib due to the applied load q are designated by M_{ob}, M_{oc}, and M_{od} (Fig. 3b).

Then the horizontal forces at the joints are determined by assuming zero moment at points b, c, and d.

$$F_a = \frac{M_{ob}}{h_1}$$

$$F_b = \frac{M_{oc} - F_a(h_1 + h_2)}{h_2}$$

$$F_c = \frac{M_{od} - F_a(h_1 + h_2 + h_3) - F_b(h_2 + h_3)}{h_3}$$

and $$F_d = -(F_a + F_b + F_c).$$

Having the horizontal thrusts F, the ring forces are obtained from the relation

$$N = \frac{F}{2 \sin \alpha},$$

which is the component of the F thrust in the direction of the rings (Fig. 3c).

In the above analysis the axis of the rib and the line of pressure will coincide at the joints only. The ordinates to the line of pressure between the joints are given by the following expressions, derived by simple statics (Fig. 3d)

$$Y_{ab} = \frac{M_o}{F_a}$$ between rings a and b.

$M_o = \Sigma M$ to right of section.

$$Y_{bc} = \frac{M_o + F_b h_1}{F_a + F_b}$$ between rings b and c.

1. F. Dischinger, Handbuch für Eisenbetonbau, (dritte Auflage; Berlin: Verlag von Wilhelm Ernst & Sohn, 1928), XII.

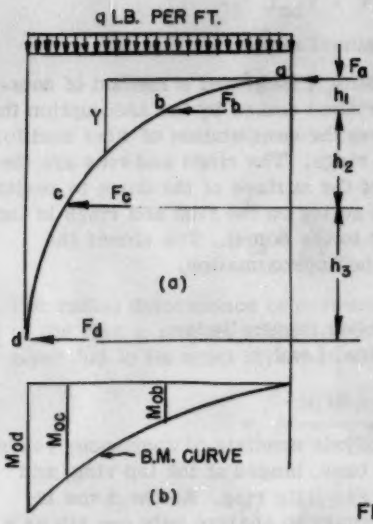

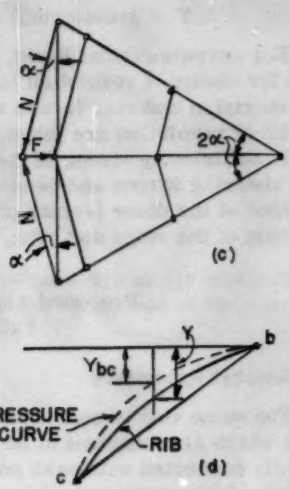

FIG. 3

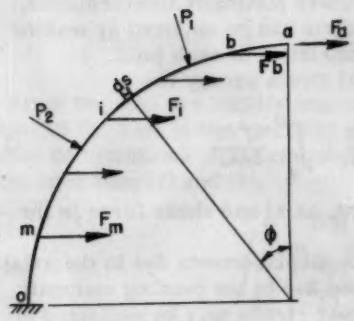

FIG. 4

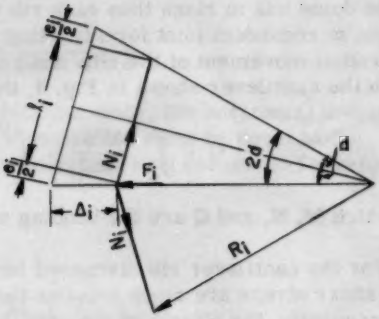

FIG. 5

$$Y_{cd} = \frac{M_o + F_b h_1 + F_c(h_1 + h_2)}{F_a + F_b + F_c}$$ between rings c and d.

The bending moments at any point in the rib, as for example between joints b and c, are

$$M = (F_a + F_b)(Y - Y_{bc}).$$

Y = geometrical ordinate to actual rib.

For unsymmetrical loads, i.e., wind loads, Dischinger's method of solution for shells of revolution is applied to ribbed domes by the assumption that the meridian and ring forces resulting from the computation of wind load for shells of revolution are taken by ribs and rings. The rings and ribs are then made sufficiently strong in the direction of the surface of the dome to resist any shearing forces and bending moments acting on the ribs and rings in the surface of the dome (vector perpendicular to the dome). The closer the spacing of the rings and ribs, the closer the approximation.

Proposed Analysis of Ribbed Domes Under Fully Symmetrical Load

1. General Procedure

The dome that is considered in this analysis consists of continuous curved ribs which are assumed to be fixed at the base, hinged at the top ring, and rigidly connected with each polygonal intermediate ring. As the dome is under a fully symmetrical load, it is necessary to analyze only one rib as a cantilever since each rib is held in equilibrium by the horizontal ring forces at each joint as shown in Fig. 4. Under this loading condition, the rings remain in a horizontal plane and only axial stresses exist in the ring members. If the dome has m rings then each rib is m times statically indeterminate. These m redundant joint forces acting on the rib can be obtained by making the radial movement of the ribs and rings consistent at each joint.

In the cantilever shown in Fig. 4, the total strain energy is

$$U = \int_a^o \frac{M^2 ds}{2EI} + \int_a^o \frac{N^2 ds}{2AE} + \int_a^o \frac{Q^2 ds}{2AG} \qquad (1)$$

in which M, N, and Q are the bending moment, axial and shear force in the rib.

For the cantilever rib discussed here, the displacements due to the axial and shear stress are much smaller than those due to the bending moments. Consequently, the effects of the axial and shear stress may be neglected in the rib. Then equation 1 reduces to the simple expression

$$U = \int_a^o \frac{M^2 ds}{2EI}$$

By application of Castigliano's theorem, the horizontal displacements in the meridian plane at joints a, b. . . . . m are

$$\Delta_a = \frac{\partial U}{\partial F_a} = \int_a^o \frac{M \frac{\partial M}{\partial F_a} ds}{EI}$$

$$\Delta_b = \frac{\partial U}{\partial F_b} = \int_a^o \frac{M \frac{\partial M}{\partial F_b} ds}{EI} \qquad (2)$$

. . . . . .

$$\Delta_m = \frac{\partial U}{\partial F_m} = \int_a^o \frac{M \frac{\partial M}{\partial F_m} ds}{EI}$$

The radial deformation of corners of the polygonal rings as for instance, Δ_i of the ring i, may be computed by considering the elongation of the ring member due to its axial stress N_i (Fig. 5) is

$$e_i = \frac{N_i 2R_i \sin \alpha}{A_i E}$$

As $$N_i = \frac{F_i}{2 \sin \alpha} \qquad (3)$$

therefore $$e_i = \frac{F_i R_i}{A_i E}$$

and $$\Delta_i = \frac{e_i}{2 \sin \alpha} = \frac{F_i R_i}{2A_i E \sin \alpha} \qquad (4)$$

Since the ribs are rigidly connected with the rings, the horizontal displacements of the ribs in the meridian plane at each joint must be equal to the radial deformations of the corresponding polygonal ring corners. Therefore, from equations (2) and (4),

$$\int_a^o \frac{M \frac{\partial M}{\partial F_a} ds}{EI} = \frac{F_a R_a}{2A_a E \sin \alpha}$$

$$\int_a^o \frac{M \frac{\partial M}{\partial F_b} ds}{EI} = \frac{F_b R_b}{2A_b E \sin \alpha} \qquad (5)$$

. . . . . .

$$\int_a^o \frac{M \frac{\partial M}{\partial F_m} ds}{EI} = \frac{F_m R_m}{2A_m E \sin \alpha}$$

By solving these m simultaneous equations, the m redundant horizontal forces F_a, F_b . . . . . F_m are obtained. The bending moments, axial and shear forces in the ribs are then easily calculated by statics and the axial forces in the polygonal rings are determined by equation (3).

If the ribs are assumed to be fixed at the top ring, the proposed method can also be applied. In this case one more redundant moment exists at the top of the rib, which can be determined by use of one more strain condition which is based on the equality of the slopes at the crown point of all ribs.

2. Neglect of Axial Strains of Rings

If the axial strains of the polygonal rings are neglected, i.e., the deformations of their corners Δ_a, Δ_b . . . . . Δ_m are equal to zero, then equation (5) reduces to the expression

$$\int_a^o \frac{M \frac{\partial M}{\partial F_a} ds}{EI} = 0$$

$$\int_a^o \frac{M \frac{\partial M}{\partial F_b} ds}{EI} = 0 \qquad (6)$$

. . . . . .

$$\int_a^o \frac{M \frac{\partial M}{\partial F_m} ds}{EI} = 0$$

In example 1, which considers a dome with 12 ribs and 4 rings under fully symmetrical uniform load, the difference between the horizontal joint forces in the dome when the axial strains of rings are considered and when they are neglected is 2.6%, 21.8%, 9.2%, and 5.4% for the forces F_a, F_b, F_c, and F_d respectively. These figures show that neglect of the axial strains of rings may result in a considerable error.

Example 1

To illustrate the use of the equations derived above, let us assume a spherical ribbed dome which is made of 12 continuous ribs and 4 polygonal rings and which is loaded with a fully symmetrical uniform load of q pound per horizontal linear foot on each rib. The dome is so constructed, that the ribs are fixed at the base, rigidly connected with the intermediate rings, and hinged at the top ring which is assumed to have no axial strains.

$$K = \frac{AE}{R} = \frac{A_bE}{R_b} = \frac{A_cE}{R_c} = \frac{A_dE}{R_d}$$

and

$$\rho = \left(\frac{R}{r}\right)^2 = \left(\frac{R_b}{r_b}\right)^2 = \left(\frac{R_c}{r_c}\right)^2 = \left(\frac{R_d}{r_d}\right)^2 = 10{,}000$$

Let us consider any one rib as shown in Fig. 6. Then by equation (5) the following four simultaneous equations are obtained:

$$\begin{aligned}
.35620F_a + .31304F_b + .19807F_c + .06460F_d &= -.22603_qR \\
.31304F_a + .27699F_b + .17808F_c + .05895F_d &= -.19643_qR \\
.19807F_a + .17808F_b + .12101F_c + .04287F_d &= -.11949_qR \\
.06460F_a + .05895F_b + .04287F_c + .01863F_d &= -.03615_qR
\end{aligned}$$

These simultaneous equations can be easily solved by the square root method which is detailed in Appendix A, and their solution is

$$F_a = -1.01062_qR \qquad F_b = +.18728_qR$$

$$F_c = +.25454_qR \qquad F_d = +.38560_qR$$

If the axial strains of the rings are neglected, then by equation (6) the following four simultaneous equations are obtained:

$$\begin{aligned}
.35620F_a + .31304F_b + .19807F_c + .06460F_d &= -.22603_qR \\
.31304F_a + .27718F_b + .17808F_c + .05895F_d &= -.19643_qR \\
.19807F_a + .17808F_b + .12120F_c + .04287F_d &= -.11949_qR \\
.06460F_a + .05895F_b + .04287F_c + .01882F_d &= -.03615_qR
\end{aligned}$$

and the solution of these equations gives

$$F_a = -.98408_qR \qquad F_b = +.14653_qR$$

$$F_c = +.27797_qR \qquad F_d = +.36486_qR$$

According to Dischinger's method described in Part I, the horizontal forces acting on the ribs are

$$F_a = -.96193_qR \qquad F_b = +.14642_qR$$

$$F_c = +.27063_qR \qquad F_d = +.35353_qR$$

As the horizontal joint forces in the meridianal plane acting on the rib have been ascertained, then the shear and axial force and bending moment at any section of the rib can be determined by statics.

3. Comparison of Proposed Method with Dischinger's Analytical Method

For the dome under a fully symmetrical load, Dischinger assumed that all the members of the dome are connected with hinges, while in example 1 the ribs are assumed to be; continuous from base to top, restrained at the base, hinged at the top ring, and rigidly connected with the intermediate rings. A comparison of the horizontal forces acting on the rib, i.e., of the ring stresses, between the results computed by Dischinger's method and the proposed method as given in example 1 shows variations of 4.8%, 21.8%, 6.3%, and 8.3% for the forces F_a, F_b, F_c, and F_d respectively. From these figures we can see that Dischinger's method, assuming the joints connected with hinges, results in a considerable discrepancy for the ring axial stresses. Moreover, for the bending moment in the ribs as shown in Table 1 and Fig. 7 Dischinger's method gives large discrepancies as compared with the more exact solution by the proposed method. Thus for a safe and economical design in practical construction, the continuity of the structure should be considered.

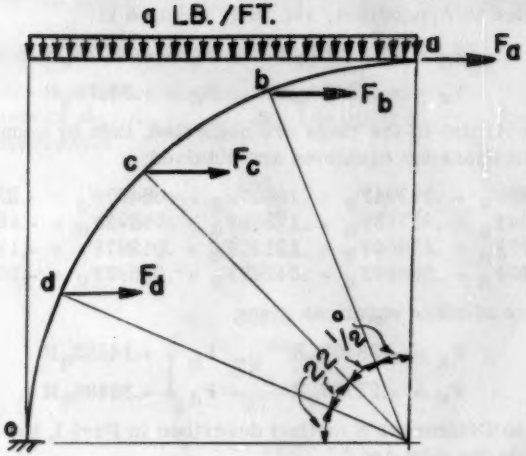

FIG. 6

TABLE 1

VALUES OF BENDING MOMENTS IN THE RIBS (IN qR^2 ft-lb)

Point	By Proposed Method		By
	Consider Ring Strain	Neglect Ring Strain	Dischinger's Method
a	0	0	0
1	+0.000057	-0.000071	-0.000177
2	+ .000384	- .000126	- .000551
3	+ .001383	+ .000240	- .000713
b	+ .003707	+ .001686	0
4	+ .000367	- .001058	- .003668
5	- .001316	- .002024	- .005746
6	- .000086	+ .000035	- .004974
c	+ .005404	+ .006462	0
7	- .002012	- .001624	- .009154
8	- .004071	- .004411	- .013099
9	- .000484	- .000532	- .010458
d	+ .013162	+ .011228	0
10	- .001002	- .001872	- .013413
11	- .006669	- .006443	- .018304
12	- .003113	- .001769	- .013956
o	+0.010047	+0.012517	0

Domes with Two Opposite Ribs Under Antisymmetrical Loads

1. Translation and Deformation of Rings

When a dome is subjected to antisymmetrical loads on two opposite ribs as shown in Fig. 8b the rings should be made as stiff as possible in the horizontal plane by placing the major axis of the ring cross section vertical. According to Dr. El-Schasly's investigation[2] the lateral bending stiffness of the members may then be neglected, and also the rings may be assumed to translate only horizontally. This condition is practically true in the case of antisymmetrical loads on ribs 12 and 6 (Fig. 8b), since the horizontal translation of the rings is equal to the algebraic sum of the translations of the respective rings in the domes with the loads on ribs 12 and 6 considered

2. El-Sayed El-Schasly, "Biegungsspannungen und Stabkräfte in Schwelderkuppeln nach Theorie und Modellversuch," Mitteilungen aus dem Institut für Baustatik, XIII (1943).

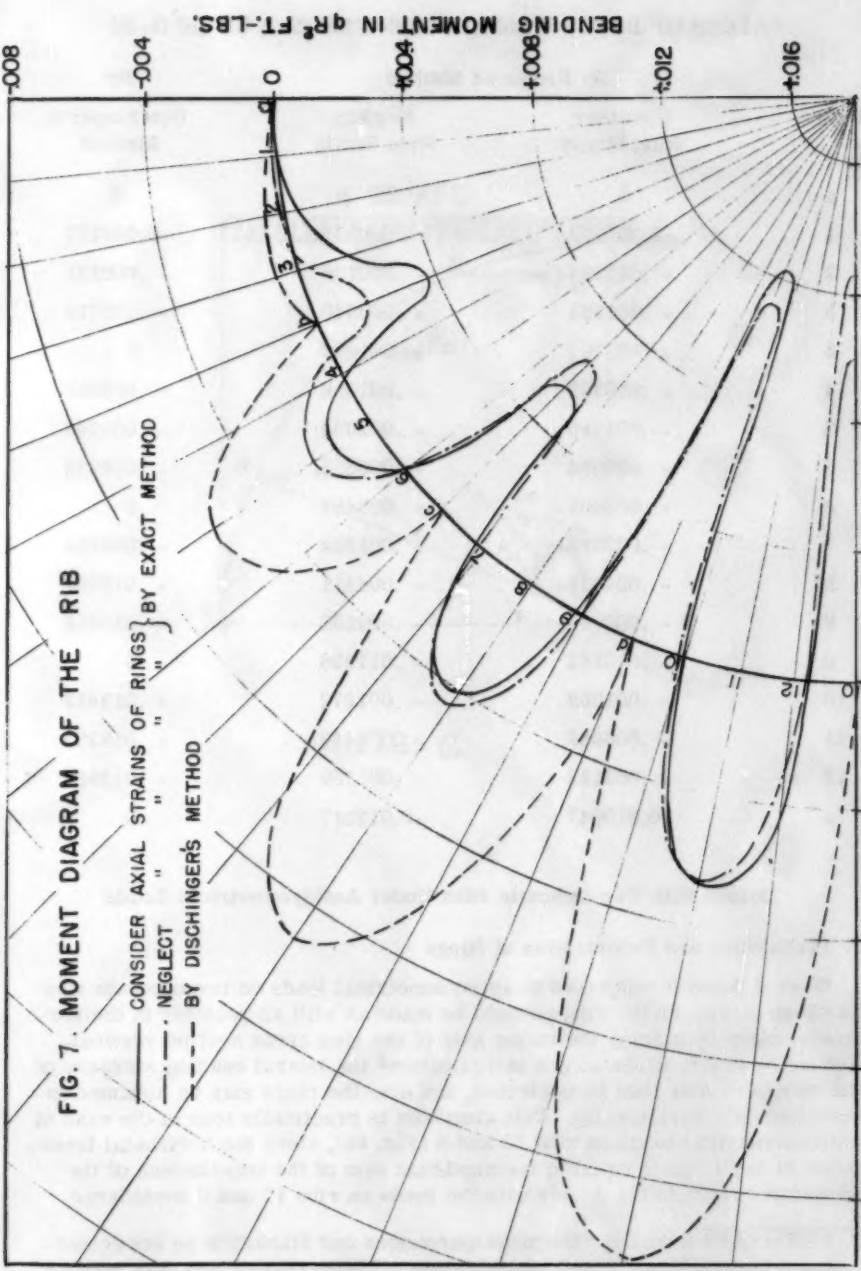

FIG. 7. MOMENT DIAGRAM OF THE RIB

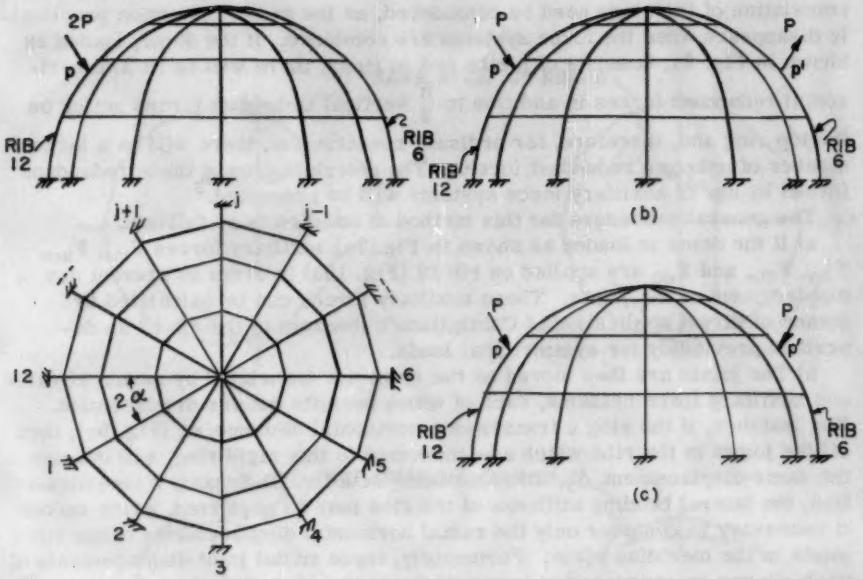
2P
p
RIB 12
RIB 6
P
p
P'
p'
RIB 12
RIB 6
(b)
j+1
j
j-1
12
6
1
5
2
4
3
2α
P
p
P
p'
RIB 12
RIB 6
(c)
(a)

FIG. 8

separately as shown in Figs. 9c and 9d. The radial distortions of the rings as indicated in Figs. 9e and 9f practically disappear when combined as they are of opposite sign. Hence the effect of ring deformation is sufficiently small as compared with that of rigid body translation, that it may be neglected and, for this reason, the rings when the dome is subjected to antisymmetrical loads may be considered as rigid elements translating only horizontally. One exception is the top ring where the vertical displacement is also considered (See Appendix B).

2. Proposed Method of Analysis

For the reasons just discussed a dome with two opposite ribs under antisymmetrical loads (Fig. 8b), may be analyzed by superposition of the effects of separate loads on the corresponding ribs as shown in Fig. 9. Only the translation of the rings need be considered, as the radial distortion practically disappears when the force systems are combined. If the dome, loaded as shown in Fig. 9a, consists of n ribs and m rings, there will be (n/2)m horizontal redundant forces in addition to $\frac{n}{2}$ vertical redundant forces acting on the top ring and, therefore, for ordinary construction, there will be a large number of unknown redundant forces. The determination of these redundant forces by use of auxiliary force systems will be presented.[3]

The general procedure for this method of solution is as follows:

a) If the dome is loaded as shown in Fig. 9a, auxiliary forces F_{vo}, F_{ao}, F_{bo}, F_{co}, and F_{do} are applied on rib 12 (Fig. 10a) in order to prevent any displacement of the joints. These auxiliary forces can be calculated by means of direct application of Castigliano's theorem to the rib 12 as described previously for symmetrical loads.

b) The joints are then moved as the rings are translated by means of various auxiliary force systems, each of which permits but one displacement. For instance, if the ring c translates a horizontal distance Δ_3 (Fig. 9c), then all the joints in the ribs which are connected to this rigid ring, will receive the same displacement Δ_3. In accordance with Dr. El-Schasly's investigation, the lateral bending stiffness of the ribs may be neglected, which makes it necessary to consider only the radial horizontal displacements of the rib joints in the meridian plane. Fortunately, these radial joint displacements of each rib can be expressed in terms of the angle, (Fig. 8a) which the plane of the rib makes with that of the loaded rib. For example, $\Delta_3 \cos 2\alpha$, $\Delta_3 \cos 4\alpha$ . . . . . $\Delta_3 \cos 2_{j\alpha}$ . . . . . $\Delta_3 \cos 2\pi$, are the horizontal joint displacements in meridian plane for ribs 1, 2 . . . . j . . . . 12 respectively. Since all ribs are identical, it is sufficient to analyze only one rib, such as rib 12, with different auxiliary force systems for different displacements Δ_1, Δ_2, Δ_3, Δ_4, and Δ_v as illustrated in Fig. 10. Each auxiliary force system can be expressed in terms of one displacement Δ by Castigliano's theorem, and the summation of all auxiliary force systems can be expressed as functions of the various Δ values. The auxiliary force systems for the other ribs can be obtained directly by multiplication of the forces for the rib 12 by functions of the corresponding angle, that the particular rib makes with rib 12. The vertical displacement of the top ring will be discussed in Appendix B.

3. L. C. Maugh, Statically Indeterminate Structures, New York: John Wiley & Sons, Inc., 1946.

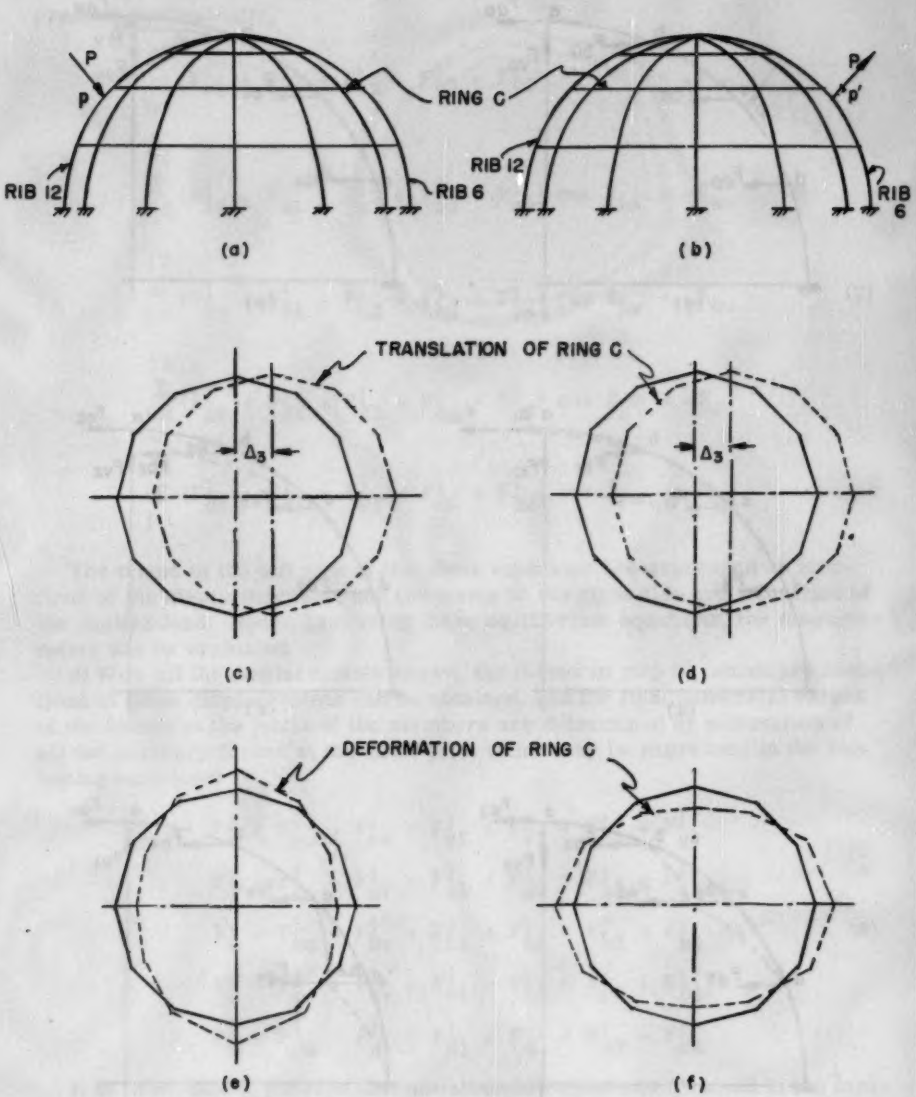
P
p
RING C
RIB 12
RIB 6
(a)
P
p'
RING C
RIB 12
RIB 6
(b)
TRANSLATION OF RING C
Δ3
(c)
Δ3
(d)
DEFORMATION OF RING C
(e)
(f)

FIG. 9

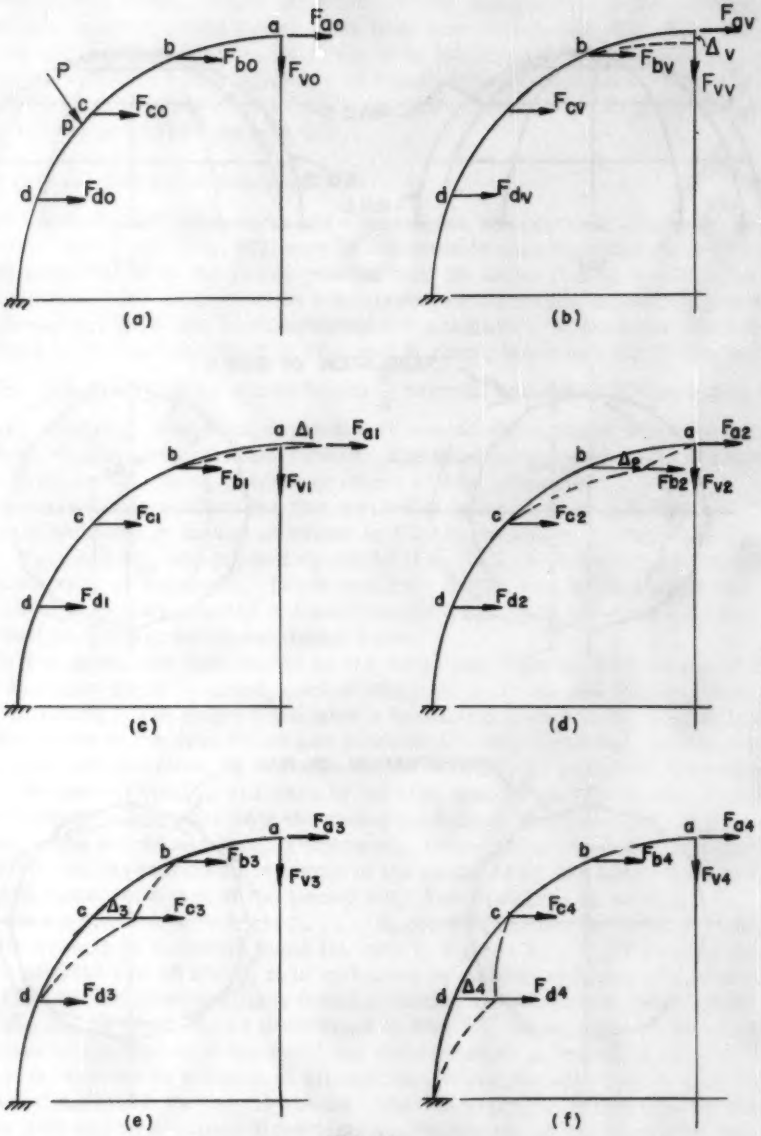
a
b
c
d
P
p
F_{ao}
F_{bo}
F_{vo}
F_{co}
F_{do}
(a)
F_{av}
Δ_v
F_{bv}
F_{vv}
F_{cv}
F_{dv}
(b)
Δ_1
F_{a1}
F_{b1}
F_{v1}
F_{c1}
F_{d1}
(c)
F_{a2}
Δ_2
F_{b2}
F_{v2}
F_{c2}
F_{d2}
(d)
F_{a3}
F_{b3}
F_{v3}
Δ_3
F_{c3}
F_{d3}
(e)
F_{a4}
F_{b4}
F_{v4}
F_{c4}
Δ_4
F_{d4}
(f)

FIG. 10

c) To satisfy the necessary equilibrium conditions of the individual rings, the summation of all auxiliary forces for the ribs must be equal to the restraining forces due to applied load on the rib 12, shown in Fig. 10a, or expressed algebraically,

$$\sum_{j=1}^{12} (F^j_{vv} + F^j_{v1} + F^j_{v2} + F^j_{v3} + F^j_{v4}) = -F_{vo}$$

$$\sum_{j=1}^{12} (F^j_{av} + F^j_{a1} + F^j_{a2} + F^j_{a3} + F^j_{a4}) \cos 2_{j\alpha} = -F_{ao}$$

$$\sum_{j=1}^{12} (F^j_{bv} + F^j_{b1} + F^j_{b2} + F^j_{b3} + F^j_{b4}) \cos 2_{j\alpha} = -F_{bo} \qquad (7)$$

$$\sum_{j=1}^{12} (F^j_{cv} + F^j_{c1} + F^j_{c2} + F^j_{c3} + F^j_{c4}) \cos 2_{j}\alpha = -F_{co}$$

$$\sum_{j=1}^{12} (F^j_{dv} + F^j_{d1} + F^j_{d2} + F^j_{d3} + F^j_{d4}) \cos 2_{j\alpha} = -F_{do}$$

The terms in the left side of the above equations are expressed as functions of the displacement Δ, and the terms in the right side are a function of the applied load. Hence by solving these equilibrium equations, the displacements can be evaluated.

d) With all the displacements known, the forces in step b), which are functions of these displacements can be obtained, and the final numerical values of the forces at the joints of the members are determined by summation of all the auxiliary forces at the same joint which may be expressed in the following equations:

$$\begin{aligned}
F^j_v &= F^j_{vo} + F^j_{vv} + F^j_{v1} + F^j_{v2} + F^j_{v3} + F^j_{v4} \\
F^j_a &= F^j_{ao} + F^j_{av} + F^j_{a1} + F^j_{a2} + F^j_{a3} + F^j_{a4} \\
F^j_b &= F^j_{bo} + F^j_{bv} + F^j_{b1} + F^j_{b2} + F^j_{b3} + F^j_{b4} \qquad (8) \\
F^j_c &= F^j_{co} + F^j_{cv} + F^j_{c1} + F^j_{c2} + F^j_{c3} + F^j_{c4} \\
F^j_d &= F^j_{do} + F^j_{dv} + F^j_{d1} + F^j_{d2} + F^j_{d3} + F^j_{d4}
\end{aligned}$$

It is important to observe that simultaneous equations obtained in the foregoing procedure will usually be the type which can be conveniently solved by the square root method, which is explained in detail in the appendix.

3. Application of the Proposed Method

The most important antisymmetrical loading on a dome is produced by wind pressure, inasmuch as it is assumed that the pressure on the windward side is

equal to the suction on the leeward, or diametrically opposite side. In general, the distribution of wind pressure on a dome is based upon a sine law[4] (Fig. 11).

$$W = W_o \sin \phi \sin \beta$$

in which

W = Wind pressure on an element of dome surface.
W_o = Wind pressure on vertical wall.

In practical design, if a lantern is built on the upper part of the dome, it may be analyzed according to the general procedure by considering different vertical displacements at the corners of the top ring. If the dome has no lantern, the top ring, in general, is comparatively very small, and, thus it may be assumed as a hinge at the crown.

Example 2

To illustrate the use of equations 7 and 8, let us assume the ribbed dome that was used in Example 1 to be loaded with an antisymmetrical load on ribs 12 and 6 (Fig. 12a).

In solving this problem, we may, at first, analyze the dome with unsymmetrical load on rib 12 (Fig. 12b) according to the described procedure.

a) By direct application of Castigliano's theorem to rib 12 restrained by the forces F_{ao}, F_{bo}, F_{co}, F_{do}, and F_{vo} as shown in Fig. 10a, in which the concentrated load P is replaced by a uniform load q lb. per ft., we may obtain the following equations:

$$\begin{aligned}
.35620F_{ao} + .31304F_{bo} + .19807F_{co} + .06460F_{do} + .50000F_{vo} &= -.22603qR \\
.31304F_{ao} + .27718F_{bo} + .17808F_{co} + .05895F_{do} + .42677F_{vo} &= -.19643qR \\
.19807F_{ao} + .17808F_{bo} + .12120F_{co} + .04287F_{do} + .25000F_{vo} &= -.11949qR \quad (a) \\
.06460F_{ao} + .05895F_{bo} + .04287F_{co} + .01882F_{do} + .07322F_{vo} &= -.03615qR \\
.50000F_{ao} + .42677F_{bo} + .25000F_{co} + .07322F_{do} + .78540F_{vo} &= -.33333qR
\end{aligned}$$

b) If any rib, for instance rib 12, is displaced a horizontal distance Δ_1 at joint a (Fig. 10c) then, by Castigliano's theorem we obtain the following equations:

$$\begin{aligned}
.35620F_{a1} + .31304F_{b1} + .19807F_{c1} + .06460F_{d1} + .50000F_{v1} &= C\Delta_1 \\
.31304F_{a1} + .27718F_{b1} + .17808F_{c1} + .05895F_{d1} + .42677F_{v1} &= 0 \\
.19807F_{a1} + .17808F_{b1} + .12120F_{c1} + .04287F_{d1} + .25000F_{v1} &= 0 \quad (b) \\
.06460F_{a1} + .05895F_{b1} + .04287F_{c1} + .01882F_{d1} + .07322F_{v1} &= 0 \\
.50000F_{a1} + .42677F_{b1} + .25000F_{c1} + .07322F_{d1} + .78540F_{v1} &= 0
\end{aligned}$$

in which $C = EI/R^3$

Similarly, for the displacements Δ_2, Δ_3, Δ_4, and Δ_v (Figs. 10d, e, f, and b) there will be four other groups of equations, of which the coefficients of the terms in the left side are same as those in equations a and b, but the

4. S. Timoshenko, Theory of Plates and Shells, (New York: McGraw-Hill Book Co., 1940).

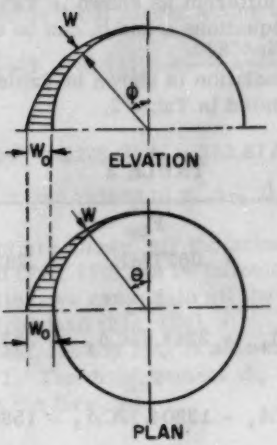

FIG. 11

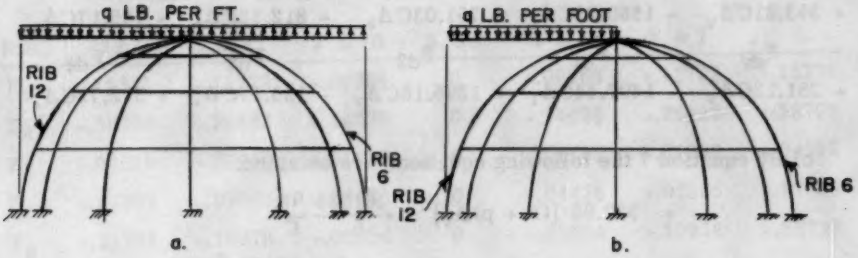

FIG. 12

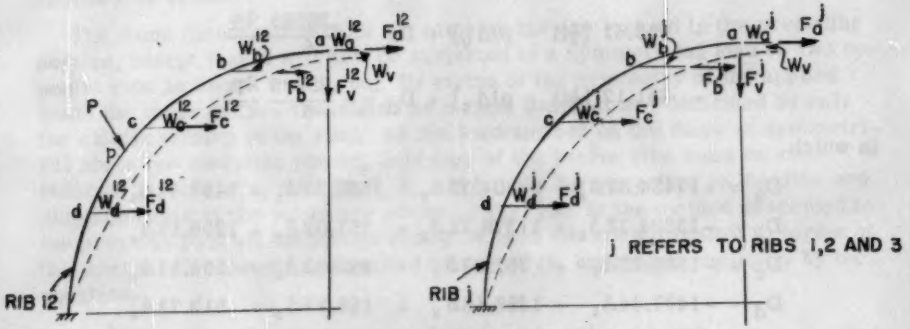

FIG. 13

terms in the right side are different as shown in Table 9. These six groups of equations, including the equations a and b, can be easily solved by the square root method.

The whole procedure of solution is shown in Table 9, and the solution for all the auxiliary forces is listed in Table 2.

TABLE 2

F_{vo}	F_{ao}	F_{bo}	F_{co}	F_{do}
$-.01835qR$	$-.88059qR$	$+.06777qR$	$+.26555qR$	$+.35605qR$
F_{vv}	F_{v1}	F_{v2}	F_{v3}	F_{v4}
$+522.98C\Delta_v$	$-2949.42C\Delta_1$	$+2245.05C\Delta_2$	$+353.81C\Delta_3$	$+251.12C\Delta_4$
F_{av}	F_{a1}	F_{a2}	F_{a3}	F_{a4}
$-2949.42C\Delta_v$	$+17424.89C\Delta_1$	$-13804.32C\Delta_2$	$-1580.23C\Delta_3$	$-1497.44C\Delta_4$
F_{bv}	F_{b1}	F_{b2}	F_{b3}	F_{b4}
$+2245.05C\Delta_v$	$-13804.32C\Delta_1$	$+11379.22C\Delta_2$	$+751.03C\Delta_3$	$+1295.16C\Delta_4$
F_{cv}	F_{c1}	F_{c2}	F_{c3}	F_{c4}
$+353.81C\Delta_v$	$-1580.23C\Delta_1$	$+751.03C\Delta_2$	$+812.32C\Delta_3$	$-155.17C\Delta_4$
F_{dv}	F_{d1}	F_{d2}	F_{d3}	F_{d4}
$+251.12C\Delta_v$	$-1497.44C\Delta_1$	$+1295.16C\Delta_2$	$-155.17C\Delta_3$	$+512.72C\Delta_4$

c) By equation 7 the following equations are obtained:

$$
\begin{aligned}
+\ 522.98\ [(1+p)\Delta_v] &= +\frac{.01835}{6}\frac{q_R}{C}\\
-\ 2949.42\ [\tfrac{1}{2}(1-p)\Delta_v] + D_a &= +\frac{.88059}{6}\frac{q_R}{C}\\
+\ 2245.05\ [\tfrac{1}{2}(1-p)\Delta_v] + D_b &= -\frac{.06777}{6}\frac{q_R}{C}\\
+\ 353.81\ [\tfrac{1}{2}(1-p)\Delta_v] + D_c &= -\frac{.26555}{6}\frac{q_R}{C}\\
+\ 251.12\ [\tfrac{1}{2}(1-p)\Delta_v] + D_d &= -\frac{.35605}{6}\frac{q_R}{C}
\end{aligned}
\qquad (c)
$$

in which

$$
\begin{aligned}
D_a &= +17424.89\Delta_1 - 13804.32\Delta_2 - 1580.23\Delta_3 - 1497.44\Delta_4\\
D_b &= -13804.32\Delta_1 + 11379.22\Delta_2 + 751.03\Delta_3 + 1295.16\Delta_4\\
D_c &= -1580.23\Delta_1 + 751.03\Delta_2 + 812.32\Delta_3 - 155.17\Delta_4\\
D_d &= -1497.44\Delta_1 + 1295.16\Delta_2 - 155.17\Delta_3 + 512.72\Delta_4
\end{aligned}
$$

The term "p" defines the rotation of the top ring as shown in Appendix B. The value of p can be taken equal to unity for small top rings.

In addition to equation c, we obtain another equation by means of moment equilibrium condition of the vertical forces acting on the top ring.

$$522.98\ [\tfrac{1}{2}(1 - p)\Delta_v] = +\frac{.01835qR}{6C} - D_v \qquad (d)$$

in which

$$D_v = -2949.42\Delta_1 + 2245.05\Delta_2 + 353.81\Delta_3 + 251.12\Delta_4$$

By use of equations c and d, the values of p, Δ_v, Δ_1, Δ_2, Δ_3, and Δ_4 can be determined.

d) As the displacements are known, all the actual joint forces in the dome under unsymmetrical load (Fig. 12b) can be calculated by equation 8. Then by principle of superposition, we can obtain all the radial joint forces in the dome under antisymmetrical load (Fig. 12a).

However, in this problem, the top ring is assumed as a hinge, for which the value of p is equal to 1. The displacement Δ_v therefore vanishes from all equations in (c) except the first one.

TABLE 3

VALUES OF RADIAL JOINT FORCES IN THE DOME WITH ANTISYMMETRICAL LOAD ON RIBS 12 and 6 (IN qR lb.)

Rib	12	1 & 11	2 & 10	3 & 9	4 & 8	5 & 7	6
F_v	-.15371	-.11722	-.06768	0	+.06768	+.11722	+.15371
F_a	-.58705	+.25422	+.14678	0	-.14678	-.25422	+.58705
F_b	+.04519	-.01956	-.01130	0	+.01130	+.01956	-.04519
F_c	+.17703	-.07666	-.04426	0	+.04426	+.07666	-.17703
F_d	+.23737	-.10278	-.05934	0	+.05934	+.10278	-.23737

Domes with Two Opposite Ribs Under Symmetrical Loads

1. Analysis of Ribs

The dome discussed here is the same as the one treated in the preceding section, except that it will now be subjected to a symmetrical load on two opposite ribs as shown in Fig. 8c. By virtue of the symmetry of the applied loads the rings are not translated as a rigid body but are deformed by only the elastic strains in the ring. As the load applied on the dome is symmetrical about two meridian planes, only four of the twelve ribs must be considered, for instance, ribs 12, 1, 2, and 3. The forces acting on the ribs and displacements at the joints are shown in Fig. 13. In the method described in the previous part all the forces acting on each rib are expressed in terms of the joint displacements and applied load, that is, expressed explicitly by the equation,

$$F_i^j \text{ or } F_v^j = f_i\ (W_v^j,\ W_a^j,\ W_b^j,\ W_c^j,\ W_d^j,\ p^j) \qquad (8a)$$

in which i refers to the number of rings a, b, c, and d; and j refers to the number of ribs 12, 1, 2, and 3.

2. Analysis of Polygonal Rings by Means of Finite Trigonometric Series

In the analysis of the rings that follows, finite trigonometrical series have been employed to advantage.[5] The internal forces are first expressed in terms of the displacements by means of Hooke's law, and by geometrical considerations. Then the expressions for the internal forces are substituted in the difference equations of equilibrium. These equations are readily satisfied by expressing both displacements and external loads as finite trigonometric series. The equations can then be solved simultaneously for the coefficients of the displacement series in terms of the coefficients of the external-load series or vice versa, and, by substituting these back in the internal force-displacement relations, formulas for the internal forces in terms of the external loads are also obtained. All these formulas are derived in Appendix C.

In deriving these formulas, shear and axial strains in the ring and the difference in length of the inner and outer circumferential fibers of the ring due to its curvature are considered. Before these formulas can be applied, the harmonic components of the loading must be known. These can be easily obtained by method of quasi-harmonic analysis.[6]

If the rings are circular in shape, the method of analysis described above can still be applied, if differential equations are used instead of difference equations of equilibrium as in polygonal rings. This case is not treated in this discussion.

3. Combination of Ribs with Rings

The radial joint forces acting on the ribs are expressed in terms of the joint displacements and applied load as illustrated in equation 8a. As the dome is subjected to a symmetrical load on two opposite ribs, the top ring will, according to the original assumption, displace vertically and remain in a horizontal plane. This vertical displacement of the top ring can be expressed in terms of the horizontal displacements of the other rings by means of equilibrium condition of the vertical forces acting on it. Thus the joint forces are finally expressed in terms of the applied load and the horizontal displacements of the joints, both of which can be represented by trigonometric series. Meanwhile, the joint forces acting on each ring are also expressed in terms of the joint displacements by trigonometric series of the type shown in equation 9, which is derived in Appendix C.

$$F_j = \frac{2 \sin \alpha}{C} \left\{ \frac{(\rho - 1)\rho'}{\rho' - 1} W_o + \sum_k \left[\frac{\gamma}{\tau} (W_k \cos 2_{kj}\alpha + W'_k \sin 2_{kj}\alpha) \right] \right\} \quad (9)$$

As the joint forces mutually acting on the rib 12 and on the rings must satisfy the equilibrium conditions, four equilibrium equations, expressed in the form of trigonometric series, are obtained, from which the joint

5. L. H. Donnell, H. B. Gibbons, and E. L. Shaw, "Analysis of Spoked Rings," Suppl. I, Report 2 of Special Committee on Airships, 1937.
6. F. V. Southwell and J. B. B. Owen, "On the Calculation of Stresses in Braced Frameworks," Great Britain Aeronautical Research Committee, Reports and Memoranda, No. 1573 (1934), (1935).

displacements can be determined. The joint forces are then obtained from the displacements by means of equations 8a or 9.

Example 3

Let us consider that the ribbed dome, which was used in Examples 1 and 2, is subjected to a symmetrical load on ribs 12 and 6 (Fig. 14).

The top ring is assumed to be very rigid so that it is not deformed but can be displaced vertically.

By the method of analysis of the rib as suggested previously, the vertical forces acting on the top ring are

$$F_v^j = (522.98W_v + 2245.05W_b^j + 353.81W_c^j + 251.12W_d^j)C + F_{vo}^j \qquad (a)$$

and the horizontal joint forces acting on rib 12 expressed in trigonometric series are:

$$\begin{aligned} F_b^{12} = K\{&(.17414W_o^b - .07676W_o^c + .02170W_o^d + .024423\tfrac{qR}{K}) \\ &+ (1.13792W_2^b + .07510W_2^c + .12952W_2^d + .022589\tfrac{qR}{K}) \\ &+ (1.13792W_4^b + .07510W_4^c + .12952W_4^d + .022589\tfrac{qR}{K}) \\ &+ (1.13792W_6^b + .07510W_6^c + .12952W_6^d + .011295\tfrac{qR}{K}) \end{aligned}$$

$$\begin{aligned} F_c^{12} = K\{&(-.07676W_o^b + .05729W_o^c - .03250W_o^d + .046328\tfrac{qR}{K}) \\ &+ (.07510W_2^b + .08123W_2^c - .01552W_2^d + .088517\tfrac{qR}{K}) \\ &+ (.07510W_4^b + .08123W_4^c - .01552W_4^d + .088517\tfrac{qR}{K}) \\ &+ (.07510W_6^b + .08123W_6^c - .01522W_6^d + .044259\tfrac{qR}{K})\} \end{aligned} \qquad (b)$$

$$\begin{aligned} F_d^{12} = K\{&(.02170W_o^b - .03250W_o^c + .03921W_o^d + .060810\tfrac{qR}{K}) \\ &+ (.12952W_2^b - .01552W_2^c + .05127W_2^d + .118684\tfrac{qR}{K}) \\ &+ (.12952W_4^b - .01552W_4^c + .05127W_4^d + .118684\tfrac{qR}{K}) \\ &+ (.12952W_6^b - .01552W_6^c + .05127W_6^d + .059342\tfrac{qR}{K})\} \end{aligned}$$

For the rings, by equation 9, the following equations are obtained:

$$\begin{aligned} F_b^{12} &= K\,(.51770W_o^b + .00050W_2^b + .01154W_4^b + .03229W_6^b) \\ F_c^{12} &= K\,(.51770W_o^c + .00050W_2^c + .01154W_4^c + .03229W_6^c) \\ F_d^{12} &= K\,(.51770W_o^d + .00050W_2^d + .01154W_4^d + .03229W_6^d \end{aligned} \qquad (c)$$

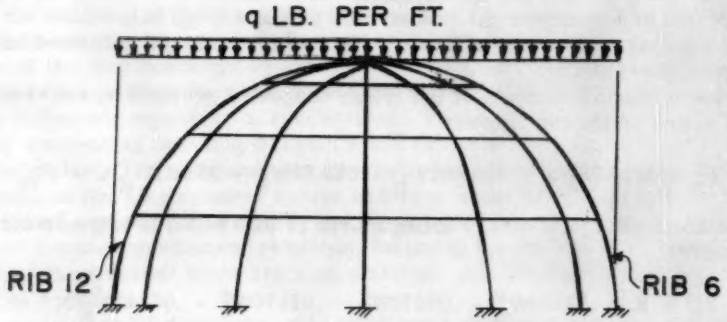

FIG. 14

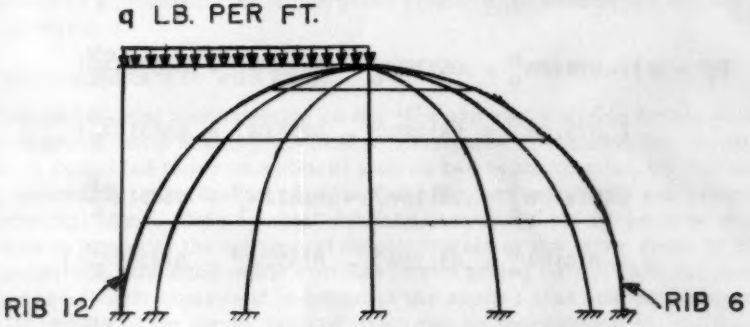

FIG. 15

By combining equations b and c, we obtain 3 equations which consists of 12 unknown trigonometrical coefficients, which can be solved by four groups of three simultaneous equations separately. The final joint forces which are calculated by equation 8 or 9 are listed in Table 4.

TABLE 4

VALUES OF RADIAL JOINT FORCES IN THE MERIDIAN PLANE WITH SYMMETRICAL LOAD ON RIBS 12 and 6 (IN qR lb.)

Rib	12 & 6	1,5,7, & 11	2,4,8, & 10	3 & 9
F_v	-.10849	-.04025	+.14283	-.09668
F_a	-.58833	+.05644	-.36236	+.18880
F_b	+.00710	+.06418	-.01714	+.08729
F_c	+.10516	-.05027	+.19023	-.13122
F_d	+.22798	-.15656	+.39229	-.31337

Proposed Method of Analysis for Ribbed Domes Under General Load Condition

1. Dome with Load on One Rib Only

As the joint forces in domes under antisymmetrical and symmetrical load on two opposite ribs (Figs. 8b and 8c) have been determined, then the joint forces in a dome with unsymmetrical loading on one rib (Fig. 8a) can be calculated by superposition of the corresponding forces for the above two loading conditions. The internal forces in the ribs are obtained by considering the individual ribs as curved cantilever members, and the internal forces of the rings are determined directly from equations 10, 11, and 12, which are derived in Appendix C.

$$M_j = \frac{R_i}{2\tan\alpha}\left\{-\frac{F_o}{\rho 1}\sum_k\left[\frac{s^2-t^2}{\gamma}\left(F_k\cos 2kj\alpha + F_k'\sin 2kj\alpha\right)\right]\right\} \quad (10)$$

$$N_{(j+1)j} = \frac{1}{2\sin\alpha}\left\{F_{o+k}\sum\left[-\frac{t(s^2-t^2)}{\gamma}\left(F_k\cos k(2j+1)\alpha + F_k'\sin k(2j+1)\alpha\right]\right\}\right. \quad (11)$$

$$Q_{(j+1)j} = \frac{1}{2\sin\alpha}\sum_k\left\{-\frac{s(s^2-t^2)}{\gamma}\left[F_k\sin k(2j+1)\alpha - F_k'\cos k(2j+1)\alpha\right]\right\} \quad (12)$$

2. Domes under General Load Condition

This paper also suggests a method of solution for a dome under a general load condition. A dome is a structure symmetrical about its axis of rotation; and, therefore, under a general load condition it can be solved by the superposition of the effects of the unsymmetrical loads on individual ribs, for which the method of analysis has been described in the previous article. Therefore, if the domes with antisymmetrical and symmetrical load on two opposite ribs have been analyzed then the problem for the dome under general loading condition can be solved by principle of superposition.

3. Comparison of Proposed Solution with Dischinger's Analytical Method

For a dome under unsymmetrical load, Dischinger[1] suggested that the method of analysis for shells of revolution may be applied to ribbed domes with the assumption that the shearing forces in the surface of the dome are taken by the bending moments of the ribs and rings (vector perpendicular to the surface of the dome). But Dischinger did not consider the bending stresses in the ribs due to the moments, of which the vector is in the surface of the dome. As a matter of fact, the latter is much greater than the former; and for this reason in this paper the latter is considered, while the former is neglected. Dischinger's method for the shells of revolution can be applied only to the dome under uniform or wind load, whereas the proposed method can be applied not only for uniform or wind load but for any type of loading. Moreover, although Dischinger's method of analysis can not be used for domes with only two or three rings, the proposed method can be applied to domes with any number of rings.

Example 4

If the ribbed dome, which has been used in parts II, III, and IV, is subjected to an unsymmetrical load q lb. per ft. on rib 12 as shown in Fig. 15; the individual joint forces can be calculated according to the results of the numerical examples in parts III and IV and are given in Table 5.

As the joint forces have been obtained, the internal forces in the ribs are computed by considering each individual rib as a cantilever member. For instance, the internal forces in rib 12 are listed in Table 6, and their diagrams are shown in Fig. 16. The internal forces in the rings are determined by equations 10, 11, and 12. For example, the internal forces in the ring c are given in Table 7, and their diagrams are plotted in Fig. 17.

SUMMARY AND CONCLUSIONS

In this paper methods of analysis for ribbed domes with rigid joints under both fully symmetrical loading and a general load condition have been developed. Under a fully symmetrical load the dome can be easily and exactly analyzed by direct application of Castigliano's theorem. Under general load condition the structure is so statically indeterminate that an exact analysis with consideration of all influences is quite complicated. However, by suitable simplification, which gives primary consideration to the important influences and neglects the subordinate ones, a practical procedure is obtained by means of principle of superposition.

The foregoing analyses lead to the following conclusions:

1. The effect of rigid connections at the joints is very significant and therefore if a safe and economical design in practical construction is desired, the members cannot be considered as connected with hinges.

2. For a dome under a fully symmetrical load, neglect of axial strains of rings may result in a considerable error.

3. For a dome with two opposite ribs under antisymmetrical load, translations of rings as a rigid body are considered, while their deformations may be neglected. In this solution the structure can be conveniently analyzed by use of auxiliary force systems.

4. For a dome with two opposite ribs under symmetrical load, only the radial deformations are considered, and the procedure can be simplified by application of finite trigonometrical series.

5. The methods of solution given can be applied to domes which are made either of curved or of straight members.

TABLE 5

VALUES OF RADIAL JOINT FORCES IN THE DOME WITH UNSYMMETRICAL LOAD ON RIB 12 (In qR lb.)

Rib	12	1 & 11	2 & 10	3 & 9	4 & 8	5 & 7	6
F_v	-.13110	-.07874	+.03758	-.04834	+.10526	+.03849	+.02261
F_a	-.58769	+.15533	-.10779	+.09440	-.25457	-.09889	-.00064
F_b	+.02615	+.02231	-.01422	+.04365	-.00292	+.04187	-.01905
F_c	+.14110	-.06347	+.07299	-.06561	+.11725	+.01320	-.03594
F_d	+.23268	-.12967	+.16648	-.15669	+.22582	-.02689	-.00470

TABLE 6

VALUES OF INTERNAL FORCES IN RIB 12

Point	Bending Moments in qR^2 ft-lb.	Axial Forces in qR lb.	Shear Forces in qR lb.
a	0	-0.58769	-0.13110
1	+0.010873	- .58162	- .09053
2	+ .017836	- .58888	- .05189
3	+ .021229	- .60860	- .01827
b^U_L	+ .021682	- .63923 - .61507	+ .00753 + .01754
4	+ .018989	- .65565	+ .03541
5	+ .015132	- .70273	+ .04096
6	+ .011393	- .75337	+ .03282
c^U_L	+ .009162	- .80437 - .70458	+ .01023 + .11002
7	- .000400	- .76293	+ .08222
8	- .006491	- .81592	+ .03952
9	- .007710	- .86036	- .01686
d^U_L	- .002792	- .89333 - .80429	- .08506 + .12991
10	- .012201	- .84478	+ .06006
11	- .014307	- .87000	- .01839
12	- .008422	- .87834	- .10216
o	+0.005816	-0.86890	-0.18776

TABLE 7

VALUES OF INTERNAL FORCES IN RING c

Joints	Bending Moments in qR^2 ft-lb.	Members		Axial Forces in qR lbs.	Shear Forces in qR lbs.
12	+0.015300				
		12-1	11-12	+0.035492	-0.063529
1 & 11	- .007954				
		1-2	10-11	+ .046074	+ .024032
2 & 10	+ .000842				
		2-3	9-12	+ .046776	- .026656
3 & 9	- .008915				
		3-4	8- 9	+ .036858	+ .063677
4 & 8	+ .014393				
		4-5	7- 8	+ .030426	- .039676
5 & 7	- .000129				
		5-6	6- 7	+0.049602	-0.031893
6	-0.011806				

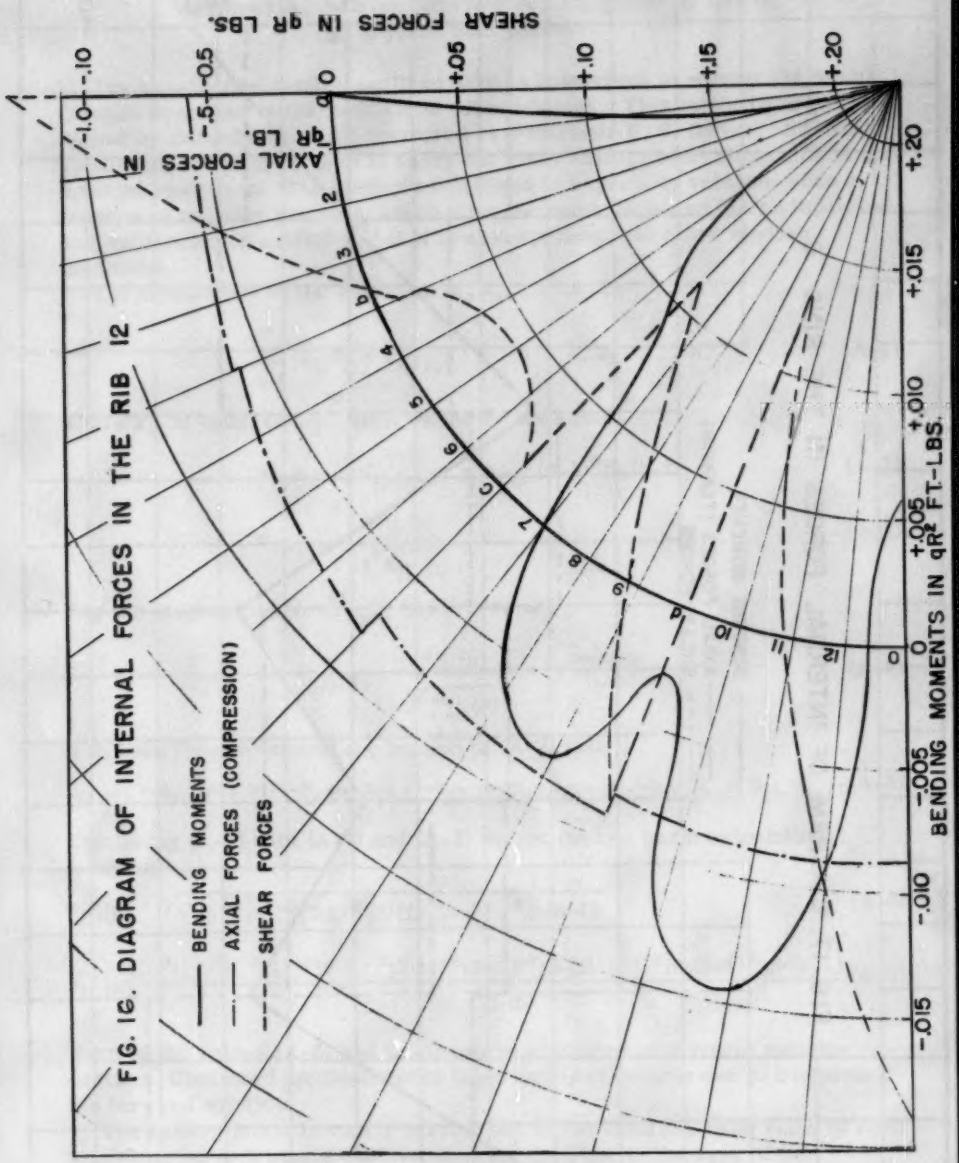

FIG. 16. DIAGRAM OF INTERNAL FORCES IN THE RIB 12

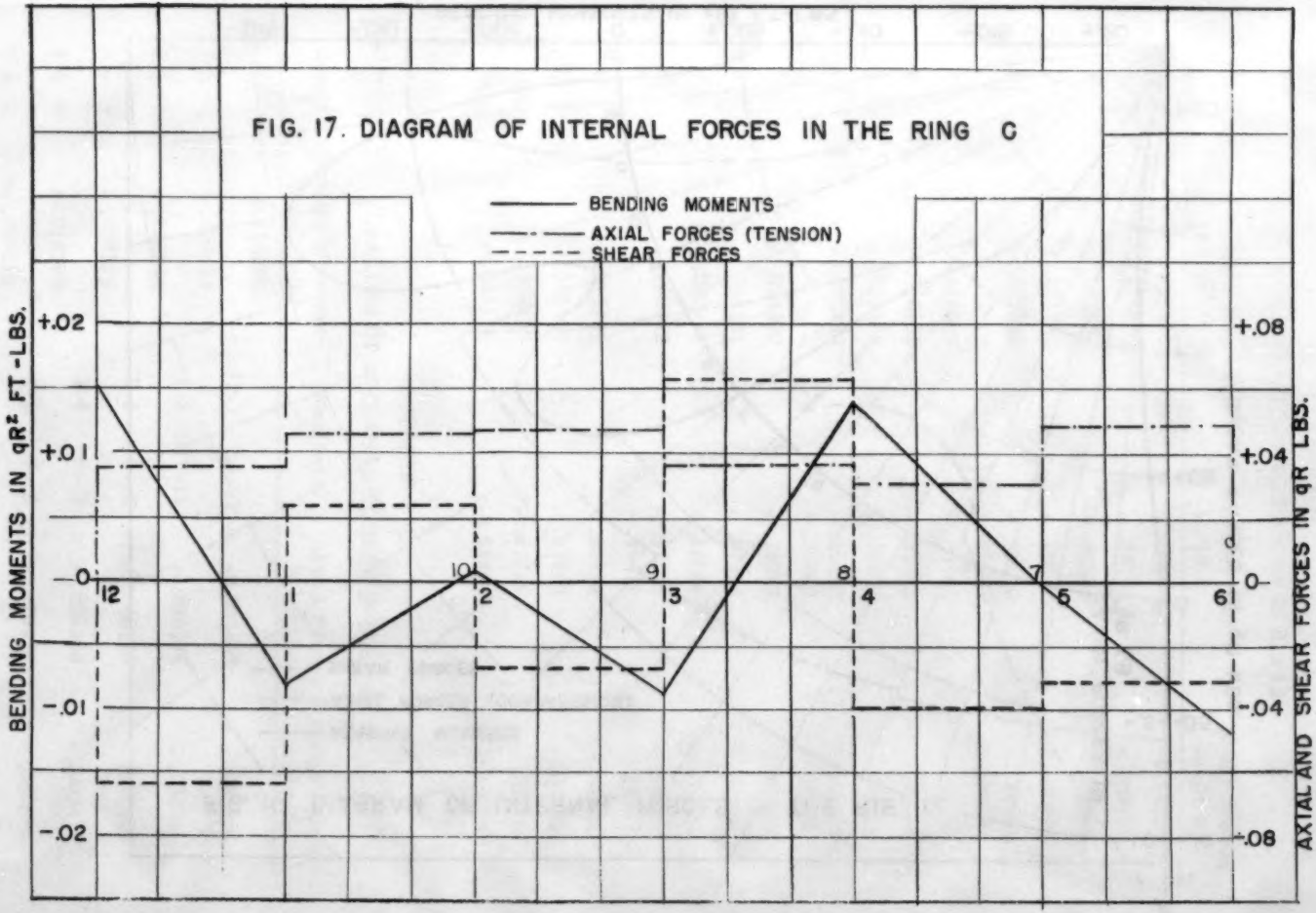

FIG. 17. DIAGRAM OF INTERNAL FORCES IN THE RING C

APPENDIXES

Appendix A. Solving Simultaneous Equations by Use of Square Root Method

The square root method outlined here is convenient in solving the simultaneous equations in the problem of ribbed domes. This method was presented by Banachiewicz and improved by Professor P. S. Dwyer,[7] so that the calculating machine is used to carry out many calculational steps as a single machine operation. The method as outlined is especially valuable when a modern calculating machine, which uses the same keyboard for multiplicand and multiplier, is available; but it is also applicable to other modern machines.

Let n equations in the variables $x_1, x_2, \ldots x_n$ be

$$\sum_{i=1}^{n} a_{ij}x_i = a_{n+1,j} \qquad j = 1, 2, \ldots, n \tag{A-1}$$

where a_{ij} is equal to a_{ji}. Then we define the values

$$a_{ij\cdot(h)} = a_{ij\cdot(h-1)} - s_{ih\cdot(h-1)}\, s_{jh\cdot(h-1)}, \tag{A-2}$$

$$s_{ij\cdot(h)} = \frac{a_{ij\cdot(h)}}{\sqrt{a_{jj\cdot(h)}}} \tag{A-3}$$

For the diagonal terms (i = j), (A-3) becomes

$$s_{jj\cdot(h)} = \frac{a_{jj\cdot(h)}}{\sqrt{a_{jj\cdot(h)}}} = \sqrt{a_{jj\cdot(h)}} \tag{A-4}$$

It follows from continued application of (A-2) that

$$a_{ij\cdot(h)} = a_{ij} - s_{i1}\, s_{j1} - s_{i2\cdot1}\, s_{j2\cdot1} - s_{i3\cdot(2)}\, s_{j3\cdot(2)} - \cdots - s_{ih\cdot(h-1)}\, s_{jh\cdot(h-1)} \tag{A-5}$$

Combining (A-5) with (A-4) and (A-3) we get the two basic calculational formulas

$$s_{jj\cdot(h)} = \sqrt{a_{jj} - s_{j1}^2 - s_{j2\cdot1}^2 - s_{j3\cdot(2)}^2 - \cdots - s_{jh(h-1)}^2} \tag{A-6}$$

$$s_{ij\cdot(h)} = \frac{a_{ij} - s_{i1}\, s_{j1} - s_{i2\cdot1} \cdot s_{j2\cdot1} - s_{i3\cdot(2)} \cdot s_{j3\cdot(2)} - \cdots - s_{ih\cdot(h-1)}\, s_{jh\cdot(h-1)}}{s_{jj\cdot(h)}} \tag{A-7}$$

Each of the values (A-6) and (A-7) can be computed as a single machine operation. Continued applications of (A-6) and (A-7) enable one to complete the forward solution.

The back solution is easily carried out by substitution. The value of each x is obtained as a single machine operation. Thus in the case of four

7. P. S. Dwyer, "The Square Root Method and Its Use in Correlation and Regression," Journal of the American Statistical Association, Vol. 40 (Dec. 1945), 493-503.

equations as illustrated in Table 8, we have

$$x_4 = \frac{s_{54.(3)}}{s_{44.(3)}}$$

$$x_3 = \frac{s_{53.(2)} - x_4 s_{43.(2)}}{s_{33.(2)}}$$

etc.

Forms for the theoretical solution and an illustration for the equations obtained in part II are presented in Table 8. The sixth column is a row sum check column. The last row results from carrying the check column through the back solution.

TABLE 8

(a) Theoretical

a_{11}	a_{21}	a_{31}	a_{41}	a_{51}	a_{61}
—	a_{22}	a_{32}	a_{42}	a_{52}	a_{62}
—	—	a_{33}	a_{43}	a_{53}	a_{63}
—	—	—	a_{44}	a_{54}	a_{64}
s_{11}	s_{21}	s_{31}	s_{41}	s_{51}	s_{61}
	$s_{22.(1)}$	$s_{32.(1)}$	$s_{42.(1)}$	$s_{52.(1)}$	$s_{62.(1)}$
		$s_{33.(2)}$	$s_{43.(2)}$	$s_{53.(2)}$	$s_{63.(2)}$
			$s_{44.(3)}$	$s_{54.(3)}$	$s_{64.(3)}$
x_1	x_2	x_3	x_4		
$1 + x_1$	$1 + x_2$	$1 + x_3$	$1 + x_4$		

(b) Illustration

F_a	F_b	F_c	F_d	a_5	Check (Sum)
-35620	.31304	.19807	.06460	-.22603	+.70588
	.27699	.17808	.05895	-.19643	+.63063
		.12101	.04287	-.11949	+.42054
			.01863	-.03615	+.14890
.5968249320	.5245089161	.3318728629	.1082394454	-.378720773	+1.182725383
	.0433635450	.0924676325	.0502137400	+.051020320	+ .237065238
		.0481678280	.0478560030	+.030713840	+ .126737671
			.0458541792	+.017681349	+ .063535528
-1.01062	+ .18728	+ .25454	+ .38560		
- .01062	+1.18728	+1.25454	+1.38560		

In the illustration, as the exact solution is desired, operation is worked out to ten decimal places. If only approximate result is required, the same number of decimal places as exists in the coefficients of the variables is sufficient for the operation.

The Solution of Associated Equations

Groups of equations, which have identical coefficients on the left, but differ on the right side, are said to be associated. The solution of these equations can be obtained in terms of general expressions on the right. The numerical values which identify a given group may be substituted in the answer. For example, the equations obtained in part III are associated as shown in Table 9. The inverse matrix is obtained by pairing of elements of columns, multiplying and adding. Each of the elements of the inverse can be obtained as a single machine operation. Thus

$$(1.67553321)\ (0) + (-19.31430578)\ (+21.9772418) + (+19.9644303)\ (-33.74012427) + (-4.09976945)\ (+10.96492017) + (-128.9715098)\ (+98.1712318) = -13804.32316$$

The results can then be expressed as

$$F_a = +17414.88675a_{61} - 13804.32316a_{62} - 1580.23134a_{63} - 1497.43967a_{64} - 2949.41671a_{65}$$

$$F_b = -13804.32316a_{61} + 11379.21537a_{62} + 751.02893a_{63} + 1295.16373a_{64} + 2245.05297a_{65}$$

$$F_c = -1580.23134a_{61} + 751.02893a_{62} + 812.32417a_{63} - 155.16838a_{64} + 353.80628a_{65}$$

$$F_d = -1497.43967a_{61} + 1295.16373a_{62} - 155.16838a_{63} + 512.71956a_{64} + 251.12495a_{65}$$

$$F_v = -2949.41671a_{61} + 2245.05297a_{62} + 353.80628a_{63} + 251.12495a_{64} + 522.97955a_{65}$$

when

$$a_{61} = -.22603qR, \quad a_{62} = -.19643qR, \quad a_{63} = -.11949qR,$$

$$a_{64} = -.03615qR, \quad a_{65} = -.33333qR,$$

we have

$$F_{ao} = -.88059qR, \quad F_{bo} = +.06777qR, \quad F_{co} = +.26555qR,$$

$$F_{do} = +.35605qR, \quad F_{vo} = -.01835qR.$$

TABLE 9

F_a	F_b	F_c	F_d	F_v
.35620	.31304	.19807	.06460	.50000
—	.27718	.17808	.05895	.42677
—	—	.12120	.04287	.25000
—	—	—	.01882	.07322
—	—	—	—	.78540
.5968249320	.5245089161	.3318728629	.1082394454	.837766605
	.0455016151	.0881226836	.0478542530	-.277925385
		.0574003080	.0475819795	-.061680446
			.0504989916	-.024248667
				+.043727802
+17424.88675	-13804.32316	-1580.23134	-1497.43967	-2949.41671
-13804.32316	+11379.21537	+ 751.02893	+1295.16373	+2245.05297
- 1580.23134	+ 751.02893	+ 812.32417	- 155.16838	+ 353.80628
- 1497.43967	+ 1295.16373	- 155.16838	+ 512.71956	+ 251.12495
- 2949.41671	+ 2245.05297	+ 353.80628	+ 251.12495	+ 522.97955

a_{61}	a_{62}	a_{63}	a_{64}	a_{65}	Check (Sum)
1	0	0	0	0	2.43191
0	1	0	0	0	2.25402
0	0	1	0	0	1.79022
0	0	0	1	0	1.25846
0	0	0	0	1	3.03539
+ 1.67553321	0	0	0	0	4.074745971
- 19.31430578	+21.97724180	0	0	0	2.566489187
+ 19.96443030	-33.74012427	+17.42150930	0	0	3.689117172
- 4.09976945	+10.96492017	-16.41517725	+19.80237560	0	10.278599395
-128.97150980	+98.17123180	+15.47117108	+10.98114225	+22.868746	18.564509230

Appendix B. Discussion of Vertical Displacement of the Top Ring

If the top ring is assumed to remain in a plane when the dome is under load, then the vertical displacements of the ring corners may be expressed in terms of Δ_v and p as shown in Fig. 18. Thus, there are six unknowns in the equation 7 as represented in the following:

$$
\begin{aligned}
f_v\,(p,\ \Delta_v) &= f_{vo}\,(q,E,I,R) && \text{(a)}\\
f_a\,(p,\ \Delta_v,\ \Delta_1,\ \Delta_2,\ \Delta_3,\ \Delta_4) &= f_{ao}\,(q,E,I,R) && \text{(b)}\\
f_b\,(p,\ \Delta_v,\ \Delta_1,\ \Delta_2,\ \Delta_3,\ \Delta_4) &= f_{bo}\,(q,E,I,R) && \text{(c)}\quad (7a)\\
f_c\,(p,\ \Delta_v,\ \Delta_1,\ \Delta_2,\ \Delta_3,\ \Delta_4) &= f_{co}\,(q,E,I,R) && \text{(d)}\\
f_d\,(p,\ \Delta_v,\ \Delta_1,\ \Delta_2,\ \Delta_3,\ \Delta_4) &= f_{do}\,(q,E,I,R) && \text{(e)}
\end{aligned}
$$

The additional unknown may be calculated by means of the moment equilibrium condition of the vertical forces acting on the top ring about the plan axis. If the top ring is so small that it is considered as a hinge at the crown, then the value of p is equal to 1.

Appendix C. Derivation of the Equations 9, 10, 11, and 12

As there are assumed to be no forces on any portion of the ring between two joints, it follows that N and Q are constant over each side and M varies linearly. The corners of the polygonal rings and the internal and external forces are labeled as shown in Figs. 19a and b. Since the sides of the ring are straight, they will behave like ordinary beams except for the effect of the short lengths $r_i \tan\alpha$ of outer boom and $-r_i \tan\alpha$ of inner boom at each end, as shown in Fig. 19c, for the left end of a side. Using Hooke's law, these will produce, at each end, an extra elongation of the beam's centroidal axis of

$$\frac{1}{2}\,\frac{2}{A_iE}\left\{(r_i\tan\alpha)\,\frac{1}{2}\,(N+\frac{M}{r_i})+(-r_i\tan\alpha)\,\frac{1}{2}\,(N-\frac{M}{r_i})\right\}=\frac{\tan\alpha\,M}{A_iE} \qquad \text{(C-1)}$$

and an extra counterclockwise rotation of the end, of

$$\frac{1}{2r_i}\,\frac{2}{A_iE}\left\{(r_i\tan\alpha)\,\frac{1}{2}\,(N+\frac{M}{r_i})-(-r_i\tan\alpha)\,\frac{1}{2}\,(N-\frac{M}{r})\right\}=\frac{\tan\alpha\,N}{A_iE} \qquad \text{(C-2)}$$

Using equation (C-1) and Hooke's law, the total elongation of the sides j(j-1) and (j+1)j are

$$
\left.
\begin{aligned}
\frac{1}{A_iE}\left\{N_{j(j-1)}2R_i\sin\alpha+\tan\alpha\,(M_j+M_{j-1})\right\}&=(W_j+W_{j-1})\sin\alpha+(V_j-V_{j-1})\cos\alpha\\
\frac{1}{A_iE}\left\{N_{(j+1)j}2R_i\sin\alpha+\tan\alpha\,(M_{j+1}+M_j)\right\}&=(W_{j+1}+W_j)\sin\alpha+(V_{j+1}-V_j)\cos\alpha
\end{aligned}
\right\}\text{(C-3)}
$$

By use of equation (C-2) and the theorem of area moments, we have (Fig. 19d)

$$\Delta_{j(j-1)}=\left\{2R_i\sin\alpha\ \frac{\tan\alpha\ N_{j(j-1)}}{A_iE}+\frac{4R_1^2\sin^2\alpha}{6A_iEr_i^2}\,(M_{j-1}+2M_j)\right\} \qquad \text{(C-4)}$$

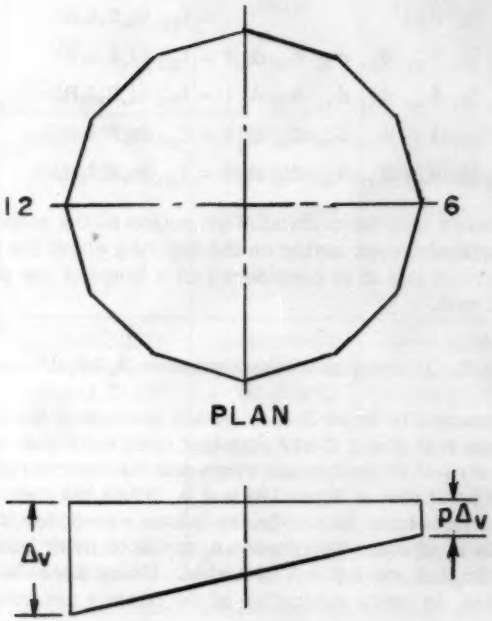

FIG. 18

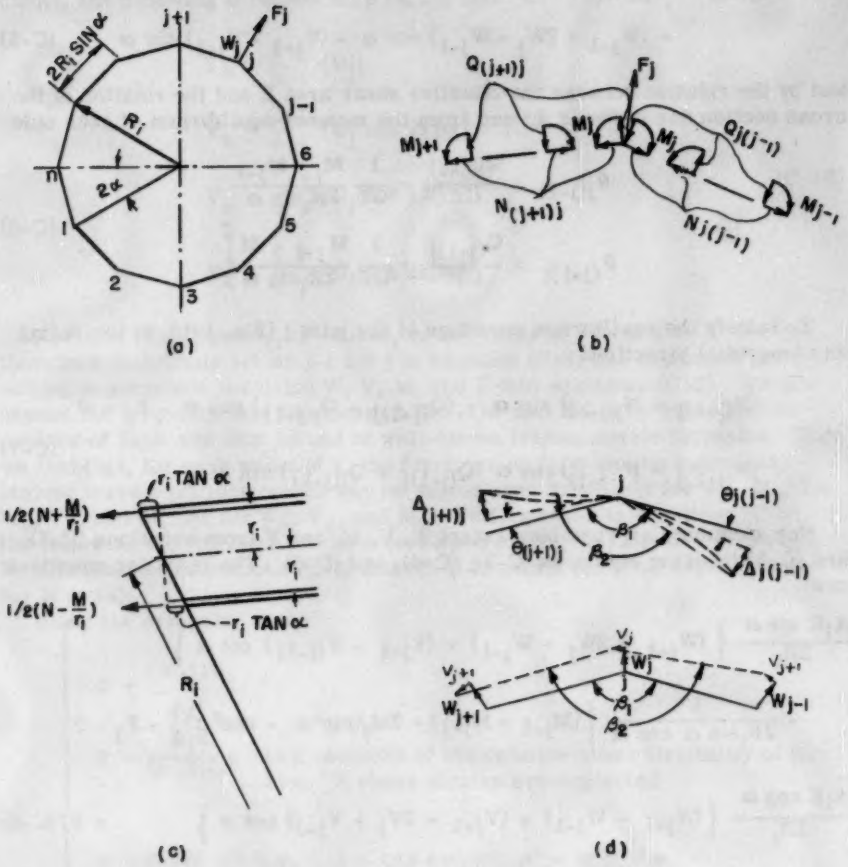
2R_i SIN α
j+1
W_j
F_j
j
j-1
R_i
2α
n
6
1
5
2
3
4
(a)
Q(j+1)j
F_j
M_j+1
M_j
M_j
Qj(j-1)
N(j+1)j
Nj(j-1)
M_j-1
(b)
r_i TAN α
1/2(N+M/r_i)
r_i
r_i
1/2(N-M/r_i)
-r_i TAN α
R_i
(c)
Δ(j+1)j
j
θj(j-1)
β_1
θ(j+1)j
β_2
Δj(j-1)
V_j
W_j
V_j+1
V_j+1
W_j+1
β_1
β_2
W_j-1
(d)

FIG. 19

$$-\Delta_{(j+1)j} = \left\{ 2R_i \sin\alpha \; \frac{\tan\alpha \; N_{(j+1)i}}{A_i E} + \frac{4R_i^2 \sin^2\alpha}{6A_i E r_i^2} \; (M_{j+1} \; 2M_j) \right. \qquad \text{(C-4)}$$

In Fig. 19d, change of angle $\beta_2 - \beta_1$ multiplied by $2R_i \sin\alpha$ is

$$\Delta_{(j+1)j} - \Delta_{j(j-1)} + 2R_j \sin\alpha \; (\theta_{(j+1)j} - \theta_{j(j-1)}$$
$$= (W_{j+1} - 2W_j + W_{j-1}) \cos\alpha - (V_{j+1} - V_{j-1}) \sin\alpha \qquad \text{(C-5)}$$

and by the relation between the effective shear area Z and the rotation of the cross section due to shear θ ; and from the moment equilibrium of each side

$$\theta_{j(j-1)} = \frac{Q_{j(j-1)}}{GZ} = \frac{1}{GZ} \frac{M_j - M_{j-1}}{2R_i \sin\alpha}$$
$$\theta_{(j+1)j} = \frac{Q_{(j+1)j}}{GZ} = \frac{1}{GZ} \frac{M_{j+1} - M_j}{2R_i \sin\alpha} \qquad \text{(C-6)}$$

To satisfy the equilibrium condition of the joint j (Fig. 19b), in the radial and tangential directions

$$(N_{(j+1)j} + N_{j(j-1)}) \sin\alpha - (Q_{(j+1)j} - Q_{j(j-1)}) \cos\alpha - F_j = 0$$
$$(N_{(j+1)j} - N_{j(j-1)}) \cos\alpha \; (Q_{(j+1)j} + Q_{j(j-1)}) \sin\alpha \qquad = 0 \qquad \text{(C-7)}$$

Now eliminate all variables except W, V, M, and F from equations (C-7) and (C-5) by using equations (C-3), (C-4), and (C-6). The resulting equations are

$$\left.\begin{aligned}
&\frac{A_i E \sin\alpha}{2R_i} \left\{ (W_{j+1} + 2W_j + W_{j-1}) + (V_{j+1} - V_{(j-1)}) \cot\alpha \right\} \\
&\quad - \frac{1}{2R_i \sin\alpha \cos\alpha} \left\{ (M_{j+1} + M_{j-1}) + 2M_j(\sin^2\alpha - \cos^2\alpha) \right\} - F_j = 0 \\
&\frac{A_i E \cos\alpha}{2R_i} \left\{ (W_{j+1} - W_{j-1}) + (V_{j+1} - 2V_j + V_{j-1}) \cot\alpha \right\} \qquad = 0 \\
&\frac{1}{\cot\alpha} \left\{ (W_{j+1} + W_{j-1}) + 2W_j (\sin^2\alpha - \cos^2\alpha) \right\} + \left(\frac{\tan^2\alpha}{A_i E} - \frac{8\rho \sin^2\alpha}{6A_i E}\right. \\
&\quad \left. - \frac{1}{GZ}\right) 2M_j + \left(\frac{\tan^2\alpha}{A_i E} - \frac{4\rho \sin^2\alpha}{6A_i E} + \frac{1}{GZ}\right) (M_{j+1} + M_{j-1}) = 0
\end{aligned}\right\} \qquad \text{(C-8)}$$

These equations are satisfied by letting

$$F_j = F_o \sum_k F_k \cos 2kj\alpha + \sum_k F_k' \sin 2kj\alpha \qquad \text{(C-9)}$$

with similar expressions for W_j, V_j, and M_j.

Any loading, if not already harmonic, can be resolved into the foregoing components by the method of quasi-harmonic analysis. For example, if the applied loads on the joints of the ring are $U_1, U_2 \ldots U_j \ldots U_n$; we may have values of F corresponding with n values represented by a definite series of circular functions as equation (C-9). For the determination of the coefficients, the following formulas may be applied:

$$
\begin{aligned}
F_o &= \frac{1}{n} \sum_j [U_j] \\
F_k &= \frac{2}{n} \sum_j [U_j \cos 2kj\alpha] \quad (0 < k < \tfrac{n}{2}) \\
F_{\frac{n}{2}} &= \frac{1}{n} \sum_j [U_j \cos j\pi] \\
F'_k &= \frac{2}{n} \sum_j [U_j \sin 2kj\alpha]
\end{aligned}
\tag{C-10}
$$

Equation (C-9) applies, of course, to any value of j from 1 to n. We can, therefore, substitute j+1 or j-1 for j in equation (C-9) and substitute the resulting expressions involving W, V, M, and F into equations (C-8). We now expand the trigonometric functions of $2k(j+1)\alpha$ and $2k(j-1)\alpha$ into sines or cosines of $2kj\alpha$ and $2k\alpha$ by use of well-known trigonometric formulas. Then we find that, for each value of k, the functions of $2kj\alpha$ can be cancelled, leaving three equations, which can be solved simultaneously for W_o, M_o; for W_k, V'_k, and M_k; or for W'_k, V_k, and M'_k. Putting these in equations (C-9), the following expressions are then developed for V_j, W_j, and M_j, which may be substituted in equations (C-3) and (C-6) to obtain the final expressions for N and Q.

Using the symbols

$$c = \frac{(\rho - 1)R_i}{A_i E}$$

$$\eta = \frac{A_i E}{(\rho - 1)GZ}$$ is a measure of the relative shear flexibility of the ring. If shear strains are neglected

$$\eta = 0$$

$$s = \cot\alpha \sin k\alpha, \qquad t = \cos k\alpha, \qquad \rho' = \rho \cos^2\alpha,$$

$$\lambda = \left(\frac{1 + 2t^2}{3}\frac{\rho'}{\rho - 1} - \frac{t^2}{\rho - 1} + s^2\eta\right); \qquad \gamma = (s^2 - t^2)^2,$$

the following equations are obtained:

$$V_j = \frac{c}{2 \sin\alpha} \sum_k \left\{ -\frac{t\lambda}{s\gamma} (F_k \sin 2kj\alpha - F'_k \cos 2kj\alpha) \right\} \tag{C-11}$$

$$W_j = \frac{c}{2 \sin\alpha} \left\{ \frac{\rho' - 1}{(\rho - 1)\rho'} F_o + \sum_k \left[\frac{\lambda}{\gamma} (F_k \cos 2kj\alpha \; F'_k \sin 2kj\alpha) \right] \right\} \tag{C-12}$$

$$F_j = \frac{2 \sin \alpha}{c} \left\{ \frac{(\rho - 1)\rho'}{\rho' - 1} W_o + \sum_k \left[\frac{\gamma}{\lambda} (W_k \cos 2kj\alpha + W_k' \sin 2kj\alpha) \right] \right\} \quad (9)$$

$$M_j = \frac{R_i}{2 \tan \alpha} \left\{ - \frac{F_o}{\rho'} + \sum_k \left[\frac{s^2 - t^2}{\gamma} (F_k \cos 2kj\alpha + F_k' \sin 2kj\alpha) \right] \right\} \quad (10)$$

$$N_{(j+1)j} = \frac{1}{2 \sin \alpha} \left\{ F_o + \sum_k \left[- \frac{t(s^2 - t^2)}{\gamma} (F_k \cos k(2j+1)\alpha + F_k' \sin k(2j+1)\alpha) \right] \right\} \quad (11)$$

$$Q_{(j+1)j} = \frac{1}{2 \sin \alpha} \sum_k \left\{ - \frac{s(s^2 - t^2)}{\gamma} \left[F_k \sin k(2j+1)\alpha - F_k' \cos k(2j+1)\alpha \right] \right\} \quad (12)$$

Paper 1106 ST 6

Journal of the
STRUCTURAL DIVISION
Proceedings of the American Society of Civil Engineers

SIMPLIFIED ANALYSIS OF RIGID FRAMES

Robert M. Barnoff,[1] J. M. ASCE
(Proc. Paper 1106)

SYNOPSIS

A procedure to reduce the time required to analyze rigid frames is presented in this paper. Formulas for balanced moments at the joints of four types of rigid frames are derived, and coefficients from these formulas are plotted on diagrams to simplify the numerical computations.

INTRODUCTION

Rigid frames, especially those used as bridge piers, are usually analyzed by moment distribution. Although this method is time-saving, it is usually necessary to solve at least four moment distribution problems for a complete structural analysis of a rigid frame used as a bridge pier. Thus the analysis becomes a time consuming task even for the most experienced designer.

A method of analysis is presented in this paper that will considerably shorten the time required to analyze rigid frames. This method applies to the most common types of rigid frames used; namely, two or three column frames with columns of equal length and the foundation end of the columns either fixed or free to rotate. All members of the frame are assumed to be prismatic and the moments of inertia of the columns for any given frame are equal. Four different loading conditions are covered in the analysis; symmetrical vertical loads, unsymmetrical vertical loads with sidesway, lateral loads caused by wind and other forces, and the moments in the columns and cap caused by shrinkage and temperature changes. The analysis consists of formulas (derived by moment distribution and slope deflection) to obtain balanced moments from fixed-end moments caused by the above loads. The formulas contain two variables; the fixed-end moments or loads on the frame, and a ratio of the rotational stiffnesses of the column and cap of the frame.

Note: Discussion open until April 1, 1957. Paper 1106 is part of the copyrighted Journal of the Structural Division of the American Society of Civil Engineers, Vol. 82, No. ST 6, November, 1956.

1. Instr. in Civ. Eng., Pennsylvania State Univ., University Park, Pa.

Although these formulas were derived for analyzing rigid frames used as bridge piers, they may be applied to any two or three column rigid frame with prismatic members and equal length columns.

A General Analysis of a Two Column Rigid Frame with Column Bases Free to Rotate

To derive equations for a general analysis of a two column rigid frame, the method of moment distribution is used. The four loading conditions discussed in the introduction are considered in the analysis. The columns are equal in length and cross-section, and all members in the frame are prismatic. In the analysis all fixed-end moments, distribution factors, stiffnesses, and moments of inertia are designated by letters. The moments on the structure are then divided into symmetric and anti-symmetric cases so that the short-cut method of moment distribution can be used. This operation is shown in Figure 1.

Notation

d_a = Distribution factor for anti-symmetric distribution.

d_s = Distribution factor for symmetric distribution.

Δ = Lateral displacement of column.

H = Height of frame from base to center line of cap.

I = Moment of inertia of member.

L = Length of a member.

$M_1, M_2, \ldots$ = Fixed-end moment in frame.

M_S = Fixed-end moment in column caused by shrinkage of cap.

M' = Symmetric fixed-end moment on frame.

M'' = Anti-symmetric fixed-end moment on frame.

$M_{AB}, M_{BA}, \ldots$ = Balanced moments on frame.

P = Vertical load on frame.

P_W = Lateral load on frame.

Q = Coefficient

R = Ratio of stiffnesses of column and cap.

S = Rotational stiffness of member. = 4 EI/L

S'' = Rotational stiffness of member with one end free to rotate. = 3 S/4

S''' = Symmetric rotational stiffness of member. = 1/2 S.

S^{iv} = Anti-symmetric rotational stiffness of member. = 3 S/2.

After the moments are divided into symmetric and anti-symmetric cases, the distribution factors are found and the moment distributions performed in Figure 2.

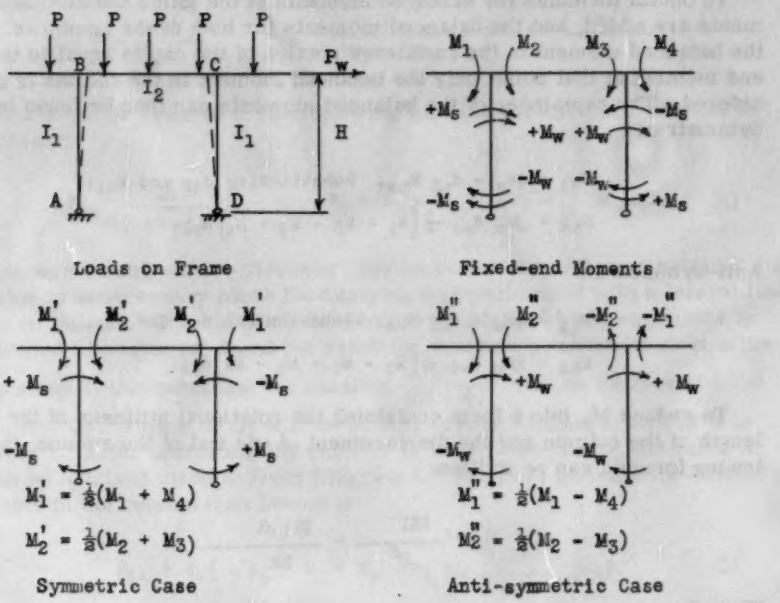

Fig. 1. Loads and Moments on Frame Divided into Symmetric and Anti-symmetric Cases.

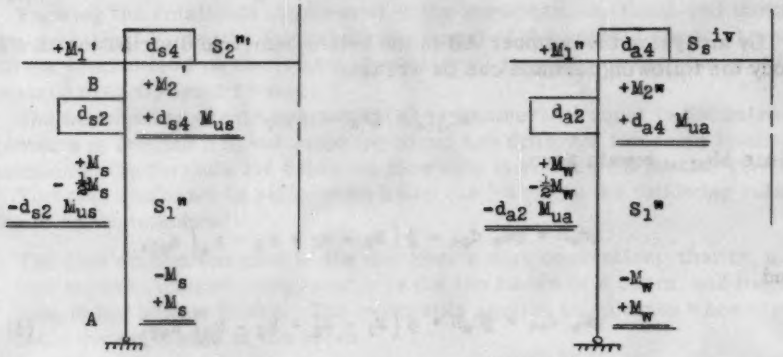

Fig. 2. Moment Distribution

To obtain formulas for balanced moments at the joints the distributed moments are added, and the balanced moments for both cases combined. Since the balanced moment in the cantilever portion of the cap is equal to the fixed-end moment at that point, only the balanced moment in the column is considered. The remainder of the balanced moments can then be found by statics.
Symmetric:

$$M_{BA} = \tfrac{1}{2}M_s - d_{s2}\,M_{us}. \quad \text{Substituting } d_{s2} \text{ and } M_{us}:$$

$$M_{BA} = \tfrac{1}{2}M_s\,d_{s4} - \tfrac{1}{2}\left[M_1 - M_2 - M_3 + M_4\right]d_{s2}. \qquad (1)$$

Anti-symmetric:

$$M_{BA} = \tfrac{1}{2}M_w - d_{a2}\,M_{ua}. \quad \text{Substituting } d_{a2} \text{ and } M_{ua}:$$

$$M_{BA} = \tfrac{1}{2}M_w\,d_{a4} - \tfrac{1}{2}\left[M_1 - M_2 + M_3 - M_4\right]d_{a2}. \qquad (2)$$

To reduce M_S into a form containing the rotational stiffness of the column, length of the column and the displacement of one end of the column; the following formula can be written:

$$M_s = \frac{6EI}{H^2} = \frac{3S_1\Delta}{2H}$$

Therefore:

$$\tfrac{1}{2}M_s\,d_{s4} = d_{s4}\,\frac{3}{4}\cdot\frac{S_1\Delta}{H} \qquad (3)$$

By analyzing the member AB in the anti-symmetric distribution as a free body the following formula can be written:

$$M_{base} + \tfrac{1}{2}P_wH = M_{top}$$

Since M_{base} equals zero,

$$\tfrac{1}{2}P_wH = \tfrac{1}{2}M_w\,d_{a4} - \tfrac{1}{2}\left[M_1 - M_2 + M_3 - M_4\right]d_{a2},$$

and

$$\tfrac{1}{2}M_w\,d_{a4} = \tfrac{1}{2}P_wH + \tfrac{1}{2}\left[M_1 - M_2 + M_3 - M_4\right]d_{a2}. \qquad (4)$$

Substituting equations 3 and 4 into equations 1 and 2 and combining equations 1 and 2 the following formula for balanced moments in the column is obtained:

$$M_{BA} = d_{s4}\,\frac{3S_1\Delta}{4H} + \tfrac{1}{2}P_w\,H - \tfrac{1}{2}\left[M_1 - M_2 - M_3 + M_4\right]d_{s2}. \qquad (5)$$

Since

$$d_{s4} = \frac{2S_2}{3S_1 + 2S_2}, \quad d_{s2} = \frac{3S_1}{3S_1 + 2S_2} \quad \text{and} \quad R = \frac{S_1}{S_2};$$

equation 5 can be reduced to the following formula for balanced moment in the column:

$$M_{BA} = \frac{3R}{6R + 4}\left[- M_1 + M_2 + M_3 - M_4 + \frac{S_2 \Delta}{H} \right] \pm \tfrac{1}{2} P_w H. \quad (6)$$

A separate analysis for sidesway correction for the anti-symmetrical distribution is unnecessary since the analysis was performed with a lateral load acting on the cap. The sidesway correction is obtained when equation 4 is substituted into equation 2 and the resulting equation combined with equation 1.

To simplify computations the quantity $\frac{3R}{6R + 4}$ will be replaced by the coefficient Q_1. Values of Q_1 will be plotted versus various values of R in Diagram 1. After computing the value of R for a given frame, the value of Q_1 can be obtained directly from Diagram 1. The final formula for balanced moments in the column then becomes:

$$M_{BA} = Q_1\left[- M_1 + M_2 + M_3 - M_4 + \frac{S_2 \Delta}{H} \right] \pm \tfrac{1}{2} P_w H. \quad (7)$$

Also;

$$M_{CD} = Q_1\left[M_1 - M_2 - M_3 + M_4 - \frac{S_2 \Delta}{H} \right] \pm \tfrac{1}{2} P_w H$$

Knowing the rotational stiffnesses of the members, the fixed-end moments due to vertical loads, the lateral displacement of the column due to shrinkage and the lateral load on the frame, the balanced moments in the column can be obtained directly from formula 7.

The balanced moments in column CD are numerical equal to the balanced moments in column AB, but since the signs are different for some loading conditions, the formula for balanced moments in column CD is also given.

To avoid confusion in signs when using the formulas the following rules should be remembered:

1) The sign convention used is the designer's sign convention: that is, a positive moment causes compression in the top fibers of a beam, and the tension in the bottom fibers. The same rule applies to columns when viewed from the right side of the paper.

2) Fixed-end moments used in deriving the formulas were positive.

3) When writing moments on a sketch of the structure, moments on beams are written on the ends of beams and moments on columns are written to the left of the column at the top, and to the right of the column at the bottom.

4) The moments at a joint are balanced when the moment on the left of the vertical centerline of a joint equals the moment on the right.

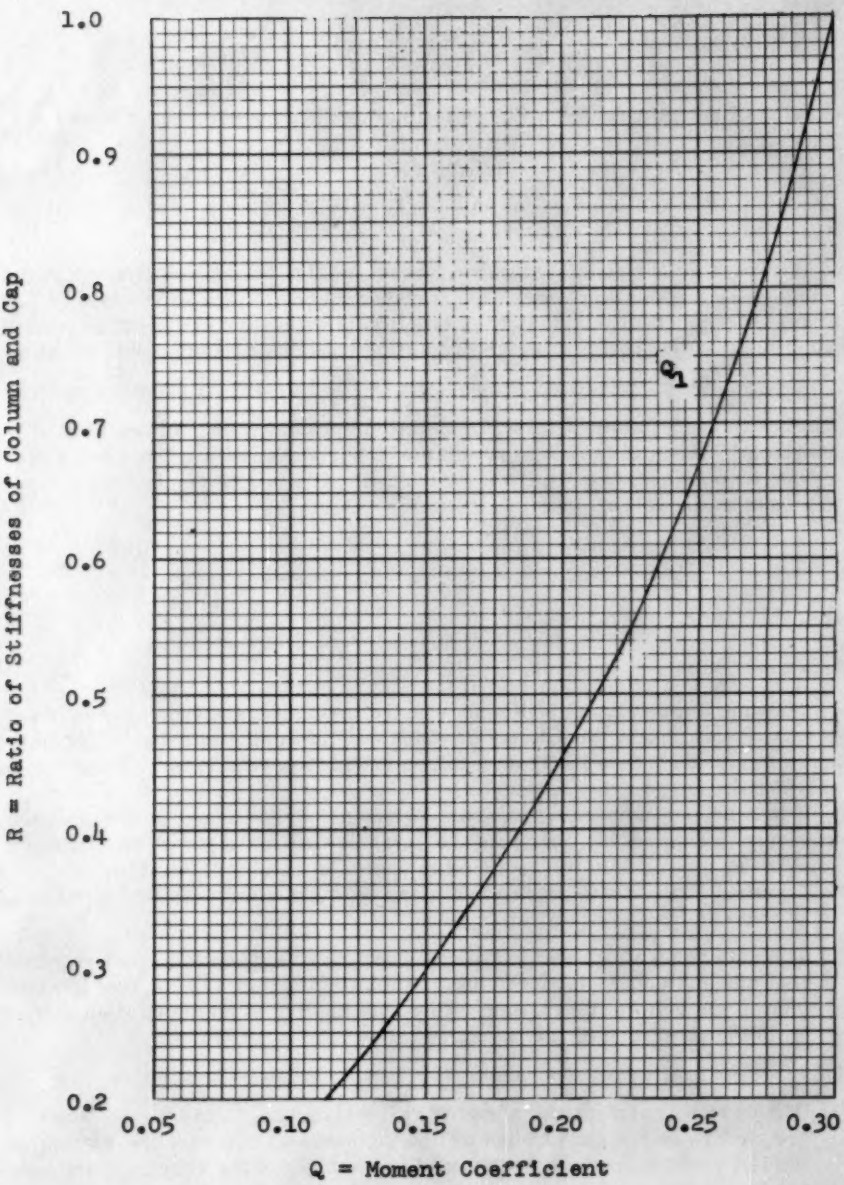

Diagram 1. Values of Q for formula 7.

Numerical Example

To illustrate the ease with which formula 7 may be used to analyze a rigid frame, the following numerical example has been worked.

Consider the frame shown in Figure 3. The frame is loaded with an unsymmetrical vertical load, a lateral load, and the cap is shortened by shrinkage and temperature change.

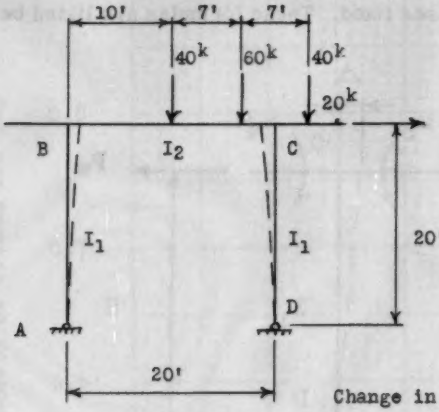

$I_1 = 8$ ft^4
$I_2 = 16$ ft^4
$E = 432{,}000$ kips/ft^2
$S_1 = 691{,}000$ ft kips
$S_2 = 1{,}382{,}000$ ft kips
$R = 691{,}000/1{,}382{,}000 = 0.5$
Change in length of cap = 0.0088 feet.

Fig. 3. Loaded Frame

Since most designers consider each loading condition separately, the problem will be worked that way. The first load to be considered will be the vertical loads acting on the cap. These loads produce the following fixed-end moments; $M_1 = 0$, $M_2 = -123$, $M_3 = -230$, and $M_4 = -160$. Since $R = 0.5$, the value of $Q_1 = 0.214$ can be obtained from Diagram 1. Substituting these values in Formula 7, the following balanced moments are obtained:

$$M_{BA} = 0.214\ (0 - 123 - 230 + 160) = -61,$$

and

$$M_{CD} = 0.214\ (0 + 123 + 230 - 160) = 61.$$

The next load to be considered will be the lateral load acting on the cap. Substituting $P_w = 20$ and $H = 20$ into formula 7, yields the following moments:

$$M_{BA} = 1/2 \times 20 \times 20 = +200,$$

and

$$M_{CD} = 1/2 \times 20 \times 20 = +200.$$

The last loading condition to be considered will be the shortening of the cap due to shrinkage and temperature changes. The total shortening of the cap is 0.0088 feet, and Δ for each column equals 0.0044 feet. Substituting this value of Δ and the appropriate values of S_2, and Q_1 and H into formula 7; the following balanced moments are obtained:

$$M_{BA} = (0.214 \times 1{,}382{,}000 \times 0.0044) / 20 = 65,$$

and $$M_{CD} = -(0.214 \times 1{,}382{,}000 \times 0.0044) / 20 = -65.$$

The balanced moments in the columns for all loading conditions have now been found by using formula 7. The remainder of the balanced moments and the shears and reactions can be found by using the laws of statics.

Two Column Rigid Frame With Column Bases Fixed

Using the same procedure as before, formulas were derived for a two column rigid frame with column bases fixed. These formulas are listed below.

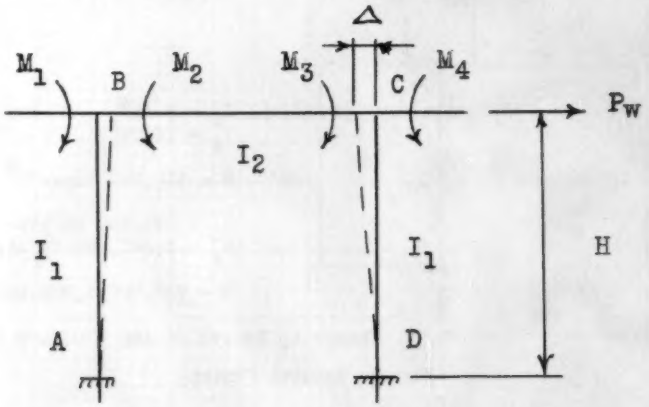

Fig. 4.

$$M_{AB} = -\frac{S_2 \Delta}{H} Q_2 \pm P_w H Q_4 + (M_1 - M_2) Q_6 + (M_4 - M_3) Q_8 \quad (8)$$

$$M_{BA} = \frac{S_2 \Delta}{H} Q_3 \pm \tfrac{1}{2} P_w H Q_5 + (M_2 - M_1) Q_7 + (M_3 - M_4) Q_9 \quad (9)$$

$$M_{DC} = \frac{S_2 \Delta}{H} Q_2 \pm P_w H Q_4 + (M_2 - M_1) Q_8 + (M_3 - M_4) Q_6 \quad (10)$$

$$M_{CD} = \frac{S_2 \Delta}{H} Q_3 \pm \tfrac{1}{2} P_w H Q_5 + (M_1 - M_2) Q_9 + (M_4 - M_3) Q_7 \quad (11)$$

Where:

$$Q_2 = \frac{3R(R+1)}{2(2R+1)}, \quad Q_3 = \frac{3R}{2(2R+1)}, \quad Q_4 = \frac{R+3}{2(R+6)}, \quad Q_5 = \frac{3}{2(R+6)},$$

$$Q_6 = \frac{R(5-R)}{2(2R+1)(R+6)}, \quad Q_7 = \frac{R(4R+13)}{2(2R+1)(R+6)}, \quad Q_8 = \frac{R(3R+7)}{2(2R+1)(R+6)},$$

and $Q_9 = \frac{11R}{2(2R+1)(R+6)}$.

The notation, sign convention and rules for using the formulas are the same as for the two column bent with column bases free to rotate. Values of Q_2 through Q_9 are plotted versus various values of R on Diagrams 2 and 3.

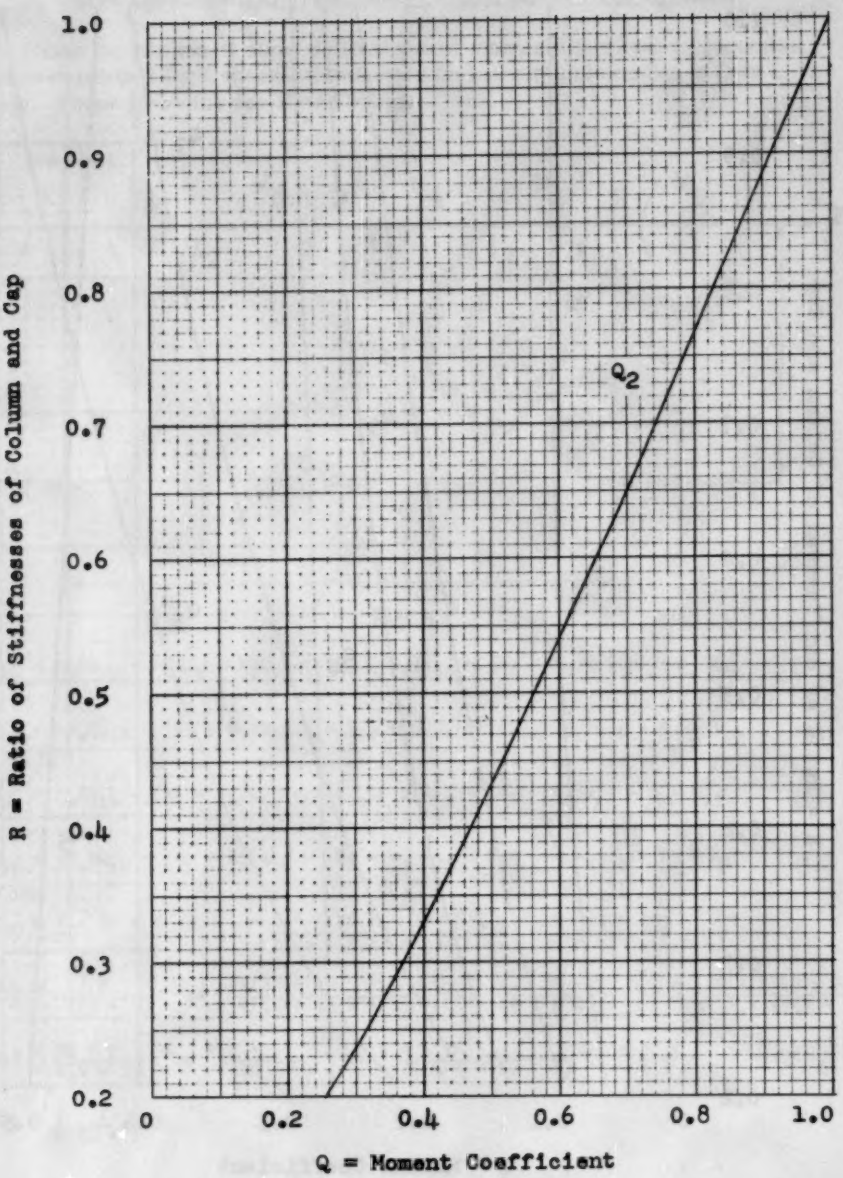

Diagram 2. Values of Q for Formulas 8, 9, 10, and 11.

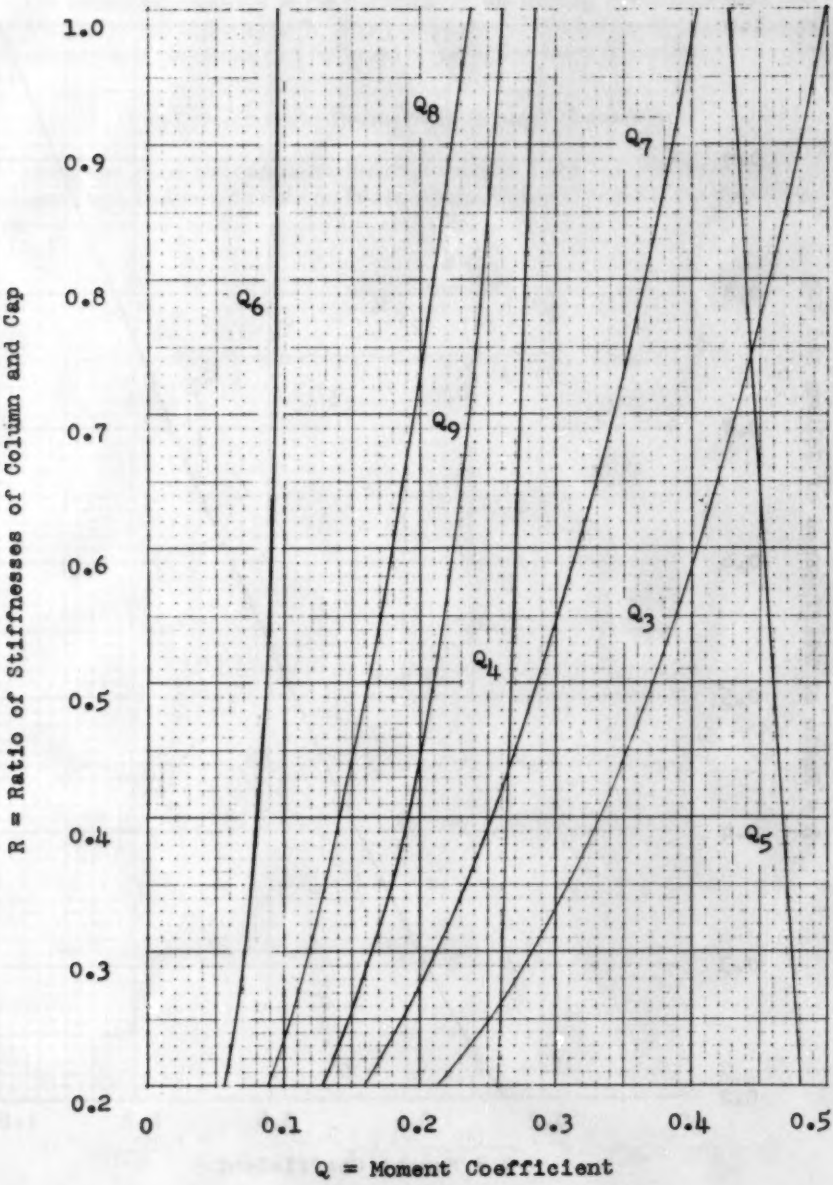

Diagram 3. Values of Q for Formulas 8, 9, 10, and 11.

Three Column Rigid Frame with Column Bases Free to Rotate

Using the method of slope deflection and moment distribution, formulas were developed for a three column rigid frame with column bases free to rotate. These formulas are listed below.

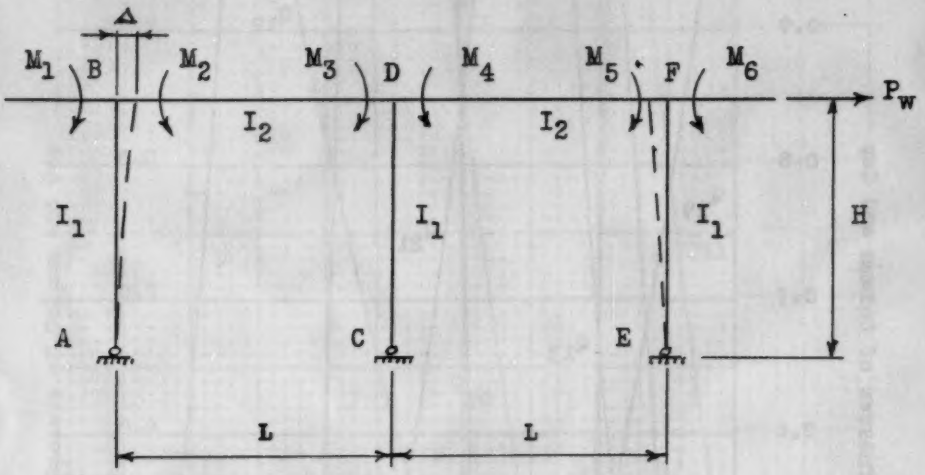

Fig. 5.

$$M_{BD} = P_w H Q_{10} + M_1 Q_{11} + M_2 Q_{12} + (M_3 - M_4) Q_{13} + (M_5 - M_6) Q_{14} + \frac{S_1 \Delta}{H} Q_{20} \quad (12)$$

$$M_{DB} = -P_w H Q_{15} - (M_1 - M_2) Q_{16} + M_3 Q_{17} + M_4 Q_{18} + (M_5 - M_6) Q_{19} - \frac{S_1 \Delta}{H} Q_{21} \quad (13)$$

$$M_{DF} = P_w H Q_{15} - (M_1 - M_2) Q_{19} + M_3 Q_{18} + M_4 Q_{17} + (M_5 - M_6) Q_{16} - \frac{S_1 \Delta}{H} Q_{21} \quad (14)$$

$$M_{FD} = -P_w H Q_{10} - (M_1 - M_2) Q_{14} - (M_3 - M_4) Q_{13} + M_5 Q_{12} + M_6 Q_{11} + \frac{S_1 \Delta}{H} Q_{20} \quad (15)$$

Where:

$$Q_{10} = \frac{1}{12} \frac{3R + 4}{R + 1} \qquad Q_{11} = \frac{3R^2 + 18R + 16}{4(3R + 4)(R + 1)} \qquad Q_{12} = \frac{R(9R + 10)}{4(3R + 4)(R + 1)}$$

$$Q_{13} = \frac{R}{4(R + 1)} \qquad Q_{14} = \frac{R(3R + 2)}{4(3R + 4)(R + 1)} \qquad Q_{15} = \frac{1}{12} \frac{3R + 2}{R + 1} \qquad Q_{16} = \frac{(3R + 2)(R + 2)}{4(3R + 4)(R + 1)}$$

$$Q_{17} = \frac{3R + 2}{4(R + 1)} \qquad Q_{18} = \frac{R + 2}{4(R + 1)} \qquad Q_{19} = \frac{4 - 3R^2}{4(3R + 4)(R + 1)} \qquad Q_{20} = \frac{3}{4} \frac{1}{R + 1}$$

$$Q_{21} = \frac{3}{8} \frac{1}{(R + 1)}$$

The notation, sign convention and rules for using the formulas are the same as those previously listed. Values of Q_{10} through Q_{21} are plotted on Diagrams 4 and 5.

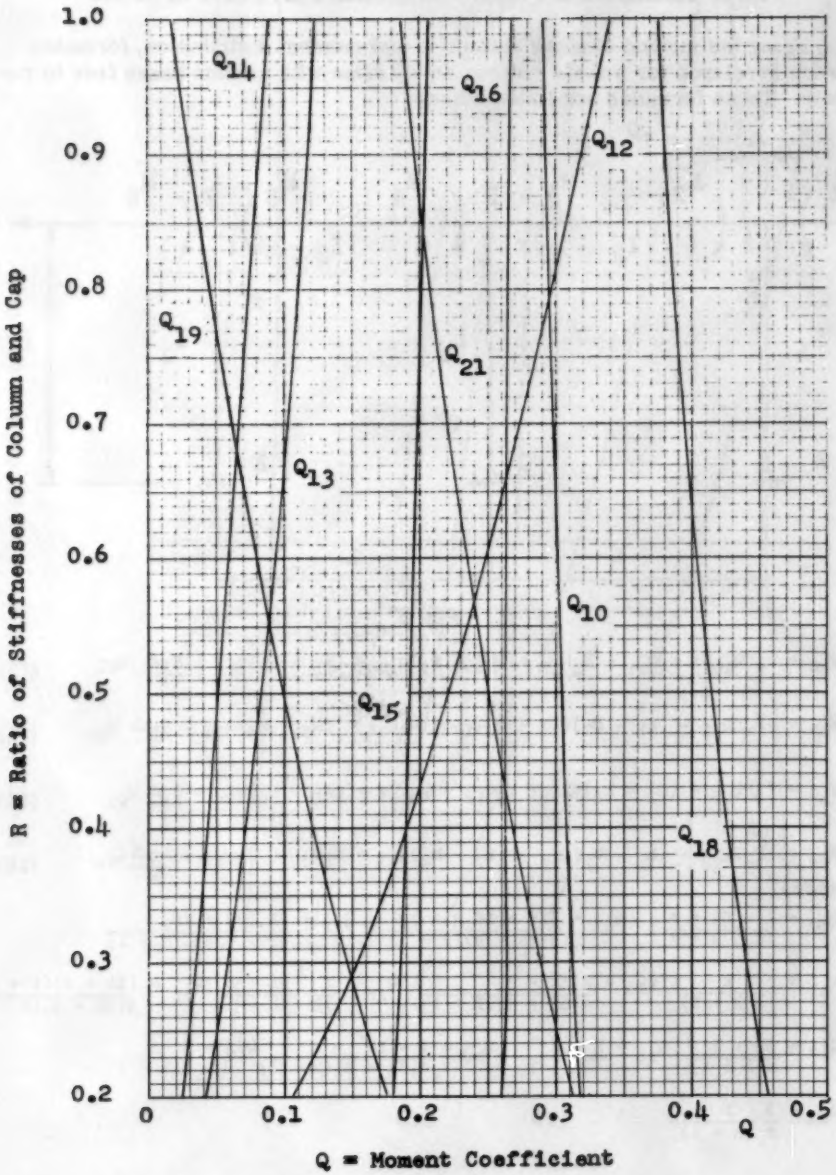

Diagram 4. Values of Q for Formulas 12, 13, 14, and 15.

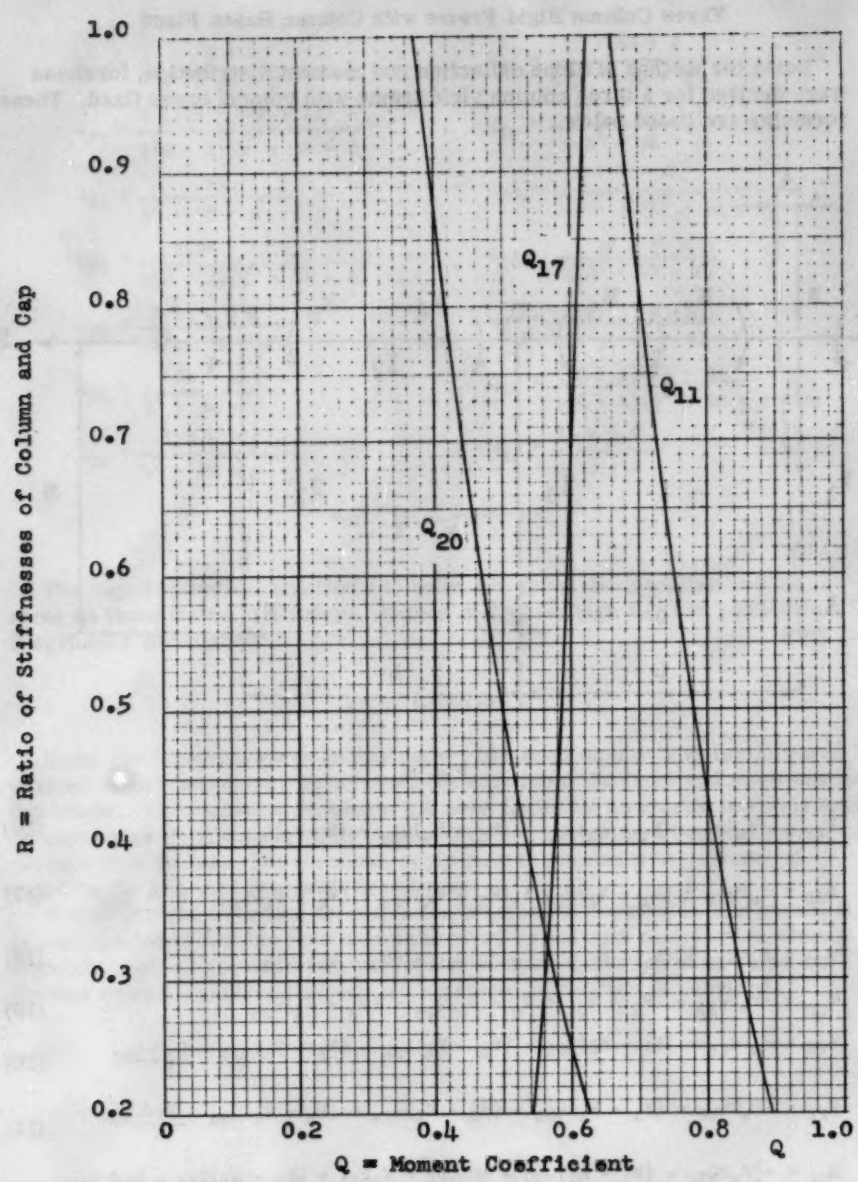

Diagram 5. Values of Q for Formulas 12, 13, 14 and 15.

Three Column Rigid Frame with Column Bases Fixed

Using the method of slope deflection and moment distribution, formulas were derived for a three column rigid frame with column bases fixed. These formulas are listed below.

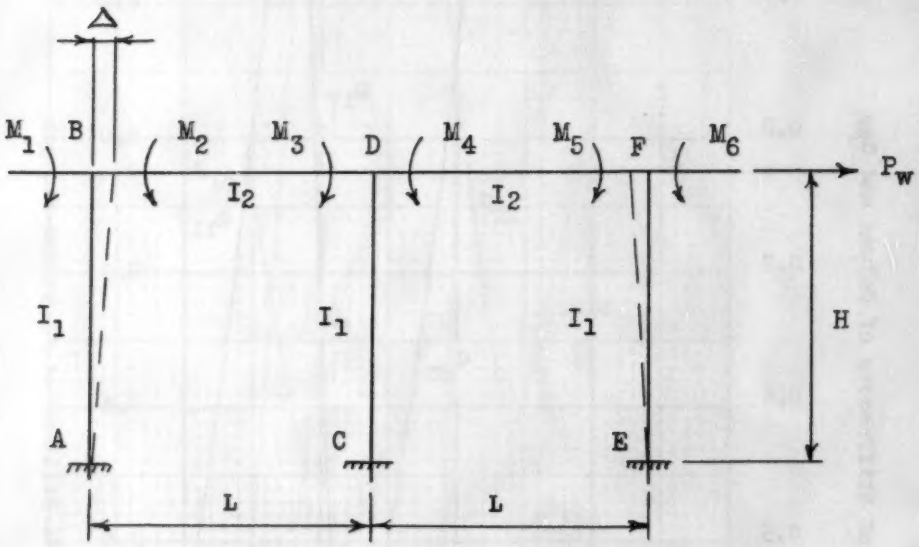

Fig. 6.

$$M_{AB} = -P_w H Q_{22} + (M_1 - M_2)Q_{23} - (M_3 - M_4)Q_{24} - (M_5 - M_6)Q_{25} - \frac{S_1 \Delta}{H} Q_{39} \quad (16)$$

$$M_{BA} = P_w H Q_{26} - (M_1 - M_2)Q_{27} + (M_3 - M_4)Q_{28} + (M_5 - M_6)Q_{29} + \frac{S_1 \Delta}{H} Q_{40} \quad (17)$$

$$M_{DC} = P_w H Q_{30} + (M_1 - M_2 + M_5 - M_6)Q_{31} - (M_3 - M_4)\, Q_{32} \quad (18)$$

$$M_{CD} = -P_w H Q_{33} - (M_1 - M_2 + M_5 - M_6)Q_{34} + (M_3 - M_4)Q_{28} \quad (19)$$

$$M_{FE} = P_w H Q_{26} + (M_1 - M_2)Q_{29} + (M_3 - M_4)Q_{28} - (M_5 - M_6)Q_{27} - \frac{S_1 \Delta}{H} Q_{40} \quad (20)$$

$$M_{EF} = -P_w H Q_{22} - (M_1 - M_2)Q_{25} - (M_3 - M_4)Q_{24} + (M_5 - M_6)Q_{23} + \frac{S_1 \Delta}{H} Q_{39} \quad (21)$$

$$M_{DF} = +\tfrac{1}{2} P_w H Q_{30} - (M_1 - M_2)Q_{35} - \tfrac{1}{2} M_3 Q_{36} + M_4 Q_{37} + (M_5 - M_6)Q_{38} - \frac{S_1 \Delta}{2H} Q_{40} \quad (22)$$

Where

$$Q_{22} = \frac{2R^2 + 9R + 6}{6(R^2 + 9R + 6)} \qquad Q_{24} = \frac{R\,(R + 2)}{2(R^2 + 9R + 6)}$$

$$Q_{23} = \frac{R(5R + 4)}{2(R + 1)(R^2 + 9R + 6)} \qquad Q_{25} = \frac{R(R^2 + 4R + 2)}{2(R + 1)(R^2 + 9R + 6)}$$

$$Q_{26} = \frac{R + 1}{R^2 + 9R + 6}$$

$$Q_{27} = \frac{R\,(2R^2 + 15R + 11)}{2(R + 1)(R^2 + 9R + 6)}$$

$$Q_{28} = \frac{2R}{R^2 + 9R + 6}$$

$$Q_{29} = \frac{R(3R + 1)}{2(R + 1)(R^2 + 9R + 6)}$$

$$Q_{30} = \frac{2R + 1}{R^2 + 9R + 6}$$

$$Q_{31} = \frac{7R}{R^2 + 9R + 6}$$

$$Q_{32} = \frac{R(R + 4)}{R^2 + 9R + 6}$$

$$Q_{33} = \frac{R^2 + 6R + 3}{3(R^2 + 9R + 6)}$$

$$Q_{34} = \frac{R(R + 5)}{2(R^2 + 9R + 6)}$$

$$Q_{35} = \frac{3 + R - 3R^2}{2(R + 1)(R^2 + 9R + 6)}$$

$$Q_{36} = \frac{5R + 6}{2(R^2 + 9R + 6)}$$

$$Q_{37} = \frac{(2R + 1)(R + 6)}{2(R^2 + 9R + 6)}$$

$$Q_{38} = \frac{(2R + 1)(2R + 3)}{2(R + 1)(R^2 + 9R + 6)}$$

$$Q_{39} = \frac{3}{4}\,\frac{R + 2}{R + 1}$$

$$Q_{40} = \frac{3}{2}\,\frac{1}{R + 1}$$

The sign convention, notation and rules for using the formulas are the same as those listed previously. Values of Q_{22} through Q_{40} are plotted on Diagrams 6 through 10.

CONCLUSIONS

Using the formulas given in this paper, balanced moments at the joints of various rigid frames may be obtained directly from the fixed end moments on the frame. The formulas eliminate the need for using an elastic analysis such as moment distribution or slope deflection when analyzing a two or three column rigid frame. The formulas apply only to frames with columns of equal length and with prismatic members.

If it is desired to derive formulas for frames not covered in this paper, it is recommended that the formulas be derived by moment distribution when a separate analysis for sidesway correction is not required, and by slope deflection when a separate analysis for sidesway correction is required.

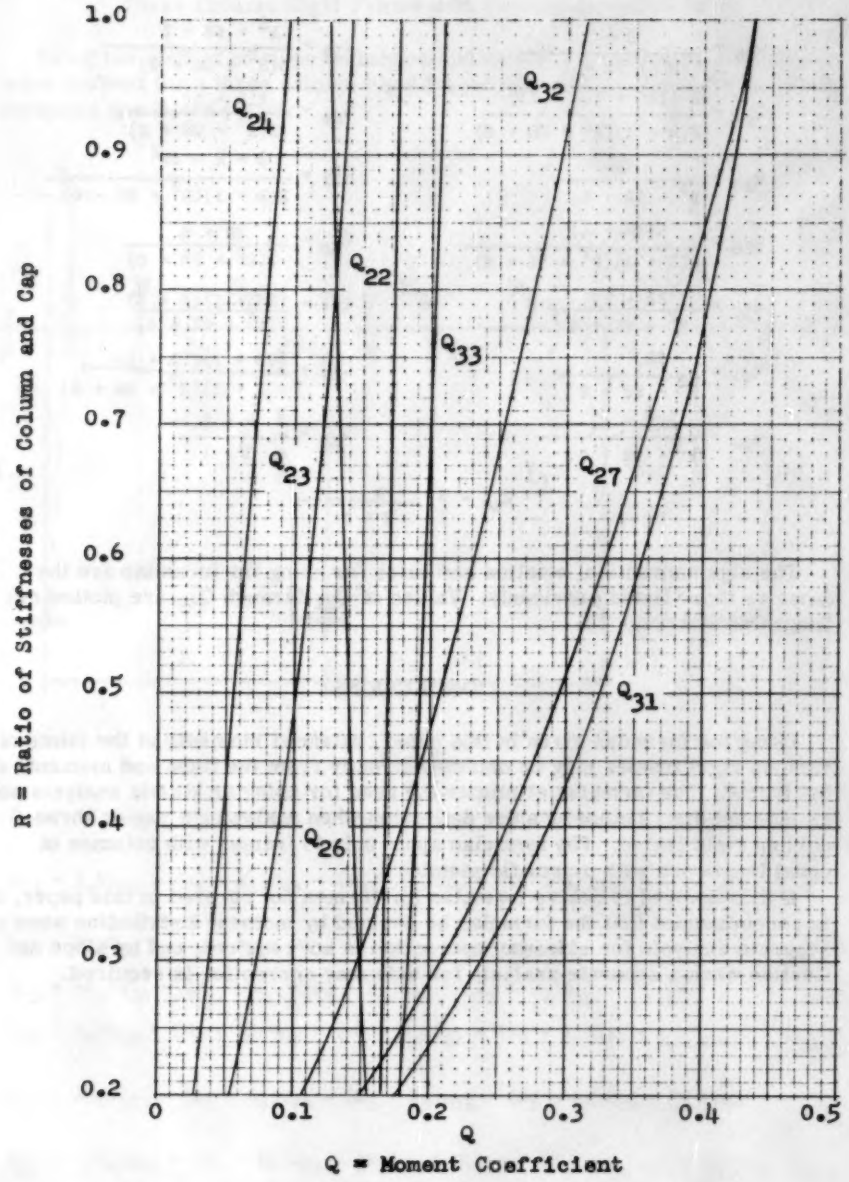

Diagram 6. Values of Q for Formulas 16, 17, 18, 19, 20, 21 and 22.

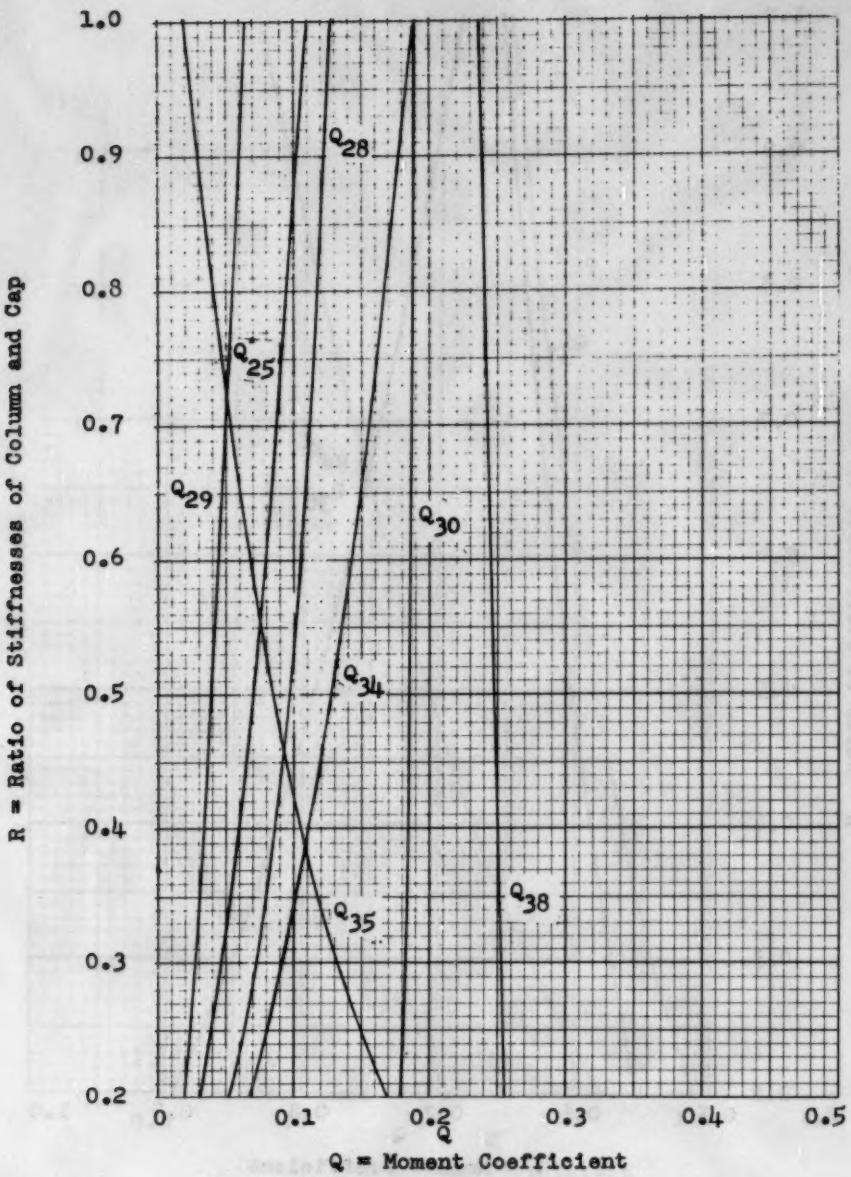

Diagram 7. Values of Q for Formulas 16, 17, 18, 19, 20, 21 and 22.

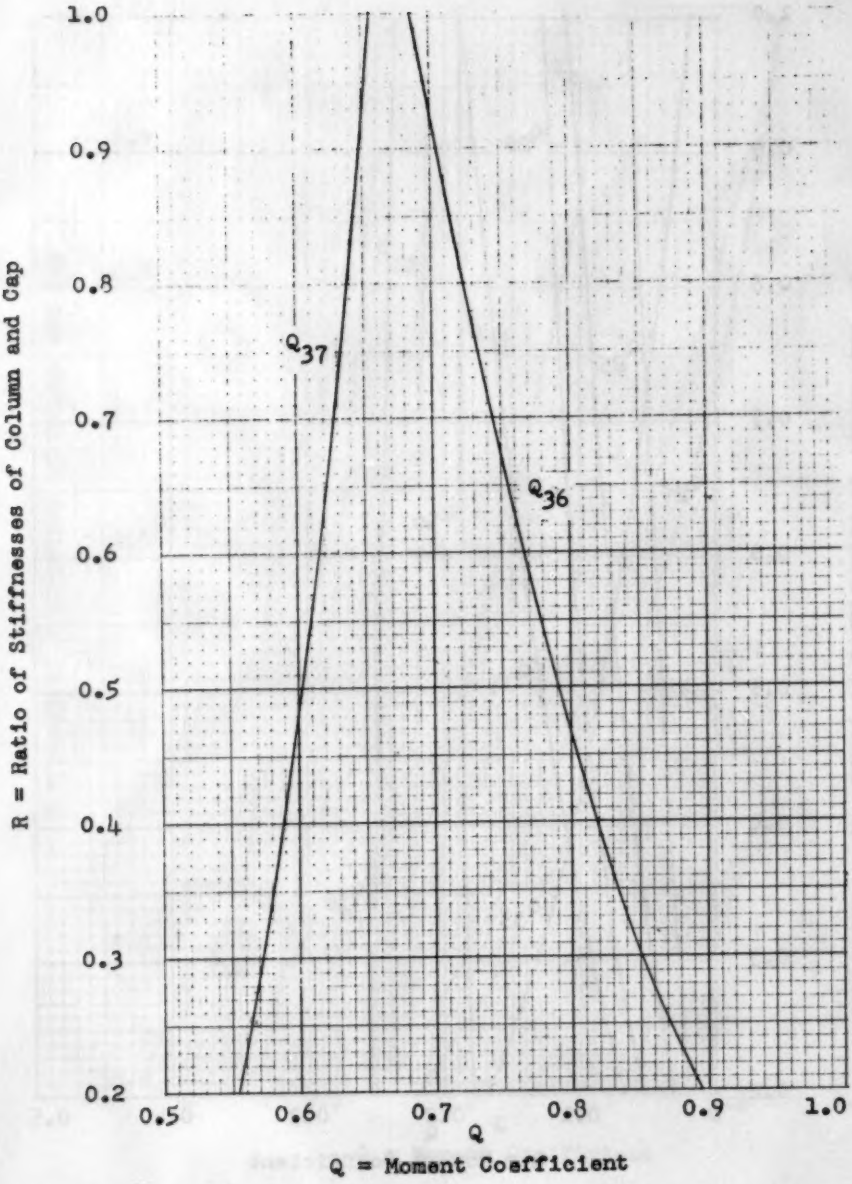

Diagram 8. Values of Q for Formulas 16, 17, 18, 19, 20, 21 and 22.

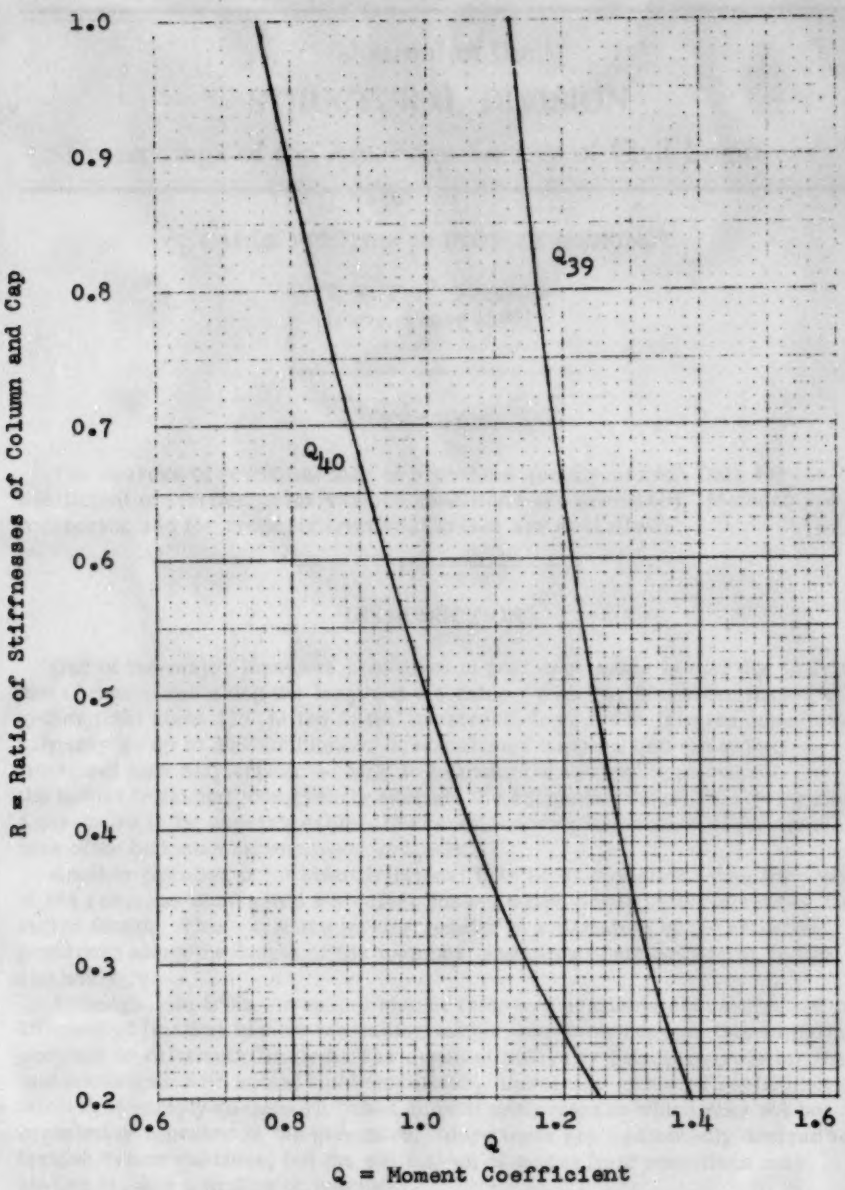

Diagram 9. Values of Q for Formulas 16, 17, 18, 19, 20, 21 and 22.

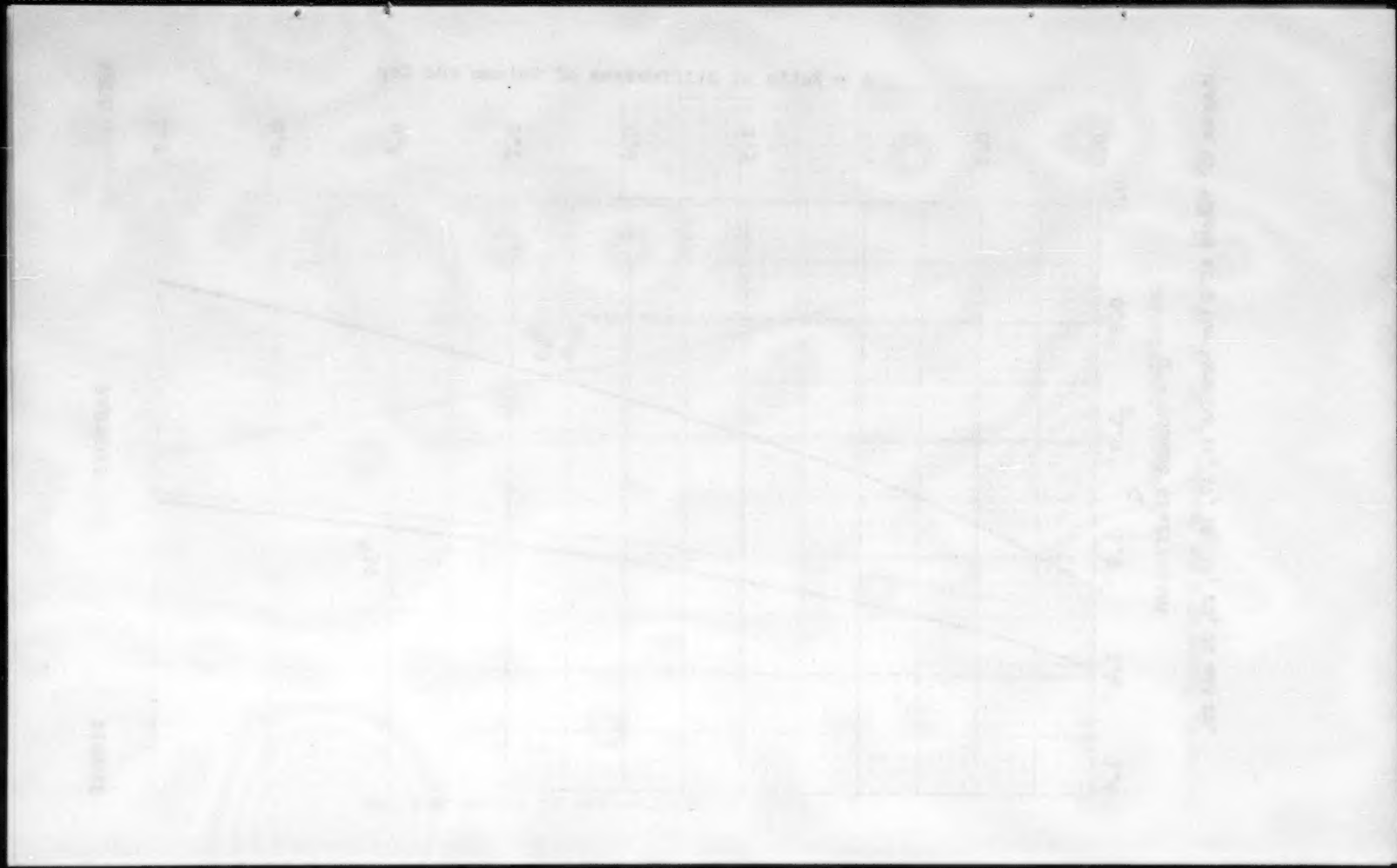

Journal of the
STRUCTURAL DIVISION
Proceedings of the American Society of Civil Engineers

CABLE FRICTION IN POST-TENSIONING[a]

T. Y. Lin,* M. ASCE
(Proc. Paper 1107)

SYNOPSIS

The sources of frictional loss of prestress are discussed. Data for the coefficient of friction under various conditions are presented. Methods for measuring and for reducing frictional losses are described.

INTRODUCTION

One of the major losses of prestress in post-tensioning is that due to frictional resistance along the length of the cable. While all the other losses together total about 15% of the initial prestress, loss due to friction occasionally may go up to 30% or higher. It sometimes happens that the expected frictional loss may appear so high as to make the design impracticable, or the actual frictional loss greatly exceeds the estimated value, thus rendering a structure to be unserviceable. Hence an accurate estimation of frictional loss often becomes an important problem.

Another peculiar point about frictional loss is its variation along the length of the cable, as contrasted with other losses which occur uniformly along the entire length. This variation of loss results in a variation of the effective prestress along the length of the member, and often complicates the design and analysis.

Although data from several series of tests are available concerning the coefficient of friction in post-tensioning cables, our knowledge on this important problem is relatively limited. The greatest difficulty lies in correlating the test conditions with actual field conditions. Hence any assumed coefficient of friction is simply guesswork based on past performance which may not be completely repeated in the structure. More tests are undoubtedly desired to furnish better guidance, but the estimation of actual field conditions may always remain a matter of judgment.

Note: Discussion open until April 1, 1957. Paper 1107 is part of the copyrighted Journal of the Structural Division of the American Society of Civil Engineers, Vol. 82, No. ST 6, November, 1956.

[a]Presented at the ASCE Convention, June, 1956, Knoxville, Tenn.

*Prof. of Civ. Eng., Univ. of California, Berkeley, Calif.

While frictional resistance in cables is an objectionable item to be contended with, it is interesting to mention that it can be an asset under certain conditions. For unbonded cables, the presence of friction prevents or restricts their slippage under load applications, and thus transforms an unbonded tendon into a partially bonded one. The ultimate strength of the beam is thus enhanced. Hence it appears desirable to coat unbonded cables with lubricants which will harden in the course of time, thus serving the dual purpose of reducing the friction during tensioning and increasing the bond after tensioning. Care must be taken, of course, to have the cables tensioned before the lubricant hardens.

Sources of Frictional Loss

There are two major sources of frictional loss. One is the loss produced by the binding of cables to the surrounding grout or concrete. This could be extremely serious and every means should be used to prevent its occurrence. Careless workmanship and unsatisfactory construction procedures may result in the sticking of cables to the surrounding material. For example, if there are holes in the sheathing which separates the cables from the concrete, fresh mortar may force its way into the sheathing and bind the cables so that it would be extremely difficult to tension them. For cables that are to be grouted for bond, it may happen that during the grouting of some cables grout finds its way into other untensioned cables, through holes in the sheathing or through intersection of the conduits. Cases have been known where it was impossible to tension the cables as a result of such leakage; but there is every reason to believe that similar incidents should not occur if proper care is exercised during construction.

The second and more common source of frictional loss is the bending of cables which can be further classified into three types:

1) Intentional bending of the cables to obtain a proper profile and location.—This is often necessary in order to obtain suitable position for the cables. For simple beams, the cables should be located near the bottom fiber at midspan but should be near the centroid of concrete section at the ends. For continuous and cantilever beams, the cables generally move from one side to another. Horizontal spreading of the cables at certain locations produces horizontal curvature in addition to the usual vertical curves.

2) Bending of wires at the anchorages.—For most systems using parallel wires, the wires are grouped together along the length of the tendon but are separated apart near the anchorages. This is true of the Freyssinet system, the Magnel system and most of the button-head systems. The angular turn of the individual wires at the anchorages produces a frictional loss of prestress so that the force at the jack differs from the stress in the wires. This is a relatively small amount of loss, say not much more than a few per cent, and hence is taken care of by overtensioning at the jack.

3) Unintentional wobbling of the cables along their length.—Even for cables that are supposed to be straight, a certain amount of wobbling will exist along their length, known as the wobbling or length effect. This wobbling is produced by the weight of the cable itself unless the supports for the cables are very closely spaced. It also results from the concreting operations, such as placing and vibrating. The amount of wobble evidently depends upon the weight of the cable, the stiffness of the cable and sheathing, the spacing and

rigidity of supports, and the amount of vibration. The resulting frictional loss is a function of the amount of wobble and the coefficient of friction.

Coefficient of Friction—Review of Previous Tests

The coefficient of friction between the cables and the surrounding materials depends upon many things, among which are the following:

1) The type of cable, whether wires, strands, or bars,
2) The surface conditions of the tendons, whether corrugated, smooth, rusted, or galvanized,
3) The surrounding material, whether paper, metal, plastic, or concrete,
4) The use of lubricants—grease, oil, wax, soluble oil, etc.
5) The sequence of tensioning—when the wires in one cable are pulled in a sequence as in the Magnel cable, the tensioned wires may press against the untensioned ones and increase the frictional loss. The tilting of grillages in the conduit as a result of tensioning operations may increase the friction between the wires.

In an effort to determine the coefficient of friction, the Cement and Concrete Association of England conducted an extensive series of experiments.[1] Average values for three different systems are listed in Table 1. One of the interesting points brought out by this series of tests was the wobble or length effect, for which a coefficient K was obtained as the loss of prestress per linear foot of cable. These values of K can be translated into an average curvature θ_k (in radians per ft of tendon) by the simple formula,

$$\theta_k = K/u$$

The wobble effect will vary greatly depending upon the amount of vibration used in placing the concrete and upon the spacing and stiffness of the supports for the cables. As an example, for Freyssinet cables in light metal sheathing, the K values can be as high as 0.0050 if heavy vibration is applied to the concrete and light-gage metal is used for sheathing without adequate supports.

Experiments were also conducted by Dr. Leonhardt of Germany to determine the coefficients of friction for different wires and strands on various underlays.[2] He also pointed out many factors that cannot be predetermined, such as thin sheet metal casings which may be worn through so that the wires slide against the concrete, or the lateral bending of wires in curved sections, or the uneven movement of the separators due to the elongation of wires. Some of his values are listed in Table 2. One of the interesting findings of his tests was the extremely low coefficient for paraffin under high pressure.

1. E. H. Cooley, Friction in Post-tensioned Prestressing Systems, and Estimation of Friction in Post-tensioned Concrete, Cement and Concrete Association, London, 1953.
2. Leonhardt, F., "Continuous Prestressed Concrete Beams," Journal, Am. Conc. Inst., March 1953 (Proc. Vol. 49), p. 617.

Table 1

FRICTIONAL COEFFICIENTS AND WOBBLE EFFECT
(Cement and Concrete Association, England)

	Freyssinet system			Magnel system			Lee-McCall system		
	u	K	θ_k	u	K	θ_k	u	K	θ_k
Duct formed by withdrawing steel tubing or rods	0.55	0	0	0.30	0.0010	.003	0.55	0.0005	.001
Rubber core unstiffened	0.55	0.0020	.004	0.30	0.0005	.002	0.55	0.0010	.002
Rubber core stiffened internally	0.55	0.0005	.001	0.30	0.0005	.002	0.55	0.0005	.001
Metal sheathing	0.35	0.0010	.003	0.30	0.0005	.002	0.30	0.0005	.002

u = coefficient of friction
K = coefficient of loss of prestress per ft of length
θ_k = average curvature of wobbling in radians per ft = K/u

Table 2

FRICTIONAL COEFFICIENTS
(Dr. F. Leonhardt)

Type of tendon	Underlay	u
Drawn wires, 0.196-in. diameter	smoothly finished concrete	0.29-0.31
	roughly finished concrete	0.35-0.44
	new black sheet metal	0.16-0.22
Two 0.079-in. wire strands	smoothly finished concrete	0.38-0.40
	roughly finished concrete	0.40-0.46
	new black sheet metal	0.19-0.22
Seven 0.099-in. wire strand	black sheet metal	0.20-0.25
	paraffin, under pressure of 30 psi	0.10
	paraffin, under pressure of 700 psi	0.02-0.025

A series of laboratory tests using Freyssinet cables of 10 x 0.2 in. wires was run in France[3] and the following coefficients of friction were obtained:

Table 3

FRICTIONAL COEFFICIENTS
(Y. Guyon)

	Max.	Min.	Ave.
Uncoated wires, paper wrapped	0.32	0.43	0.37
Uncoated wires, metal sheathed	0.36	0.25	0.32
Bitumen-painted wires, paper wrapped	0.08	0.10	0.09
Bitumen-painted wires, metal sheathed	0.17	0.22	0.19

Since these cables were relatively short, varying from 2'-4" to 5'-9", length effect was negligible. Some doubts were cast on the accuracy of the low frictional coefficients obtained for the bitumen-painted wires wrapped in paper. It is generally believed that the coefficient of 0.19 for the bitumen-painted wires in metal sheathing should hold true also for the paper wrapping. Depending upon the amount of coating, the coefficient can evidently vary within wide limits.

Recent Measurements of Friction in the U.S.A.

Several series of measurements were recently made in the United States to determine the coefficient of friction in actual structures. Four such series are discussed herein, using respectively Freyssinet cables, Roebling strands, high tensile rods and button-headed wires.

(I) Richmond Reservoir, Freyssinet cables—During the construction of the Richmond Reservoir Tank of 200-ft. diameter, 1954, Freyssinet cables were wrapped around the tank in quadrants of a circle and pulled from both ends. The cables were of 18 x 0.196-in. wires and the average length of cables was 1977 in. The maximum initial jacking stress in the wires was set at 200,000 psi. The procedure for jacking was as follows: jack both ends to 10% of the desired initial stress, then jack one end to 85%, then the other end to 80%, then both ends simultaneously to 100%.

Due to construction reasons, the cables were left in the sheathing for more than a month before they were pulled. During tensioning, cable elongation and jack pressure were recorded for each cable in order to obtain the coefficients of friction, some of which are listed in Table 4.

Due to the high value of friction encountered in these cables, it was decided to re-tension them after a few months. During re-tensioning, it was found

3. Guyon, Y. "PRESTRESSED CONCRETE," John Wiley and Sons, N.Y., 1953, pp. 84-94.

Table 4

FRICTIONAL COEFFICIENTS, RICHMOND RESERVOIR

GROUP NO.	NO. OF CABLES	VALUE OF COEFF. OF FRICTION MAX.	MIN.	AVERAGE
A	34	0.88	0.54	0.71
B	18	0.79	0.33	0.66
C	20	0.82	0.36	0.60

that numerous wires were broken as a result of corrosion. Consequently, all cables were replaced with new ones. In order to reduce the coefficient of friction for the new cables, the steel sheath was blown clean with water under pressure.

The following records the coefficient of friction as encountered by some of these new cables, also computed from cable elongation:

Table 5

FRICTIONAL COEFFICIENTS,

RICHMOND RESERVOIR, NEW CABLES

GROUP NO.	NO. OF CABLES	VALUE OF COEFF. OF FRICTION MAX.	MIN.	AVERAGE
D	12	0.59	0.32	0.44
E	13	0.59	0.31	0.42
F	16	0.61	0.31	0.45

In computing the coefficients of friction for Tables 4 and 5, no attempt was made to separate the wobble effect from the curvature effect, thus resulting in apparently high values of coefficients. Since relatively heavy vibration was employed in placing the concrete, it would be proper to assume the length effect K to be 0.0015 per ft for the cables. The cables were pulled from both ends and the length is one half of 1977 in. or 82.4 ft., while the curvature was 45 degrees or 0.785 radians. Hence the actual coefficient of friction u, after allowing for the wobble effect, can be computed from the apparent coefficient u_1 by the following formula,

$$u = u_1 - KL/\theta$$
$$= u_1 - 0.0015 \times 82.4/.785$$
$$= u_1 - 0.16$$

Thus the coefficients u_1 in Tables 4 and 5 can be recalculated and listed as in Table 6.

Table 6

FRICTIONAL COEFFICIENTS, RICHMOND RESERVOIR
(ASSUMING K = 0.0015/FT)

GROUP NO.	NO. OF CABLES	VALUES OF COEFFICIENT OF FRICTION		
		MAX.	MIN.	AVERAGE
A	34	0.72	0.38	0.55
B	18	0.63	0.16	0.50
C	20	0.66	0.20	0.44
D	12	0.43	0.16	0.28
E	13	0.43	0.15	0.26
F	16	0.45	0.15	0.29

It is interesting to note the appreciable difference in frictional coefficients between groups A, B, and C for the uncleaned ducts and the groups D, E, and F for the thoroughly cleaned ones. This brings out the significance of construction procedures which may seriously affect the values of frictional coefficients.

(II) Eureka Bridge, Roebling Strands—Seven 105-ft prestressed concrete girders designed by the California Division of Highways were made in the Petaluma plant of Ben C. Gerwich, Inc., 1955. 1-1/8 in. Roebling strands with a net steel area of 0.751 sq. in. were enclosed in thin metal corrugated sheathing and supported at about 2-ft intervals. Internal vibration was applied to the fresh concrete.

The tensioning procedure was as follows:

1) Tension one end to one-half the desired total elongation, recording the jacking force F_1 as indicated by gage pressure.
2) Tension the second end and record the force F_2 required to loosen the nut. Continue tensioning this second end until full prestress F_3 was reached.
3) Retension the first end, recording the force F_4 required to loosen the nut. Continue tensioning up to full prestress.

Based on the force required to loosen the nut at one end as compared to the force previously applied to the other end, it is possible to compute the total percentage of frictional loss from one end to the other, thus,

$$\text{Ratio of loss} = \frac{F_1 - F_2}{F_1} \quad \text{or} \quad \frac{F_3 - F_4}{F_4}$$

Cable groups M and N had practically no intended curvature, hence the frictional loss can be attributed almost entirely to the length effect, say a loss of 14% in a length of 105 ft, thus,

$$KL = 0.14$$
$$K = 0.14/105 = 0.0013$$

Assuming the length effect to be the same for all the other strands, coefficient of friction u can be computed by the following formula and listed in Table 7.

$$\mu = \frac{\frac{F_1 - F_2}{F_1} - KL}{\theta} \quad \text{or} \quad \frac{\frac{F_3 - F_4}{F_3} - KL}{\theta}$$

From Table 7, it can be seen that the coefficient of friction varies from a minimum of 0.29 for Group J to 0.35 for Groups G and H.

Table 7

FRICTIONAL COEFFICIENTS, STRANDS FOR EUREKA BRIDGE

Group No.	No. of strands	Curvature radians	F_1 kips	F_2 kips	$\frac{F_1-F_2}{F_1}$	u	F_3 kips	F_4 kips	$\frac{F_3-F_4}{F_3}$	u
G	14	0.23	65	51	0.21	0.30	117	91	0.22	0.35
H	14	0.20	66	55	0.17	0.15	119	94	0.21	0.35
J	14	0.17	64	54	0.16	0.12	116	94	0.19	0.29
K	14	0.03	66	56	0.15		115	97	0.16	
N	14	0.01	65	56	0.14		114	98	0.14	

(III) Eureka Bridge, High Tensile Rods.—Four 105-ft girders of this bridge were prestressed with high tensile rods of 1-1/8 in. diameter, manufactured by Rods, Inc., of Berkeley, California. They were also enclosed in thin metal sheathing and supported at about 2-ft intervals. The construction and tensioning procedure was identical to the girders using the strands described above. Data and computation for frictional loss are shown in Table 8. Due to the

Table 8

FRICTIONAL COEFFICIENTS, RODS FOR EUREKA BRIDGE

Group No.	No. of strands	Curvature, radians	F_1 kips	F_2 kips	$\frac{F_1-F_2}{F_1}$	u	F_3 kips	F_4 kips	$\frac{F_3-F_4}{F_3}$	u
P	8	0.22	61	57	0.066	0.11	102	98	0.039	
Q	8	0.18	65	61	0.062	0.10	106	100	0.057	0.08
R	8	0.15	63	59	0.063	0.14	105	99	0.057	0.10
S	8	0.07	64	60	0.062	0.29	103	98	0.049	0.10
T	8	0.040	65	61	0.062		104	101	0.029	

relative stiffness of the rods, their wobbling was almost unnoticeable. Using the losses for group T, which had very slight curvature effect, the whole wobble coefficient K can be estimated to be 0.0004 per ft. Assuming K = 0.0004, the coefficient of friction for groups P, Q, R, and S are computed as shown. Both the wobble coefficient and the coefficient of friction are seen to be rather low for these rods. However, the tests were not extensive enough to justify definite conclusion.

(IV) Laboratory beam, General Prestressing Cables.—A short series of tests was conducted on a 20-ft prestressed concrete beam at the University of California. A General Prestressing cable[4] made of 6 x 1/4" headed wires was greased with mastic and wrapped in paper. It was bent with a curvature of 0.21 radian near the midspan of the beam. The cable was tensioned from one end and the force accurately measured by a calibrated jack gage. The force at the non-jacking end was measured simultaneously with a dynamometer whose SR4 gage raed to an accuracy of 1/2%. No strain gages were installed along the length of the cable. The results of tests are recorded as follows:

Test 1 - Force applied at jacking end = 15,000 lb
Force recorded at non-jacking end = 13,600 lb

This indicated a frictional loss of 9.3% which can be approximately divided into:

Length effect KL = 0.0010 x 20 = 2%
Curvature effect $u\theta$ = 0.35 x 0.21 = 7.3%

After 3 minutes, the force at the non-jacking end increased to 13,920 lb, indicating a gradual slipping of the cable had taken place so that the coefficient u was reduced to about 0.25

Test 2 - The above jacking force of 15,000 lb was completely released and then re-applied. Maximum loss at the non-jacking end was only 6% and the average loss in four trials was 5%, which indicated a coefficient of friction of only 0.14.

Test 3 - One end was jacked to 18,000 lb., the non-jacking end had a force of 16,650 lb., indicating a loss of 7.5% or a coefficient of friction of 0.26. After 2 minutes, to measure the effect of temporary over-tensioning, the jacking force was lowered to 15,000 lb, and the force at the non-jacking end reduced itself to 16,500 lb, indicating a loss in the other direction of 9.1%, or a coefficient of friction of 0.34. When the jacking force was completely released, the non-jacking end had a residual force of 1000 lb which diminished to 750 lb. after 5 minutes, indicating a certain amount of sticking between the wires and the wrapping.

While the coefficient of friction obtained from such an isolated test cannot be taken as a good average value, it seems evident that for coated wires, there is an instantaneous value of frictional coefficient which will decrease with time.

4. Made by Western Concrete Structures, Los Angeles, California.

Reduction of Frictional Losses

The first step in reducing frictional losses lies in the design stage. Two simple ways to keep down frictional losses are to limit the length of tendons and to reduce their curvature. Generally speaking, the length is not a major factor until it exceeds one or two hundred feet. For example, corresponding to K = 0.0010, the loss of prestress in 100 ft is KL = 0.0010 x 100 = 10%. Curvature is not significant until the total angular change exceeds 20 or 30 degrees. For example, with u = 0.30 and $\theta = 20^0$ or 0.35 radians, the frictional loss is nearly 0.30 x 0.35 = 10%. The total frictional loss is the sum of the two but can be reduced to half by tensioning from both ends. Thus, a tendon 100 ft. long with an intended curvature of 20^0 would suffer a maximum frictional loss of about 10% if tensioned from both ends.

The second step in reducing frictional losses lies in the care exercised during construction. First of all, tendons must be carefully wrapped so as to avoid any leakage of mortar through the sheathing. Then the wobble effect can be reduced by providing strong and frequent supports for the tendons. The spacing of the supports will depend upon the size and stiffness of the tendons, and, in general, should not be more than 2 or 4 ft apart. Reasonably rigid holds for the tendons at the anchorages will also help to straighten them. Care should be exercised during concreting operations so as not to displace the tendons.

A third approach is to reduce the coefficient of friction between the tendon and the surrounding material. This is accomplished in a number of ways, by choosing tendons with proper surface conditions; for example, corrugated tendons and rusted tendons will have higher frictional coefficients. The type and surface conditions of the surrounding material, whether metal sheathing, paper, or plastic, or concrete, will affect the amount of friction, although we do not yet have enough data concerning the relative values of each.

Lubrication has been used to reduce frictional losses. Water-soluble lubricants which can be washed away have been suggested where it was desired to establish bond between steel and concrete. Grease, asphalt and wax have been successfully applied to lubricate unbonded cables or for the portion of cables which are intended to be unbonded. Certain types of asphaltic mix tend to harden as time goes on and may result in high frictional loss.

Frictional losses can be totally or partially balanced by over-tensioning. The amount of over-tensioning is necessarily limited by the strength of the tendons and should not be carried too far. A common rule is not to tension the tendons to over 75% or 80% of its ultimate strength.

Tensioning from both ends is a common method for reducing frictional loss. Re-tensioning is sometimes suggested as another means of balancing frictional losses. Actually, if the maximum jacking stress is limited, re-tensioning will not reduce the frictional loss as such, but will balance some of the losses due to creep and shrinkage. For unbonded cables which will slip with time, re-tensioning or sustained tensioning will help to reduce frictional losses.

Computation for Frictional Losses

When the coefficient of friction and the wobble effect are known or assumed, it is a simple matter to compute the magnitude of frictional losses.

The exact formula for frictional loss takes the well-known exponential form,

$$f_2 = f_1 e^{-u\theta - KL}$$

where f_2 and f_1 = unit stress in steel at points 2 and 1

e = natural log base
u = coefficient of friction
θ = angular change or curvature in radians
K = coefficient for wobble effect per ft
L = length of cable in ft

When the value of $u\theta + KL$ does not exceed 0.20 or 0.30, the following simplified formula will yield very nearly correct answers,

$$f_2 = f_1 (1 - u\theta - KL)$$

No attempt will be made here to present the method of computation for frictional losses. Readers are referred to treatise on prestressed concrete[5] for detailed examples.

In a paper by M. J. Montagnon,[6] a very convenient monograph was presented which gives the relation between frictional loss, cable elongation, and the coefficient of friction, Fig. 1. Four scales are shown in the figure,

Scale 1 - Tension at jacking end, in ksi
Scale 2 - Average tension for the cable in ksi (for computing cable elongation)
Scale 3 - Tension at non-jacking end, in ksi
Scale 4 - $KL + u\theta$

From these four scales, it is only necessary to know two values in order to determine the remaining two. An example is given in Fig. 1.

CONCLUSION

Frictional loss is not a serious problem for relatively short and straight cables if reasonable care is taken during construction. For cables with a lot of curvature or with length over 100 or 200 ft, efforts should be made to reduce frictional loss to a minimum or to make proper allowance for the loss.

Presently, we have some data concerning the coefficient of friction for post-tensioned cables so that approximate design can be made. When more exact values of frictional loss are desired, test should be run to determine the coefficient of friction and the length effect for the particular conditions.

5. Lin, T. Y., "DESIGN OF PRESTRESSED CONCRETE STRUCTURES," John Wiley and Sons, Inc., 1955, pp. 92-109. Also reference C.A.C.A. above.
6. Montagnon, M. J., "Aspects Practiques de la Precontrainte par Cables—Le Problème des Frottements," Supplément aux Annales de L'Institut Technique du Batiment et des Travaux Publics, Paris, June, 1954, pp. 504-520.

ACKNOWLEDGMENT

In addition to the various sources of information already cited, the writer wishes to acknowledge the following persons for helping supply the data presented in this paper: Mr. L. E. Hanson, East Bay Municipal Utility District, Oakland, Calif.; Mr. Don Scott, Bridge Department, State of California; Mr. Jack Weiss of Ben. C. Gerwich Inc., San Francisco, Calif.; Mr. James Libby of Freyssinet Company, N.Y.; and Mr. Howard R. May, research engineer, University of California.

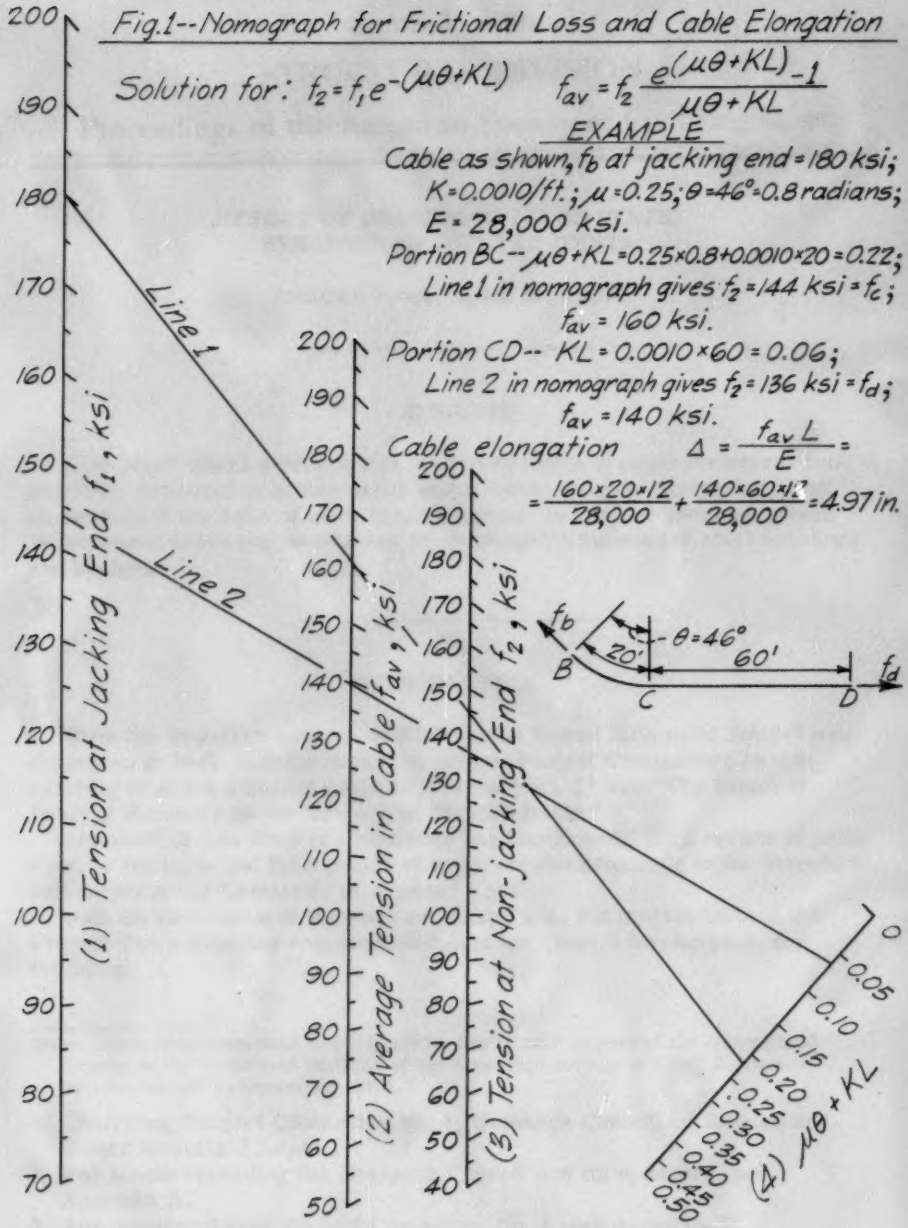

Fig.1--Nomograph for Frictional Loss and Cable Elongation

Solution for: $f_2 = f_1 e^{-(\mu\theta + KL)}$ $\quad f_{av} = f_2 \dfrac{e^{(\mu\theta+KL)} - 1}{\mu\theta + KL}$

EXAMPLE

Cable as shown, f_b at jacking end = 180 ksi;
$K = 0.0010$/ft.; $\mu = 0.25$; $\theta = 46° = 0.8$ radians;
$E = 28{,}000$ ksi.

Portion BC -- $\mu\theta + KL = 0.25 \times 0.8 + 0.0010 \times 20 = 0.22$;
Line 1 in nomograph gives $f_2 = 144$ ksi $= f_c$;
$f_{av} = 160$ ksi.

Portion CD -- $KL = 0.0010 \times 60 = 0.06$;
Line 2 in nomograph gives $f_2 = 136$ ksi $= f_d$;
$f_{av} = 140$ ksi.

Cable elongation $\Delta = \dfrac{f_{av} L}{E} =$

$= \dfrac{160 \times 20 \times 12}{28{,}000} + \dfrac{140 \times 60 \times 12}{28{,}000} = 4.97$ in.

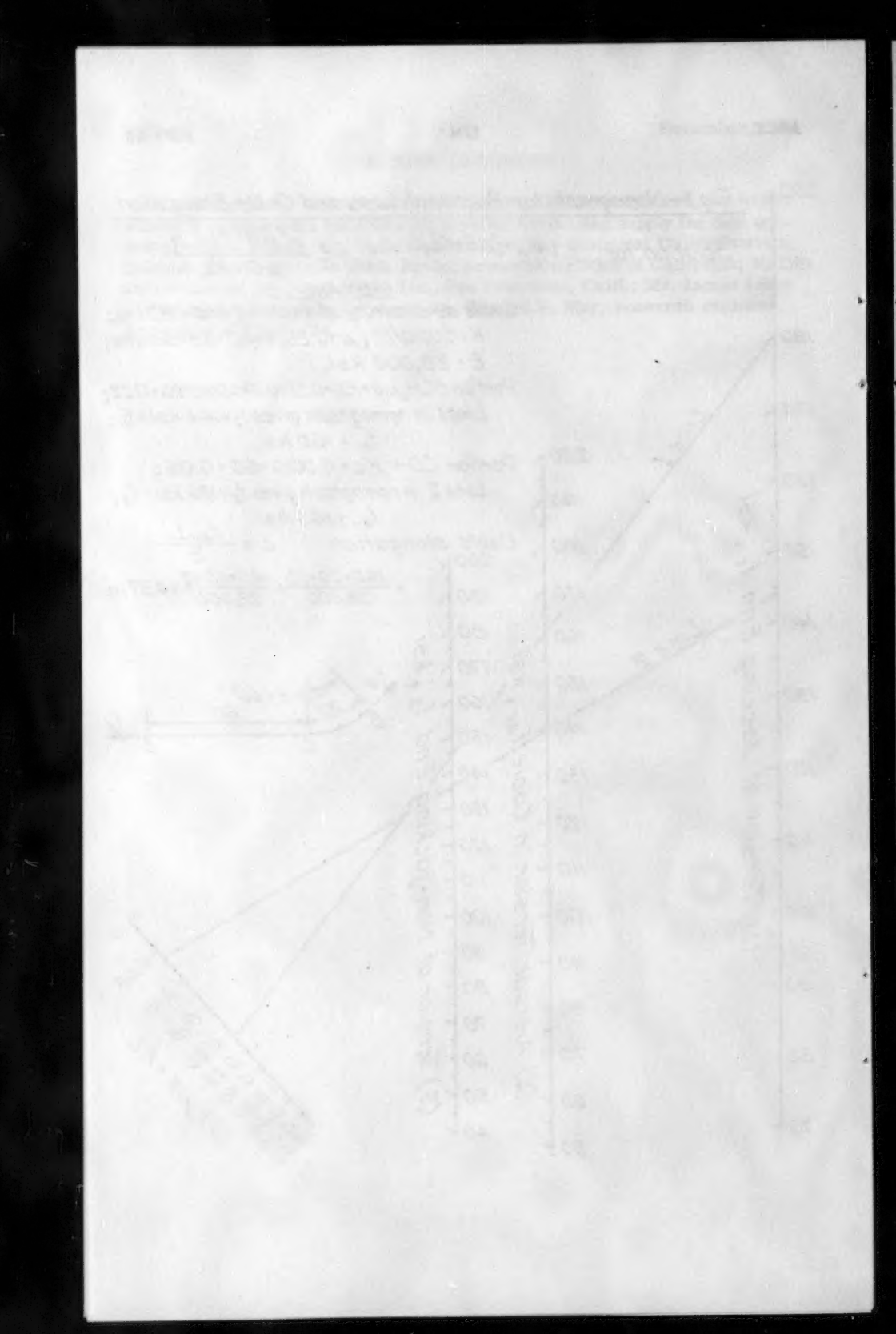

Paper 1108 ST 6

Journal of the
STRUCTURAL DIVISION
Proceedings of the American Society of Civil Engineers

EFFECT OF BEARING RATIO ON STATIC STRENGTH OF RIVETED JOINTS

Jonathan Jones,[1] HON. M. ASCE

SYNOPSIS

This paper offers evidence that in riveted joints of usual structural proportions, subjected to substantially static loads, the joint strength will not be reduced if the ratio of rivet bearing stress to axial or shearing stress is increased above that sanctioned by most specifications for steel buildings and bridges.

INTRODUCTION

When the Research Council on Riveted and Bolted Structural Joints[2] was organized in 1947, it designated appropriate Project Committees for the handling of seven different projects. Project No. 1[3] was "The Effect of Bearing Pressure on the Strength of Riveted Joints."

The work of this Project Committee has comprised: (1) a review of prior work on the topic and (2) a series of experimental programs in the structural laboratory of the University of Illinois.[4]

With the conclusion of its work and based upon the content thereof the Project Committee has recommended, and the Council has adopted, the following

Note: Discussion open until April 1, 1957. Paper 1108 is part of the copyrighted Journal of the Structural Division of the American Society of Civil Engineers, Vol. 82, No. ST 6, November, 1956.

1. Chairman, Project Committee No. 1, Research Council on Riveted and Bolted Structural Joints.
2. For a note regarding the Research Council and its sponsors, see Appendix A.
3. For membership of Project Committee No. 1, see Appendix B.
4. For details of these programs see References 7, 8, 9, 10.

CONCLUSIONS

For riveted joints of normal design[5] in medium structural steel comparable to that defined in A.S.T.M. Specification A7, riveted in accordance with good commercial practice employing rivet steel comparable to that defined in A.S.T.M. Specification A141;

1. Under static loading, the strength of a joint loaded in tension is not reduced by reason of bearing pressure, if the ratio of this to the net tensile stress on the main material does not exceed 2.25.

$$\frac{\text{Bearing pressure} = s_b = \text{Breaking Load} \div (\text{No. of rivets} \times \text{cold rivet dia.} \times \text{plate thickness})}{\text{Net tension} = s_t = \text{Breaking Load} \div \text{Net tensile area as defined by spec.}} \leqq 2.25$$

2. Under static loading the strength of a joint loaded in compression or shear is not reduced by reason of bearing pressure, if the ratio of this to the shearing stress on the rivets does not exceed 3.00.

$$\frac{\text{Bearing pressure} = s_b}{\text{Rivet shear} = s_s} = \frac{\text{As defined in the preceding}}{\text{Breaking load} \div \text{area of total shearing surfaces of rivets}} \leqq 3.00$$

3. In joints with not more than two rivets in the line of stress the foregoing conclusions hold true only if the "end distance" or distance from rivet to unloaded end of piece is sufficient to obviate the splitting out of the rivet through this end portion.

The details of this latter requirement have not been explored in this project. Such possible end weakness has on the contrary been avoided in the specimens tested under this project, by following the end distance requirement of A.I.S.C. Specification[6] Sect. 23 (f).

4. For the ratio of rivet shear to plate tension commonly found in American specifications for steel bridges and buildings, the foregoing limits may be conveniently expressed thus:

Static Tension	$S_t : S_s : S_b = 1.00 : 0.75 : 2.25$	
Static Compression or Shear	$S_s : S_b = 1.00 : 3.00$	
Thus: For statically loaded members in Buildings,	20 000 : 15 000 : 45 000	(in psi)
" " " " " Bridges,	18 000 : 13 500 : 40 500	(in psi)

5. No reason is found for differentiating between the allowable bearing pressure on a rivet stressed in single shear and that on a rivet stressed in double shear.

---

5. Normal design for a tensile joint contemplates that the "g/d" ratio shall not exceed about 5 if the theoretical tensile efficiency is to be attained. g = distance center to center of holes, transverse to line of tensile force. d = diameter of rivet. See Reference 11.
6. Specifications for the Design, Fabrication and Erection of Structural Steel for Buildings, American Institute of Steel Construction, New York City, February, 1946.

6. At the above recommended unit stresses, bearing in single shear joints will virtually never be critical, nor its computation necessary.

7. These conclusions are not applicable to "high-strength" steels.

Incidental Considerations

1. If $S_b : S_s = 3.00 : 1.00$,

	Single Shear	Double Shear
Value of one rivet =	$S_s \cdot \frac{\pi d^2}{4}$	$S_s \cdot \frac{\pi d^2}{2}$
Then $3.00\ S_s \cdot d \cdot t$ =	do.	do.
$\frac{t}{d}$ =	$\frac{\pi}{3 \times 4}$	$\frac{\pi}{3 \times 2}$
=	0.26	0.52
If d = 3/4" minimum t =	0.19"	0.38"
7/8"	0.23"	0.46"
1"	0.26"	0.52"

It is evident from the thicknesses ordinarily encountered in important bridge construction that most joints, whether in single or in double shear, will not require the making of computations based on a bearing criterion.

2. Before discussing data from the test programs executed under this project, it seems appropriate to set down the following general considerations:

"High bearing pressure" is only another way of saying "thin connected material" (thin as related to the rivet used); under working loads, because of the clamping action of the rivets, there may or may not be any actual bearing.

A rivet of short grip (driven, say, through a certain number of plies of thin material) does not have the clamping force of a rivet of long grip (driven, say, through the same number of plies of thicker material). On geometrical reasoning this should not be so, and it is presumably a function of rivet constitution and head behavior.

A rivet of short grip will as a practical commercial average, fill its hole more closely than a rivet of long grip.

Initial slip, which represents the overcoming of friction and which brings actual bearing into existence as its consequence, may, therefore, start sooner with rivets of short grip (thin material, "high bearing") than with rivets of long grip (thick material, "low bearing"); but should proceed over less distance before bringing up in actual bearing.)

In static loading, after initial slip has been arrested by bearing, three conditions are to be distinguished:

a) If the critical plate is being stressed in tension, and there is an insufficient distance from the rivet to the unstressed end of the piece, failure can occur through the bulging out, and ultimate

bursting open of the plate, beyond the rivet and in line with the load (This type of failure is recognized and prescribed against, in the A.I.S.C. Specifications,[6] but not in standard American specification for bridges).

b) If the critical plate is stressed in tension, and there is sufficient end distance, and the ratio of computed bearing stress to tensile stress (the "bearing ratio") does not exceed that recommended in the foregoing, failure will not occur by the crushing of material at the surfaces in bearing, since this will be preceded by the failure of the critical plate on some transverse line.

c) If the critical plate is being stressed in compression or shear, then after initial slip produces actual bearing it is quite possible for thin material to fail by the flowing of the metal at the surfaces in bearing. The criterion is, the magnitude of the stress per rivet vs. the product of rivet diameter and plate thickness.

Background for Project Programs

At the time this project was undertaken, there was little record of joint tests in which the bearing ratio had been high, or of tests specifically directed toward establishing a safe upper limit of bearing.

In 1938 the present Project chairman had prepared for A.I.S.C. a memorandum digesting such German, and American, tests on this topic as he had been able to locate. The most pertinent of these were:

Reference No. 2.[7] Specimens contained three rivets in line, about 5/8" dia. in double shear. The plates were alternatively 1/2" or 1/4" ($S_b : S_s = 2 :$ 1 or 4 : 1). The thicker plates failed by rivet shear with a factor of safety of 3.37; the thinner plates failed "in bearing" (what this failure comprised is not described) with a factor of safety of 3.02.

Reference No. 3. Similar tests were made, and it was found that for equal safety as between tension and bearing, measured by ultimate load, the ratio $S_b:S_t$ might be allowed to go as high as 3.21.

The German Specifications adopted at this time a bearing ratio of 2.50 for static and 2.00 for dynamic loads, the latter being based on the concept of failure at 2 000 000 cycles.

Reference No. 4. (These are Dr. Graf's original fatigue tests on one-rivet connections). For stress ratios of 1 : 0.93 : 2.50 he found that a pulsating load of zero to 29 900 psi tension reached 2 000 000 cycles without failure. This was, however, a "coasing" test with initial cycles at a succession of lower and gradually increased loads.

Reference No. 5. The pulsating fatigue strength of a riveted joint is here compared to that of a bar containing a drilled hole; the latter being accepted as an upper limit to the resistance to be expected from a structure. The conclusion is reached that a stress ratio 1 : 0.80 : 2.50 will yield a pulsating fatigue strength from 100 to 120 percent of that of a drilled bar, therefore, satisfactory for design specifications.

7. Reference numbers refer to list following this text.

Reference No. 6. These were static tests of single-rivet specimens with stress ratios varying in steps from 1 : 0.97 : 1.78 to 1 : 0.97 : 3.56. The breaking load for the specimen with highest bearing was within 3 percent of that with lowest bearing, and attained 66 000 psi in tension on net section, as against the coupon ultimate of 65 000.

Static Tests Under Project No. 1

Summary of First or 1949 Static Series

For further details see Reference No. 8.

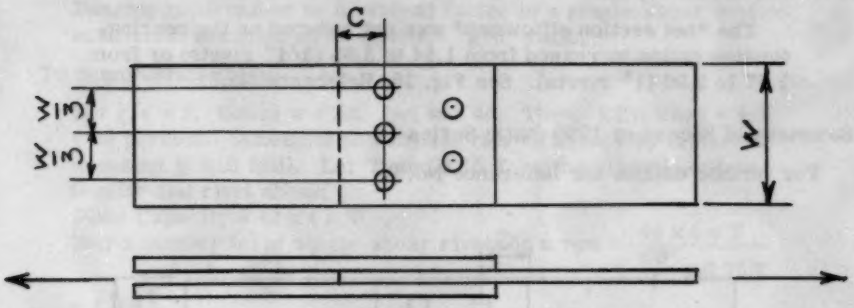

Fig. 1
From Fig. 1, Ref. No. 8

For 3/4"	center plate w =	6.46",	c = 1 1/2"	Bearing Ratio 1.29:1	3/4" Rivets
5/8		7.40	1 1/2	1.54:1	
1/2		8.82	1 3/4	1.91:1	
3/8		11.17	2 3/8	2.55:1	
5/16		13.05	2 1/2	3.05:1	
For 1"	center plate w =	8.53",	c = 1 3/4"	1.28:1	1" Rivets
13/16		9.97	2	1.57:1	
5/8		12.30	2 1/4	2.04:1	
1/2		14.82	3 1/8	2.54:1	
7/16		16.63	3 1/4	2.90:1	

This 1949 Series gave disappointingly low "test efficiencies," meaning by this the ratio of breaking load to the product of the "theoretical" net section by the coupon ultimate strength. Moreover, the break patterns were erratic; including, contrary to the expectation under specification rules for net section a few zigzag breaks through three rivets and a few rivet failures; whereas the design expectation was a break across the two rivets in the outer row (plate-tension : rivet-shear ratio, 1 : 0.83).

In retrospect it is seen that the Series was unfortunately designed in that some of the theoretical net sections were illusory, and the theoretical efficiencies unattainable. The theoretical efficiency of the widest and thinnest specimens was, for example,

$$\frac{13.05 - 2 \times 13/16}{13.05} = 87.5$$ and their

"g/d" ratio $$\frac{1/3 \times 13.05}{13/16} = 5.35.$$

Such efficiencies are known, as from the results of Program 2, to be illusory at such "g/d" ratios. See for instance Reference No. 11. For this Series, therefore, the actual values of "net section efficiency" (the percentage developed in tests, of the net area times coupon ultimate) attained are beside the point. The very interesting and pertinent observation that can be made from this Series is, that:

> The "net section efficiency" was not reduced as the bearing-tension ratios increased from 1.54 to 3.05 (3/4" rivets) or from 1.57 to 2.90 (1" rivets). See Fig. 15, Reference No.8.

Summary of Second or 1950 Static Series

For further details see Reference No. 9

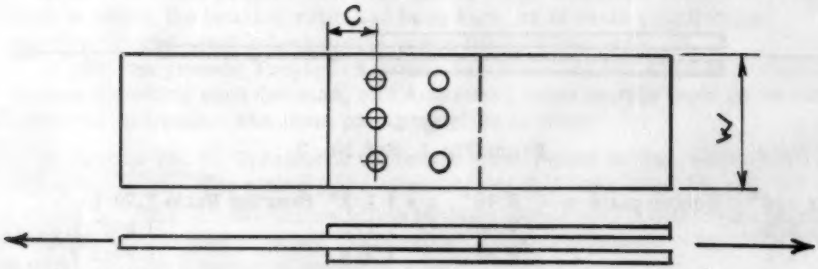

Fig. 2
From Fig. 1, Ref. No. 9

For 5/16" outer plates	w = 8.80,	c = 1 1/2	Bearing Ratio	1.41:1	3/4" Rivets
1/4	10.38	1 3/4		1.77:1	
3/16	13.04	2 1/2		2.36:1	
For 3/8 " outer plates	w = 10.02,	c = 1 3/4		1.37:1	7/8" Rivets
5/16	11.48	2		1.65:1	
1/4	13.64	2 1/2		2.06:1	
3/16	17.24	3 1/4		2.75:1	
For 7/16" outer plates	w = 11.26,	c = 1 3/4		1.34:1	1" Rivets
3/8	12.62	2		1.57:1	
5/16	14.50	2 1/2		1.88:1	
1/4	17.32	3		2.35:1	

Whereas in the 1949 Series the inner plate was critical and the rivets delivered to it the forces due to double shear, in the 1950 Series, the inner plate was held to a constant and non-critical thickness for each of the three

rivet sizes, and the critical bearing was on the outer plates, where the rivets were stressed in single shear and subjected to cantilever bending.

Most of these specimens developed a "net section efficiency" of 100 percent or more. Three developed 99, 98 and 96 percent respectively. One (No. 50-7) developed only 89 percent, and that was at a bearing ratio of 2.75, the highest in its group. Here again, however, the "g/d" ratio was 6.60; so that with out present regard for that ratio we would not expect the "theoretical efficiency" to be confirmed. There was no significant change in behavior as the bearing ratio increased from 1.41 to 2.35.

The point of major significance to be derived from a study of this Series is that:

> Bearing ratio cannot be a critical factor in a single-shear tension connection designed on an efficient "g/d" ratio.

To demonstrate this:

> Let g/d = 5. Gross w = 5d. Net w = 4d. Theo. Efficiency = 4/5 = 80 percent. (Attempts to increase this efficiency by further increasing g will fail). Let T and 0.75 T be the allowable plate tension and rivet shear.
>
> Plate Capacity = $4d \times t \times T$
>
> Req'd number (n) of single-shear rivets in a row = $\dfrac{4d \times t \times T}{\frac{\pi d^2}{4} \times 0.75\,T}$
>
> $n = 6.8\dfrac{t}{d}$
>
> Bearing stress = $\dfrac{4d \times t \times T}{6.8\frac{t}{d} \times dt} = 0.57\dfrac{d}{t}\,T$. Therefore:

In Buildings, if the maximum rivet be 7/8" and the thinnest material for computed stress be 1/4", the bearing stress in a single-shear connection of maximum efficiency cannot exceed .59 x 7/8 ÷ 1/4 = 2.07 times the allowable tensile stress.

In Bridges, if the maximum rivet be 1" and the thinnest material for computed stress be 3/8", the bearing stress in a connection of maximum efficiency cannot exceed .59 x 1 ÷ 3/8 = 1.57 times the allowable tensile stress.

In both cases, when the "theoretical efficiency" is reduced below 80 percent by closer spacing of the rivet lines, the bearing ratio will be further reduced.

Therefore, in the vast majority of single-shear tension-member connections, no attention need be paid to bearing pressure.

There is no reason, according to this Series of tests, to prescribe for single-shear connections a lower unit bearing than for double-shear; however, since in 20 out of these 33 specimens there were rivet failures, suspicion is aroused that in single-shear connections the customary shear-tension ratio of 0.75 admits of a greater possibility of rivet failure than in double-shear connections. The pursuit of this thought through comparison with other data was not within the scope of Project 1.

Unless the bearing ratio in this Series exceeded 2.06, (1) the plate developed its coupon strength or more, and (2) the rivets developed 45 000 psi in shear (or more when plate failure did not conclude the test).

Summary of Third, or 1951 Static Series

For further details see Reference No. 10.

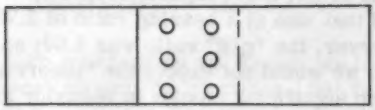

51 - 1 to 51 - 6

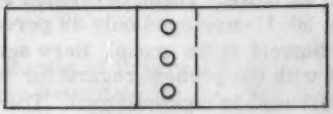

50 - x6, 50 - x7

Fig. 3
From Fig. 1, Ref. No. 10

Six tensile designs were tested, Nos. 51-1 to 51-6. Nos. 51-1, 2, 3 employed 3/4" rivets; Nos. 51-4, 5, 6 employed 1" rivets. For each design number three duplicate specimens were procured from one fabricator and three from another, as a check on possible differences. Such differences were usually quite small, as measured by breaking load, but in one instance were as 57.2 to 68.1 ksi.

The objective in selecting this type was to re-test in double-shear with a more reasonable g/d ratio (max. 5.24) than had been used in 1949 Series. While there was still some scatter, a marked improvement in this respect was attained.

For the 3/4" rivet series, with bearing ratios of 1.56, 1.76 and 2.01, the "net section efficiencies" (as previously defined) were .98, 1.00 and .97.

For the 1" rivet series, with bearing ratios of 1.45, 1.71 and 2.09, the "net section efficiencies" were .90, .94 and .85. This last was the first instance of a reduction of "net section efficiency" at a bearing ratio so little over 2.00.

Two single-shear designs were tested, Nos. 50-x6, x7, using a single transverse row of three 7/8" rivets. The outer or critical plates were 1/4" and 3/16", bearing ratios 2.06 and 2.74. This latter thickness confirms the necessity for going outside of normal design to create a single-shear bearing ratio much over 2.00.

The six specimens with bearing ratio of 2.06 developed "net section efficiency" of 1.00. Those with bearing ratio of 2.74 developed 0.97 (specimens from one fabricator) and 0.82 (from the other).

The Conclusions above stated for single-shear joints, drawn from the 1950 tests, were thus confirmed.

(Efficiencies found in these tests did not approach those that would be predicted from the Schutz "g/d" Rule as discussed in Reference No. 11.)

This Series included also six designs for testing in compression, each containing six 3/4" rivets in two longitudinal rows, or three in each line parallel to the application of stress.

In three designs the inner or double-shear plate was critical, with ratios of bearing: shear of 1.88, 2.36 and 4.71. In the other three the outer or single-shear plates were critical, with ratios of 1.88, 2.35 and 3.14.

In all compressive tests with bearing : shear ratio not over 2.36, the ultimate compressive stress (maximum load divided by gross area) exceeded the coupon yield point of the critical material. In the tests with still higher bearing : shear ratios, buckling intervened and established the maximum load.

These compressive tests were introduced as an extension of a shorter and simpler program conducted in 1948 and reported in Reference No. 7. These comprise specimens with one rivet, and specimens with two rivets, in line of stress, with critical inner or double-shear plate of thickness 7/16", 3/8" and 5/16". Rivets were 3/4". Nominal bearing : shear ratios were respectively 2.77, 3.13 and 3.77.

All of the one-rivet specimens failed by rivet shear, with no decrease of ultimate load as between bearing: shear ratios of 2.77 and 3.13; and with a drop off of only 3 to 4 percent as between 3.13 and 3.77.

Of the six two-rivets specimens, one test was stopped a little beyond the yield load for examination of conditions around the holes in the inner plate. The other five failed by buckling of the inner plate, at compressive stresses between 65 000 and 88 000 psi, with no decrease of ultimate load as between bearing-shear ratios of 2.77 and 3.13.

Measurements of slip at the yield point (a combination of plate strain and rivet slip) were made, and showed slight differences. The slips thus measured on specimens with bearing : shear ratio of 3.13 were slightly below those on specimens with ratio of either 2.77 or 3.77; and consequently inconclusive.

REFERENCES

1. W. M. Wilson: "Fatigue Tests of Riveted Joints." Bulletin 302, University of Illinois Experiment Station, 1938.
2. H. Kayser: "Tests on the Shearing and Bearing Strength of Riveted Connections." "Der Stahlbau," 17 April 1931.
3. Same: "Further Tests on (the foregoing)." "Der Stahlbau," 13 October 1933.
4. Otto Graf: "Fatigue Tests of Riveted Joints." "Der Bauingenieur," 1932, #29-30.
5. K. Schaechterle: "Fatigue Strength of Riveted and Welded Joints." Publ. of I.A.B.S.E., Vol II., 1934.
6. Jonathan Jones: "Static Tests of Riveted Joints." "Civil Engineering," p. 287., May 1940.

*7. W. M. Wilson and W. H. Munse: "Tests of Riveted Joints with High Rivet Bearing." Progress Report, University of Illinois Experiment Station, Aug. 1, 1948.

*8. Becker, Sinnamon and Munse: "The Effect of Bearing Pressure on the Static Strength of Riveted Joints." Presented as a Masters Thesis by W. K. Becker, University of Illinois, January 1951.

*9. Massard, Sinnamon and Munse: "(Same Title as Ref. 8)." Presented as a Masters Thesis by J. M. Massard, University of Illinois, January 1952.

*10. Bergendoff and Munse: "(Same Title as Ref. 8)." Presented as a Masters Thesis by R. C. Bergendoff, University of Illinois, June 1953.

*11. Schutz, F. W., Jr., "The Efficiency of Riveted Structural Joints." Presented as a Doctorate Thesis by F. W. Schutz, Jr., University of Illinois, September 1952.

*Unpublished, but microfilms of all reports presented as a Masters or Doctorate Thesis can be secured from the University of Illinois Library.

APPENDIX A

It being generally recognized that existing practice in the design of riveted and bolted connections has been empirically developed from experience and that many of these practices and the joint capacities predicated thereon, are not supported by definite scientific data, the Research Council on Riveted and Bolted Structural Joints was organized in 1947 to carry on such investigations as may be deemed necessary to determine the suitability and capacity of various types of joints used in fabricated structural frames. It is the expectation that the work of the Council will result in the promulgation of more economical and efficient practices.

SPONSORING ORGANIZATIONS.

American Institute of Steel Construction, Inc.
American Iron and Steel Institute
American Society of Civil Engineers
Association of American Railroads
Canadian Institute of Steel Construction, Inc.
The Engineering Foundation
State of Illinois, Division of Highways
University of Illinois
Industrial Fasteners Institute
Northwestern University
U.S. Dept. of Commerce, Bureau of Public Roads
University of Washington

APPENDIX B

MEMBERSHIP OF PROJECT COMMITTEE NO. 1.

Jonathan Jones, Hon. Member A.S.C.E., Chairman
Raymond Archibald, Member A.S.C.E.
Frank Baron, Member A.S.C.E.
W. H. Munse, Member A.S.C.E.
C. Neufeld, Member A.S.C.E.
N. M. Newmark, Member A.S.C.E.
T. C. Shedd, Member A.S.C.E.
W. M. Wilson, Hon. Member A.S.C.E.
L. T. Wyly, Member A.S.C.E.
R. B. Murphy, Division of Highways, State of Illinois.

Journal of the
STRUCTURAL DIVISION
Proceedings of the American Society of Civil Engineers

CONTENTS

DISCUSSION
(Proc. Paper 1112)

(Over)

Note: Paper 1112 is part of the copyrighted Journal of the Structural Division of the American Society of Civil Engineers, Vol. 82, ST 6, November, 1956.

Page

Discussion of
"CALCULATION OF PRESSURE OF CONCRETE ON FORMS"

by Rolf Schjodt
(Proc. Paper 680)

CORRECTIONS.--On page 2, at the bottom, the author's title should be Dr. techn. instead of Junior Technician. On page 3, in Eq. 6, the term $\frac{\kappa}{\lambda} \frac{\gamma_0}{\gamma + \gamma_0 \kappa}$ should be changed to $\frac{\kappa}{\lambda} \frac{\gamma_0}{\gamma - \gamma_0 \kappa}$.

Discussion of
"NATURAL FREQUENCIES OF CONTINUOUS FLEXURAL MEMBERS"

by A. S. Veletsos and N. M. Newmark
(Proc. Paper 735)

CORRECTIONS.—In the authors' closure to this paper, which appeared as part of Proceedings Paper 1067 (September, 1956), the first two sentences of the second paragraph on page 1067-3 were reproduced incorrectly. These sentences should be changed to read:

> It may be of interest to note that, in the course of the investigation which resulted in the present paper, the writers studied several alternate procedures, including the procedures described by Mr. Karol. An account of these procedures together with a brief discussion of their relative merits are contained in pp. 31-37 of Ref. (15).

Discussion of "ANALYSIS OF ARCHES BY FINITE DIFFERENCES"

by Ephraim G. Hirsch and E. P. Popov
(Proc. Paper 829)

EPHRAIM G. HIRSCH,* and E. P. POPOV,** A.M. ASCE.—The writers express their thanks to Messrs. Chang and Sawyer for their discussions which contribute significantly to the value of the paper. Their interest in the paper is gratifying.

Mr. Chang is correct in stating that for the case considered by the authors in the example, the sum of all the upward deflections of the arch rib should equal the sum of the downward deflections. However, his analysis indicating that the sum of the vertical deflections at odd stations is zero and that the sum of vertical deflections at even stations is also zero is true only for a special reason. In the analysis of the arch the "three-point central difference" approximation was used to convert Eq. 2 into an algebraic set of equations. A characteristic of this approximation is that when it is applied to a first order differential equation, which Eq. 2 is, no relationship between the consecutive even and odd stations can be obtained. Each of the resulting algebraic equations in effect "skips" every other station. This situation may be avoided by using the "five-point central difference" approximation.(17) However, since this procedure considerably complicates the resulting matrix of equations, and yields only a small improvement in the accuracy of the results, its use is usually not warranted.

As noted by Mr. Chang, Eq. 2 was not used at Station 4. A clarification of this point seems necessary. Due to the nature of the "three-point finite difference" approximation and the nature of Eq. 2 itself, an application of Eq. 2 at Station 4 yields $\zeta_5 = \zeta_3$, regardless of the loading conditions. This is with axial strains neglected. For symmetrical loading of a symmetrical arch such a result is in direct contradiction to what is readily evident from considerations of symmetry. There the horizontal displacements for similarly situated points on either side of the crown must be equal and opposite. This incompatible situation may be avoided either by using the "five-point finite difference" approximation if it is desired to obtain an equation at the crown or by avoiding an equation written for the crown point. The latter procedure was used in the illustrative example and a sufficient number of equations was obtained by utilizing the known boundary conditions at both ends.

Professor Sawyer's contribution to the paper is particularly valuable. The writers concur in the necessity of including an additional term in the basic differential Eq. 1 for cases when the effect of rib shortening due to axial force is to be considered. Hence, Eq. 1-A stated by Professor Sawyer is the complete equation for an arch rib and should supersede Eq. 1 of the paper.

* Private, United States Army; formerly student at Univ. of California, Berkeley, Calif.
** Prof. of Civ. Eng., Univ. of California, Berkeley, Calif.

CORRECTION* to Eq. (2) on page 829-4 of the paper. The last term of the equation is to read as follows:

$$-\left(\frac{N}{EA} - \alpha t\right)\left(1 + \tan^2\theta\right)$$

* Correction through the courtesy of Mr. Sawyer.

Discussion of "INFLUENCE LINES FOR REACTIONS OF CONTINUOUS TRUSSES"

by Andrew John Pyka
(Proc. Paper 914)

HOWARD H. MULLINS.[1]—The author is to be commended for his service in bringing to the attention of the profession the application of another method of analysis for determining the stresses in statically indeterminate framed structures. One has but to look at many bridges in the United States today to realize that these structures are obviously not suited to the location and that some statically indeterminate type such as a continuous truss, an arch, a suspension bridge of either the self-anchored type or externally anchored type, a continuous tied arch, or others, would have been more pleasing from an aesthetic standpoint and in many instances more economical. There is evidently some basic reason for such a situation. The writer ventures the opinion that this situation came about, in part at least, because of the lack of widespread knowledge among bridge designers concerning the various methods available for stress analysis. Some years ago one often heard, as the reason for avoiding the use of statically indeterminate type bridges, that the stresses in such structures would be seriously affected by settlement of the foundation. In recent years this situation has improved considerably due perhaps to the ease with which such phenonema may be investigated by some of the modern methods now available to bridge designers.

It is a well known fact that a method of stress analysis which may be very appealing to one designer may be considered indirect, laborious and difficult to apply by another. It is also true that all methods of analysis cannot be applied to all types of structures with equal facility. It sometimes develops that, in trying to apply some of the newer and more glamorous methods of analysis, they become difficult, or break down entirely, and one is forced to resort to one of the classical methods for a solution. For this reason it is particularly desirable that the bridge designer have information in regard to, and be able to apply, all of the available methods of analysis.

In the introduction to the Paper, the author, while admitting that the method of elastic weights "has its advantages in that it is a definite time saver when applied to parallel chord continuous trusses . . ." appears to imply that the method is difficult when applied to curved chord trusses or other types of trusses, such as the continuous truss, the framed arch, etc. The writer has found the method to be equally advantageous for all types of framed structures.

When deciding on the method to be used in computing the stresses in statically indeterminate structures the selection of the redundants is sometimes all important in reducing the work involved in the solution. It appears to have been a rather common practice for many years when designing fixed plate rib steel arches, fixed concrete arches, and fixed concrete and steel frames to work about the elastic center of the structure. It does not, however, appear

1. Asst. Chief, Civ. Eng. Dept., Engr. Research and Development Labs., Fort Belvoir, Va.

to be the general practice to do so when analyzing framed structures, despite the fact that the method is equally applicable and often more expeditious of application.

The author takes as an example, to illustrate the application of his method of analysis, the interesting Continuous Tied Arch constructed over the Mississippi River at Dubuque, Iowa, and opened to traffic in 1943. This type of bridge has become quite popular since 1940; similar bridges having been constructed over the Mississippi River at Minneapolis, Minn., the Kanawha River at Charleston, W. Va., the Missouri River at Jefferson City, Mo. and elsewhere. The writer was fortunate in having the opportunity in 1939 to design the first bridge of this type built in the United States. The bridge was constructed over the Meramec River near St. Louis, Mo. and opened to traffic in 1941. The writer sketched the method of analysis used in the design in an article published in ENGINEERING NEWS-RECORD June 5, 1941, Volume p 869.

Statically indeterminate structures are termed singly indeterminate, twofold indeterminate, threefold indeterminate, etc., depending on how many reactions, moments, or stresses must be removed to permit computation of the stresses in the remaining statically determinate system by simple statics. Then elastic equations must be written involving each of the redundants removed. Thus to accomplish a solution, we must have as many equations as we have redundants.

The writer proposes to show the application of the method of least work to the solution of several of the more important types of bridge trusses, namely:

a) A continuous Tied Arch,
b) A 3-Span Continuous Truss,
c) A 2-Span Continuous Truss,
d) A 2-Hinged Tied Arch, and
e) A 2-Hinged Externally Anchored Arch.
f) A Fixed Arch

The Continuous Tied Arch

Shown in Fig. 1 is the Meramec River Continuous Tied Arch. The total work in such a structure is

$$\omega = \frac{1}{2} \sum \frac{S^2 L}{AE} \qquad (1)$$

in which,

S = stress in any member of the structure,
L = length of the member
A = gross sectional area of the member, and
E = modulus of elasticity of the material.

The structure is three fold indeterminate and, therefore, three equations are required. If we let Xa, Xb and Xc indicate the three unknown reactions, stresses or moments, we get, by differentiating Equation (1) with respect to each unknown,

$$\frac{\delta \omega}{\delta X_a} = \sum \frac{SL}{AE} \cdot \frac{\delta S}{\delta X_a} = 0 \cdot \quad (2)$$

$$\frac{\delta \omega}{\delta X_b} = \sum \frac{SL}{AE} \cdot \frac{\delta S}{\delta X_b} = 0 \cdot \quad (3)$$

$$\frac{\delta \omega}{\delta X_c} = \sum \frac{SL}{AE} \cdot \frac{\delta S}{\delta X_c} = 0 \cdot \quad (4)$$

The stress in each individual member of the truss can be expressed as

$$S = S_o + S_a X_a + S_b X_b + S_c X_c \quad (5)$$

in which,

So = the stress due to the applied loads on the statically determinate base system after removal of redundants,
Sa = stress due to Xa = 1,
Sb = stress due to Xb = 1, and
Sc = stress due to Xc = 1

Differentiating Equation (5) with respect to each of the unknowns, Xa, Xb and Xc,

$$\frac{\delta S}{\delta X_a} = S_a \quad (6)$$

$$\frac{\delta S}{\delta X_b} = S_b \quad (7)$$

$$\frac{\delta S}{\delta X_c} = S_c \quad (8)$$

Substituting the value of S from Equation (5) in Equations (2), (3) and (4) and the appropriate derivative from Equations (6), (7) and (8) the necessary three equations are as follows:

$$\sum \frac{S_o S_a L}{AE} + X_a \sum \frac{S_a^2 L}{AE} + X_b \sum \frac{S_a S_b L}{AE} + X_c \sum \frac{S_a S_c L}{AE} = 0 \quad (9)$$

$$\sum \frac{S_o S_b L}{AE} + X_a \sum \frac{S_a S_b L}{AE} + X_b \sum \frac{S_b^2 L}{AE} + X_c \sum \frac{S_b S_c L}{AE} = 0 \quad (10)$$

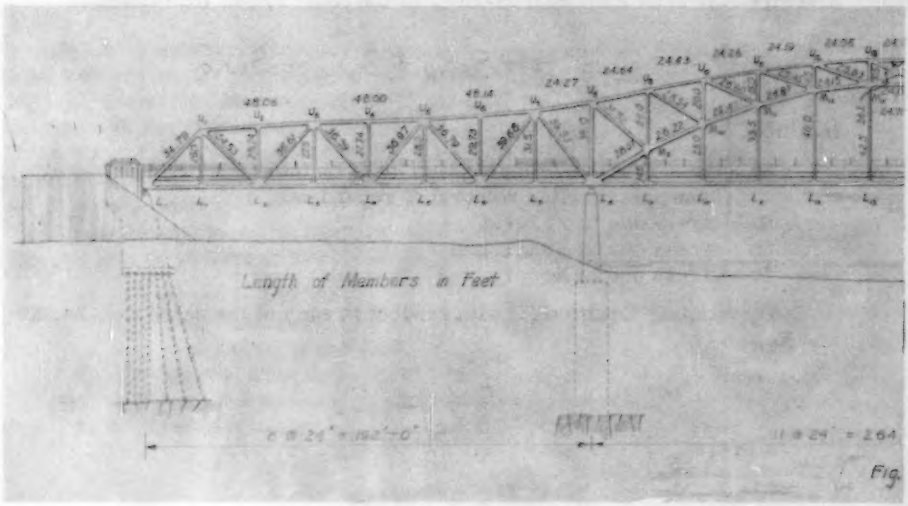

Fig.

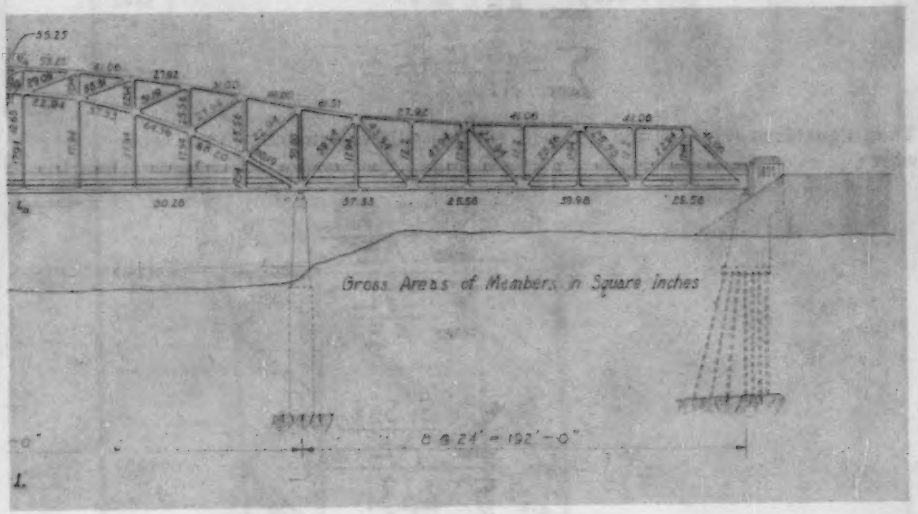
Gross Areas of Members in Square Inches
6 @ 24' = 192'-0"

$$\sum \frac{S_o S_c L}{AE} + X_a \sum \frac{S_a S_c L}{AE} + X_b \sum \frac{S_b S_c L}{AE} + X_c \sum \frac{S_c^2 L}{AE} = 0 \quad (11)$$

These three simultaneous equations could be solved for the unknowns. The work of computation is substantially reduced if the coordinate axes are located so that certain terms of Equations (9), (10) and (11) are zero. The axes are located so that

$$\sum \frac{S_a S_b L}{AE} = 0 \quad (12)$$

$$\sum \frac{S_b S_c L}{AE} = 0 \quad (13)$$

$$\sum \frac{S_a S_c L}{AE} = 0 \quad (14)$$

Then Equations (9), (10) and (11) will contain only one unknown each from which

$$X_a = - \frac{\sum \frac{S_o S_a L}{AE}}{\sum \frac{S_a^2 L}{AE}} \quad (15)$$

$$X_b = - \frac{\sum \frac{S_o S_b L}{AE}}{\sum \frac{S_b^2 L}{AE}} \quad (16)$$

$$X_c = - \frac{\sum \frac{S_o S_c L}{AE}}{\sum \frac{S_c^2 L}{AE}} \quad (17)$$

The condition expressed by Equations (12), (13) and (14) will be satisfied if the axes are located as shown in Fig. 2. The intersection of the axes is located by Equation (14).

The stresses Sc due to the force Xc = 1 acting at a distance y above the arch springing line may be expressed thusly,

$$S_c = y S_a + S_H \quad (18)$$

where S_H is the stress in the two-hinged arch shown in Fig. 2c, due to H = 1.

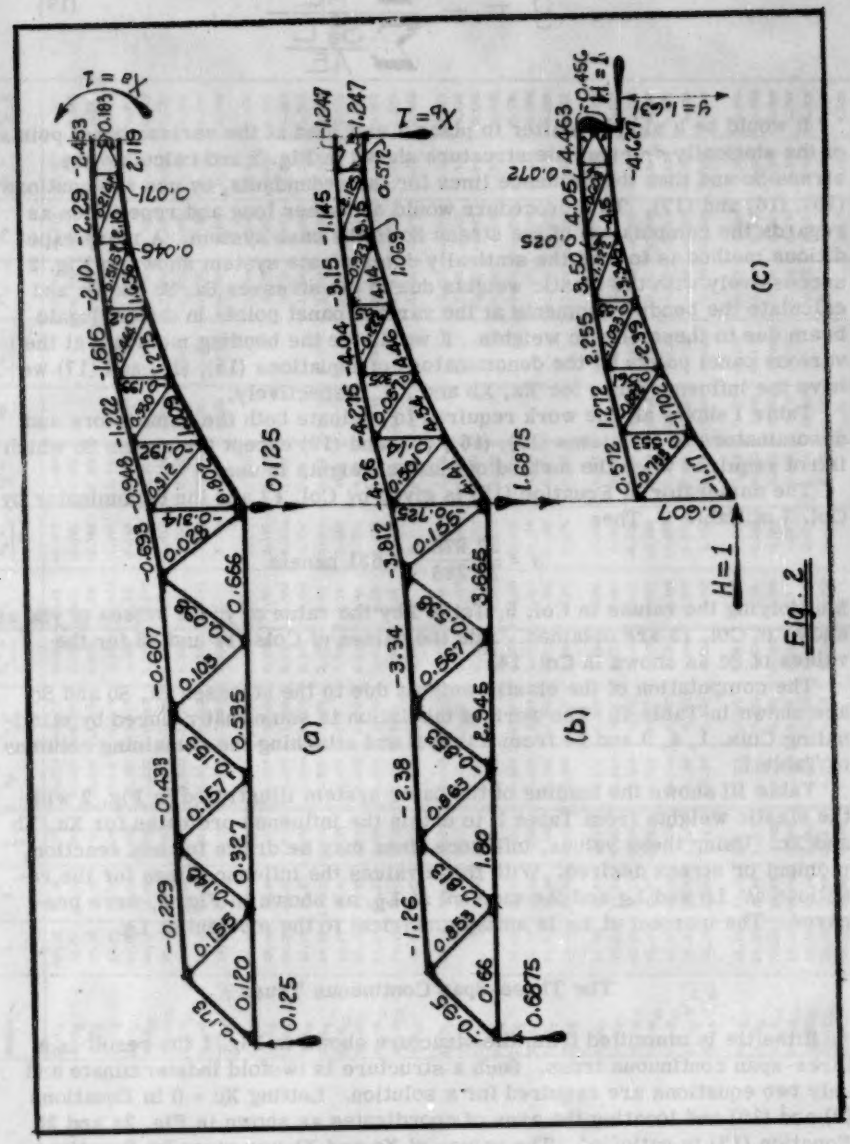

Fig. 2

Substituting this value of Sc in Equation (14) and solving,

$$y = -\frac{\sum \frac{S_a S_H L}{AE}}{\sum \frac{S_a^2 L}{AE}} \qquad (19)$$

It would be a simple matter to place a unit load at the various panel points of the statically determinate structure shown in Fig. 2 and calculate the stress So and then the influence lines for the redundants, by use of Equations (15), (16) and (17). This procedure would be rather long and repetitious as regards the computation of the stress So in the base system. A more expeditious method is to load the statically determinate system shown in Fig. 2 successively with the elastic weights due to the stresses Sa, Sb and Sc and calculate the bending moments at the various panel points in the conjugate beam due to these elastic weights. If we divide the bending moments at the various panel points by the denominators of Equations (15), (16) and (17) we have the influence lines for Xa, Xb and Xc, respectively.

Table I shows all the work required to evaluate both the numerators and denominators of Equations (15), (16), (17) and (19) except the stress So which is not required when the method of elastic weights is used.

The numerator of Equation (19) is given by Col. 12 and the denominator by Col. 7 of Table I. Then

$$y = \frac{37.970}{23.286} = 1.631 \text{ panels}$$

Multiplying the values in Col. 5, Table I by the value of y, the values of ySa as shown in Col. 13 are obtained. Add the values of Cols. 11 and 13 for the values of Sc as shown in Col. 14.

The computation of the elastic weights due to the stresses Sa, Sb and Sc are shown in Table II. The work of tabulation is somewhat reduced by eliminating Cols. 1, 4, 9 and 14 from Table II and attaching the remaining columns to Table I.

Table III shows the loading of the basic system illustrated in Fig. 2 with the elastic weights from Table II to obtain the influence ordinates for Xa, Xb and Xc. Using these values, influence lines may be drawn for any reaction, moment or stress desired. With these values the influence lines for the reactions at Lo and L_8 and the moment at L_8, as shown in Fig. 3, were prepared. The moment at L_8' is antisymmetrical to the moment at L_8.

The Three-Span Continuous Truss

If the tie is ommitted from the structure shown in Fig. 1 the result is a three-span continuous truss. Such a structure is twofold indeterminate and only two equations are required for a solution. Letting Xc = 0 in Equations (9) and (10) and locating the axes of coordinates as shown in Fig. 2a and 2b Equation (12) is satisfied. The values of Xa and Xb are given by Equations (15) and (16), and are as shown in Table III for The Continuous Tied Arch. Using these values of Xa and Xb, the influence lines for the moment at L_8 and the reactions at Lo and L_8, as shown in Fig. 4 were prepared.

TABLE I

1	2	3	4	5	6	7	8	9	10	11	12	13	14	15	16
Member	L	A	$\frac{L}{A}$	S_a	$\frac{S_a L}{A}$	$\frac{S_a^2 L}{A}$	S_b	$\frac{S_b L}{A}$	$\frac{S_b^2 L}{A}$	S_H	$\frac{S_a S_H L}{A}$	yS_a	S_o	$\frac{S_o L}{A}$	$\frac{S_a^2 L}{A}$
U_1-U_3	48.08	41.06	1.171	-0.229	-0.268	0.061	-1.26	-1.475	1.858			-0.374	-0.374	-0.437	0.163
U_3-U_5	48.00	41.06	1.168	-0.433	-0.506	0.219	-2.38	-2.782	6.621			-0.706	-0.706	-0.826	0.583
U_5-U_7	48.14	27.92	1.725	-0.607	-1.046	0.635	-3.34	-5.758	19.225			-0.990	-0.990	-1.706	1.69
U_7-U_8	24.27	61.61	0.395	-0.693	-0.274	0.190	-3.812	-1.505	5.740			-1.130	-1.130	-0.446	0.504
U_8-U_9	24.64	49.00	0.503	-0.948	-0.477	0.452	-4.26	-2.143	9.128	0.572	-0.273	-1.545	-0.973	-0.490	0.476
U_9-U_{10}	24.43	31.00	0.788	-1.222	-0.963	1.177	-4.275	-3.367	14.40	1.272	-1.225	-1.992	-0.720	-0.567	0.409
U_{10}-U_{11}	24.26	27.92	0.869	-1.616	-1.404	2.270	-4.04	-3.51	14.175	2.255	-3.166	-2.635	-0.380	-0.330	0.126
U_{11}-U_{12}	24.19	41.06	0.589	-2.100	-1.236	2.598	-3.15	-1.855	5.845	3.5	-4.33	-3.425	0.075	0.044	0.005
U_{12}-U_{13}	24.06	55.25	0.434	-2.29	-0.993	2.272	-1.145	-0.496	0.569	4.06	-4.020	-3.735	0.315	0.137	0.043
$\frac{1}{2}(U_{13}-U'_{13})$	12.00	55.25	0.216	-2.463	-0.531	1.302	0	0	0	4.463	-2.366	-4.000	0.463	0.100	0.046
L_0-L_2	48.00	25.56	1.877	0.120	0.225	0.027	0.66	1.238	0.818			0.196	0.196	0.367	0.072
L_2-L_4	48.00	39.98	1.201	0.327	0.393	0.128	1.80	2.161	3.893			0.533	0.533	0.640	0.341
L_4-L_6	48.00	25.56	1.877	0.535	1.004	0.536	2.945	5.528	16.275			0.873	0.873	1.638	1.428
L_6-L_8	48.00	37.33	1.285	0.666	0.856	0.571	3.665	4.710	17.26			1.086	1.086	1.396	1.515
L_8-M_9	28.07	110.19	0.255	0.802	0.204	0.164	4.41	1.123	4.955	-1.170	-0.239	1.308	0.138	0.035	0.006
M_9-M_{10}	26.22	88.20	0.297	1.009	0.3	0.303	4.54	1.350	6.13	-1.702	-0.511	1.645	-0.057	-0.017	0.001
M_{10}-M_{11}	25.47	64.36	0.396	1.276	0.505	0.644	4.46	1.766	7.88	-2.39	-1.206	2.079	-0.311	-0.123	0.038
M_{11}-M_{12}	24.87	37.33	0.666	1.656	1.103	1.828	4.14	2.756	11.42	-3.345	-3.692	2.70	-0.645	-0.430	0.277
M_{12}-M_{13}	24.15	22.94	1.053	2.10	2.21	4.643	3.15	3.315	10.44	-4.50	-9.95	3.424	-1.076	-1.133	1.220
$\frac{1}{2}(M_{13}$-	12.00	24.71	0.486	2.119	1.028	2.178	0	0	0	-4.627	-4.758	3.454	-1.173	-0.57	0.668
L_0-U_1	34.79	41.06	0.847	-0.173	-0.147	0.025	-0.95	-0.806	0.766			-0.282	-0.282	-0.239	0.067
U_1-L_2	33	22.94	1.505	0.155	0.233	0.036	0.853	1.283	1.096			0.253	0.253	0.380	0.096
L_2-U_3	1	25.56	1.432	-0.148	-0.212	0.031	-0.813	-1.165	0.947			-0.241	-0.241	-0.346	0.083
U_3-L_4	3...00	25.56	1.424	0.157	0.224	0.035	0.865	1.228	1.061			0.256	0.256	0.365	0.093
L_4-U_5	36.97	22.94	1.611	-0.155	-0.250	0.039	-0.853	-1.375	1.172			-0.253	-0.253	-0.407	0.103
U_5-L_6	36.79	43.94	0.837	0.103	0.086	0.009	0.567	0.475	0.269			0.168	0.168	0.141	0.024
L_6-U_7	39.68	43.94	0.903	-0.096	-0.089	0.009	-0.538	-0.486	0.261			-0.160	-0.160	-0.144	0.023
U_7-L_8	39.53	59.94	0.660	0.028	0.019	0.001	0.155	0.102	0.016			0.046	0.046	0.030	0.001
U_8-M_9	31.52	22.94	1.374	0.312	0.429	0.134	0.601	0.689	0.345	-0.733	-0.314	0.509	-0.224	-0.308	0.069
U_9-M_{10}	28.64	27.94	1.022	0.330	0.337	0.111	0.067	0.068	0.003	-0.822	-0.277	0.538	-0.284	-0.290	0.085
U_{10}-M_{11}	26.60	31.19	0.853	0.444	0.379	0.168	-0.222	-0.189	0.042	-1.093	-0.414	0.724	-0.369	-0.315	0.116
U_{11}-M_{12}	25.45	36.31	0.721	0.615	0.371	0.191	-0.923	-0.665	0.614	-1.322	-0.491	0.84	-0.482	-0.347	0.167
U_{12}-M_{13}	25.63	29.09	0.882	0.214	0.187	0.040	-2.125	-1.873	3.980	-0.603	-0.114	0.349	-0.264	-0.224	0.067
$\frac{1}{2}(U_{13}-M'_{13})$	13.10	10.00	1.31	0.183	0.240	0.044	-1.247	-1.634	2.075	-0.456	-0.109	0.298	-0.158	-0.207	0.033
$\frac{1}{2}(M_{13}-U'_{13})$	13.10	10.00	1.31	0.183	0.240	0.044	1.247	1.634	2.075	-0.456	-0.109	0.298	-0.158	-0.207	0.033
U_8-L_8	35.00	50.00	0.7	-0.314	-0.220	0.069	-0.725	-0.508	0.368	0.807	-0.133	-0.512	0.096	0.067	0.006
U_9-M_9	26.00	25.56	1.017	-0.192	-0.195	0.038	0.14	0.143	0.020	0.563	-0.106	-0.313	0.240	0.244	0.059
U_{10}-M_{10}	20.00	25.56	0.782	-0.199	-0.156	0.031	0.306	0.239	0.073	0.561	-0.087	-0.325	0.237	0.185	0.044
U_{11}-M_{11}	15.00	22.94	0.654	-0.200	-0.131	0.026	0.5	0.327	0.164	0.550	-0.072	-0.326	0.224	0.146	0.033
U_{12}-M_{12}	11.50	17.94	0.641	0.046	0.030	0.001	1.069	0.686	0.733	0.028	0	0.075	0.10	0.064	0.006
U_{13}-M_{13}	10.50	12.65	0.83	0.071	0.059	0.004	0.572	0.475	0.272	-0.072	-0.004	0.116	0.044	0.036	0.002
Tie	132.00	30.26	4.362	0						1.00			1.0	4.362	4.362
Σ						23.286			172.982		-37.970				18.168

TABLE II

1	2	3	4	5	6	7	8	9	10	11	12	13	14	15	16	17	18
Member	r_1	r_2	$\frac{S_a L}{A}$	$\frac{100 \cdot S_a L}{r_1 A}$	Acts At	$\frac{100 \cdot S_a L}{r_2 A}$	Acts At	$\frac{S_b L}{A}$	$\frac{100 \cdot S_b L}{r_1 A}$	Acts At	$\frac{100 \cdot S_b L}{r_2 A}$	Acts At	$\frac{S_c L}{A}$	$\frac{100 \cdot S_c L}{r_1 A}$	Acts At	$\frac{100 \cdot S_c L}{r_2 A}$	Acts At
U_1-U_3	26.2		-0.268	1.023	L_2			-1.475	5.630	L_2			-0.457	1.668	L_2		
U_3-U_5	27.74		-0.506	1.824	L_4			-2.782	10.300	L_4			-0.826	2.975	L_4		
U_5-U_7	29.6		-1.046	3.532	L_6			-5.755	19.445	L_6			-1.706	5.762	L_6		
U_7-U_8	34.6		-0.274	0.791	L_8			-1.505	4.350	L_8			-0.446	1.289	L_8		
U_8-U_9	25.3		-0.477	1.885	M_9			-2.145	8.470	M_9			-0.490	1.935	M_9		
U_9-U_{10}	19.65		-0.963	4.900	M_{10}			-3.367	17.140	M_{10}			-0.667	2.887	M_{10}		
U_{10}-U_{11}	14.85		-1.404	9.460	M_{11}			-3.510	23.640	M_{11}			-0.330	2.225	M_{11}		
U_{11}-U_{12}	11.41		-1.236	10.830	M_{12}			-1.855	16.250	M_{12}			0.044	-0.387	M_{12}		
U_{12}-U_{13}, $\frac{1}{2}(U_{13}-U'_{13})$	10.48		-0.993	9.470	M_{13}			-0.496	4.735	M_{13}			0.137	-1.302	M_{13}		
	10.5		-0.551	5.060	M_{13}			0		M_{13}			0.100	-0.955	M_{13}		
L_0-L_2	28.0		0.225	0.902	U_1			1.236	4.956	U_1			0.367	1.470	U_1		
L_2-L_4	27.5		0.393	1.428	U_3			2.161	7.860	U_3			0.640	2.326	U_3		
L_4-L_6	28.0		1.004	3.586	U_5			5.528	19.745	U_5			1.638	5.848	U_5		
L_6-L_8	31.5		0.856	2.716	U_7			4.710	14.960	U_7			1.396	4.430	U_7		
L_8-M_9	29.9		0.204	0.683	U_8			1.123	3.758	U_8			0.035	0.117	U_8		
M_9-M_{10}	23.8		0.3	1.261	U_9			1.350	5.672	U_9			-0.017	-0.071	U_9		
M_{10}-M_{11}	18.85		0.506	2.680	U_{10}			1.766	9.370	U_{10}			-0.123	-0.654	U_{10}		
M_{11}-M_{12}	14.47		1.103	7.625	U_{11}			2.756	19.050	U_{11}			-0.430	-2.966	U_{11}		
M_{12}-M_{13}	11.42		2.21	19.350	U_{12}			3.315	29.040	U_{12}			-1.133	-9.930	U_{12}		
$\frac{1}{2}(M_{13}-M'_{13})$	10.5		1.028	9.800	U_{13}			0.0		U_{13}			-0.570	-5.430	U_{13}		
L_0-U_1	17.25		-0.147	0.849	L_1			-0.805	4.664	L_1			-0.239	1.385	L_1		
U_1-L_2	17.25	18.25	0.233	-1.352	L_1	1.278	U_2	1.283	-7.440	L_1	7.032	U_2	0.380	-2.206	L_1	2.085	U_2
L_2-U_3	17.2	18.02	-0.212	-1.233	U_2	1.176	L_3	-1.165	-6.770	U_2	6.460	L_3	-0.346	-2.010	U_2	1.918	L_3
U_3-L_4	18.15	18.3	0.224	-1.232	L_3	1.221	U_4	1.228	-6.770	L_3	6.715	U_4	0.365	-2.008	L_3	1.992	U_4
L_4-U_5	18.0	18.18	-0.250	-1.387	U_4	1.373	L_5	-1.375	-7.635	U_4	7.560	L_5	-0.407	-2.262	U_4	2.238	L_5
U_5-L_6	18.26	19.42	5.086	-0.472	L_6	0.444	U_6	0.475	-2.598	L_5	2.444	U_6	0.14	-0.769	L_5	0.724	U_6
L_6-U_7	17.98	19.05	-0.089	-0.492	U_5	0.465	L_7	-0.486	-2.702	U_6	2.550	L_7	-0.144	-0.803	U_6	0.758	L_7
U_7-L_8	19.12	21.25	0.019	-0.097	L_7	0.087	U_8	0.102	-0.535	L_7	0.481	U_8	0.030	-0.158	L_7	0.142	U_8
U_8-M_9	26.65	19.80	0.429	-1.608	L_8	2.166	U_9	0.689	-2.583	L_8	3.478	U_9	-0.306	1.155	L_8	-1.554	U_9
U_9-M_{10}	21.85	18.82	0.537	-1.542	M_9	2.004	U_{10}	0.058	-0.267	M_9	0.347	U_{10}	-0.290	1.328	M_9	-1.726	U_{10}
U_{10}-M_{11}	18.05	13.54	0.379	-2.098	M_{10}	2.798	U_{11}	-0.189	1.048	M_{10}	-1.398	U_{11}	-0.315	1.744	M_{10}	-2.325	U_{11}
U_{11}-M_{12}	14.15	10.85	0.371	-2.622	M_{11}	3.420	U_{12}	-0.665	4.700	M_{11}	-6.130	U_{12}	-0.347	2.453	M_{11}	-3.200	U_{12}
U_{12}-M_{13}	10.76	9.85	0.189	-1.752	M_{12}	1.918	U_{13}	-1.873	17.400	M_{12}	-19.060	U_{13}	-0.224	2.081	M_{12}	-2.278	U_{13}
$\frac{1}{2}(U_{13}-M'_{13})$	9.62		0.240	-2.492	M_{13}			-1.634	16.980	M_{13}			-0.207				
$\frac{1}{2})M_{13}-U'_{13})$	9.62		0.240	2.492	U_{13}			1.634	16.980	U_{13}			-0.207				
U_8-L_8	34.95	24.0	-0.220	-0.629	L_8	0.916	M_9	-0.506	-1.453	L_8	2.115	M_9	0.067	0.190	L_8	-0.277	M_9
U_9-M_9	29.7	24.0	-0.195	-0.658	M_9	0.814	M_{10}	0.145	0.480	M_9	-0.594	M_{10}	0.244	0.823	M_9	-1.017	M_{10}
U_{10}-M_{10}	29.95	24.0	-0.166	-0.520	M_{10}	0.649	M_{11}	0.239	0.796	M_{10}	-0.994	M_{11}	0.185	0.618	M_{10}	-0.771	M_{11}
U_{11}-M_{11}	30.0	24.0	-0.131	-0.436	M_{11}	0.545	M_{12}	0.327	1.090	M_{11}	-1.362	M_{12}	0.146	0.488	M_{11}	-0.610	M_{12}
U_{12}-M_{12}	22.9	24.0	0.030	0.129	M_{12}	-0.123	M_{13}	0.688	2.994	M_{12}	-2.856	M_{13}	0.(	0.280	M_{12}	-0.267	M_{13}
U_{13}-M_{13}	166.8		0.059	0.035	M_{13}			0.475	0.285	M_{13}			0.036	0.022	M_{13}		

TABLE III

Panel Point	Influence Line for Moment Xa				Influence Line for Shear Xb				Influence Line for Tie Xc			
	Load	Shear	Ma	Inf. Ord Xa	Load	Shear	M_b	Inf. Ord X_b	Load	Shear	Mc	Inf. Ord Xc
L_0	-5.776				-31.918				-9.422			
L_1	0.399	-5.776	-5.776	-0.030	2.180	-31.918	-31.918	-0.022	0.650	-9.422	-9.422	-0.075
L_2	1.068	-5.377	-11.153	-0.058	5.892	-29.738	-61.656	-0.043	1.743	-8.772	-18.194	-0.144
L_3	1.372	-4.309	-15.462	-0.080	7.550	-23.846	-85.502	-0.059	2.236	-7.029	-25.223	-0.200
L_4	1.658	-2.937	-18.399	-0.095	9.380	-16.296	-101.798	-0.071	2.705	-4.793	-30.016	-0.238
L_5	4.487	-1.279	-19.678	-0.101	24.707	-6.916	-108.714	-0.075	7.317	-2.088	-32.104	-0.254
L_6	3.484	3.208	-16.470	-0.085	19.187	17.791	-90.923	-0.063	5.683	5.229	-26.875	-0.213
L_7	3.084	6.692	-9.778	-0.050	16.965	36.978	-53.945	-0.037	5.030	10.912	-15.963	-0.126
L_8	-0.676	9.776			4.553	53.943			2.893	15.942		
L_9	4.028	9.100	9.100	0.047	19.948	58.496	58.496	0.041	2.184	18.835	18.835	0.149
L_{10}	7.780	13.128	22.228	0.115	28.107	78.444	136.940	0.095	1.852	21.019	34.854	0.316
L_{11}	17.474	20.908	43.136	0.222	46.088	106.551	243.491	0.169	-0.896	22.871	62.725	0.497
L_{12}	32.522	38.382	81.518	0.420	58.192	152.639	396.130	0.275	-11.766	21.975	84.700	0.671
L_{13}	26.150	70.904	152.422	0.785	17.064	210.831	606.961	0.421	-10.210	10.209	94.909	0.751
	$Xa = \frac{24\ Ma}{25.285 \times 2 \times 100} = 0.00515\ Ma$				$Xb = \frac{24\ Mb}{172.98 \times 2 \times 100} = 0.000694\ Mb$				$Xc = \frac{24\ Mc}{15.168 \times 2 \times 100} = 0.007915\ Mc$			

NOTE: Moments Xa are in panel units

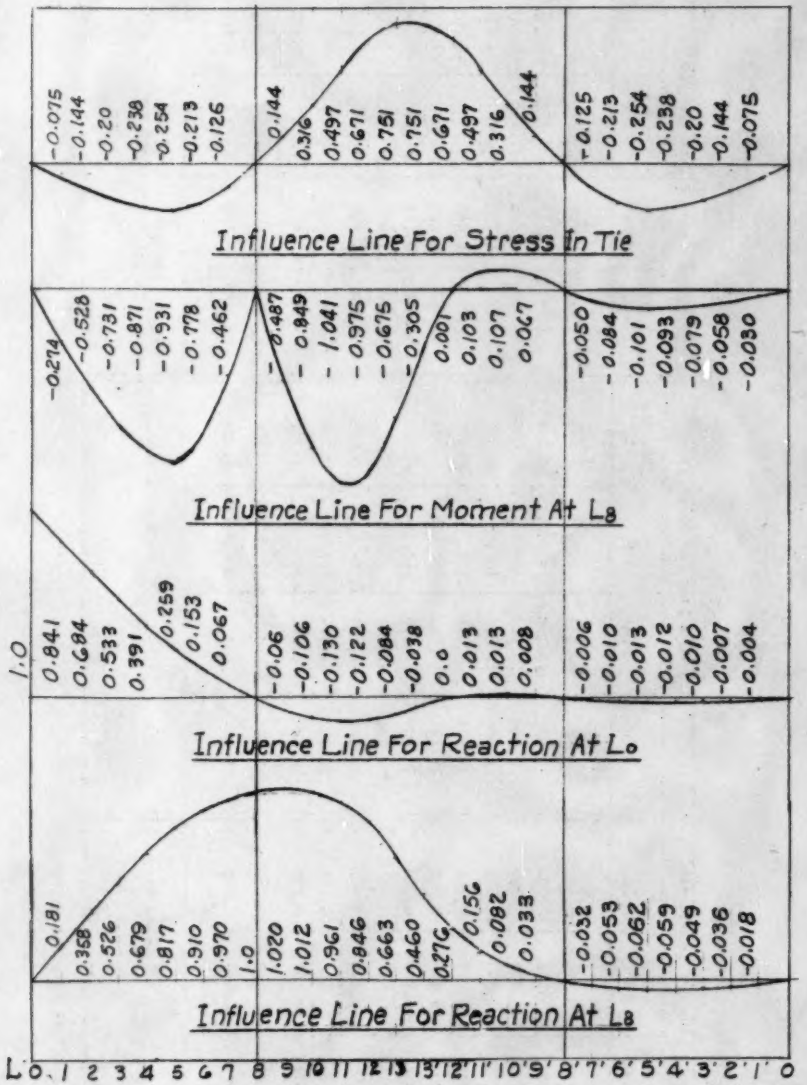
-0.075 -0.144 -0.20 -0.238 -0.254 -0.213 -0.126
0.144 0.316 0.497 0.671 0.751 0.751 0.671 0.497 0.316 0.144
-0.125 -0.213 -0.254 -0.238 -0.20 -0.144 -0.075
Influence Line For Stress in Tie
-0.274 -0.528 -0.731 -0.871 -0.931 -0.778 -0.462
-0.487 -0.849 -1.041 -0.975 -0.675 -0.305 0.001 0.103 0.107 0.047
-0.050 -0.084 -0.101 -0.093 -0.079 -0.058 -0.030
Influence Line For Moment At L8
1.0
0.841 0.684 0.533 0.391 0.259 0.153 0.067
-0.06 -0.106 -0.130 -0.122 -0.084 -0.038 0.0 0.013 0.013 0.008
-0.006 -0.010 -0.013 -0.012 -0.010 -0.007 -0.004
Influence Line For Reaction At L0
0.181 0.358 0.526 0.679 0.817 0.910 0.970 1.0 1.020 1.012 0.961 0.846 0.663 0.460 0.276 0.156 0.082 0.033
-0.032 -0.053 -0.062 -0.059 -0.049 -0.036 -0.018
Influence Line For Reaction At L8
L 0 1 2 3 4 5 6 7 8 9 10 11 12 13 13' 12' 11' 10' 9' 8' 7' 6' 5' 4' 3' 2' 1' 0

Fig. 3

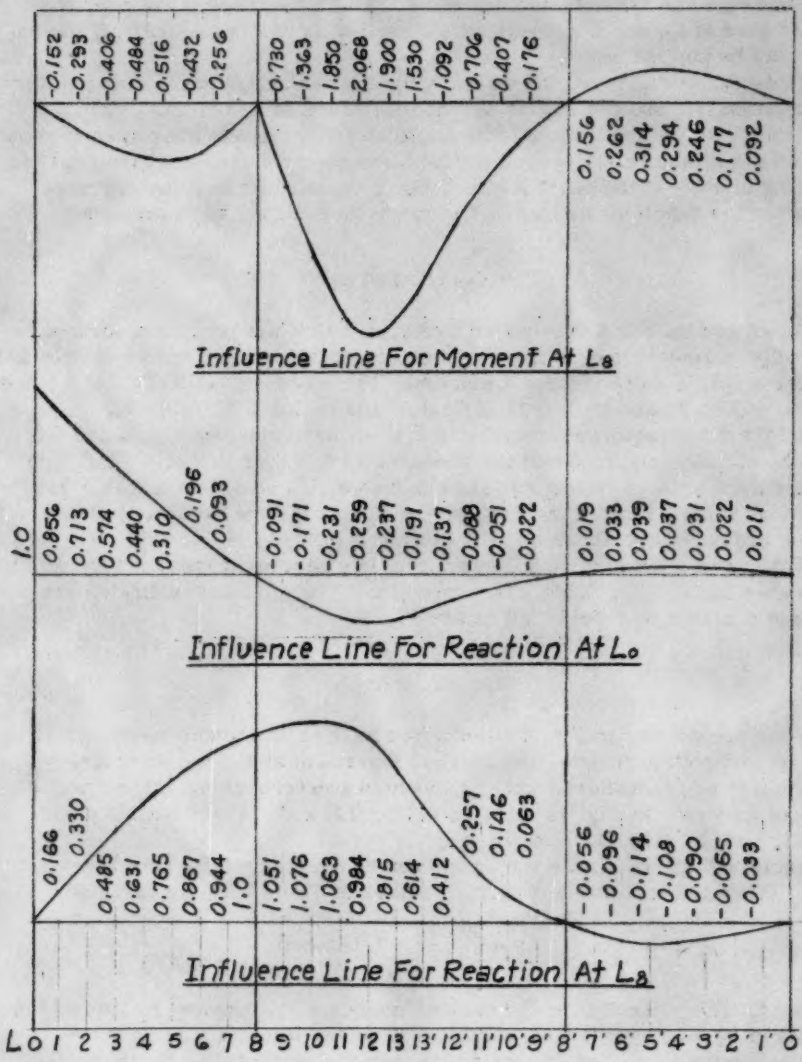
-0.152 -0.293 -0.406 -0.484 -0.516 -0.432 -0.256
-0.730 -1.363 -1.850 -2.068 -1.900 -1.530 -1.092 -0.706 -0.407 -0.176
0.156 0.262 0.314 0.294 0.246 0.177 0.092
Influence Line For Moment At La
1.0
0.856 0.713 0.574 0.440 0.310 0.196 0.093
-0.091 -0.171 -0.231 -0.259 -0.237 -0.191 -0.137 -0.088 -0.051 -0.022
0.019 0.033 0.039 0.037 0.031 0.022 0.011
Influence Line For Reaction At Lo
0.166 0.330 0.485 0.631 0.765 0.867 0.944 1.0
1.051 1.076 1.063 0.984 0.815 0.614 0.412
0.257 0.146 0.063
-0.056 -0.096 -0.114 -0.108 -0.090 -0.065 -0.033
Influence Line For Reaction At La
Lo 1 2 3 4 5 6 7 8 9 10 11 12 13 13' 12' 11' 10' 9' 8' 7' 6' 5' 4' 3' 2' 1' 0'

Fig. 4

The Two-Span Continuous Truss

The two-span continuous truss shown in Fig. 5 is singly indeterminate and only one equation is necessary for a solution. If the truss is cut over the center pier at L_8 and a moment Xa = 1 applied as shown in Fig. 6, Equation (15) may be applied.

Table IV shows the work necessary for the evaluation of the denominator of Equation (15) and the elastic weights due to the stresses Xa.

Table V shows the loading of the statically determinate base system shown in Fig. 6 with the elastic weights. The influence ordinates are given in Col. 5 and are in units of the panel length. Using these ordinates, the influence lines for the reactions at Lo and L_8, as shown in Fig. 7 were prepared.

The Two-Hinged Arch

Shown in Fig. 8 is a two-hinged tied arch which has been used quite often in bridge engineering practice. Such structures are singly indeterminate and Equation (15) is sufficient for a solution. The stresses due to Xa = H = 1 are shown in Fig. 2c and in Col. 11 of Table I and in Col. 5 of Table VI.

All the work required for evaluation of the denominator of Equation (15) and the elastic weights due to the stresses Xa is shown in Table VI.

The arch span is loaded with the elastic weights as shown in Table VII. Col. 5 of Table VII gives the influence ordinates for the horizontal thrust. These ordinates are shown as an influence line in Fig. 9.

If the arch is externally anchored it is only necessary that the term for the tie shown in Col. 7 of Table VI be ommitted. The influence ordinates are then as shown in Col. 6 of Table VII and in Fig. 9.

The Fixed Arch

If the arch shown in Fig. 8 is anchored against horizontal movement at U_8 and against both horizontal and vertical movement at L_8, the structure becomes a fixed framed arch and is three-fold indeterminate. If the axes are located as shown in Fig. 10 Equations (12), (13) and (14) are satisfied and Equations (15), (16), (17) and (18) apply.

Table VIII shows all the work required by Equations (15), (16), (17) and (19). Using the total value of Cols. 7 and 12 of Table VIII, the value of

$$y = \frac{38.014}{20.783} = 1.83 \text{ panels}$$

is found. The value S_c, for the various members, is found by multiplying the values of S_a as shown in Col. 5 Table VIII by the value of y found above.

A tabulation of the elastic weights due to the stresses S_a, S_b and S_c is shown in Table IX.

The conjugate beam is loaded with the elastic weights shown in Table IX. This operation is illustrated by Table X.

Using the influence ordinates for X_a, X_b and X_c, as determined by Table X, the influence lines for thrust, reaction and moment at L_8 were prepared and are shown in graph form in Fig. 11.

The proportions and sections shown for this fixed arch, and for some of the

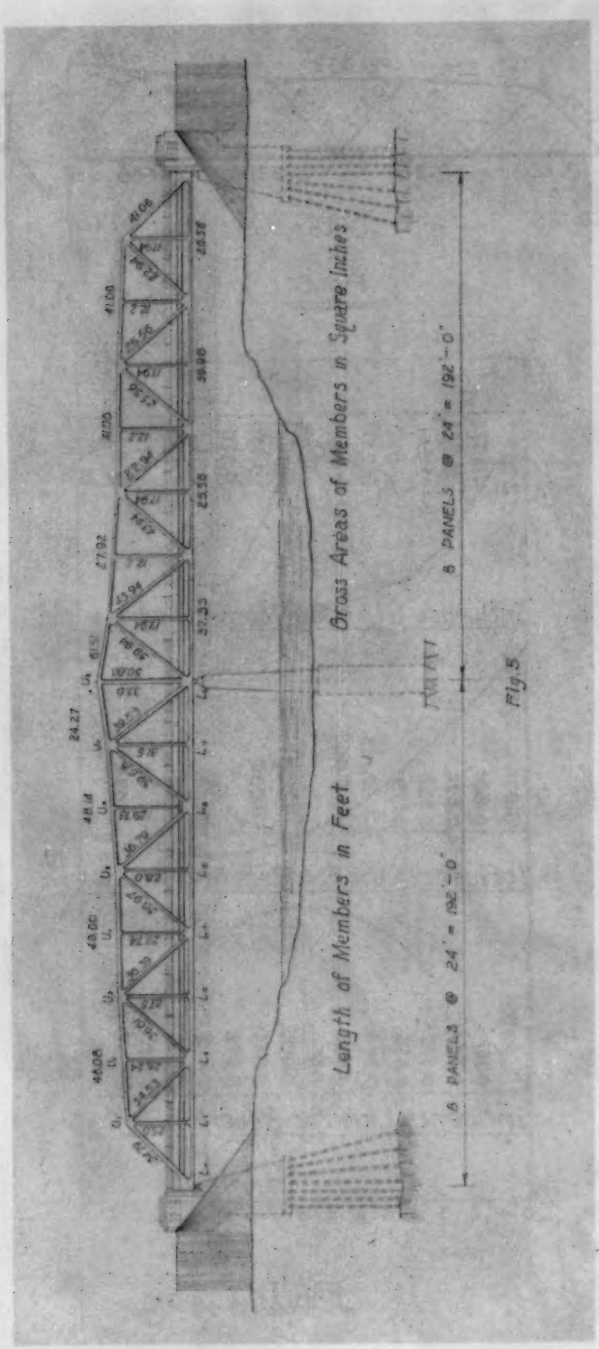
Gross Areas of Members in Square Inches
Length of Members in Feet
6 PANELS @ 24' = 192'-0"
8 PANELS @ 24' = 192'-0"

Fig.5

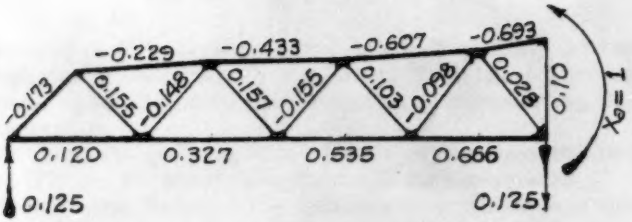
-0.173
-0.229
-0.433
-0.607
-0.693
0.155
-0.148
0.157
-0.155
0.103
-0.098
0.028
0.10
1 = ∑x
0.120
0.327
0.535
0.666
0.125
0.125

Fig. 6

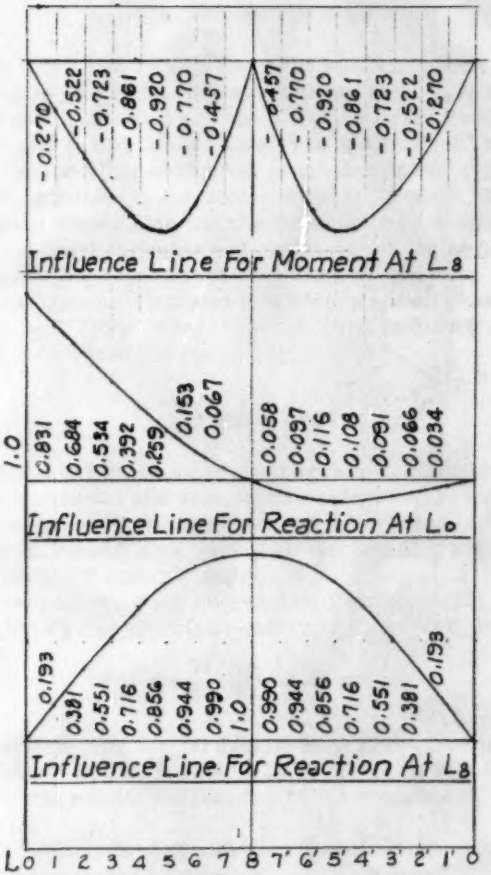
-0.270
-0.522
-0.723
-0.861
-0.920
-0.770
-0.457
-0.457
-0.770
-0.920
-0.861
-0.723
-0.522
-0.270
Influence Line For Moment At L8
1.0
0.831
0.684
0.534
0.392
0.259
0.153
0.067
-0.058
-0.097
-0.116
-0.108
-0.091
-0.066
-0.034
Influence Line For Reaction At L0
0.193
0.381
0.551
0.716
0.856
0.944
0.990
1.0
0.990
0.944
0.856
0.716
0.551
0.381
0.193
Influence Line For Reaction At L8
L0 1 2 3 4 5 6 7 8 7' 6' 5' 4' 3' 2' 1' 0

Fig. 7

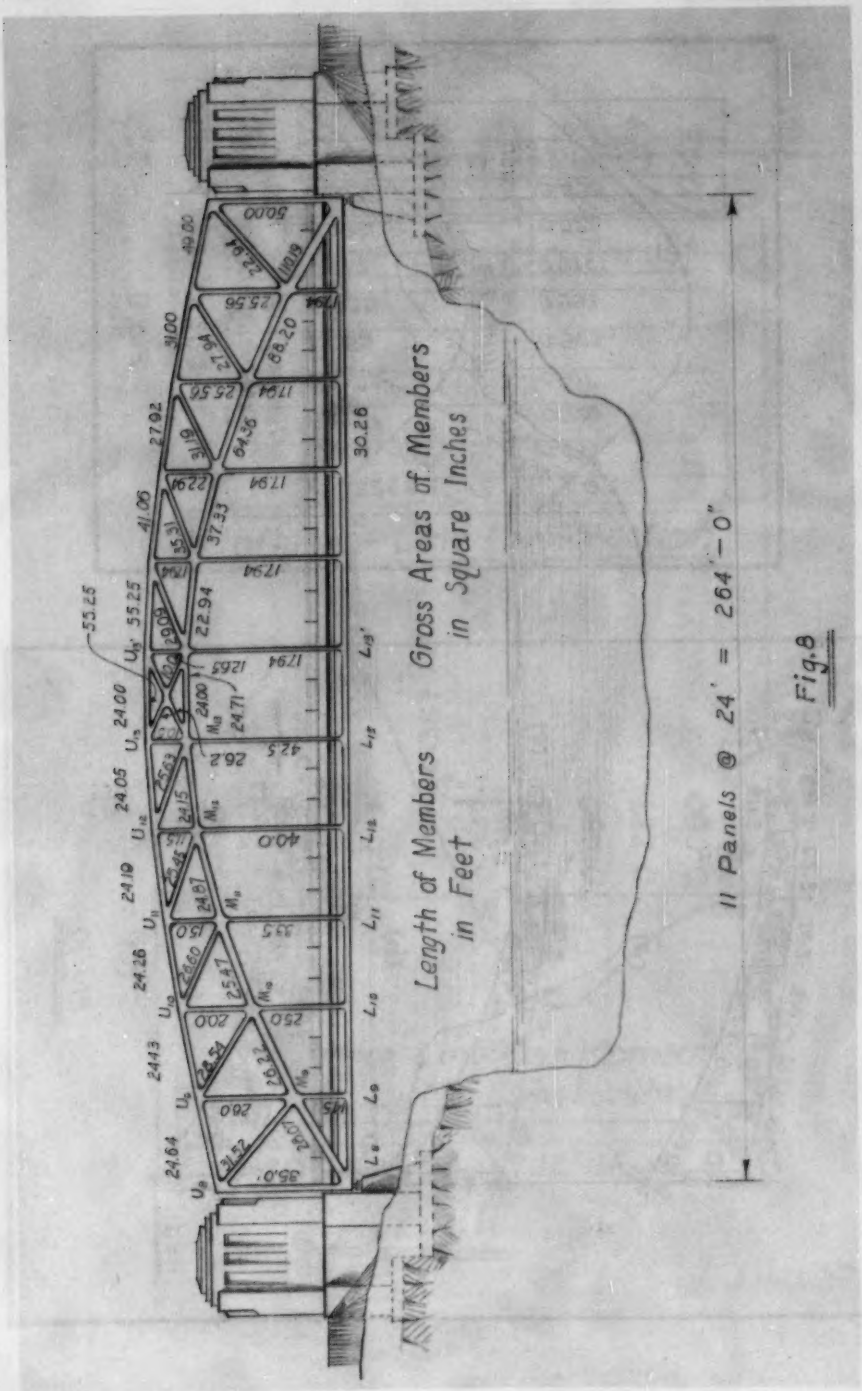
Length of Members in Feet
Gross Areas of Members in Square Inches
11 Panels @ 24' = 264'-0"

Fig.8

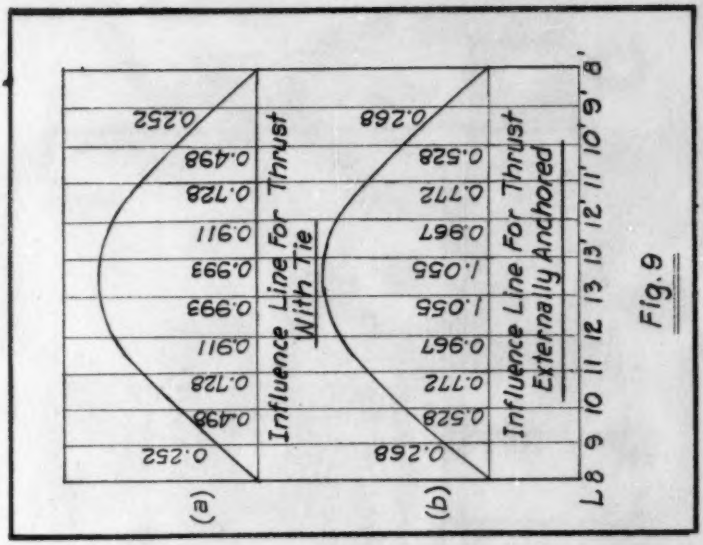
(a)
0.252
0.498
0.728
0.911
0.993
0.993
0.911
0.728
0.498
0.252
Influence Line For Thrust With Tie
(b)
0.268
0.528
0.772
0.967
1.055
1.055
0.967
0.772
0.528
0.268
Influence Line For Thrust Externally Anchored
L 8 9 10 11 12 13 13' 12' 11' 10' 9' 8'

Fig. 9

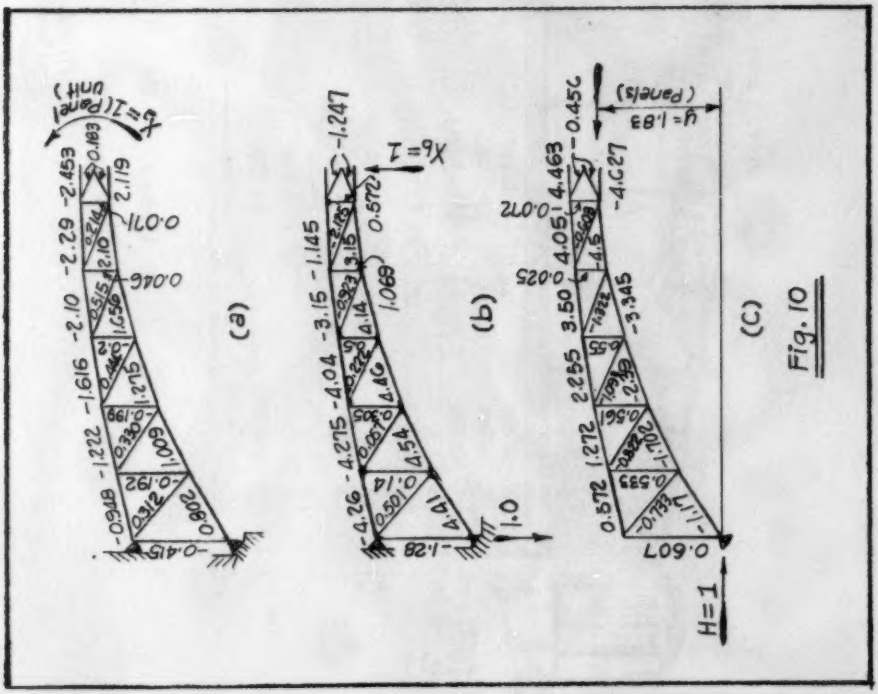
(a)
(b)
(c)
H=1
1.0
X6=1
u=1.83 (Panels)

Fig. 10

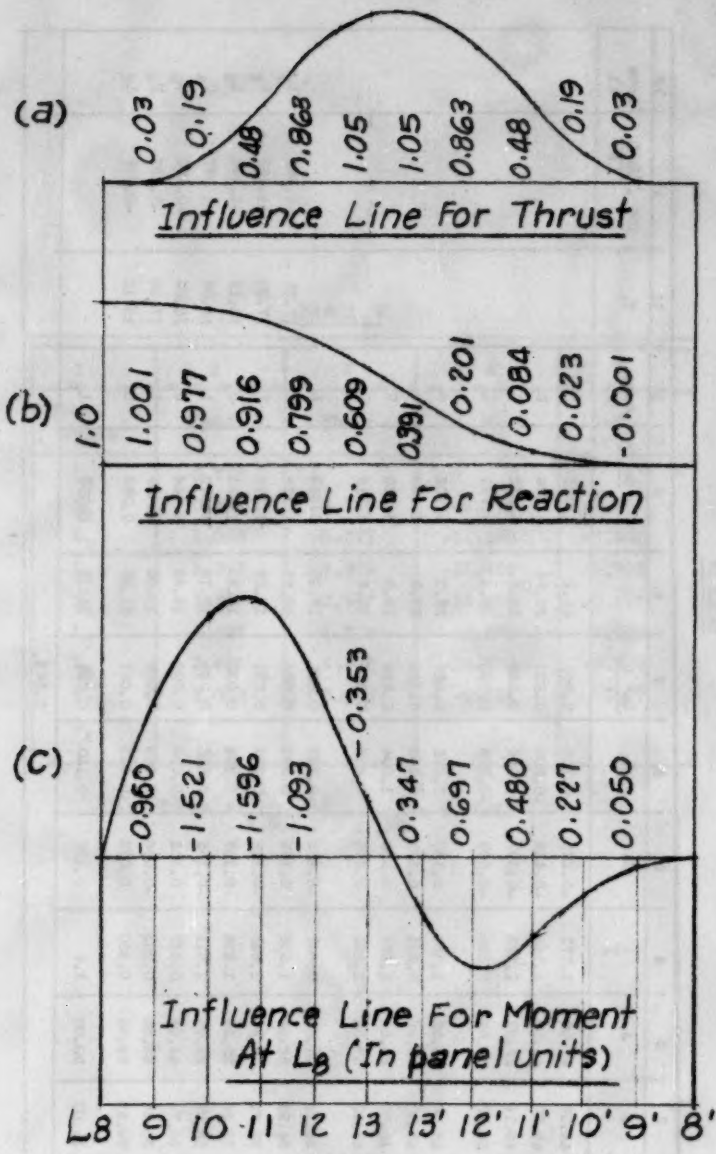
(a)
0.03
0.19
0.48
0.863
1.05
1.05
0.863
0.48
0.19
0.03
Influence Line for Thrust
(b)
1.0
1.001
0.977
0.916
0.799
0.609
0.391
0.201
0.084
0.023
-0.001
Influence Line For Reaction
(c)
-0.960
-1.521
-1.596
-1.093
-0.353
0.347
0.697
0.480
0.227
0.050
Influence Line For Moment
At L8 (In panel units)
L8 9 10 11 12 13 13' 12' 11' 10' 9' 8'

Fig. 11

TABLE IV

1	2	3	4	5	6	7	8	9	10	11	12	13
Member	L	A	$\frac{L}{A}$	Sa	$\frac{Sa\ L}{A}$	$\frac{Sa^2\ L}{A}$	r_1	$\frac{100}{r_1} \cdot \frac{Sa\ L}{A}$	Acts At	r_2	$\frac{100}{r_2} \cdot \frac{Sa\ L}{A}$	Acts At
U_1-U_3	48.08	41.06	1.171	-0.229	-0.268	0.061	26.2	1.023	L_2			
U_3-U_5	48.00	41.06	1.168	-0.433	-0.506	0.220	27.74	1.824	L_4			
U_5-U_7	48.14	27.92	1.723	-0.607	-1.046	0.635	29.6	3.532	L_6			
U_7-U_8	24.27	61.51	0.395	-0.693	-0.274	0.190	34.6	0.791	L_8			
L_0-L_2	48.00	25.56	1.877	0.120	0.225	0.027	25.0	0.902	U_1			
L_2-L_4	48.00	39.98	1.201	0.327	0.393	0.128	27.5	1.428	U_3			
L_4-L_6	48.00	25.56	1.877	0.535	1.004	0.538	28.0	3.586	U_5			
L_6-L_8	48.00	37.32	1.285	0.666	0.856	0.570	31.5	2.716	U_7			
L_0-U_1	34.79	41.06	0.847	-0.173	-0.147	0.025	17.25	0.849	L_1			
U_1-L_2	34.53	22.94	1.505	0.155	0.233	0.036	18.25	1.278	U_2	17.25	-1.352	L_1
L_2-U_3	36.61	25.56	1.432	-0.148	-0.212	0.031	18.02	1.176	L_3	17.20	-1.233	U_2
U_3-L_4	36.39	25.56	1.424	0.157	0.224	0.035	18.30	1.221	U_4	18.15	-1.232	L_3
L_4-U_5	36.97	22.94	1.611	-0.155	-0.250	0.039	18.18	1.373	L_5	18.00	-1.387	U_4
U_5-L_6	36.79	43.94	0.837	0.103	0.086	0.009	19.42	0.444	U_6	18.26	-0.472	L_5
L_6-U_7	39.68	43.94	0.903	-0.098	-0.089	0.009	19.05	0.465	L_7	17.98	-0.492	U_6
U_7-L_8	39.53	59.94	0.660	0.028	0.019	0.001	21.25	0.089	U_8	19.12	-0.099	L_7
U_8-L_8	35.00	50.00	1.4	0.100	0.140	0.014	240.0	0.006	L_8			
Σ						2.568						

TABLE V

1	2	3	4	5
Panel Point	Load	Shear	M	Inf Ord. Xa
L_0	-5.776			
L_1	0.399	-5.776	-5.776	-0.27
L_2	1.068	-5.377	-11.153	-0.522
L_3	1.372	-4.309	-15.462	-0.723
L_4	1.658	-2.937	-18.399	-0.861
L_5	4.487	-1.279	-19.678	-0.920
L_6	3.484	3.208	-16.470	-0.770
L_7	3.082	6.692	-9.778	-0.457
L_8				

$$\text{Inf. Ord } Xa = \frac{24M}{2.568 \times 2 \times 100} = 0.0468M$$

TABLE VI

1	2	3	4	5	6	7	8	9	10	11	12	13
Member	L	A	$\frac{L}{A}$	S_a	$S_a \frac{L}{A}$	$S_a^2 \frac{L}{A}$	r_1	$\frac{100}{r_1} \cdot \frac{S_a L}{A}$	Acts At	r_2	$\frac{100}{r_2} \cdot \frac{S_a L}{A}$	Acts At
U_8-U_9	24.64	49.00	0.503	0.572	0.288	0.164	25.5	-1.157	M_9			
U_9 -U_{10}	24.48	31.00	0.788	1.272	1.003	1.277	19.65	-5.110	M_{10}			
U_{10}-U_{11}	24.28	27.92	0.869	2.256	1.960	4.420	14.85	-13.200	M_{11}			
U_{11}-U_{12}	24.19	41.06	0.589	3.5	2.060	7.225	11.41	-18.060	M_{12}			
U_{12}-U_{13}	24.05	55.25	0.434	4.05	1.756	7.120	10.48	-16.770	M_{13}			
$\frac{1}{2}(U_{13}$-$U'_{13})$	12.00	55.25	0.216	4.463	0.965	4.310	10.50	-9.180	M_{13}			
L_8-M_9	28.07	110.19	0.255	-1.170	-0.298	0.349	29.9	-0.997	U_8			
M_9-M_{10}	26.22	88.20	0.297	-1.702	-0.506	0.862	23.8	-2.180	U_9			
M_{10}-M_{11}	25.47	64.36	0.396	-2.39	-0.947	2.260	18.85	-5.025	U_{10}			
M_{11}-M_{12}	24.87	37.33	0.666	-3.345	-2.230	7.460	14.47	-15.400	U_{11}			
M_{12}-M_{13}	24.15	22.94	1.053	-4.5	-4.740	21.300	11.42	-41.500	U_{12}			
$\frac{1}{2}(M_{13}$-$M'_{13})$	12.00	24.71	0.486	-4.627	-2.250	10.410	10.5	-21.450	U_{13}			
U_8-M_9	31.52	22.94	1.374	-0.733	-1.007	0.738	26.65	3.785	U_8	19.80	-5.090	M_9
U_9-M_{10}	28.54	27.94	1.022	-0.822	-0.841	0.691	21.85	3.850	U_9	16.82	-5.0	M_{10}
U_{10}-M_{11}	26.60	31.19	0.853	-1.093	-0.935	1.020	18.05	5.180	U_{10}	13.54	-6.91	M_{11}
U_{11}-M_{12}	25.45	35.31	0.721	-1.322	-0.953	1.262	14.15	6.740	U_{11}	10.85	-8.80	M_{12}
U_{12}-M_{13}	25.63	29.09	0.882	-0.603	-0.532	0.321	10.76	4.940	U_{12}	9.85	-5.42	M_{13}
$\frac{1}{2}(U_{13}$-$M'_{13})$	13.10	10.00	1.31	-0.456	-0.598	0.273						
$\frac{1}{2}(M_{13}$-$U_{13})$	13.10	10.00	1.31	-0.456	-0.598	0.273						
U_8-L_8	35.00	50.00	0.7	0.607	0.425	0.258	41.10	1.034	L_8	24.0	-1.770	M_9
U_9-M_9	26.00	25.56	1.017	0.553	0.563	0.311	29.70	1.900	M_9	24.0	-2.35	M_{10}
U_{10}-M_{10}	20.00	25.56	0.782	0.561	0.438	0.246	29.95	1.465	M_{10}	24.0	-1.828	M_{11}
U_{11}-M_{11}	15.00	22.94	0.654	0.550	0.359	0.198	30.00	1.198	M_{11}	24.0	-1.496	M_{12}
U_{12}-M_{12}	11.50	17.94	0.641	0.025	0.016		22.90	0.070	M_{12}	24.0	-0.067	M_{13}
U_{13}-M_{13}	10.50	12.65	0.830	-0.072	-0.060	0.004	21.00	-0.286	M_{13}	24.0	0.250	M_{13}
Tie	132.00	30.26	4.362	1.0	4.362	4.362						
						27.114						

TABLE VII

1	2	3	4	5	6
Panel Point	Load	Shear	M	Inf.Ord for H_t	Inf.Ord for H
L_8	162.376	0	0	0	0
M_9	-4.377	162.376	162.376	0.252	0.268
M_{10}	-10.840	157.999	320.375	0.498	0.528
M_{11}	-29.400	147.159	467.534	0.728	0.772
M_{12}	-64.836	117.759	585.293	0.911	0.967
M_{13}	-52.923	52.923	638.216	0.993	1.055

$$H_t = X_a = \frac{24M}{77.144 \times 2 \times 100} = 0.001555M \text{ with tie}$$

$$H = X_a = \frac{24M}{72.752 \times 2 \times 100} = 0.00165M \text{ without tie}$$

TABLE VIII

1	2	3	4	5	6	7	8	9	10	11	12	13	14	15	16
Member	L	A	$\frac{L}{A}$	S_a	$\frac{S_aL}{A}$	$\frac{S_a^2L}{A}$	S_b	$\frac{S_bL}{A}$	$\frac{S_b^2L}{A}$	S_H	$\frac{S_aS_HL}{A}$	yS_a	J_c	$\frac{S_cL}{A}$	$\frac{S_c^2L}{A}$
U_8-U_9	24.64	49.00	0.503	-0.948	-0.477	0.452	-4.26	-2.143	9.128	0.572	-0.273	-1.735	-1.163	-0.585	0.681
U_9-U_{10}	24.43	31.00	0.788	-1.222	-0.963	1.177	-4.275	-3.367	14.40	1.272	-1.225	-2.24	-0.968	-0.764	0.738
U_{10}-U_{11}	24.26	27.92	0.869	-1.616	-1.404	2.270	-4.04	-3.51	14.175	2.255	-3.166	-2.955	-0.7	-0.607	0.425
U_{11}-U_{12}	24.19	41.06	0.589	-2.100	-1.236	2.598	-3.15	-1.855	5.845	3.5	-4.33	-3.84	-0.34	-0.200	0.068
U_{12}-U_{13}	24.05	55.25	0.434	-2.29	-0.993	2.272	-1.145	-0.496	0.569	4.05	-4.020	-4.19	-0.14	-0.061	0.008
$\frac{1}{2}(U_{13}$-$U'_{13})$	12.00	55.25	0.216	-2.453	-0.531	1.302	0	0	0	4.463	-2.368	-4.49	-0.027	-0.006	0
L_8-M_9	28.07	110.19	0.255	0.802	0.204	0.164	4.41	1.123	4.955	-1.170	-0.239	1.466	0.296	0.076	0.022
M_9-M_{10}	26.22	88.20	0.297	1.009	0.3	0.303	4.54	1.350	6.13	-1.702	-0.511	1.845	0.143	0.042	0.006
M_{10}-M_{11}	25.47	64.36	0.396	1.275	0.506	0.644	4.46	1.766	7.88	-2.39	-1.206	2.33	-0.06	-0.024	0.001
M_{11}-M_{12}	24.87	37.33	0.666	1.656	1.103	1.828	4.14	2.756	11.42	-3.345	-3.692	3.03	-0.315	-0.210	0.066
M_{12}-M_{13}	24.15	22.94	1.053	2.10	2.21	4.643	3.15	3.315	10.44	-4.50	-9.95	3.84	-0.66	-0.694	0.458
$\frac{1}{2}(M_{13}$-$M'_{13})$	12.00	24.71	0.486	2.119	1.028	2.178	0	0	0	-4.627	-4.758	3.87	-0.757	-0.368	0.279
U_8-M_9	31.52	22.94	1.374	0.312	0.429	0.134	0.501	0.689	0.345	-0.733	-0.314	0.571	-0.162	-0.223	0.036
U_9-M_{10}	28.54	27.94	1.022	0.330	0.337	0.111	0.057	0.058	0.003	-0.822	-0.277	0.604	-0.218	-0.223	0.049
U_{10}-M_{11}	26.60	31.19	0.853	0.444	0.379	0.168	-0.222	-0.189	0.042	-1.093	-0.414	0.813	-0.280	-0.239	0.067
U_{11}-M_{12}	25.46	35.31	0.721	0.515	0.371	0.191	-0.923	-0.665	0.614	-1.322	-0.491	0.943	-0.379	-0.273	0.104
U_{12}-M_{13}	25.63	29.09	0.882	0.214	0.187	0.040	-2.125	-1.873	3.980	-0.603	-0.114	0.391	-0.212	-0.187	0.040
$\frac{1}{2}(U_{13}$-$M'_{13})$	13.10	10.00	1.31	0.183	0.240	0.044	-1.247	-1.634	2.075	-0.456	-0.109	0.335	-0.121	-0.158	0.019
$\frac{1}{2}(M_{13}$-$U'_{13})$	13.10	10.00	1.31	0.183	0.240	0.044	1.247	1.634	2.075	-0.456	-0.109	0.335	-0.121	-0.158	0.019
U_8-L_8	35.00	50.00	0.7	-0.415	-0.291	0.120	-1.28	-0.895	1.146	0.607	-0.177	-0.759	-0.162	-0.106	0.016
U_9-M_9	26.00	25.56	1.017	-0.192	-0.195	0.038	0.14	0.143	0.020	0.553	-0.108	-0.351	0.202	0.206	0.042
U_{10}-M_{10}	20.00	25.56	0.782	-0.199	-0.156	0.031	0.305	0.239	0.073	0.561	-0.087	-0.364	0.197	0.154	0.030
U_{11}-M_{11}	15.00	22.94	0.654	-0.200	-0.131	0.026	0.5	0.327	0.164	0.550	-0.072	-0.366	0.184	0.120	0.022
U_{12}-M_{12}	11.50	17.94	0.641	0.046	0.030	0.001	1.069	0.686	0.733	0.025	0	0.084	0.109	0.070	0.008
U_{13}-M_{13}	10.50	12.65	0.83	0.071	0.059	0.004	0.572	0.475	0.272	-0.072	-0.004	0.13	0.068	0.049	0.003
						20.783			96.484		-38.014				3.207

TABLE IX

1	2	3	4	5	6	7	8	9	10	11	12	13	14	15	16	17	18
Member	r_1	r_2	$\frac{S_a L}{A}$	$\frac{100 \cdot S_a L}{r_1 A}$	Acts At	$\frac{100 \cdot S_a L}{r_2 A}$	Acts At	$\frac{S_b L}{A}$	$\frac{100 \cdot S_b L}{r_1 A}$	Acts At	$\frac{100 \cdot S_b L}{r_2 A}$	Acts At	$\frac{S_c L}{A}$	$\frac{100 \cdot S_c L}{r_1 A}$	Acts At	$\frac{100 \cdot S_c L}{r_2 A}$	Acts At
U_8-U_9	25.3		-0.477	1.885	M_9			-2.143	8.470	M_9			-0.585	2.31	M_9		
U_9-U_{10}	19.85		-0.963	4.900	M_{10}			-3.367	17.160	M_{10}			-0.764	3.89	M_{10}		
U_{10}-U_{11}	14.85		-1.404	9.480	M_{11}			-3.510	23.640	M_{11}			-0.607	4.08	M_{11}		
U_{11}-U_{12}	11.41		-1.236	10.830	M_{12}			-1.855	16.250	M_{12}			-0.2	1.754	M_{12}		
U_{12}-U_{13}	10.48		-0.993	9.470	M_{13}			-0.498	4.735	M_{13}			-0.061	0.582	M_{13}		
$\frac{1}{2}(U_{13}-U'_{13})$	10.8		-0.531	5.080	M_{13}			0.0					-0.006	0.057	M_{13}		
L_8-M_9	29.9		0.204	0.683	U_8			1.123	3.755	U_8			0.076	0.254	U_8		
M_9-M_{10}	23.8		0.3	1.261	U_9			1.350	5.672	U_9			0.042	0.177	U_9		
M_{10}-M_{11}	18.85		0.845	2.680	U_{10}			1.766	9.370	U_{10}			-0.024	-0.127	U_{10}		
M_{11}-M_{12}	14.47		1.105	7.625	U_{11}			2.756	19.050	U_{11}			-0.210	-1.452	U_{11}		
M_{12}-M_{13}	11.42		2.21	19.350	U_{12}			3.315	29.040	U_{12}			-0.894	-6.075	U_{12}		
$\frac{1}{2}(M_{13}-M'_{13})$	10.8		1.028	9.800	U_{13}			0.0					-0.368	-3.506	U_{13}		
U_8-M_9	26.65	19.80	0.429	-1.608	L_8	2.166	U_9	0.688	-2.583	L_8	3.478	U_9	-0.223	0.837	U_8	-1.126	M_9
U_9 -M_{10}	21.85	16.82	0.337	-1.542	M_9	2.004	U_{10}	0.058	-0.267	M_9	0.347	U_{10}	-0.223	1.021	U_9	-1.325	M_{10}
U_{10}-M_{11}	18.06	13.54	0.379	-2.098	M_{10}	2.798	U_{11}	-0.189	1.048	M_{10}	-1.398	U_{11}	-0.239	1.325	U_{10}	-1.765	M_{11}
U_{11}-M_{12}	14.15	10.85	0.371	-2.622	M_{11}	3.420	U_{12}	-0.665	4.700	M_{11}	-4.130	U_{12}	-0.273	1.93	U_{11}	-2.514	M_{12}
U_{12}-M_{13}	10.76	9.83	0.189	-1.752	M_{12}	1.918	U_{13}	-1.873	17.400	M_{12}	-19.06	U_{13}	-0.187	1.736	U_{12}	-1.902	M_{13}
$\frac{1}{2}(U_{13}-U'_{13})$	9.82		0.240	-2.492	M_{13}			-1.634	16.980	M_{13}			-0.158				
$\frac{1}{2}(M_{13}-U'_{13})$	9.82		0.240	2.492	U_{13}			1.634	16.980	U_{13}			-0.158				
U_8-L_8	34.95	24.0	-0.291	-0.833	L_8	1.213	M_9	-0.895	-2.56	L_8	3.73	M_9	-0.106	-0.303	L_8	0.442	M_9
U_9-M_9	29.7	24.0	-0.195	-0.658	M_9	0.814	M_{10}	0.143	0.480	M_9	-0.594	M_{10}	0.206	0.694	M_9	-0.858	M_{10}
U_{10}-M_{10}	29.95	24.0	-0.156	-0.520	M_{10}	0.649	M_{11}	0.230	0.796	M_{10}	-0.994	M_{11}	0.154	0.514	M_{10}	-0.642	M_{11}
U_{11}-M_{11}	30.0	24.0	-0.131	-0.436	M_{11}	0.545	M_{12}	0.327	1.090	M_{11}	-1.362	M_{12}	0.120	0.400	M_{11}	-0.5	M_{12}
U_{12}-M_{12}	22.9	24.0	0.030	0.129	M_{12}	-0.125	M_{13}	0.686	2.994	M_{12}	-2.856	M_{13}	0.070	0.305	M_{12}	-0.291	M_{13}
U_{13}-M_{13}	21.0	24.0	0.069	0.281	M_{13}	-0.266	M_{13}	0.475	2.26	M_{13}	-1.975	M_{13}	0.049	0.233	M_{13}	-0.204	M_{13}

TABLE X

	Influence Line for Moment Xa				Influence Line for Shear Xb				Influence Line for Thrust Xc			
	Load	Shear	Ma	Inf.Ord Xa	Load	Shear	Mb	Inf.Ord Xb	Load	Shear	Mc	Inf.Ord Xc
L_8	-1.758				-1.386				0.788			
L_9	4.325	-1.758	-1.758	-0.010	21.563	-1.385	-1.385	-0.001	3.518	0.788	0.788	0.03
L_{10}	7.780	2.567	0.809	0.005	28.107	20.178	18.793	0.023	3.419	4.306	5.094	0.19
L_{11}	17.474	10.347	11.156	0.064	46.088	48.285	67.078	0.084	2.551	7.725	12.819	0.48
L_{12}	32.522	27.821	38.977	0.225	58.202	94.373	161.451	0.201	-5.294	10.276	23.095	0.865
L_{13}	26.150	60.343	99.320	0.573	17.064	152.575	314.026	0.391	-5.031	4.982	28.077	1.060
	$Xa = \frac{24\ Ma}{20.783 \times 2 \times 100} = 0.005775\ Ma$				$Xb = \frac{24\ Mb}{96.484 \times 2 \times 100} = 0.001245\ Mb$				$Xc = \frac{24\ Mc}{3.207 \times 2 \times 100} = 0.0374\ Mc$			

NOTE: Moments Xa are in panel units.

other examples given in this discussion, would not be used in an actual design; however, they serve to illustrate the application of this method of stress analysis.

The analysis of the stresses in the various examples has been shown in considerable detail in order to illustrate all the work involved. Using this method of analysis it is obvious there are no simultaneous equations to solve. Slide rule computations are sufficiently accurate and for many cases much time may be saved.

Discussion of
"ANALYSIS OF COLLAR SLABS FOR SHELLS OF REVOLUTION"

by Gunhard Oravas
(Proc. Paper 916)

CORRECTIONS.—On page 916-5 the following formulas were omitted:

$$M_{\Delta F} = \left(\frac{h}{2 K^2 \sin \alpha \, k_\alpha} \right) \Delta_F \, E$$

and

$$H_{\Delta F} = \left(\frac{h}{a K \sin^2 \alpha \, k_\alpha} \right) \Delta_F \, E$$

in which

$$k_\alpha = 1 - \frac{\cot a}{2 K}$$

On page 5, under the heading "Procedure for Continuity Analysis" in item b, the phrase "The rotations of the intersections . . . " should be changed to "The intersections . . . "

On page 8 the final moments for the spherical shell should be changed to

$$\begin{array}{r} -5.00 \\ \underline{(-0.3)(1.5 = -0.45} \\ -5.45 \text{ ft k / ft} \end{array}$$

In Fig. 7 on page 14 the moment of 1.1 ft k should be changed to 5.45 ft k / ft and the direction of the reactions (6.54 k) should be reversed.

Discussion of "HEAVY AND TALL BUILDING PROBLEMS IN MEXICO CITY"

by Leonardo Zeevaert
(Proc. Paper 917)

LEONARDO ZEEVAERT,[1] A.M. ASCE.—The author appreciates the discussion presented by Dr. Emilio Rosenblueth extending the subject on the earthquake problem. The philosophy with which the 43-storey building "Latino Americana Tower" in Mexico City was finally designed may be found in proceedings of the World Conference on Earthquake Engineering held June 12-16, 1956, in Berkeley, University of California; "Aseismic Design of Latino Americana Tower in Mexico City" by N. M. Newmark and L. Zeevaert. This paper explains in detail the different steps in the design of the building. Aseguradora Anahuac Building was designed following the same philosophy as finally adopted in Latino Americana Tower.

The calculations were made following Dr. Newmark's method of analysis first known to the author in 1948 by personal communication while working with him in this particular problem. The method to find the modes of vibration is primarily based on numerical proceedures similar to those described in paper No. 2202 Transactions Vol. 108 (1943) by Dr. N. M. Newmark.

The same probabilistic equation as published by Messrs. L. E. Goodman, E. Rosenblueth and N. M. Newmark, Transactions Vol. 120 (1955), was used as a general criterion to estimate the probable design shears. The results obtained by means of equation: $V_D = \sqrt{\Sigma\ V_n^2}$, are very valuable to estimate the most probable shears to design the building. The values of "V_n" are the shears induced by the first modes of vibration of the building, in this case up to the fourth mode. However, it should be not forgotten that the building may be excited strongly during an earthquake in any one of the modes of vibration enclosing the period of the ground motion. The probable shears under this condition should be also carefully investigated.

The writer agrees that flexibility in the first floor is limited to a certain extent, primarily because of possible large deflections; and secondly, because of architectural demands. However, Dr. Rosenblueth will agree with the writer that a flexible building in the first floors is more economical and better suited to resist tremors. The stresses originated in the superstructure will be smaller for the same intensity of ground motion as those transmitted in a building with very rigid first floor structure as obtained when designing with a uniform seismic coefficient. In buildings like those mentioned in the paper flexibility of the upper floors it is very important to take this into consideration when making the seismic stress analysis.

Concerning the use of deep foundations for buildings like the ones mentioned above, the necessity is obvious from the Soil Mechanics point of view. Considering the earthquake problem Dr. Rosenblueth should consider that

1. Prof., Soil Mechanics and Foundation Eng., Univ. of Mexico, Mexico City, Mexico.

there are other items more important as the overturning moment induced to the building during an earthquake. From aseismic design point of view, and considering subsoil conditions in Mexico City, the effect of lateral movement in the foundation is a phenomenon that takes place during earthquakes and should be seriously considered. Heavy buildings in Mexico City on wood piles and with no basement, but a shallow foundation, have seriously damaged neighbour lighter buildings during an earthquake because of the foundation sidesway movement set during the earthquake.

The design of foundations using the combination of friction piles and point bearing piles as stated by Dr. Rosenblueth, is undersirable because of the large relative movement of friction piles vs. point bearing piles set by the well known surface subsidence, in spite that any one of these groups may be provided with load adjustment and measuring devices in order to control the proper load on each pile. The best practice regardless the use of load control devices is to be consistent in the pile foundation design.

Discussion of
"TESTS ON BOLTED CONNECTIONS IN LIGHT-GAGE STEEL"

by George Winter
(Proc. Paper 920)

R. B. MATTHIESEN,[1] J.M. ASCE, and R. L. MOORE,[2] A.M. ASCE.—The design procedures proposed by the author make use of the tensile properties of the materials to account for the various modes of failure which he observed. It can be shown that the author's results in Figs. 8 and 9 are in reasonable agreement with what might be expected if one considers that the nominal tensile, bearing, or shear stress governs the ultimate strength of the joint, irrespective of the type of failure which occurs.

For connections with a single row of fasteners, the ratio of the nominal tensile stress on the net section, σ_n, to the tensile ultimate strength of the material, σ_t, is given by the following formula when the nominal bearing stress governs the ultimate strength of the joint:

$$\frac{\sigma_n}{\sigma_t} = \frac{\sigma_b}{\sigma_t} \frac{d/s}{1 - d/s} \qquad (A)$$

where σ_b is the bearing ultimate strength,

d is the diameter of the bolt, and

s is the transverse spacing of the bolts.

From Fig. 7 and Table 2, it can be deduced that for the author's tests, $\frac{\sigma_b}{\sigma_t}$ is about 3.6 if the e/d ratio is equal to 3.5 or greater. This value of $\frac{\sigma_b}{\sigma_t}$ has been substituted in Equation A and the resulting equation has been plotted in Figs. A and B, which are reproductions of the author's Figs. 8 and 9. It can be seen that the trend of the author's results is in reasonable agreement with the trend indicated by Equation A. For specimens having e/d ratios less than 3.5, the curve representing Equation A would be lower than indicated in Figs. A and B. Thus, the relatively low values of stress on the net section of specimens with low values of d/s (i.e., less than 0.225) might be a result of the high bearing or longitudinal-shearing stresses in these specimens, even though tension failures occurred.

On the other hand, it can be shown that for connections with a single row of bolts, the ratio of the nominal tensile stress on the net section, σ_t, to the tensile ultimate strength, σ_n is given by the following formula when shear stress in the bolts governs the ultimate strength:

1. Eng. Design Div., Alcoa Research Labs., New Kensington, Pa.
2. Asst. Chief, Eng. Design Div., Alcoa Research Labs., New Kensington, Pa.

$$\frac{\sigma_n}{\sigma_t} \frac{\tau_b}{\sigma_t} \frac{k\pi}{4} \frac{(d/t)(d/s)}{1 - d/s} \qquad \text{(B)}$$

where τ_b is the shear ultimate strength of the bolts,

k is the number of shear planes,

d is the diameter of the bolts,

s is the transverse spacing of the bolts, and

t is the plate thickness.

Equation B is similar to Equation A. If the proper values for all of the terms in Equation B were known, it could be plotted in Figs. A and B. Since the d/t ratios for the author's specimens range from about 3 to about 21, it is impractical to attempt to plot Equation B. However, for d/t ratios of about 4 for double-shear joints or 8 for single-shear joints, and with $\frac{\tau_b}{\sigma_t}$ equal to 0.6 (as in Figs. 10 and 11), Equation B would be equivalent to Equation A. Thus, the relatively low values of stress on the net section of specimens with low d/s ratios might be correlated with high bolt-shearing stresses as well as with high bearing or longitudinal-shearing stresses. In this connection, the work of Fefferman and Langhaar[1] is of interest. From an extensive investigation of riveted connections in plates of aluminum alloy 2024-T4, these investigators developed correction factors to be applied to an analysis of riveted connections based on the nominal tensile, bearing, and shear properties of the material. These correction factors account for the apparent lowering of the net-section tensile stress which results from high bearing or shear stresses as well as from the perforations in the plate.

It is of interest to point out that Equation (3) describes surprisingly well the results of bearing tests of aluminum alloy sheet and plate. If the term σ_y in Equation (3) is replaced by $0.7\,\sigma_t$, which is approximately true for the author's materials as indicated by Table 2, and values of 1-1/2 and 2 are substituted for e/d to cover the edge distances investigated in aluminum, the resulting expressions will be:

$$\sigma_b = 1.5\,\sigma_t, \text{ for } e/d = 1.5, \text{ and}$$

$$\sigma_b = 2.0\,\sigma_t, \text{ for } e/d = 2.0$$

Almost identical relationships exist between the bearing and tensile properties of a wide range of aluminum alloy sheet and plate products used in structural design (Ref. 2, 3 and 4).

Corresponding linear relationships exist between bearing yield strengths (stress producing permanent hole elongation = 0.02d) and tensile yield strengths for aluminum.[2]

$$\sigma_{by} = 1.4\,\sigma_{ty}, \text{ for } e/d = 1.5, \text{ and}$$

$$\sigma \quad = 1.6\,\sigma \quad, \text{ for } e/d = 2.0$$

Rather large reductions in bearing ultimate strengths have been observed for aluminum alloys with ratios of e/d = 2 when the ratios of diameter to thickness (d/t) exceed 4. Although bolted connections provide greater support against lateral buckling under high bearing stresses than the type of bearing specimen used with the aluminum alloys, some of the scatter in Figs. 5, 6 and 7 may be attributable to the effect of the d/t ratios, considering the wide range of values covered in the author's tests.

In aluminum-alloy connections, when a rivet or bolt is used in conjunction with a relatively thin plate, i.e., when d/t is greater than 3, the plate apparently has a tendency to cut into the rivet and cause a lowering of the shear strength of the rivet.(5,6) This lowering of the shear strength is greater in double-shear connections than in single-shear connections. Since, as suggested by the author, a similar phenomenon undoubtedly occurs in light-gage steel connections, it would seem that the results in Figs. 10 and 11 for specimens which fail by shearing the bolts, Type IV failures, would show less scatter if the shear strength were plotted against the ratio diameter to plate thickness, d/t, rather than against the bolt diameter, per se.

REFERENCES

1. "Investigations of 24S-T Riveted Tension Joints," by R. L. Fefferman and H. L. Langhaar, Journal of the Aeronautical Sciences, March, 1947.
2. "Strength of Metal Aircraft Elements," Dept. of Air Force, Dept. of Navy, Dept. of Commerce, Bulletin ANC-5, June, 1955.
3. "Specifications for Structures of Aluminum Alloy 6061-T6," ASCE, Proceedings Paper No. 970, Journal of the Structural Division, May, 1956.
4. "Specifications for Structures of Aluminum Alloy 2014-T6," ASCE, Proceedings Paper No. 971, Journal of the Structural Division, May, 1956.
5. "The Shear Strength of Aluminum Alloy Driven Rivets as Affected by Increasing d/t Ratios," by E. C. Hartmann and C. Wescoat, NACA Technical Note No. 947, July, 1944.
6. Alcoa Structural Handbook, Aluminum Company of America, Pittsburgh, Pennslyvania, 1955.

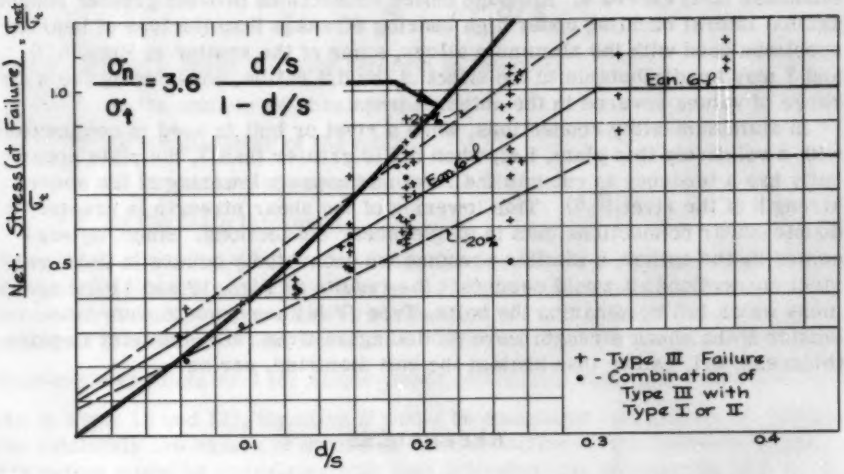

FIG. A TYPE III FAILURES, SINGLE SHEAR TESTS

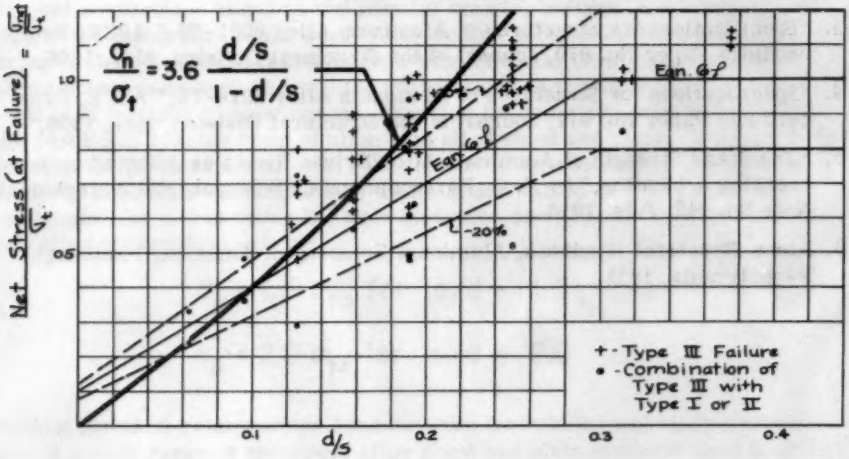

FIG. B TYPE III FAILURES, DOUBLE SHEAR TESTS

Discussion of
"DYNAMIC STRESSES IN CONTINUOUS PLATE GIRDER BRIDGES"

by Roy C. Edgerton and Gordon W. Beecroft
(Proc. Paper 973)

R. K. L. WEN,* J.M. ASCE.—One of the essential points that this paper has brought out is the importance of "deck roughness" in relation to the dynamic response of the two bridges studied. If the bridge deck and approach are smooth, it has been indicated by both experiments and mathematical analyses that, within practical ranges of parameters, a sprung or an unsprung load will seldom cause any serious dynamic effects on the structure.(1)** The maximum dynamic stresses in these cases are of the order of 10 to 15 per cent larger than the maximum static stresses. Field tests on highway bridges, however, have rather consistently shown that the maximum dynamic deflection or stress may well be expected to be 25 per cent and often more than 30 per cent larger than the maximum static response. Analytical studies and laboratory experiments(1)(2) have also shown that large dynamic stresses can exist in a bridge, if the sprung part of the vehicle has been oxcillating vertically as it enters onto the bridge. This vertical oscillation of the vehicle may have been excited by the unevenness of the approach to the bridge.

On highway bridges there is no apparent counterpart of such periodic forcing as that acting on railway bridges due to the centrifugal force of wheel unbalance in locomotives. The effect of axle-spacing has been conceived by many engineers to be similar to that of a periodic forcing and to be the cause of a possible resonant state of the bridge vehicle system. However, available information, though limited,(3)(4) is indicative of the fact that this effect is very much less serious than that which would be expected from the above mentioned conception. It appears logical, therefore, to attribute the major remaining source of large dynamic stresses in highway bridges directly or indirectly*** to "road roughness" or "deck roughness."

After reading much of the literature on the subject of dynamic stresses in highway bridges, the writer has received the impression that the term "roadway roughness" or "deck roughness" as related to highway bridge dynamics has not been sufficiently well defined and does not always refer to the same physical condition of the road or deck. With a view toward helping the understanding and clarification of the subject, the writer believes it desirable to discuss the subject of "deck roughness" in some detail. The following suggested terminology is admittedly somewhat arbitrary. Nevertheless, it does describe, at least qualitatively, different physical characteristics of a deck surface to which the vehicle and the bridge respond in different ways.

---

* Research Associate in Civ. Eng., Univ. of Illinois, Urbana, Ill.

** Numerals in parentheses refer to items in the list of references at the end of this discussion.

*** By "indirect" is meant that "deck roughness" may induce vertical and/or pitching oscillations of the sprung part of the vehicle, which in turn may cause large dynamic effects on the bridge.

Any deviation of a roadway surface from the assumption of a perfectly smooth and horizontal profile, an assumption usually made in a mathematical analysis of bridge vibrations, may be called "unevenness." Unevenness may be of three types: (1) obstructions, (2) roughness, (3) profile variation.

"Obstructions" include any abrupt changes of appreciable magnitude in the elevation of the roadway surface. They are also characterized by their localized presence on the road. When a vehicle runs over an obstruction, impact in the true sense of the word takes place. Many experiments have been conducted on bridges with trucks rolling over an artificial obstruction such as a 3/4" x 4" or 2" x 4" plank.(5)(6) Under this condition, the resulting maximum dynamic stress can easily exceed the maximum static stress by 50 per cent or more. Fortunately the frequency of occurrence of obstructions on a properly maintained bridge deck is very small.

The case of a vehicle passing over an obstruction on a flexible bridge deck is susceptible to mathematical analysis. Results of some exploratory analytical studies(7) of this kind indicate that the order of magnitude of the dynamic stresses and deflections of the bridge is in line with those shown by field tests.

"Roughness" differs from obstructions by its much smaller deviation from smoothness, and also by its more distributed nature on the surface of the road or deck. It might be called metaphorically the texture of the road surface. The response of a bridge with a generally rough deck (as defined in this discussion) to moving loads is probably similar to that of a structure to forces or disturbances of high frequencies and small magnitudes. There is some experimental evidence that this situation is not a very serious one. For example, the vibration record of a bridge with a 2-1/2" Irving grating deck(8) traversed by a heavy truck shows that the maximum excess dynamic deflection is only about 5 per cent of the maximum static deflection. Such a deck may be considered a typical rough surface. Cracks and joints on decks, if not opened up too widely or faulted may properly be considered as localized "roughness."

"Profile variation" comprises a continuous deviation from the assumed smooth and horizontal surface. It includes the initial deflection of the bridge due to its dead load, the design grade of the deck, the inherent unevenness of the deck due to the imperfection of surface paving and leveling during construction, and any general changes in the profile of the bridge due to subsequent exposure of the deck to traffic and weather or other causes. The deck profiles obtained by taking elevations at 10-ft. intervals along the spans shown in the authors' Fig. 11 can be considered as unevenness of this type. It may be observed from this figure that the greater portion of the "total deviations" for the North Dillard Bridge comes from the continuous upward deviation from true grade from Sta. 3+00 to about 3+80. These deviations do not represent "obstructions" or "roughness" as previously defined; they represent the difference between the "profile variation" and the design grade.

Profile variation will cause no shock or real impact effect on the vehicle or the bridge. Instead it will produce a continuous forcing or disturbance acting on the vehicle which of course reacts on the bridge. The predominant frequencies of this disturbance are lower than those due to roughness.

The effect of profile variation is also susceptible to mathematical analysis by numerical methods, provided the variation is known.(9) However, in practice, the exact profile is not available until a bridge is completed and subsequent exposure of the deck to traffic and weather may modify it to some extent.

In view of the probability that "obstructions" rarely occur, and "roughness" may need not cause great concern, research on the effect of deck unevenness might be directed to the problem of "profile variation." Accumulation of records such as those shown in the authors' Fig. 11 for a number of representative bridges is a good start. In recent years, in dealing with random disturbances in general, the technique of spectral analysis has often been applied and found useful. Both this approach and statistical analyses may prove helpful in interpreting the records of profile variation and in providing some rational basis for predicting the influence of this factor on the magnitude of the dynamic stresses and deflections in highway bridges.

In the latter part of the paper, the authors present an approximate analytical solution for the increased vehicle reaction on the bridge due to its deck unevenness. The authors assume that "the deck contour could be represented by a sinusoidal curve" with a wave length of 25 ft. and a wave height of 1/4 in., and that the vehicle speed was 37 mph. Reference is also made to pp. 238-240 of Timoshenko's book, "Vibration Problems in Engineering," Second Edition. The writer finds it not possible to reproduce from the above mentioned information the value of 36,600 lb. given in the paper as the increased vehicle pressure due to the "wavy contour" of the deck. The authors' comment on this point will be appreciated.

It is not clear to the writer whether by "a sinusoidal curve" the authors mean a series of 25 ft. sine waves or just one single wave preceded and followed by a smooth surface. For the first interpretation of the assumption of "wavy contour," a small variation of the wave length or of the vehicle speed could produce true resonance, so that the increased pressure could theoretically approach infinity. As to the second interpretation, it is difficult to conceive the physical similarity between the actual deck contour and the assumed representation. In both cases, the increased vehicle pressure is directly proportional to the assumed height of the wave.

In view of the rather arbitrary nature of the assumed physical condition for the analysis and the sensitiveness of the result to the variation of the assumed quantities, the writer is of the opinion that such type of analysis as given in pp. 973-25 serves only as a rough check of the order of magnitude of the dynamic responses of the bridges tested. While this may have been the intention of the authors, the significance of this type of analysis does not seem congruous with that of the results of the experiments which were so well presented in the paper.

The analysis of dynamic stresses in highway bridges is a difficult problem. It might be mentioned, however, that although a satisfactory analytical method for studying the vibration of this type of continuous bridge is still lacking. In recent years, substantial progress has been made in the analysis of simply supported bridges, as a reference to the literature listed at the end of this discussion will show. With the aid of modern high speed electronic computers, analyses can now be performed which can take into account the effects of such variables as axle spacing, vertical oscillation and pitching action of vehicles, vehicle springs and tires, flexibility and the actual deck profile of the bridge. Work of this kind is now being carried out in the Civil Engineering Department of the University of Illinois.

With reference to the discrepancies found in the measured static and dynamic stresses and their theoretical or computed values, it may be mentioned that the study of dynamic stresses in highway bridges is still in its early stages as indicated by the fact that research workers in this field often

face the difficulty of defining what actually is the object they are looking for. It may be emphasized that at present it is probably advantageous to focus attention on the relation between the experimental static and dynamic stresses, and that between the theoretical static and dynamic stresses. In other words, cross comparisons of these quantities of stress would needlessly complicate the picture at the present stage. For the convenience of a narrowed-down scope of investigation and to obtain a proper perspective of the problem of highway bridge dynamics at this time, it seems desirable to separate the study of the prediction of dynamic stresses from that of static stresses, although experimental data for both can be obtained from the same test set-up.

In short, it seems that the study of bridge stresses and deflections may be pursued along two lines: (1) the study of the actual value of the static response; (2) the study of the ratio of the dynamic response to the static response. By studying the latter ratio, the study of the dynamic aspect of bridge response can, in fact, be thought of as independent of the accuracy of the prediction of static response. For the purpose of predicting the actual value of the dynamic response, any advance made by the static response study can usually be utilized. However, the present concept of dealing with dynamic response of highway bridges does not really involve the requirement of an accurate prediction of its actual value. This is indicated by the manner in which provisions to take care of bridge "impact" are made in the present AASHO specifications. In view of the foregoing, therefore, the fact that the measured static stresses differ appreciably from the calculated values need not, for the time being, unduly concern those engaged in a study of dynamic stresses.

REFERENCES

1. Tung, T. P., Goodman, L. E., Chen, T. Y., and Newmark, N. M., "Highway Bridge Impact Problems," Highway Research Board, Bulletin No. 124, 1955, Washington, D. C., p. 121, Fig. 8; p. 124, Fig. 11; p. 125, Fig. 12.

2. Taylor, J. E., "Experimental Study on a Sprung Mass with Initial Oscillation," M. S. Thesis, University of Illinois, Sept. 1955.

3. Inglis, C. E., "Theory of Transverse Oscillations in Girders and Its Relation to Live Load and Impact Allowances," Minutes of Proceedings of the Institution of Civil Engineers, Vol. 218, p. 258, Fig. 11.

4. Boehning, R. H., "Single and Tandem Axle Dynamic Effects on a Highway Bridge Model," M. S. Thesis, University of Illinois, 1953, p. 40, Fig. 33.

5. "Impact in Highway Bridges," Final Report of the ASCE Special Committee on Highway Bridge Impact, ASCE Transactions Vol. 95, 1931.

6. Foster, G. M., "Test on Rolled Beam Bridges Using H20-S16 Loading," Highway Research Board, Research Report 14-B, Washington D. C., 1952, p. 10.

7. University of Illinois, Civil Engineering Studies, Structural Research Series No. 24, "Highway Bridge Impact Investigation," Second Progress Report, 1952, pp. 99-109.

8. Biggs, John M. and Suer, Herbert S., "Vibration Measurements on Simple-Span Bridges," Highway Research Board, Bulletin No. 124, 1955, Washington D. C., p. 12, Fig. 14.

9. University of Illinois, Civil Engineering Studies, Structural Research Series No. 24, "Highway Bridge Impact Investigation," Second Progress Report, 1952, pp. 111-117.

Discussion of "DEVELOPMENT AND DESIGN OF THE WALT WHITMAN BRIDGE"

by Milton Brumer and C. W. Hanson
(Proc. Paper 1019)

CEVDET Z. ERZEN.[1]—A very interesting paper is presented by Messrs. Milton Brumer and C. W. Hanson on the development and design of the Walt Whitman Bridge. The paper is especially commendable for exhibiting new design features. In recent years, the most studied feature of design of suspension bridges has been the problem arising due to the oscillation of the bridge, particularly in the torsional mode. This paper reveals some radical deviation from the old conventional methods in that it does not after some tedious aero-dynamic analysis base final depth of the truss on an arbitrarily established ratio of depth to length.

In safe-guarding against torsional oscillation, the authors reveal the importance of the double lateral system, and that a double lateral system increased the torsional stiffness of this particular bridge three fold. Inasmuch as this does not say a thing about what that initial torsional stiffness is without the double lateral system, it however reveals the importance of such a system. This on the other hand does not mean that a bridge that has a single lateral system shall fail. There can be given examples of existing suspension bridges that possess only single lateral system. The most practical approach to establishing a criterean for the stability of suspension bridges is by making a comparative study of the torsional stiffness of the existing bridges whose aero-dynamic behaviors are known. This has been done in an empirical way by Mr. O. H. Ammann to study the vertical oscillation of a suspension bridge. Mr. Ammann fixes the degree of stability of a bridge in vertical oscillatory mode. His method is empirical, but what he calls "stiffness index" gives an idea about the stability of the bridge as compared with those existing bridges whose behavior are known.

An unpublished paper by the writer started while in the employ of Ammann and Whitney, Consulting Engineers, New York City, dealt with the problem of torsional oscillation of suspension bridges and was based, for the purpose of establishing the necessary equations to study the phenomenan, on a paper by the writer entitled, "Analysis of Suspension Bridges by the Minimum Energy Principle" which appeared in Vol. 15 of the "Publications" of the International Association for Bridge and Structural Engineering. According to this analysis it was found that the torsional stiffness of the bridge is directly proportional to the sum of horizontal cable pull due to dead load and a term expressed as

$$\frac{4k}{b^2}$$

where k is the torsional modulus of the torsion box of the bridge and b is the distance between the trusses. In case of a single lateral system k becomes

1. Cons. Engr., New York, N. Y.

zero and thus the torsional stiffness becomes proportional to the dead load of the bridge only. This relationship revealed why in a heavy bridge with no double lateral system the bridge is stable against torsional oscillations. A very good example for this is George Washington Bridge. Another important factor is the length of the bridge. It appears that the stiffness is a function of the square of the length. However the length effect is reduced by the moment of inertia of the stiffening trusses.

According to a study made by the writer based on the above mentioned paper, the susceptibility of various suspension bridges to torsional oscillation is found in the following order:

1. Old Tacoma Narrows Bridge
2. Deer Isle (without diagonal stays)
3. Thousand Island (without diagonal stays)
4. Old Bronx-Whitestone
5. Old Golden Gate
6. New Bronx-Whitestone
7. Walt Whitman Bridge (without double lateral system)
8. Golden Gate Bridge (with double lateral system)
9. George Washington Bridge
10. Walt Whitman Bridge (with double lateral system)
11. Delaware Memorial Bridge
12. New Tacoma Narrows Bridge.

From the above tabulation it may be conceived that it is not altogether necessary to provide double lateral system to prevent torsional oscillations. The weight and the width of the bridge if sufficiently great will produce the effect of the torsion box as in the case of George Washington Bridge. It is interesting to note that, in the particular case of Walt Whitman Bridge, it wouldn't be necessary to provide a torsion box as the weight and the width and the relatively short span would make the bridge rather stable. However, the relatively low cost of the double lateral system further guarantees the safety of the bridge.

CORRECTIONS.—On page 1019-24, the second sentence of the third paragraph under the Section entitled Cables, Suspenders and Cable Anchor Chains, which reads "The material of the wrapping wire is required to meet the same specifications as that of the cable wire.", should be deleted and the following substituted therefor: "The material of the wrapping wire is a soft annealed galvanized steel having a minimum ultimate tensile strength of 70,000 p.s.i. The specimens cut from the wire after galvanizing are required to show an elongation of at least 10 percent in 10 inches as observed under tension."

PROCEEDINGS PAPERS

The technical papers published in the past year are identified by number below. Technical-division sponsorship is indicated by an abbreviation at the end of each Paper Number, the symbols referring to: Air Transport (AT), City Planning (CP), Construction (CO), Engineering Mechanics (EM), Highway (HW), Hydraulics (HY), Irrigation and Drainage (IR), Power (PO), Sanitary Engineering (SA), Soil Mechanics and Foundations (SM), Structural (ST), Surveying and Mapping (SU), and Waterways and Harbors (WW) divisions. Papers sponsored by the Board of Direction are identified by the symbols (BD). For titles and order coupons, refer to the appropriate issue of "Civil Engineering." Beginning with Volume 82 (January 1956) papers were published in Journals of the various Technical Divisions. To locate papers in the Journals, the symbols after the paper numbers are followed by a numeral designating the issue of a particular Journal in which the paper appeared. For example, Paper 861 is identified as 861 (SM1) which indicates that the paper is contained in issue 1 of the Journal of the Soil Mechanics and Foundations Division.

VOLUME 81 (1955)

NOVEMBER: 825(ST), 826(HY), 827(ST), 828(ST), 829(ST), 830(ST), 831(ST)[c], 832(CP), 833(CP), 834(CP), 835(CP)[c], 836(HY), 837(HY), 838(HY), 839(HY), 840(HY), 841(HY)[c].

DECEMBER: 842(SM), 843(SM)[c], 844(SU), 845(SU)[c], 846(SA), 847(SA), 848(SA)[c], 849(ST)[c], 850(ST), 851(ST), 852(ST), 853(ST), 854(CO), 855(CO), 856(CO)[c], 857(SU), 858(BD), 859(BD), 860(BD).

VOLUME 82 (1956)

JANUARY: 861(SM1), 862(SM1), 863(EM1), 864(SM1), 865(SM1), 866(SM1), 867(SM1), 868(HW1), 869(ST1), 870(EM1), 871(HW1), 872(HW1), 873(HW1), 874(HW1), 875(HW1), 876(EM1)[c], 877(HW1)[c], 878(ST1)[c].

FEBRUARY: 879(CP1), 880(HY1), 881(HY1)[c], 882(HY1), 883(HY1), 884(IR1), 885(SA1), 886(CP1), 887(SA1), 888(SA1), 889(SA1). 890(SA1), 891(SA1), 892(SA1), 893(CP1), 894(CP1), 895(PO1) 896(PO1), 897(PO1), 898(PO1), 899(PO1), 900(PO1), 901(PO1), 902(AT1)[c], 903(IR1)[c], 904(PO1)[c], 905(SA1)[c].

MARCH: 906(WW1), 907(WW1), 908(WW1), 909(WW1), 910(WW1), 911(WW1), 912(WW1), 913(WW1)[c], 914(ST2), 915(ST2), 916(ST2), 917(ST2), 918(ST2), 919(ST2), 920(ST2), 921(SU1), 922(SU1), 923(SU1), 924(ST2)[c].

APRIL: 925(WW2), 926(WW2), 927(WW2), 928(SA2), 929(SA2), 930(SA2), 931(SA2), 932(SA2)[c], 933(SM2), 934(SM2), 935(WW2), 936(WW2), 937(WW2), 938(WW2), 939(WW2), 940(SM2), 941(SM2), 942(SM2)[c], 943(EM2), 944(EM2), 945(EM2), 946(EM2)[c], 947(PO2), 948(PO2), 949(PO2), 950(PO2), 951(PO2), 952(PO2)[c], 953(HY2), 954(HY2), 955(HY2)[c], 956(HY2), 957(HY2), 958(SA2), 959(PO2), 960(PO2).

MAY: 961(IR2), 962(IR2), 963(CP2), 964(CP2), 965(WW3), 966(WW3), 967(WW3), 968(WW3), 969(WW3), 970(ST3), 971(ST3), 972(ST3)[c], 973(ST3), 974(ST3), 975(WW3), 976(WW3), 977(IR2), 978(AT2), 979(AT2), 980(AT2), 981(IR2), 982(IR2)[c], 983(HW2), 984(HW2), 985(HW2)[c], 986(ST3), 987(AT2), 988(CP2), 989(AT2).

JUNE: 990(PO3), 991(PO3), 992(PO3), 993(PO3), 994(PO3), 995(PO3), 996(PO3), 997(PO3), 998(SA3), 999(SA3), 1000(SA3), 1001(SA3), 1002(SA3), 1003(SA3)[c], 1004(HY3), 1005(HY3), 1006(HY3), 1007(HY3), 1008(HY3), 1009(HY3), 1010(HY3)[c], 1011(PO3)[c], 1012(SA3), 1013(SA3), 1014(SA3), 1015(HY3), 1016(SA3), 1017(PO3), 1018(PO3).

JULY: 1019(ST4), 1020(ST4), 1021(ST4), 1022(ST4), 1023(ST4), 1024(ST4)[c], 1025(SM3), 1026(SM3), 1027(SM3), 1028(SM3)[c], 1029(EM3), 1030(EM3), 1031(EM3), 1032(EM3), 1033(EM3)[c].

AUGUST: 1034(HY4), 1035(HY4), 1036(HY4), 1037(HY4), 1038(HY4), 1039(HY4), 1040(HY4), 1041(HY4)[c], 1042(PO4), 1043(PO4), 1044(PO4), 1045(PO4), 1046(PO4)[c], 1047(SA4), 1048(SA4)[c], 1049(SA4), 1050(SA4), 1051(SA4), 1052(HY4), 1053(SA4).

SEPTEMBER: 1054(ST5), 1055(ST5), 1056(ST5), 1057(ST5), 1058(ST5), 1059(WW4), 1060(WW4), 1061(WW4), 1062(WW4), 1063(WW4), 1064(SU2), 1065(SU2), 1066(SU2)[c], 1067(ST5)[c], 1068(WW4)[c], 1069(WW4).

OCTOBER: 1070(EM4), 1071(EM4), 1072(EM4), 1073(EM4), 1074(HW3), 1075(HW3), 1076(HW3), 1077(HY5), 1078(SA5), 1079(SM4), 1080(SM4), 1081(SM4), 1082(HY5), 1083(SA5), 1084(SA5), 1085(SA5), 1086(PO5), 1087(SA5), 1088(SA5), 1089(SA5), 1090(HW3), 1091(EM4)[c], 1092(HY5)[c], 1093(HW3)[c], 1094(PO5)[c], 1095(SM4)[c].

NOVEMBER: 1096(ST6), 1097(ST6), 1098(ST6), 1099(ST6), 1100(ST6), 1101(ST6), 1102(IR3), 1103(IR3), 1104(IR3), 1105(IR3), 1106(ST6), 1107(ST6), 1108(ST6), 1109(AT3), 1110(AT3)[c], 1111(IR3)[c], 1112(ST6)[c].

---

c. Discussion of several papers, grouped by Divisions.

AMERICAN SOCIETY OF CIVIL ENGINEERS

OFFICERS FOR 1957

PRESIDENT

MASON GRAVES LOCKWOOD

VICE-PRESIDENTS

Term expires October, 1957:
FRANK A. MARSTON
GLENN W. HOLCOMB

Term expires October, 1958:
FRANCIS S. FRIEL
NORMAN R. MOORE

DIRECTORS

Term expires October, 1957:
JEWELL M. GARRELTS
FREDERICK H. PAULSON
GEORGE S. RICHARDSON
DON M. CORBETT
GRAHAM P. WILLOUGHBY
LAWRENCE A. ELSENER

Term expires October, 1958:
JOHN P. RILEY
CAREY H. BROWN
MASON C. PRICHARD
ROBERT H. SHERLOCK
R. ROBINSON ROWE
LOUIS E. RYDELL
CLARENCE L. ECKEL

Term expires October, 1959:
CLINTON D. HANOVER, Jr.
E. LELAND DURKEE
HOWARD F. PECKWORTH
FINLEY B. LAVERTY
WILLIAM J. HEDLEY
RANDLE B. ALEXANDER

PAST-PRESIDENTS

Members of the Board

WILLIAM R. GLIDDEN

ENOCH R. NEEDLES

EXECUTIVE SECRETARY
WILLIAM H. WISELY

TREASURER
CHARLES E. TROUT

ASSISTANT SECRETARY
E. L. CHANDLER

ASSISTANT TREASURER
CARLTON S. PROCTOR

PROCEEDINGS OF THE SOCIETY

HAROLD T. LARSEN
Manager of Technical Publications

PAUL A. PARISI
Editor of Technical Publications

COMMITTEE ON PUBLICATIONS

JEWELL M. GARRELTS, *Chairman*

HOWARD F. PECKWORTH, *Vice-Chairman*

E. LELAND DURKEE
MASON C. PRICHARD
R. ROBINSON ROWE
LOUIS E. RYDELL